

UNIVERSITÀ DEGLI STUDI DI NAPOLI “FEDERICO II”

**SCUOLA DI DOTTORATO “SCIENZE DELLA TERRA”
“Giuseppe De Lorenzo”**

Dottorato in Scienze ed Ingegneria del Mare

in consorzio con
**SECONDA UNIVERSITÀ DI NAPOLI
UNIVERSITÀ “PARTHENOPE” NAPOLI**
in convenzione con
**ISTITUTO PER L’AMBIENTE MARINO COSTIERO – C.N.R.
STAZIONE ZOOLOGICA “ANTON DOHRN”**

XXIII ciclo

Tesi di Dottorato

**Nitrogen and Phosphorus dynamics in coastal areas:
common pattern, peculiarities and ecological
implications**

Candidato: Dott. Francesca Margiotta Tutor: Dott. Vincenzo Saggiomo

Co-Tutor: Dott. Raffaella Casotti

Il Coordinatore del Dottorato: Prof. Alberto Incoronato

ANNO 2011

Thesis abstract.....	- 3 -
Chapter 1: Background and aims of the work.....	- 5 -
1.1 Nitrogen and phosphorus in marine environment.....	- 6 -
1.1.1 The Nitrogen Cycle.....	- 6 -
1.1.2 The Phosphorus Cycle	- 9 -
1.2 Coastal zone.....	- 10 -
1.3 Long -term time series	- 12 -
1.4 Aims of the study.....	- 13 -
Chapter 2: Materials and methods.....	- 15 -
2.1 Physical and meteorological data	- 16 -
2.1.1 Hydrology.....	- 16 -
2.1.2 Precipitation data	- 16 -
2.2 Treatment and analyses of samples	- 16 -
2.2.1 Inorganic nutrients.....	- 16 -
2.2.2 Total N and P.....	- 16 -
2.2.3 Particulate N and P	- 16 -
2.2.4 Organic N and P.....	- 17 -
2.2.5 Chlorophyll a (Chl a)	- 17 -
2.2.6 Heterotrophic bacteria abundance.....	- 17 -
2.2.7 Enzymatic activity	- 17 -
2.3 Statistical analyses.....	- 18 -
2.3.1 Principal component analysis	- 18 -
2.3.2 Box plot.....	- 18 -
2.3.3 Time-series decomposition	- 19 -
2.3.4 Multivariate multiple regression.....	- 19 -
Chapter 3: Surface N and P dynamics along the Campania coast (2001-2006)	- 20 -
3.1 Specific aims of the chapter.....	- 21 -
3.2 Study Area	- 21 -
3.2.1 Campania Region	- 21 -
3.2.2 Sampling Strategy	- 22 -
3.3 Results.....	- 24 -
3.3.1 Hydrological features.....	- 24 -
3.3.2 Nutrients	- 33 -
3.3.3 Environmental characterization of the Campania coast	- 47 -
3.4 Discussion	- 50 -
Chapter 4: Water column distribution and time evolution of N and P at a coastal site of the Gulf of Naples (2002-2009).....	- 57 -
4.1 Specific aims of the chapter.....	- 58 -
4.2 Study area.....	- 58 -
4.2.1 Gulf of Naples	- 58 -
4.2.2 Sampling strategy	- 59 -
4.3 Results.....	- 60 -
4.3.1 Temperature.....	- 61 -
4.3.2 Salinity	- 66 -
4.3.3 Dissolved Inorganic Nitrogen (DIN)	- 71 -
4.3.4 Phosphate	- 82 -
4.3.5 N/P ratio in the inorganic dissolved pool	- 87 -
4.3.6 Phytoplankton biomass (Chl a).....	- 94 -
4.3.7 Precipitations	- 99 -
4.4 Discussion	- 101 -

Chapter 5: Detailed vertical distribution and seasonality of N and P as related to microbial activity (2008-2009)	- 108 -
5.1 <i>Specific aims of the chapter</i>	- 109 -
5.2 <i>Sampling strategies</i>	- 109 -
5.3 <i>Results</i>	- 109 -
5.3.1 Total N and P.....	- 110 -
5.3.2 Particulate N and P	- 115 -
5.3.3 Dissolved Organic N and P.....	- 119 -
5.3.4 N and P compositions	- 124 -
5.3.5 N/P ratios	- 128 -
5.3.6 Heterotrophic bacteria.....	- 134 -
5.3.7 Carbon distribution and ratios in heterotrophic bacteria and phytoplankton	- 136 -
5.3.8 Hydrolytic enzyme activities	- 138 -
5.4 <i>Discussion</i>	- 140 -
Chapter 6: Conclusions	- 145 -
References.....	- 148 -

Thesis abstract

The research carried out during this Ph.D. thesis has been focused on the study of the Nitrogen and Phosphorus dynamics in different marine ecosystems along the coast of the Campania Region (Southern Italy).

Coastal systems are often stressed by intense anthropogenic pressures, whose characteristic space and time scales significantly differ from those of the natural forcings. As a consequence, understanding the coastal marine ecosystem functioning and dynamics is a complex and extremely important issue. In fact, coastal management and remediation requires a deep knowledge of the mechanisms ruling each different system.

The approach adopted during this research involves increasing levels of complexity. At first, the surface distribution in time and space of N and P has been investigated using data from previous samplings along the Campania Region coastal system. The data used were collected in the frame of the National Project Si.Di.Mar (Sistema Difesa Mare). For each sampling site, the mean composition and the interannual and seasonal variability have been analyzed for each N and P form. A classification of the different areas has been obtained, based on chemical properties. The main mechanisms influencing N and P dynamics in each area have then been identified. N and P display significant differences depending on the area considered, both in terms of absolute concentrations and relative ratios. The stations inside the Gulf of Gaeta and the Gulf of Naples show a high nutrient load and variability derived from terrigenous inputs, and are characterized by eutrophic-mesotrophic conditions. Conversely, inside the Gulf of Salerno (and particularly in its southern part), terrigenous inputs are quite low, coastal waters display meso-oligotrophic conditions and the N and P dynamics is influenced by the exchanges with the open ocean. The inorganic fraction predominates at stations close to river mouths, while organic forms dominate the remaining sites. Nitrates represent the dominant component of the inorganic dissolved Nitrogen (DIN) next to Sarno and Picentino rivers, whereas ammonium represents about 50% of the DIN near the Sarno river. High concentrations of ammonium and phosphate were found in the Gulf of Naples, clearly marking the intense anthropic pressure on the area. Finally, a marked seasonality of the N/P ratio in the inorganic pool has been observed at all sites, independently of their specific chemical characteristics. These data, however, lacked resolution on the vertical dimension and were limited to inorganic total pools of N and P.

As a second step, the N and P dynamics along the water column and its relation to selected physical parameters has been thoroughly investigated analyzing eight years of data from the long-term fixed station MareChiara, in the Gulf of Naples. The influence of interannual signals, seasonal cycles and specific events on the distribution of N and P has been estimated through a multiplicative decomposition technique. Selected physical parameters (temperature and salinity) and meteorological forcings (precipitations) have been analyzed to highlight their role in

modulating N and P dynamics. The analysis showed that the inorganic N comes from different sources. Ammonium dominates in the surface layer, and it is mainly related to terrigenous inputs, while the nitrates display two different enrichment mechanisms. In the surface layer, terrigenous input prevail, whereas other processes act on the deeper part of the water column (namely, remineralization and sub-surface circulation/mixing). Precipitations generally increase both N and P, but more in N, causing an increase of the N/P ratio. This data suggest that the chemical characteristics of the water masses can be used as tracers of the nutrient sources.

Thirdly, a more detailed analysis of N and P concentrations, partition and stoichiometry has been carried out with the aim of describing the vertical distribution and temporal variability of each nutrient pool (dissolved inorganic, dissolved and particulate organic). Moreover, enzymatic activity (aminopeptidase and alkaline phosphatase) and phytoplankton and heterotrophic bacteria biomass have been measured, in order to better define the role of the microbial communities on N and P dynamics. The data highlight a strong temporal variability, especially in the surface layer and also show that N and P dynamics is significantly influenced by biological activity, in particular for what he particulate pool is concerned. In addition, physical processes also strongly affect inorganic N and P dynamics and this interaction is key to understand to unveil the main mechanisms of nutrient dynamics in coastal waters.

Chapter 1: Background and aims of the work

1.1 Nitrogen and phosphorus in marine environment

Nitrogen (N) and Phosphorus (P) are essential macronutrients for all living organisms, as they are found in a range of biomolecules with a variety of cellular roles.

Though their concentrations are low compared to seawater's major constituents, N and P are extremely important to the biology of the oceans.

The alteration in the partition between dissolved and particulate phase and between the inorganic and organic pools, and the ratio between Nitrogen and Phosphorus availability, may severely influenced primary production and microbial metabolism (e.g., Lipitser et al, 2011). These effects are more frequent in the regions influenced by terrestrial loads.

In the following, an overview of what is presently known about the N and P cycles is reported.

1.1.1 The Nitrogen Cycle

The Nitrogen pathway represents one of the most complex biogeochemical cycles on the Earth, and also influences many other elements of primary importance for the marine ecosystems, such as Carbon and Phosphorus. Nitrogen can exist in different chemical forms and, in the marine environment, it occurs in 5 relatively stable oxidation states. It can be found as nitrate, NO_3^- (oxidation state +V), nitrite, NO_2^- (+III), nitrous oxide, N_2O (+I), molecular nitrogen, N_2 (0), and ammonia, NH_4^+ (-III). Moreover, there are several organic nitrogen compounds, mainly in the form of amino-groups (-III).

All these oxidation states, and the resulting large number of nitrogen species, give rise to many redox reactions that transform one specie to another (Fig 1.1). Most of these reactions are biologically mediated by marine organisms.

The process that quantitatively dominates the marine nitrogen cycle is the assimilation of nitrate or ammonium into organic nitrogen by marine phytoplankton (Gruber, 2008).

NH_4 is considered the preferred source of nitrogen for phytoplankton, because its assimilation does not involve a redox reaction and therefore little energy is required (Zehr and Ward, 2002). On the contrary, the assimilation of NO_3 implies the reduction of nitrogen from state +V to -III, and consequently requires a considerable amount of energy. Most of phytoplankton organisms have the enzyme necessary to undertake this reaction. However, *Prochlorococcus* and some strains of *Synechococcus* lack the ability to use NO_3 as source of nitrogen (Moore et al., 2002).

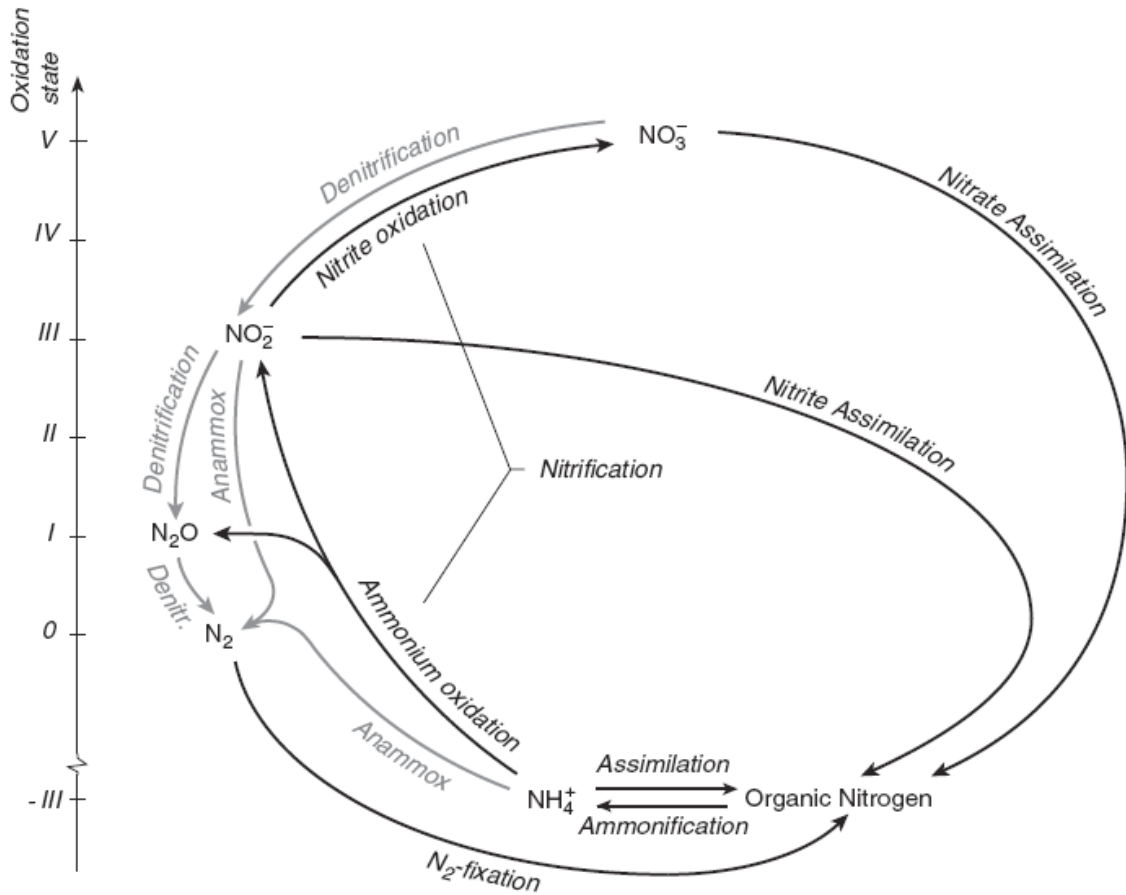
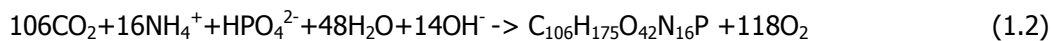


Fig 1.1 - Major chemical forms and transformations of nitrogen in the marine environment. The various chemical forms of nitrogen are plotted versus their oxidation state. Processes shown in grey occur in anoxic environments only (from Gruber, 2008).

The assimilation of nitrogen by phytoplankton is strongly coupled to the photosynthetic fixation of carbon and to the assimilation of phosphate. Assuming that the average composition of the organic matter in phytoplankton follows the stoichiometry reported by Anderson, (1995), the reaction of synthesis of organic matters can be written as:



if NO_3^- is used as source of N, or as:



if NH_4^+ is the nitrogen source (Gruber, 2008).

However, it is important to stress that these stoichiometric ratios are obtained as averages, and observed phytoplankton composition may deviate considerably from these ratios (Geider and LaRoche, 2002; Klausmeier et al., 2004; Arrigo, 2005).

Furthermore, even if phytoplankton has historically been considered the primary consumer of inorganic nitrogen, some studies have highlighted that marine bacteria appear to have very efficient NH_4^+ uptake systems (Suttle et al., 1990) and, under some conditions, compete effectively with phytoplankton for NO_3^- (Kirchman and Wheeler, 1998; Kirchman et al., 1994).

Most of the fixed organic nitrogen in the ocean is returned back to nitrate by remineralization processes in three different steps: ammonification, ammonium oxidation and nitrite oxidation (these two latter processes, combined, are usually called nitrification).

The ammonification is the reverse reaction of the assimilation (equation 1.2), done by heterotrophic bacteria, which use the oxidation of organic carbon to CO₂ as source of energy. The nitrification occurs in two different steps (equations 1.3 and 1.4),



most often done by two distinct groups of aerobic organisms (*Nitrosomonas spp.*, an ammonium oxidizer, and *Nitrobacter spp.*, a nitrite oxidizer). Nitrification requires the presence of O₂ and tends to be limited by light.

The processes that occur in anoxic environments are: denitrification and anamox. Denitrification is the can be considered as the inverse reaction of nitrogen assimilation (equation 1.1) and it is done by heterotrophic bacteria in anaerobic environment.

The anammox is an anaerobic process that removes fixed nitrogen from marine environment:



It is used as source of energy from chemo-autotrophic bacteria.

Finally, the N₂ biological fixation, is the conversion of molecular nitrogen N₂ into organic nitrogen. The most conspicuous N₂ fixing organism is the *Trichodesmium*, even if there are many other organisms known to fix nitrogen, including uni-cellular bacteria (Zehr and Ward, 2002) and cyanobacteria that live endosymbiotically with diatoms (e.g., Carpenter et al., 1999).

Looking at the nitrogen inventory in the ocean, N₂ represents the largest amount (~94%), while the remaining 6% is in fixed forms. Among them, NO₃⁻ is the most abundant (~80%), followed by the dissolved inorganic nitrogen DON (~12%). The remaining fixed forms, particulate nitrogen (PN), NO₂⁻, NH₄⁺ and NO₂, account together for less than 0.3% (Gruber, 2008).

The mean oceanic vertical distribution of NO₃ displays near surface depletion and enrichment at depth, driven by the biological pump. NH₄ and NO₂ show a maximum around 50-80m, in the lower part of the euphotic zone and rapidly decrease below this depth. These two labile species accumulate only when their generation rate overwhelms their consumption. In the case of NH₄, this occurs in the deeper parts of the euphotic zone. At these depths, organic nitrogen is rapidly remineralized but the uptake of produced NH₄ is already limited by light. Near the bottom of the euphotic zone or below, where the light is low enough not to inhibit the nitrification, part of the NH₄ is oxidized to NO₃, creating NO₂ as intermediate product.

The DON is a heterogeneous mixture of biologically labile compounds, which turn over at scales of the order of days to weeks, and refractory components, which persist for months to hundreds of years. The more refractory forms are quantitatively dominant, but their importance as potential N source is by far exceeded by the less abundant labile compounds (Bronk, 2002). The chemical composition of DON is still largely unknown and only the 4-9% has been characterized (Benner,

2002). By the way, DON is known to include urea, dissolved combined amino acids, free amino acid, humic and fulvic substances, nucleic acids.

The vertical profiles of DON generally display enrichment at the surface and lower concentrations in the deeper part of the water column. DON concentrations tend to be inversely correlated with NO_3 as depth increases, and at the surface DON and NO_3 are also often inversely correlated over time (Bronk, 2002). DON originates from several biotic and abiotic sources: the abiotic sources include DON and DOP transport via overland runoff, rivers, streams and groundwater (Valiela et al., 1990; Tobias et al., 2001) the biotic sources include phytoplankton, bacteria, microzooplankton and zooplankton releases (Carlson, 2002).

The particulate organic nitrogen (PN) represents only the 0.5% of the total organic nitrogen pool, but, since some part of it is heavy enough to sink, it plays a key role in the marine biological pump. PN can exhibit a wide spectrum of sizes, ranging from very fine suspended particles up to large aggregates, such as marine snow or faecal pellets. Most of the time, PN concentrations are higher at the surface, while they decrease quasi-exponentially with depth. In the euphotic zone, most of the PN is believed to be living matter, although its composition has never been characterized until now.

1.1.2 The Phosphorus Cycle

Compared to N, the P cycle is relatively simple. Phosphorus lacks the gas phase and it is unaffected by redox cycling. The marine P cycle consists of a series of transformations between dissolved inorganic, particulate organic, and dissolved organic forms (Hutchins and Fu, 2008), as schematized in the diagram presented in Fig. 1.2.

Phosphorus is primarily delivered to the ocean via continental weathering. This P is transported to the ocean primarily in the dissolved and particulate phases via riverine influx. However, atmospheric deposition through aerosols, volcanic ash, and mineral dust is also important, particularly in remote oceanic locations (Paytan and McLaughlin, 2007).

The inorganic forms of P consist mainly of orthophosphates ($\sim 1\% \text{H}_2\text{PO}_4$, $87\% \text{HPO}_4$, $12\% \text{PO}_4$ at pH 8, $T=20^\circ\text{C}$, salinity 33, (Kester and Pytkowicz, 1967), pyrophosphates (P_2O_7), condensed cyclic (metaphosphates) and linear (poliphosphates) polymers of various molecular weights (Karl and Bjorkman, 2002).

The chemical composition of organic P is relatively unknown. In the organic dissolved fraction, particular compound classes have been identified, such as phosphates esters, phosphonates and organic condensed phosphate, phosphonucleotides, nucleic acids and phospholipids (Benitez-Nelson, 2000).

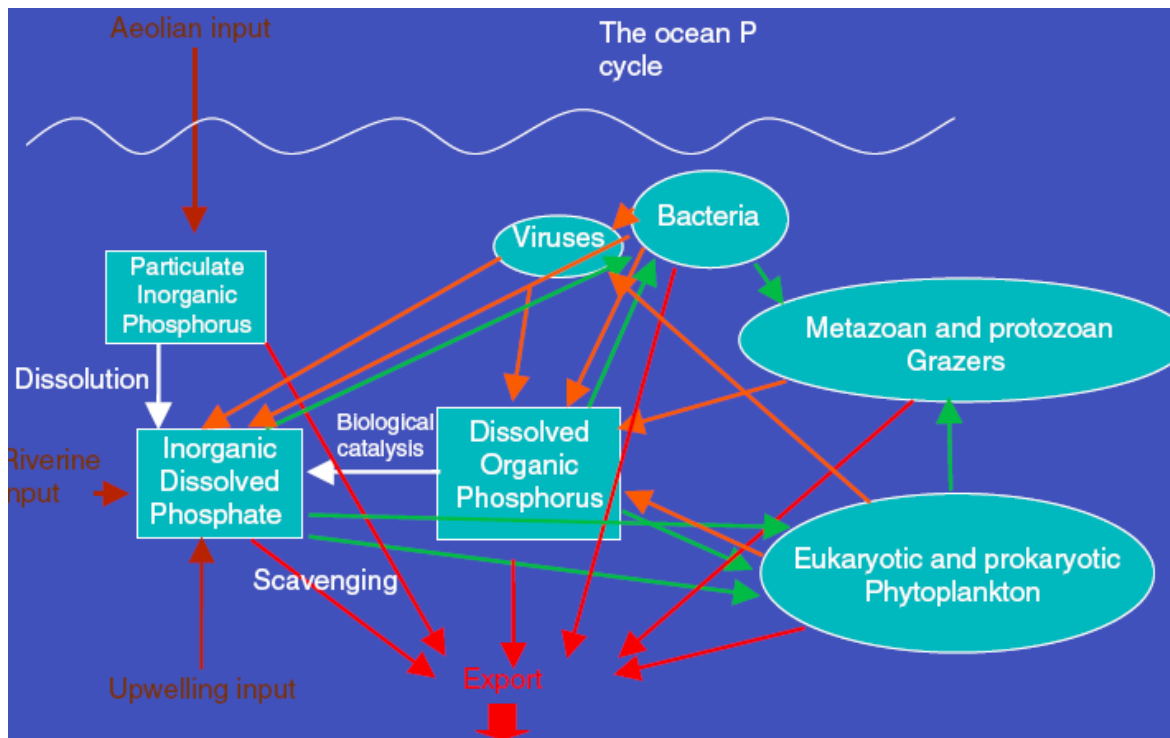


Fig. 1.2 - A conceptual diagram of important pools and fluxes in the marine P cycle (from Hutchins and Fu 2008). Non-living pools (rectangles), living pools (ovals), new inputs (brown text and arrows), transformations between non-living pools (white arrows), biological uptake pathways (green arrows), regeneration pathways (orange arrows), export pathways (red arrows).

The inorganic P is rapidly assimilated by phytoplankton, while some of the organic P compounds can be hydrolyzed by enzymes synthesized by bacteria and phytoplankton and subsequently assimilated (Azam et al., 1983). In addition, cell lysis releases enzymes (phosphomono- and phosphodiesterases, nucleases, nucleotidases, kinases) with greater or lesser substrate specificity that act to liberate orthophosphate from organic P compounds (Lehninger, 1975).

As observed in the previous section for nitrogen, the vertical distribution of the organic P pools are inversely correlated to the inorganic dissolved phosphates as depth increases, while at the surface DOP and PO_4 are often inversely correlated over time (eg, Karl et al., 2001). Moreover, recent studies highlighted that the P cycle is highly affected by scavenging. A large fraction of PP can be adsorbed at cell surface (even larger than intracellular P). The fraction of scavenged P increases in senescent phytoplankton populations. This is a unique property of inorganic phosphate; as laboratory experiments showed that DOP grown-phytoplankton do not exhibit any surface-adsorbed P (Sanudo-Wilhelmy et al., 2004; Fu et al., 2005).

1.2 Coastal zone

The coastal zone is the transitional area between land and sea (Fig. 1.3), including the coastal marshland, estuaries, it is generally considered to extend from the coastline to the continental shelf break (~200 m), occupying 7.6% of the seafloor (Sverdrup et al., 1942).

Coastal zones are highly dynamic systems, characterized by their relationships with adjacent land and ocean, by atmospheric forcing and terrigenous inputs, and by the structure of their water

bodies and underlying seafloors. In these areas, the physical factors fluctuates at spatial and temporal scales ranging from 10^{-2} m (e.g., turbulent motions) to 10^3 Km (e.g., barrier migration) and from 10^2 s (e.g., swash-backwash) to 10^4 yr (e.g. sea level changes) (Comín et al., 2004). Rivers are the major pathway for the delivery of land-based nutrients from watersheds (drainage basins) to coastal systems. In addition, submarine groundwater discharge and direct atmospheric deposition can be important pathways for the delivery of nutrient (Jickells, 1998). From the biological point of view, these areas represent the richest part of the oceans: coastal zone accounts for nearly 30% of total net primary production of the global ocean (6.9×10^{15} g C yr⁻¹) and at least 90% of the world's fish catch (Alongi, 2004).

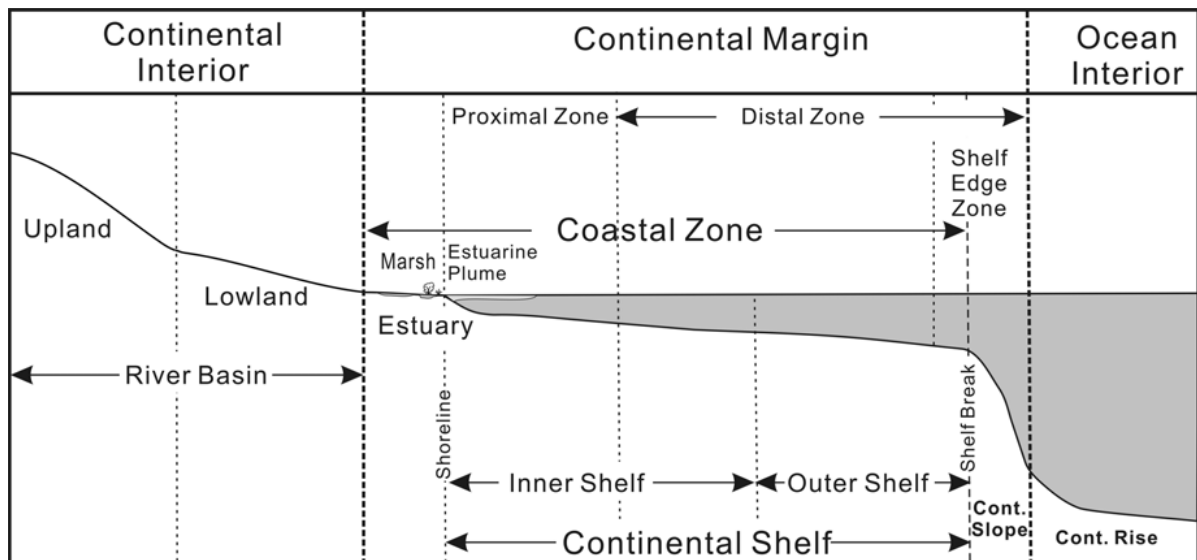


Fig. 1.3 - Schematic classification of the geological provinces of the ocean (from Liu et al., 2010)

As a consequence, the coastal zone is also one of the most valuable and vulnerable areas of the Earth's habitats. Coastal areas are used for food supply, as a source of renewable and non-renewable resources, for transportation, as well as for waste disposal and for recreation purposes (Jickells, 1998). More than half of Earth's population resides within 100km of the coast (Vitousek et al., 1997) and this number is constantly increasing, especially in tropical and subtropical areas, where, due to severe poverty and limited resources, the ocean is an important source for subsistence (Fleming et al., 2006).

During the last century, the coastal ocean has been exposed to large anthropogenic perturbations mainly related to human activities on land. Prolonged and intensive use of fertilizers, change in land use, deforestation and discharge of industrial and municipal waste have contributed, worldwide, to the eutrophication of rivers and coastal waters (Rabouille et al., 2001).

Strong increases have occurred in nitrogen and phosphorus loads. Examples are provided, for instance, by the analyses of time series of measurements conducted in the Black Sea (Cociasu et al., 1996), in the central and northern Baltic Sea (Nehring, 1992; Bonsdorff et al., 1997), in the central Irish Sea (Allen et al., 1998) and in the Wadden Sea (G. C. Cadée and Hegeman, 2002).

The larger amounts of nutrients have been hypothesized to have caused increases in phytoplankton biomass and primary production with respect to unperturbed systems, as recorded in the Wadden Sea (G.C. Cadée, 1992), in the Irish Sea (Allen et al., 1998) and in Chesapeake Bay (Harding and Perry, 1997). Smith, 2006, found a strong positive correlation between phytoplankton growth and nutrients in 92 estuarine and coastal marine sites worldwide. On the other hand, as phytoplankton biomass increases, water transparency decreases and the reduced light availability may limit benthic algal and plant growth and may stimulate the microbial metabolism, causing dramatic changes in sediment chemistry and oxygen consumption (J.E. Cloern, 2001).

Marine ecosystems heavily impacted by human activities also showed changes in species composition. A remarkable shift in the ratio of centric:pennate diatoms was found in the sedimentary records of Chesapeake Bay (Cooper, 1995), while enhanced frequency of non-diatom blooms was recorded in the Black Sea (Bodeanu, 1993) and in the Dutch Wadden Sea. In this latter site, increases in the length of *Phaeocystis* blooms were recorded until 1994, probably linked to anomalous phosphate concentrations (G. C. Cadée and Hegeman, 2002). Moreover, an increase in frequency and intensity of harmful algal blooms (HABs) on a world-wide scale has been reported in the last decades. Even if their causes are still under debate, it seems that high or unbalanced nutrient input is a necessary, but not sufficient, condition (Maso and Garces, 2006).

Human activities have affected the base as well the top of marine food web (Vitousek et al., 1997). Rapid change in species compositions and loss of biodiversity occur when there is an imbalance between removal and resource enrichment (Worm et al., 2002). Overfishing has led to a decrease in grazer and high-level consumer populations (eg. shellfish, finfish) as well as to changes in the trophic structure (Jackson et al., 2001).

Understanding how human-induced changes interact with and affect the structure and the functioning of coastal ecosystems is a major research challenge (Paerl et al., 2006), but, compared to open waters, coastal area dynamics are less predictable and more difficult to interpret due to the number of processes acting on very different space and time scales.

1.3 Long -term time series

Over the past few decades, it has become clear that the management of marine resources needs to be grounded in sound knowledge of coastal zone dynamics, as a critical part of predicting the outcome of future environmental changes (A. Zingone et al., 2010a).

Long-term time series are increasingly recognized as valuable tools for quantifying the long-term status of coastal oceans and for assessing the relative importance of varying environmental and anthropogenic influences on coastal ecosystems globally (Borkman et al., 2009).

To provide the scientific community, policy makers, and society with the knowledge and predictive understanding necessary to conserve, protect, and manage ecosystems, their biodiversity, a network of research sites located in a wide array of ecosystems worldwide has been created: the Long-Term Ecological Research network (LTER).

Moreover, in the latest years, monitoring activities of the coastal waters are undertaken by several countries in application of regional, national or supranational laws (e.g. European Directives).

In 2000, the European Parliament and the Council adopted the European Union (EU) Water Framework Directive (WFD), which provides a framework for the protection of groundwater, inland surface waters, transitional waters (estuaries) and coastal waters. The overall aim of the WFD was:

- to prevent further deterioration, protect and enhance the environmental status of aquatic systems;
- to promote the sustainable use of water while progressively decreasing or eliminating discharges, losses and emissions of pollutants and other pressures for the long-term protection and enhancement of the aquatic environment (Andersen et al., 2006).

A key problem in this kind of research is the difficulty in maintaining long time-series. For instance, in spite of an exponential increase in the initiation of long-term physical, chemical and biological monitoring programmes in the ocean since World War II, 40% of these time-series were stopped during the 1980s because monitoring the environment was seen as poor science by science administrators (C.M. Duarte et al., 1992). However, the negative perception of long-term monitoring only altered during the late 1990s, when the consequences of climate change were seen both scientifically and politically as being important. This has markedly improved the fortunes of long term researches, with many new time-series starting up (Hays et al., 2005).

1.4 Aims of the study

The nutrient dynamics in coastal areas is expected to depend strongly on the characteristics of the system considered, primarily because of the wide range of possible regimes controlling the exchange and mixing between coastal waters and the open oceans, but also in relation to the different sources and processes involved. Thus, all studies of coastal dynamics and related complex biogeochemical cycles begin by looking at specific regions, in order to identify and understand the main possible mechanisms driving the ecosystem functioning and the impact of the natural and anthropogenic pressures on its evolution. Once the a single system is deeply understood, results are extrapolated to propose a general model of coastal ecosystem functioning.

This strategy is at the base of the work presented in this thesis. The work involved a multi-scale approach with increasing levels of complexity that was applied to study of the N and P dynamics in the coastal areas of Campania region (Southern Italy). The aim of this work is to identify common patterns and/or peculiarities among different environments and to elucidate the interactions between the nutrient dynamics and the microbial communities.

The multi-scale approach (from large areas to selected stations, from few parameters at the surface to several parameters along the entire water column) was followed to overcome the limitation in both the datasets available and the possibility to carry out new intense analytical activities over wide areas and with sufficient time coverage to resolve the main processes driving the system variability. In fact, while enough historical data exist to classify the main systems along

the Campania coasts and to identify long-term variations, additional parameters were needed to give a more complete view on the N and P cycle.

The specific objectives of this work can thus be summarized in three main points:

- 1) In Chapter 3, the N and P (total, inorganic and organic) surface distribution in different ecosystems along the Campania coasts, collected in the framework of the Italian environmental coastal monitoring program Si.di.Mar, have been analysed. The specific aims were: to characterize the different sites based upon their physical and chemical properties, in order to elucidate the mechanisms driving N and P dynamics and to discern common patterns in N and P seasonality.
- 2) In Chapter 4, the temporal and vertical distribution of inorganic N and P, based on the data collected between 2002 and 2009 at the LTER-MareChiara station, have been analyzed. The influence of temperature and salinity, as well as meteorological forcings (precipitations) have been investigated in order to evaluate their role in driving N and P dynamics. Moreover, the phytoplankton biomass distribution has been analysed to elucidate its relation and eventual feedback on the inorganic dissolved N and P variability.
- 3) In Chapter 5, additional measurements of the total, particulate and dissolved organic N and P pools have been realized, in order to characterize their vertical and temporal distribution of N and in P in terms of concentration, partition and stoichiometry. Moreover, the abundance of the heterotrophic bacteria, their relative contributions to the total C (phytoplankton plus heterotrophic bacteria) and the enzymatic activities (aminopeptidase and alkaline phosphatase) have been analyzed in order to elucidate the role of the microbial communities in the N and P cycles in coastal waters.

Chapter 2: Materials and methods

2.1 Physical and meteorological data

2.1.1 Hydrology

Downwelling profiles of temperature and salinity were acquired by means of Conductivity Temperature Depth (CTD) profilers.

During the surveys carried out in the framework of the Si.Di.Mar Project (chapter 3), a SBE 19plus (Sea-Bird electronic) CTD was used, while the sample for the determinations of nutrients were collected using a horizontal Niskin bottle (capacity 1.2 l).

At LTER-MareChiara station (chapters 4 and 5), temperature and salinity profiles were acquired by means of an SBE 911plus CTD. The CTD was connected to a Sea-Bird Electronics automatic Carousel sampler (rosette), equipped with 12 Niskin bottles (12 l); water samples for chemical and biological analyses were drawn from the Niskin bottles.

In both cases, the data were processed (mediated to one meter) using the SeaSoft Data Processing Software.

2.1.2 Precipitation data

The precipitation data were collected at the meteorological station of the DISAM (Parthenope University), located in Naples (coordinates 40°50.19' N; 14°15.21' E). The data were kindly provided by Prof. Giorgio Budillon. In 2007, the precipitation data were not available starting from the 24th of April 2007 until the 30th of June.

2.2 Treatment and analyses of samples

2.2.1 Inorganic nutrients

Samples for nitrate (NO₃), nitrite (NO₂), ammonium (NH₄), orthophosphates (PO₄) and silicate (SiO₄) determinations were collected in high density polyethylene vials directly from the Niskin bottles, and immediately stored at -20°C until analysis. The analyses were performed by the technicians of the Zoological Station "A. Dohrn", utilizing an Autoanalyzer Technicon II series up to 2005 and, starting from 2006, using a FlowSys Systema Autoanalyzer. Both instruments were equipped with five continuous flux channels. The analyses were performed following Hansen and Grasshoff, 1983

The Dissolved inorganic nitrogen (DIN) was calculated as the sum of nitrate, nitrite and ammonium.

2.2.2 Total N and P

For the determination of total nitrogen (TN) and total phosphorus (TP), 50 ml of sample were added to 5 ml of a basic persulfate mixture in a borosilicate vial. The concentrations of N and P were measured with the autoanalyzer after digestion at 120 °C for 30 min., using the adjustments proposed by Valderrama, 1981 to the original methods by Koroleff (1976 a, b).

2.2.3 Particulate N and P

For the determination of particulate N and P, the protocol described by Pujo-Pay and Raimbault, 1994 was followed. The seawater (100-300ml) was filtered on precombusted (450 °C for 4 h) GF/F glass fibre filters. The filters were rinsed in HCl (10%) and cleaned with deionized water (DIW) immediately before the filtration. Samples were stored at -20°C until the analyses were performed.

The filters were placed in borosilicate vials, adding 20ml of DIW and 2.5ml of oxidizing mixture and then autoclaved (120 °C for 30 min). After the digestion, PN and PP were determined as NO₃ and PO₄, respectively.

2.2.4 Organic N and P

The total organic N and P (TON and TOP) were calculated as:

TON=TN-DIN and TOP=TP-PO₄.

The dissolved organic N and P (DON and DOP) were calculated as :

DON=TON-PN and PON=DOP-PO₄.

As the DON and DOP concentrations were determined combining three different analytical procedures, their accuracy might be differently affected by the errors in each of the analytical procedures. However, this is the only possible way to get an estimate of DON and DOP, as a direct measurement still does not exist.

2.2.5 Chlorophyll a (Chl a)

For the determination of Chlorophyll *a*, sea water samples were filtered on Whatman glass-fibre filters (GF/F, Ø 25mm). The filters were immediately stored in liquid nitrogen until analysis. In the laboratory, the samples were extracted in 90% neutralized acetone, and analyzed utilizing a Spex Fluoromax spectrofluorometer up to 2006, and starting from 2007, utilizing a SHIMADZU (mod. RF-5301PC) spectrofluorometer. The analytical procedure followed was proposed by Holm-Hansen et al., 1965. The instrument was calibrated daily with a solution of pure chlorophyll *a*, extracted from *Anacystis nidulans* (Sigma).

Total carbon biomass of phytoplankton cells was estimated using a Carbon to Chl *a* ratio of 50 (Fuhrman et al., 1989).

2.2.6 Heterotrophic bacteria abundance

Bacterial have been counted by flow cytometry using standard methods (Marie et al., 1997). Data have been kindly provided by Cecilia Balestra and Raffaella Casotti of the Stazione Zoologica A. Dohrn. Samples were fixed with a mix of glutaraldehyde 0.05 % and paraformaldehyde 1 % (final concentration), frozen in liquid nitrogen and stored at – 80 until analysis. The flow cytometer used is a Becton-Dickinson FACScalibur with standard filters and Ar laser at 488 nm.

Bacterial cell numbers were converted to carbon (pg C l⁻¹) using the factor of 20 fg C per bacterium (Campbell et al., 1994).

2.2.7 Enzymatic activity

Hydrolytic enzyme activities were measured with fluorogenic analogs of natural substrates (Hoppe, 1993) derived from 7-amino-methyl-coumarin (AMC) and 4-methyl-umbelliferone (MUF). Aminopeptidase activity (AMA) was assayed as the hydrolysis rate of L-leucine-AMC, while alkaline phosphatase (APA) was assayed using MUF derivatives. Enzyme activities measured using fluorogenic substrates were expressed in terms of rate of MUF or AMC production.

Hydrolysis rates were measured (after evaluation of saturating concentrations) by incubating 2.5 ml subsamples with 200 µM (final concentration) leucine-AMC substrates and 50 µM (final

concentration) MUF-phosphate for 1 h, at *in situ* temperature in the dark. The fluorescence released by enzymatic cleavage of the artificial substrates was measured fluorometrically, in triplicate, at 380 / 365 nm excitation and 440 / 455 nm emission for AMC/MUF substrates using SHIMADZU (mod. RF-5301PC) spectrofluorometer. Standard solutions of MUF and AMC were used to calibrate the fluorometer.

2.3 Statistical analyses

2.3.1 Principal component analysis

The principal component analysis (PCA) is an ordination method aimed to represent the data in a reduced space. PCA realizes a rigid rotation of the original system of coordinates, so that the new axes (called principal components) are orthogonal to one another and correspond to the directions along which the maximum variance of the data is found. Principal Components are generally sorted as a function of the percentage of variance of the original data they explain, and a small number of components is generally sufficient to explain the major part of the variance (generally much smaller than the number of samples in the dataset) Each principal component is actually a linear combination of the original variables and the original data can thus be obtained as linear combinations of the principal components.

In this study PCA, based on correlation matrix, have been performed using STATISTICA 6.0 package.

2.3.2 Box plot

In descriptive statistics, a box plot (also known as a box-and-whisker diagram or plot) is a way of graphically depicting groups of numerical data through their five-number summaries:

- the 25th percentile (Q1), which correspond to the bottom of the box
- the median (Q2), bold band inside the box
- the 75th percentile (Q3), the top of the box
- $Q1 - 1.5 * (Q3 - Q1)$, the bottom of the whisker
- $Q3 + 1.5 * (Q3 - Q1)$, the top of the whisker

The distance $Q3 - Q1$ is also called interquartile range (IQR). Any data not included between the whiskers is plotted as an outlier, with a small circle.

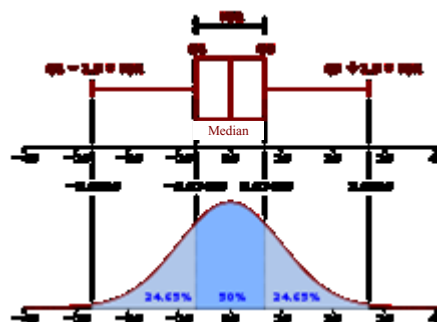


Fig. 2.1 - Boxplot and a probability density function of a Normal $N(0,1\sigma^2)$ Population

The R environment was used to graph the box plot.

2.3.3 Time-series decomposition

The package 'wq' (water quality), developed by James E. Cloern and Jassby, 2010, has been used for the analyses of the time-series. More in details, the function **decompTs** allows the decomposition of a monthly time series by a multiplicative seasonal model:

$$c_{ij} = Cy_i m_j \epsilon_{ij} \quad (2.2),$$

where c_{ij} is the concentration in year i and month j ; C is the long-term mean; y_i is the annual effect; m_j is the average seasonal (in this case monthly) effect; and ϵ_{ij} is the residual series, which is called "events".

The annual effect is simply the annual mean

$$Y_i = (1/12) \sum_{j=1}^{12} c_{ij} \quad (2.3)$$

divided by the long term mean

$$y_i = Y_i / C \quad (2.4).$$

The average monthly effect is given by

$$m_j = (1/N) \sum_{i=1}^N M_{ij} / Y_i \quad (2.5)$$

Where M_{ij} is the value of month j in the year i and N is the total number of years.

The events component is obtained by:

$$\epsilon_{ij} = c_{ij} / Cy_i m_j \quad (2.6)$$

Patterns that are highly variable from year to year will result in an average seasonal pattern of relatively low amplitude (i.e., low range of monthly values) compared to the amplitudes in individual years. An average seasonal pattern with high amplitude therefore indicates both high amplitude and a recurring pattern for individual years.

2.3.4 Multivariate multiple regression

To test the relationships between the different variables measured in the water column multivariate multiple regression analyses using the DISTLM forward procedure included in the PRIMER 6+ package. In particular, the following tests were carried out:

- variance in the inorganic nutrient pool composition as explained by all other variables;
- variance in the particulate organic pool composition as explained by all other variables;
- variance in the dissolved organic pool composition as explained by all other variables.

Chapter 3: Surface N and P dynamics along the Campania coast (2001-2006)

3.1 Specific aims of the chapter

The aim of this chapter is to investigate the Nitrogen (N) and Phosphorus (P) dynamics in the coastal waters of Campania region. The work is based on the dataset collected in the framework of the Italian Coastal Ecosystem Monitoring Project SiDiMar (Sistema Difesa Mare) and represents a first attempt to classify the different Campania coastal waters from their chemical and physical properties, discussing the different trophic regimes as identified by nutrient concentration ratios and variability. More in details, the vertical profiles of temperature and salinity, as well as the N and P surface distribution (in the total, dissolved inorganic and total organic pools) and their relative ratios have been analysed to:

- characterize the different investigated sites on the base of their physical and chemical properties and characteristic patterns;
- elucidate the mechanisms that drive N and P dynamics in coastal waters;
- discern common pattern in N and P seasonality;
- compare our results with other coastal sites.

3.2 Study Area

3.2.1 Campania Region

The Campania region is located on the eastern side of the Central Tyrrhenian Sea and has a coastline of 450Km. The coast is composed by four main embayments (Gulf of Gaeta, Naples, Salerno and Policastro) that differ for their morphological structures and social–economic coastal development, which determine complex hydrographic and biological conditions. All the four gulfs are basically characterized by the general cyclonic circulation of the Tyrrhenian Sea (from South-East to North-West). However, a recent study (Rio et al., 2007) has highlighted the presence of an anticyclonic recirculation cell located off Naples (centered at 14°E; 40.5°N) in the mean surface currents. Moreover, Rinaldi et al., 2010, have highlighted that sub-basin and mesoscale variability has a major impact on the surface circulation in the whole central-southern Tyrrhenian Sea, involving significantly higher levels of kinetic energy with respect to the mean circulation. They thus suggest that the cyclonic circulation is very often overcome by mesoscale instabilities along the Campania coasts. The northern part of Campania coasts (comprising the Gulf of Gaeta and Naples) is more densely populated, especially in the area surrounding the city of Naples, and is characterized by a high anthropogenic load of urban, industrial and agricultural origin. In addition, the Volturno River (the largest in Campania) and the Sarno River (the most polluted river in Europe) have a very strong impact on the ecosystems of the two gulfs. On the contrary, the southern part (Gulf of Salerno and of Policastro) is less populated, and includes protected and pristine areas; the only relevant freshwater input is the Sele River, that is rapidly diluted in the Tyrrhenian waters.

Several biological studies were carried out ever since the second half of the 19th century in the Gulf of Naples, but only from the '80s more detailed investigations have been conducted on the

interactions between physical, chemical and biological properties (Carrada et al., 1980, Carrada et al., 1981; A. Zingone et al., 1990, Casotti et al., 2000, Ribera d'Alcalà et al., 1989). Moreover, a coastal station located two nautical miles offshore the city of Naples has been sampled since 1984 (Scotto di Carlo et al., 1985; Ribera d'Alcalà et al., 2004). On the other hand, information on the Gulf of Salerno is very sparse and only related to occasional sampling (Marino et al., 1984) and, to the best of our knowledge, there is no information at all covering the Gulf of Gaeta (GoG).

The previous studies highlighted some differences between the Gulf of Naples (GoN) and the Gulf of Salerno (GoS). The Gulf of Naples displays pronounced gradients in hydrographical and biological parameters from the coast to the open sea, with a very evident spatial variability, mainly related to the presence of several terrestrial inputs. The phytoplankton assemblage is diatom-dominated in the GoN while dinoflagellates and small flagellates predominate in the GoS. Finally, the boundary between inshore and offshore waters is very different. In the GoN, coastal waters extend approximately to the 100m isobath in summer, but extend over greater areas during the rest of the year. In contrast, in the GoS, coastal waters are generally restricted to nearshore areas and very often offshore waters almost reach the coast line.

3.2.2 Sampling Strategy

This study was conducted in the framework of the Italian Coastal Ecosystem Monitoring Project SiDiMar (Sistema Difesa Mare). Seven sites were sampled biweekly from June 2001 till December 2006 on board of R/V Vettoria (Fig. 3.1). For each monitored site, three stations were sampled along a transect extending from 100m off the coastline to a maximum of 3 km offshore (coastal, mid-transect and outer stations). The bathymetry ranged from 6 to 7 m at the coastal stations, from 10 to 36m at mid-transect stations, and from 15 to 50m in the outer stations.

One site was located in the Gulf of Gaeta, at Volturno River mouth (Foce Volturno, FV). Three sites were located in the GoN, in correspondence of the densely populated areas of Naples (NA) and Portici (PO) and off the Sarno River mouth (Foce Sarno, FS). Other three sites were located in the GoS, one off the Picentino River mouth (Foce Picentino, FP) and two sites in the southernmost area of the GoS, in front of the 'Cilento e Valle di Diano' national park (Punta Tresino, PT and Punta Licosa, PL). Due to the pristine conditions of the area, the PL stations represented the 'control stations' (blanks) of the Campania Region in the SiDiMar Project.

The position and the characteristics of the sampling stations are reported in Tab. III.1.

At each station, temperature and salinity profiles were acquired (CTD probe), and samples for inorganic nutrients and total nitrogen and total phosphorus determination were collected at the surface (-0.5m). The detailed analytical procedures are reported in the 'material and methods' (Chapter 2).



Fig. 3.1 - Si.Di.Mar Project Sampling stations (2001-2006).

Tab. III.1 - Coordinates and characteristics of all the sampling stations.

Transect name	Station Code	Distance from the coast (m)	Depth (m)	Lat. N	Long. E	Area's characteristics
Foce Volturno	FV1	500	7	41° 01' 00"	13° 54' 45"	River Mouth (large)
	FV2	1000	10	41° 00' 50"	13° 54' 27"	
	FV3	3000	15	41° 00' 13"	13° 53' 23"	
Napoli	NA4	100	6	40° 49' 43"	14° 14' 35"	Densely populated
	NA5	800	30	40° 49' 22"	14° 14' 38"	
	NA6	1480	50	40° 48' 59"	14° 14' 40"	
Portici	PO7	200	7	40° 49' 02"	14° 19' 28"	Densely populated
	PO8	750	18	40° 48' 46"	14° 19' 14"	
	PO9	1300	50	40° 48' 31"	14° 19' 01"	
Foce Sarno	FS10	200	6	40° 43' 35"	14° 28' 11"	River Mouth (polluted)
	FS11	1000	18	40° 43' 24"	14° 27' 41"	
	FS12	3000	48	40° 42' 57"	14° 26' 25"	
Foce Picentino	FP13	500	7	40° 36' 51"	14° 50' 40"	River Mouth (small)
	FP14	1000	11	40° 36' 43"	14° 50' 19"	
	FP15	3000	27	40° 36' 29"	14° 49' 01"	
Punta Tresino	PT16	100	6	40° 19' 12"	14° 56' 18"	Pristine
	PT17	1000	36	40° 19' 29"	14° 55' 47"	
	PT19	1850	50	40° 20' 07"	14° 55' 17"	
Punta Licosa	PL19	100	6	40° 15' 19"	14° 54' 19"	Pristine (blank)
	PL20	800	26	40° 15' 42"	14° 54' 12"	
	PL21	1360	50	40° 16' 05"	14° 54' 10"	

3.3 Results

3.3.1 Hydrological features

In this section the temperature and salinity profiles have been analysed in order to characterize the different environments on the base of their hydrological features and to discern common spatial and temporal patterns.

To investigate the temporal variability of temperature and salinity over the whole water column, contour plots of this two parameters have been reported for the outermost stations of each transect. In order to characterize the interannual variability, the minimum and maximum temperature and salinity at the surface and as mean values (from the surface to the bottom) have been reported for the coastal and outermost stations for each transect.

Finally, in order to characterize the seasonal signals at monthly scale, box plots of temperature values and of salinity anomalies have been reported for the surface and for the mean values over the whole water column.

3.3.1.1 Temperature

Temperature ranged between 10.63 (09/03/2005) and 29.30 °C (18/08/2003), recorded at the surface at station FV1 and at -1.5m depth at station FS10, respectively. The lowest temperatures were recorded in the years 2005 and 2006. Minimum and maximum temperature values integrated over the whole water column and at the surface of the coastal and outermost stations for each

transect are reported in Table III.2. The highest values of surface temperature were observed in summer 2003 in all the seven sites.

Temperature variations have a significant effect on the stratification of the water column, thus influencing the vertical transport and mixing processes. However, in the shallow stations, the sampled layer displays very little vertical differences in all seasons. Consequently, we have analyzed the temporal variability of the temperature over the entire water column only at the outermost stations of each transect (Fig. 3.2). Temperature showed the typical seasonal cycle of the temperate areas with four main conditions: 1) homotherm water column during winter, with recurrent events of mixing; 2) gradual thermal stratification during spring; 3) strong thermocline in summer; 4) progressive destratification/mixing in autumn.

The largest oscillations between summer and winter temperatures were recorded near the rivers, in particular in proximity of the Volturno, due both to the large outflow of the river and to the shallowness of the water column. The same interannual variability was recognized at all the sampling sites: a progressive decrease in winter temperatures was observed starting from 2002 till winter 2006. The mean temperatures of the water column in the period January – March exhibited about 1°C of difference between 2002 and 2006.

In summer 2003 the difference between the surface and the mean temperature of the water column in the outermost stations was more pronounced than in the other years of the study, because the rapid warm-up affected only the surface layers. On the contrary, during summer 2006, the highest values of the mean temperatures were recorded in the deepest stations (Tab. III.2) (eg. more than 23°C in the GoS), even if the surface temperatures were lower than those observed in 2003.

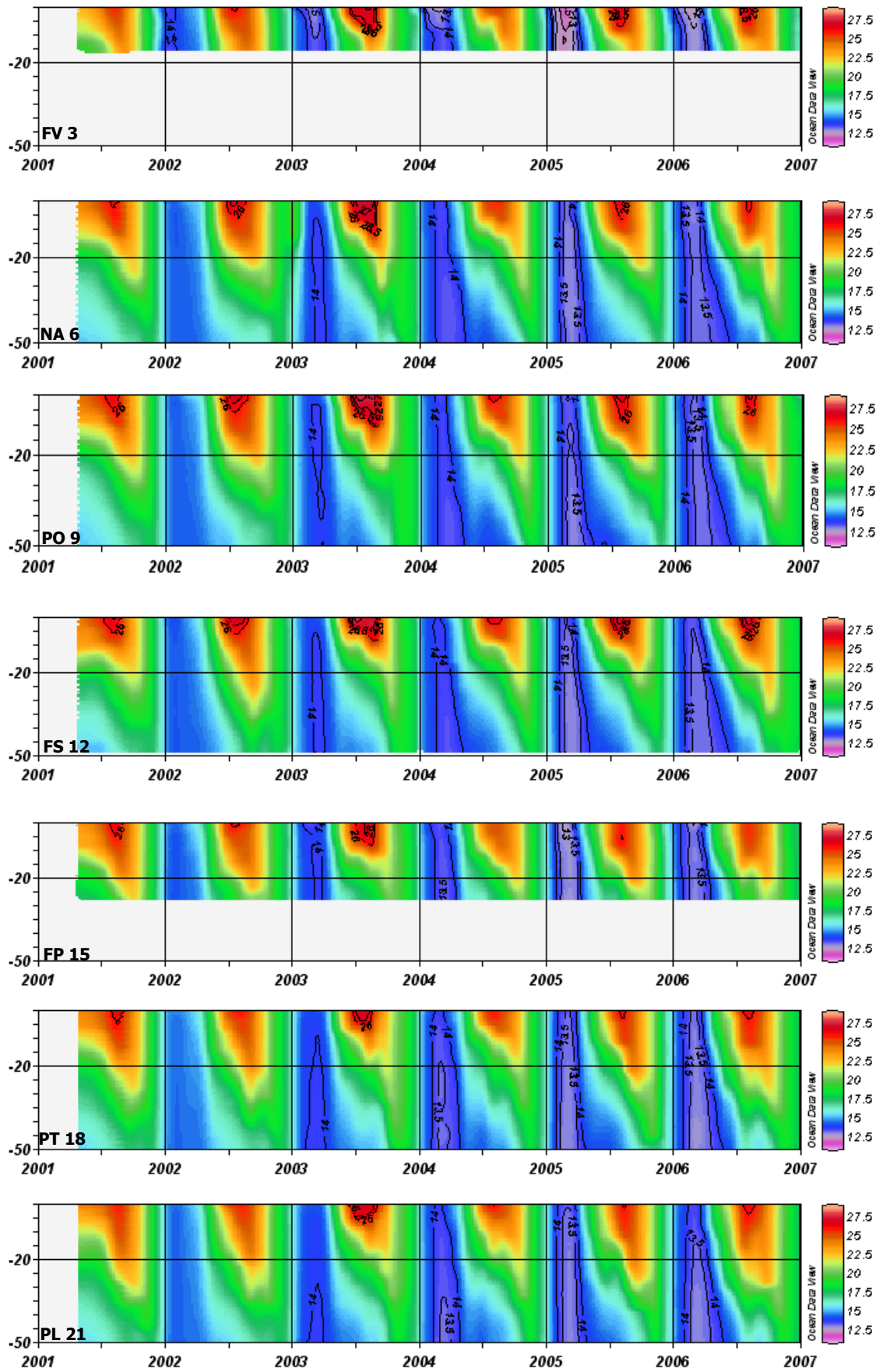


Fig. 3.2 - Contour plot of temperature (°C) at the outer stations of each transect

Tab. III.2- Yearly minimum and maximum temperatures at surface and as mean values (surface-bottom) of the coastal and outer stations of each transect.

Surface temperature		FV1	FV3	NA4	NA6	PO7	PO9	FS10	FS12	FP13	FP15	PT16	PT18	PL19	PL21
min	2002	12.98	13.51	14.04	14.38	14.15	14.16	14.18	13.70	13.95	14.40	14.38	14.59	14.44	14.30
	2003	12.50	12.62	13.78	13.89	14.02	13.60	13.83	13.70	13.41	12.76	13.52	13.76	13.64	14.02
	2004	11.36	11.87	13.37	13.00	13.32	13.27	13.75	13.50	12.80	13.04	12.59	13.43	13.27	13.51
	2005	10.63	10.96	12.40	12.59	13.07	12.90	13.09	12.82	12.60	12.35	12.77	12.74	12.97	13.02
	2006	11.47	12.24	13.16	13.08	13.11	13.15	12.80	12.72	11.49	12.30	12.99	12.90	13.08	13.25
	max	2001	26.45	27.00	27.57	27.45	28.70	27.70	28.30	27.75	27.68	27.61	27.73	27.63	26.75
2002		26.38	26.43	27.39	27.63	27.93	27.54	27.80	27.85	28.00	27.86	27.22	26.97	26.12	26.23
2003		29.08	28.76	28.48	28.39	28.74	28.91	29.23	29.17	27.71	27.62	28.22	28.12	28.14	28.23
2004		26.22	26.57	26.53	26.72	27.31	27.13	28.03	27.59	26.06	25.49	26.51	26.18	26.93	26.90
2005		27.97	28.38	27.69	27.69	28.55	28.81	28.15	29.22	27.58	27.46	27.62	27.49	27.56	27.50
2006		27.64	27.56	27.17	26.81	28.81	27.66	27.94	27.78	26.02	26.30	27.27	27.20	27.12	27.04
Mean temperature															
min	2002	13.25	13.72	14.14	14.34	14.22	14.38	14.24	14.16	14.01	14.25	14.29	14.46	14.38	14.31
	2003	12.87	12.70	13.67	13.75	13.93	13.84	13.73	13.76	13.47	13.71	13.54	13.81	13.64	13.84
	2004	12.78	13.13	13.37	13.35	13.36	13.40	13.75	13.43	12.91	13.15	12.55	13.15	13.24	13.32
	2005	11.55	11.72	12.40	12.82	13.07	13.01	13.07	12.88	12.70	12.91	12.74	12.92	12.91	12.99
	2006	12.43	12.73	13.23	13.06	13.12	13.24	12.97	13.25	11.58	13.02	12.99	12.93	13.08	13.12
	max	2001	24.99	25.77	27.30	21.48	27.91	21.58	28.14	21.78	27.36	25.49	27.49	22.35	26.60
2002		26.09	25.29	27.13	21.50	26.86	21.69	27.49	23.46	26.55	24.53	27.21	23.20	25.94	22.92
2003		28.15	27.12	28.32	21.58	28.33	21.33	28.53	21.34	27.67	23.89	28.09	21.00	27.87	20.97
2004		25.23	24.77	26.33	21.22	26.50	21.54	27.04	21.49	25.87	23.40	25.99	20.91	26.00	20.96
2005		27.62	25.99	27.41	20.87	28.36	20.87	26.87	21.20	27.46	24.18	27.60	22.19	27.51	22.50
2006		26.63	25.56	26.99	21.91	27.26	22.02	27.14	22.23	25.88	24.04	26.62	23.20	26.87	23.25

In order to characterize this seasonality, 'climatological' statistics have been computed on monthly bins considering all surface values recorded at all stations. The surface temperature displays a clear seasonal pattern (Fig 3.3). A decrease of surface temperature is generally observed from the start of the year up to the first part of March, when the lowest median value is reached. Thus, February and March are the colder months. Temperature increases from March up to July-August, when the highest values are observed. A new decrease until the end of the year is observed.

To investigate the integrated effect of the seasonality on the water column properties in the outer stations of each transect, we have also analyzed the mean temperature from the surface to the bottom (Fig 3.4). The mean temperatures clearly exhibit a lower variability compared to the surface values. The lowest values are still recorded in March. Afterward, a more gradual increase is observed compared to surface values, leading to a maximum of ~20°C in September. Starting from September the mean temperature starts decreasing again.

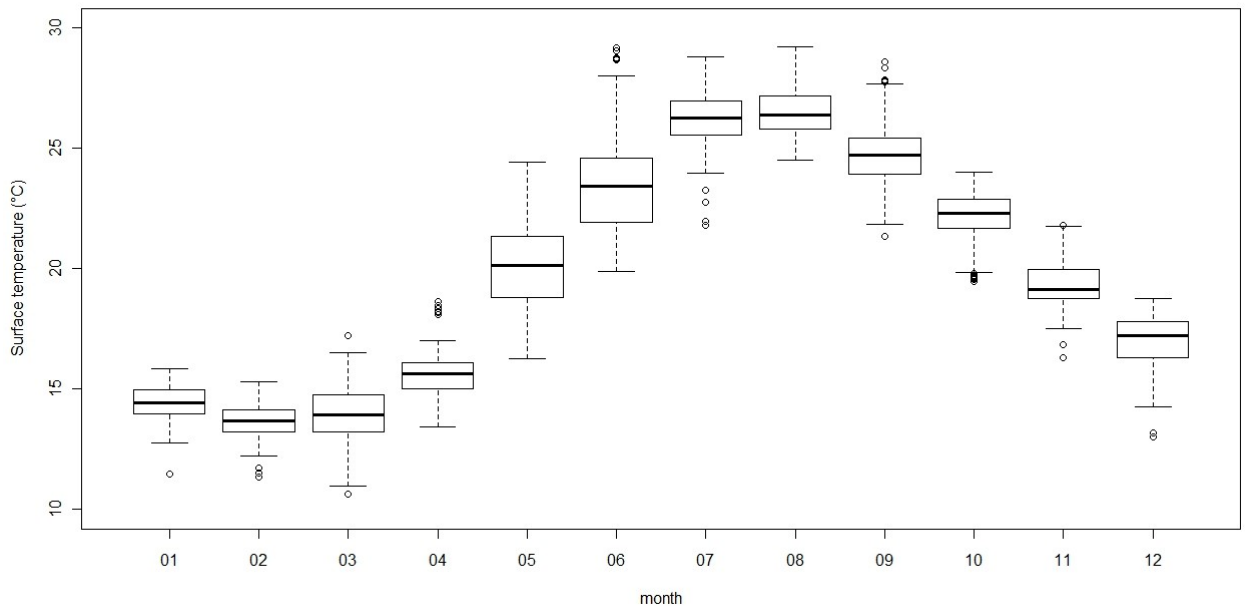


Fig. 3.3 - Seasonal cycle of surface temperature for all the sampling stations (box-plot by month).

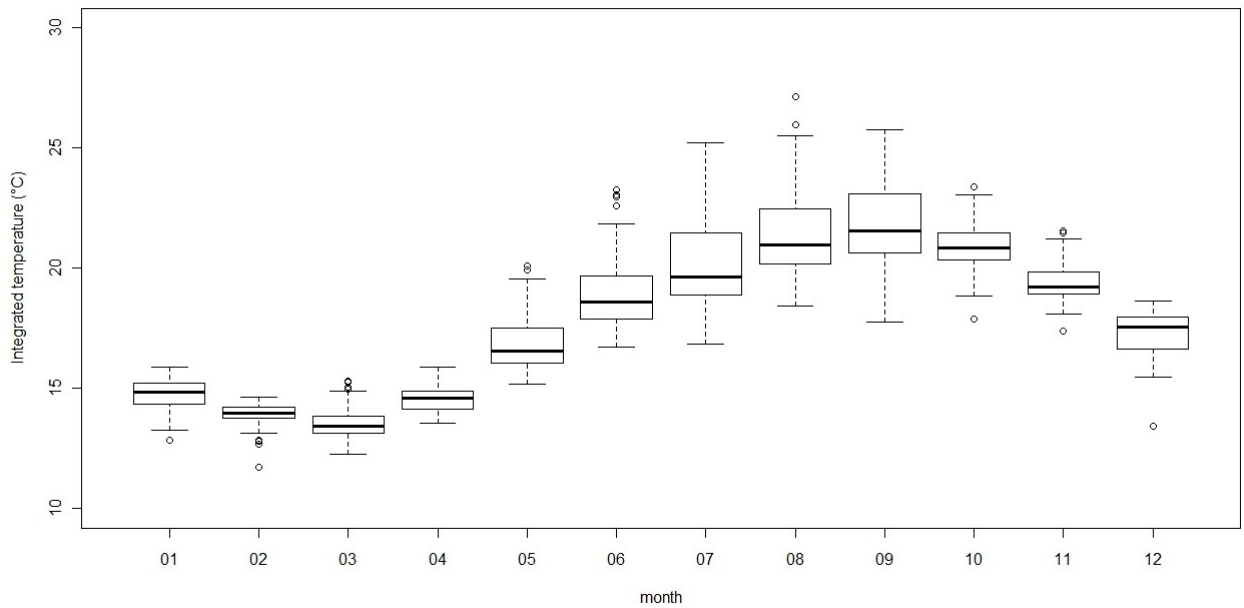


Fig. 3.4 - Seasonal cycle of mean temperature (surface-bottom) for the outer stations of each transect (box-plot by month).

3.3.1.2 Salinity

The salinity exhibited values in the range 18.23 – 38.49, recorded at FS10 at surface (29/05/2006) and at FV3 at -10m depth (05/09/2005), respectively. While temperature variability is mostly due to seasonality, salinity variations are mainly related to the different freshwater inputs in each sampling site.

The lowest salinities were clearly found near the river mouths, notably in proximity of the Sarno River, while the stations located in the southern part of the region (PT and PL) were less affected by terrestrial inputs and displayed values always greater than 37 (Fig. 3.5). Only in one case (26/03/2004), extremely low salinities (up 34.76) were observed off Punta Tresino, in the first 4 m of the water column. This anomaly was even more pronounced in the outermost station (PT18).

Notwithstanding the strong influence of the terrestrial inputs, the same interannual variability was detected at all the outermost stations. A decrease in salt content from 2001 till spring 2004 and a new increase from 2004 up to the end of 2006 were recorded. In fact, values higher than 38.0 were never recorded from May 2003 till September 2004, while salinities higher than 38.2 were observed in autumn 2006 in all the gulfs (Fig. 3.5, Tab. III.3).

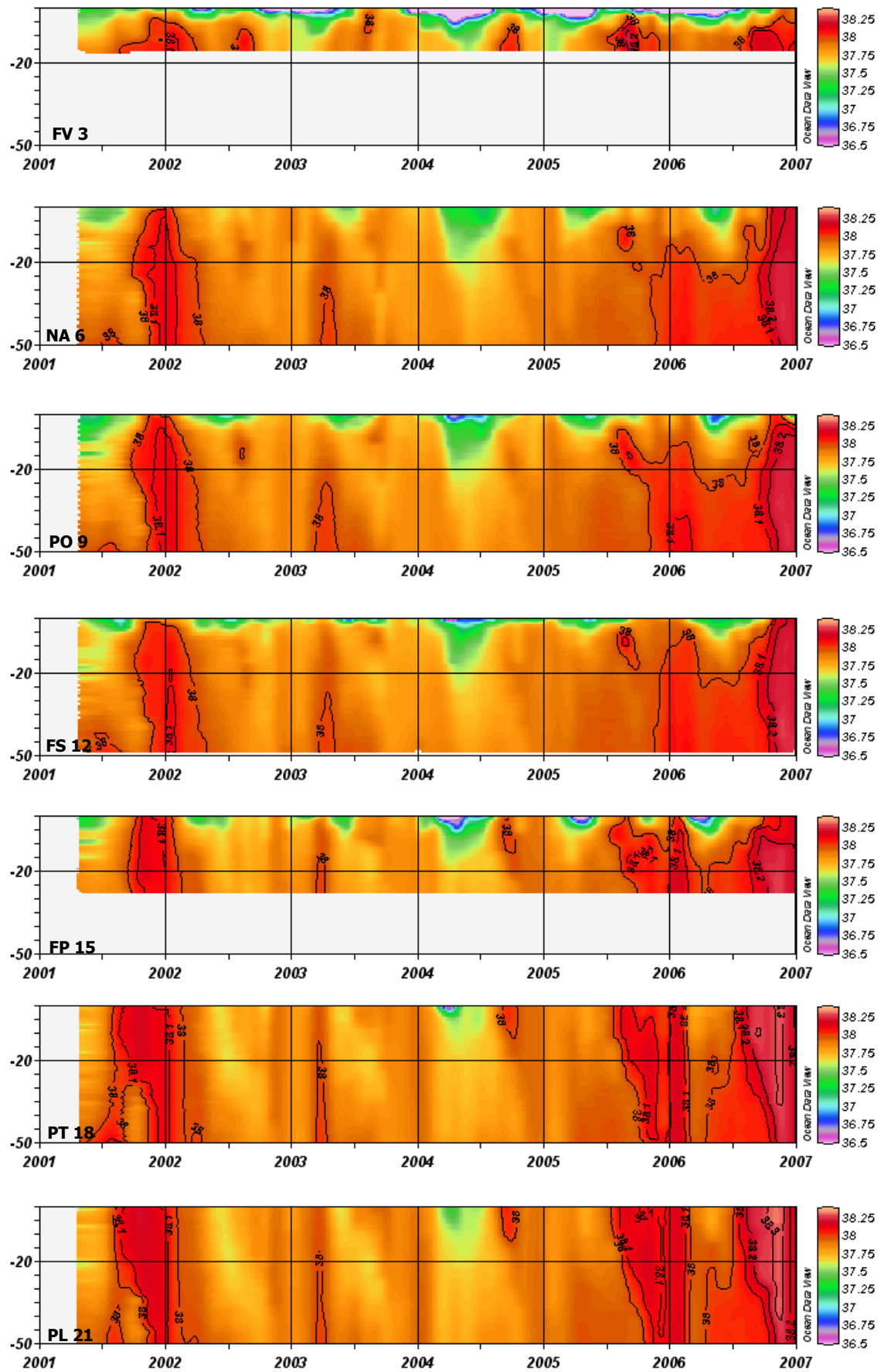


Fig. 3.5 - Contour plot of salinity at the outer stations of each transect.

Tab. III.3- Yearly minimum and maximum salinities at surface and as mean values (surface-bottom) of the coastal and outer stations of each transect.

Surface salinity		FV1	FV3	NA4	NA6	PO7	PO9	FS10	FS12	FP13	FP15	PT16	PT18	PL19	PL21
min	2001	34.60	36.82	36.57	37.06	35.24	36.97	23.03	36.00	36.94	37.22	37.72	37.59	37.73	37.60
	2002	34.18	35.68	37.05	37.48	35.74	36.97	24.53	36.80	34.53	37.20	37.67	37.43	37.56	37.61
	2003	30.80	34.38	37.09	37.38	36.43	36.85	21.61	36.08	36.90	36.55	37.67	37.61	37.61	37.57
	2004	25.82	25.46	36.87	37.04	36.61	36.30	27.56	35.89	35.19	34.38	36.72	34.76	37.36	37.06
	2005	29.72	32.94	36.76	36.89	36.44	36.56	28.29	36.47	34.51	35.71	37.75	37.65	37.68	37.70
	2006	27.81	32.17	36.79	36.98	36.31	36.72	18.23	36.93	30.07	36.12	37.60	37.71	37.67	37.62
max	2001	37.72	37.91	38.06	38.08	38.04	38.12	37.84	38.05	38.12	38.20	38.23	38.26	38.25	38.25
	2002	37.67	37.89	38.07	38.12	38.02	38.05	37.82	38.10	37.93	38.17	38.18	38.17	38.18	38.17
	2003	37.76	37.99	37.87	38.03	37.88	37.92	37.76	37.95	37.98	38.02	38.05	38.03	38.04	38.03
	2004	37.35	37.73	37.90	37.89	37.77	37.84	37.22	37.89	37.80	38.06	38.11	38.12	38.10	38.13
	2005	37.79	37.86	38.06	38.14	38.02	38.07	37.58	38.05	37.98	38.23	38.22	38.19	38.22	38.21
	2006	37.92	38.08	38.22	38.22	38.13	38.26	37.87	38.26	38.18	38.27	38.38	38.37	38.40	38.37
Mean salinity															
min	2001	36.24	37.43	37.15	37.65	36.52	37.61	34.82	37.73	37.16	37.51	37.77	37.75	37.77	37.70
	2002	36.98	37.43	37.28	37.80	37.08	38.12	35.24	37.72	36.72	37.55	37.66	37.70	37.60	37.72
	2003	35.79	37.13	37.09	37.75	37.20	37.75	34.61	37.77	37.44	37.62	37.68	37.71	37.63	37.71
	2004	35.65	36.30	36.94	37.57	36.73	37.53	34.91	37.51	36.30	37.29	37.09	37.55	37.39	37.57
	2005	35.79	36.91	37.05	37.72	36.80	37.79	35.91	37.77	36.90	37.45	37.76	37.77	37.71	37.74
	2006	35.85	37.17	37.06	37.77	36.67	37.80	32.33	37.88	34.29	37.54	37.71	37.89	37.66	37.93
max	2001	37.92	38.10	38.08	38.12	38.08	38.12	38.03	38.08	38.13	38.19	38.24	38.13	38.25	38.18
	2002	38.01	38.03	38.08	38.15	38.09	38.14	38.01	38.12	37.99	38.15	38.18	38.17	38.18	38.17
	2003	37.95	38.08	37.88	37.97	37.90	37.97	37.83	38.01	38.01	38.04	38.03	38.04	38.03	38.03
	2004	37.83	37.95	37.90	37.92	37.84	37.88	37.65	37.92	37.97	38.01	38.11	37.96	38.10	37.97
	2005	37.88	38.24	38.08	38.05	38.01	38.07	37.98	38.00	38.03	38.08	38.22	38.20	38.21	38.21
	2006	38.11	38.15	38.24	38.26	38.19	38.28	38.08	38.29	38.22	38.31	38.38	38.35	38.40	38.37

Similarly, a more pronounced seasonal signal could be evidenced only looking at the anomalies in the salt content in the outermost stations and separating the transects off the river mouths (FV3, FS12, FP15) from the others. The salinity anomalies were calculated as the difference between the single observation and the average value over the sampling period at the corresponding station. In order to characterize this seasonality, 'climatological' statistics have been computed on monthly bins that are displayed in figures 3.6 and 3.7. The stations located in proximity of the rivers showed a larger variability compared to the other stations, and some differences in the seasonal signal. Surface salinities displayed the lowest values in March-April near the river mouths and in May-July at the other stations. The same shift was observed in the anomaly of the mean salinity: the lowest values in salt content were observed in April near the rivers and later (May-June) at the other sampling sites (Fig. 3.6, 3.7).

The highest salinities (surface and mean values) were recorded in autumn-winter at all the stations.

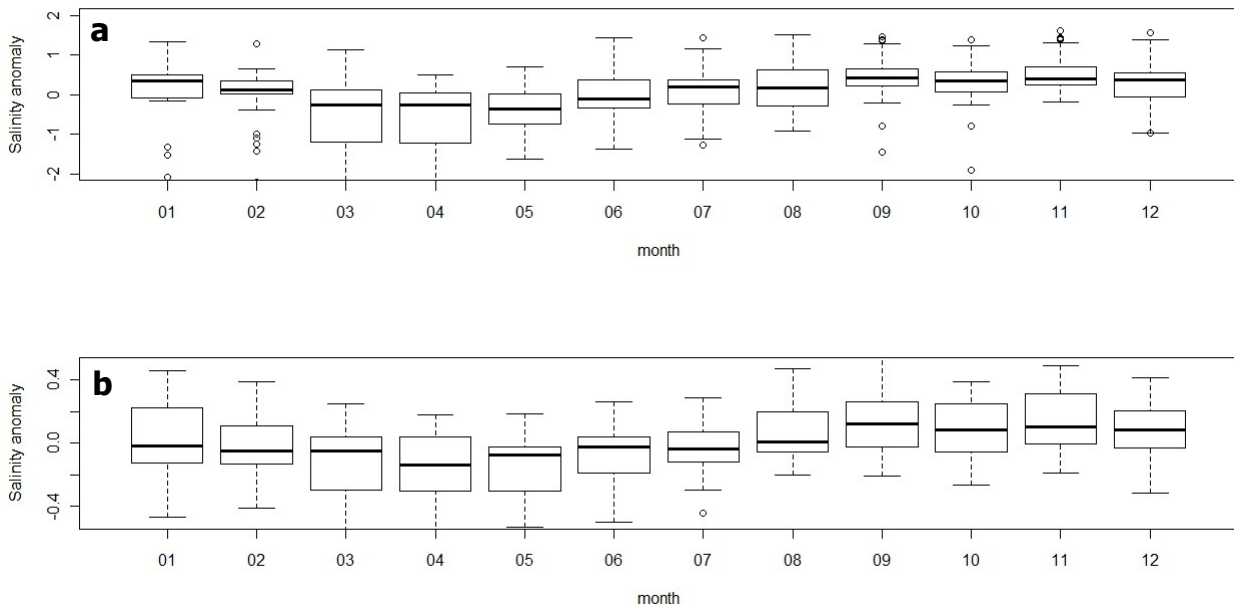


Fig. 3.6 – Seasonal cycle of (a) surface and (b) mean (surface -bottom) salinity anomalies at the outer stations off the river mouths (FV3, FS12, FP15), box-plot by month.

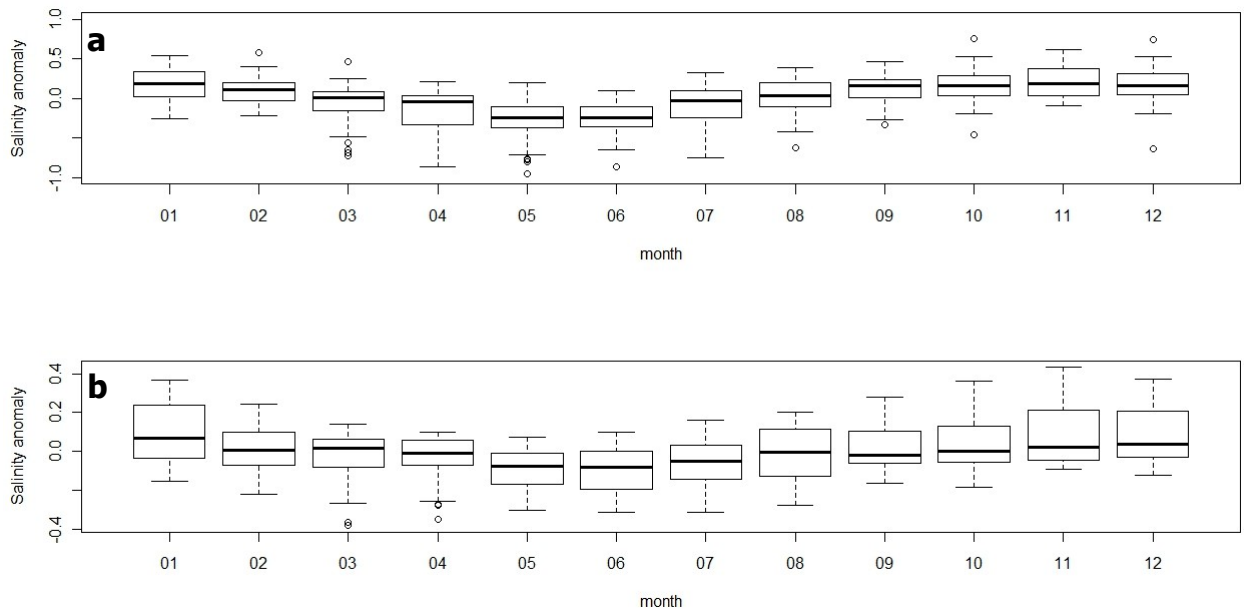


Fig. 3.7 – Seasonal cycle of (a) surface and (b) mean (surface -bottom) salinity anomalies at the outer stations not influenced by the river mouths (NA6, PO9, PT18, PL21), box-plot by month.

3.3.2 Nutrients

The variability and distribution of Nitrogen (N), Phosphorus (P) and the N/P ratio, in the total, dissolved inorganic and total organic pools, have been investigated at different temporal scales. First, we investigated the climatological mean concentration (and associated standard deviation), looking at the spatial distribution only, to describe the typical conditions along the Campania coasts. Successively, we focused on yearly means (and associated standard deviations), to evidence interannual variations and eventual anomalous years. Finally, in order to investigate the seasonal signals and the mechanisms driving the variations in the N/P ratio at seasonal scale, we computed the monthly anomalies with respect to the climatological averages at each station, looking also at main components of the dissolved inorganic nitrogen (DIN). However, as significant differences are observed at the different sites, not only in terms of mean concentrations but also in terms of associated variability, in order to evidence eventual differences in the seasonal signal phase, we also normalized the anomalies dividing them by the associated standard deviation. The results are detailed in the following sections.

3.3.2.1 Nitrogen

The total nitrogen (TN) concentrations displayed a noticeable variability and ranged from 373.36 mmol m^{-3} (11/03/2003) and 3.03 mmol m^{-3} (05/09/2003), recorded at FS10 and PT16, respectively. The highest values are found in proximity of the Volturno and Sarno rivers and the lowest in the pristine areas of PL and PT (Fig. 3.8). A pronounced coast-offshore gradient is present at all the sampling sites, except in the southernmost area (PT and PL), characterized by similar values of TN.

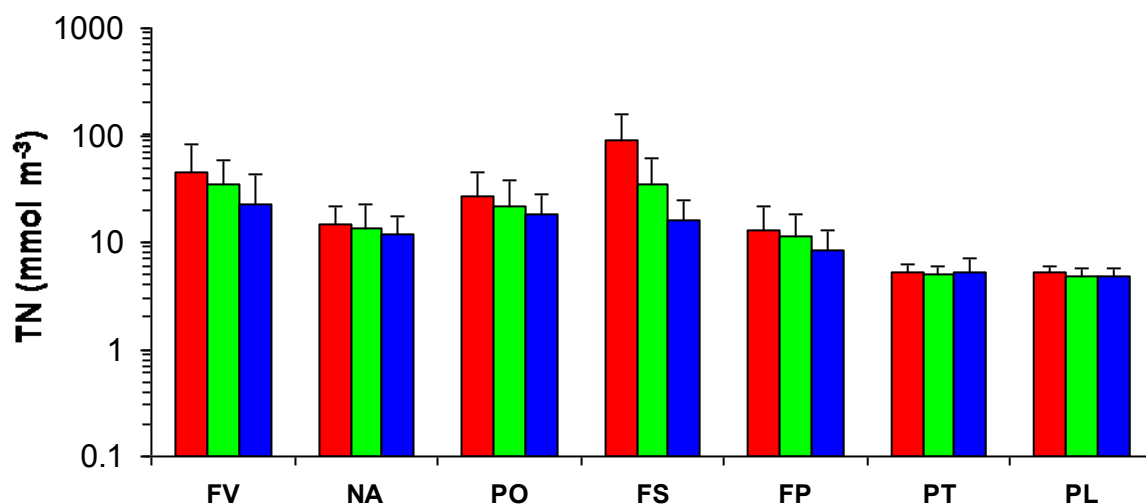


Fig. 3.8 - Averaged concentration (2002-2006) and standard deviation of TN (log scale) at each sampling site (■ coastal, ■ mid-transect and ■ outer stations).

The yearly averaged values of TN do not display a significant interannual variability, except near the Volturno River (Tab. III.4). Starting from 2004, higher values of TN were observed at the FV stations, compared to those recorded in the years 2002-2003.

Tab. III.4 - Yearly averaged values of TN (mmol m^{-3}) and standard deviations at each sampling station.

Transect	Station	2002	2003	2004	2005	2006
FV	coastal	29.18±18.64	33.76±33.68	56.70±45.68	49.36±32.72	56.00±35.62
	mid-transect	21.78±9.54	29.68±23.81	41.34±32.70	41.47±22.42	38.33±21.50
	outer	16.69±6.49	20.87±16.44	25.36±22.45	28.09±26.35	24.26±17.95
NA	coastal	13.31±6.07	15.35±6.99	14.17±5.45	14.99±7.41	15.88±8.69
	mid-transect	11.91±6.65	13.65±5.13	12.48±5.68	17.51±16.07	12.41±4.87
	outer	11.20±4.55	12.44±5.16	11.94±5.18	13.29±7.10	11.73±3.63
PO	coastal	26.22±15.18	29.76±17.45	29.66±24.32	25.70±12.29	23.83±15.92
	mid-transect	24.78±14.96	20.41±12.47	19.58±15.47	21.83±12.88	24.11±22.14
	outer	18.32±8.80	17.04±8.75	17.92±7.56	19.60±9.76	19.27±12.22
FS	coastal	83.26±57.50	83.19±80.97	74.47±64.43	89.33±60.15	112.53±63.26
	mid-transect	29.94±25.64	28.32±17.07	42.71±30.41	35.72±25.12	37.44±31.15
	outer	15.37±5.99	15.23±7.55	18.75±11.83	16.39±9.11	13.70±6.90
FP	coastal	12.64±4.44	10.11±3.36	14.35±6.08	11.14±4.91	17.11±15.62
	mid-transect	12.03±4.77	8.87±3.44	10.27±5.44	12.30±9.18	12.85±7.83
	outer	7.72±1.65	8.44±5.26	8.13±3.99	9.03±4.27	9.65±4.21
PT	coastal	5.50±0.87	5.06±0.93	5.25±1.24	5.58±1.32	4.92±0.82
	mid-transect	5.47±0.69	5.07±0.98	4.55±0.79	5.03±0.99	4.70±0.52
	outer	5.46±1.10	5.34±1.39	5.28±3.23	5.10±0.79	4.89±0.79
PL	coastal	5.20±0.64	5.15±0.89	5.13±1.21	5.13±0.96	5.10±0.84
	mid-transect	5.34±0.67	4.80±0.65	4.62±0.80	4.58±0.67	4.95±0.66
	outer	5.31±0.64	5.00±0.88	4.44±0.68	4.79±0.68	4.86±0.67

The DIN was calculated as the sum of NO_3 , NO_2 and NH_4 . As observed for the TN, also the DIN displays a wide range of concentrations: from $248.10 \text{ mmol m}^{-3}$ (11/03/2003) and 0.09 mmol m^{-3} (22/09/2004), recorded at FS10 and PT16, respectively. The spatial distribution of DIN follows the

same pattern observed for the TN: highest values and remarkable inshore-offshore gradients in the northern part, lowest concentrations and absence of gradients in the southernmost zone (Fig. 3.9).

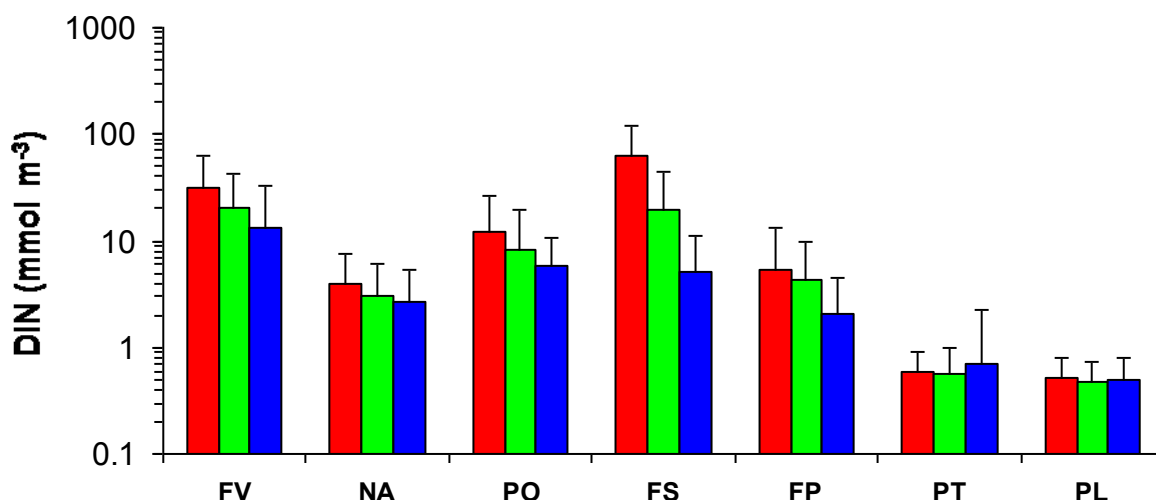


Fig. 3.9 - Averaged concentration (2002-2006) and standard deviation of DIN (log scale) at each sampling site (■ coastal, ■ mid-transect and ■ outer stations).

The yearly averaged DIN (Tab. III. 5) generally shows higher values in the latest years of the monitoring program (2004-2006) compared to the first period (2002-2003).

Tab III.5 - Yearly averaged values and standard deviations of DIN (mmol m⁻³) at each sampling station.

Transect	Station	2002	2003	2004	2005	2006
FV	coastal	15.30±17.82	21.92±31.13	43.21±40.68	32.96±32.82	41.40±33.34
	mid-transect	9.59±9.84	19.06±23.90	28.30±28.14	24.45±22.38	22.54±21.17
	outer	6.55±6.84	10.87±15.38	15.45±21.70	18.56±26.17	15.27±18.72
NA	coastal	3.35±2.47	3.57±2.56	3.46±2.61	4.31±3.39	5.33±5.87
	mid-transect	2.16±2.14	2.83±2.48	2.64±2.60	4.24±4.32	3.23±2.76
	outer	1.62±1.31	2.29±2.38	2.44±3.33	3.71±3.21	3.40±2.75
PO	coastal	11.44±12.33	13.28±10.35	16.16±24.91	10.93±7.58	8.17±5.19
	mid-transect	9.98±10.68	5.48±4.20	6.00±3.61	8.89±11.12	11.01±19.29
	outer	5.57±4.25	4.12±3.51	6.66±5.33	6.50±5.14	6.43±5.73
FS	coastal	56.88±48.06	52.71±63.73	55.24±59.93	66.26±55.85	84.21±62.52
	mid-transect	15.57±22.52	13.20±13.06	27.46±31.57	20.02±24.13	21.63±30.12
	outer	3.82±2.79	4.11±3.57	8.66±10.66	5.63±4.44	3.51±3.88
FP	coastal	4.80±4.62	2.67±2.50	7.17±5.81	3.56±2.26	8.69±15.10
	mid-transect	3.92±4.02	2.32±2.47	4.22±4.48	5.79±7.34	5.10±6.91
	outer	1.24±0.91	1.90±2.90	2.51±3.35	2.64±2.32	2.21±1.70
PT	coastal	0.51±0.19	0.48±0.32	0.62±0.28	0.75±0.38	0.63±0.34
	mid-transect	0.45±0.22	0.42±0.30	0.64±0.49	0.76±0.60	0.58±0.35
	outer	0.49±0.28	0.44±0.34	1.19±3.29	0.84±0.53	0.61±0.44
PL	coastal	0.46±0.19	0.39±0.20	0.49±0.25	0.67±0.38	0.55±0.29
	mid-transect	0.42±0.17	0.34±0.16	0.45±0.24	0.58±0.27	0.54±0.32
	outer	0.48±0.22	0.39±0.23	0.45±0.22	0.64±0.34	0.56±0.34

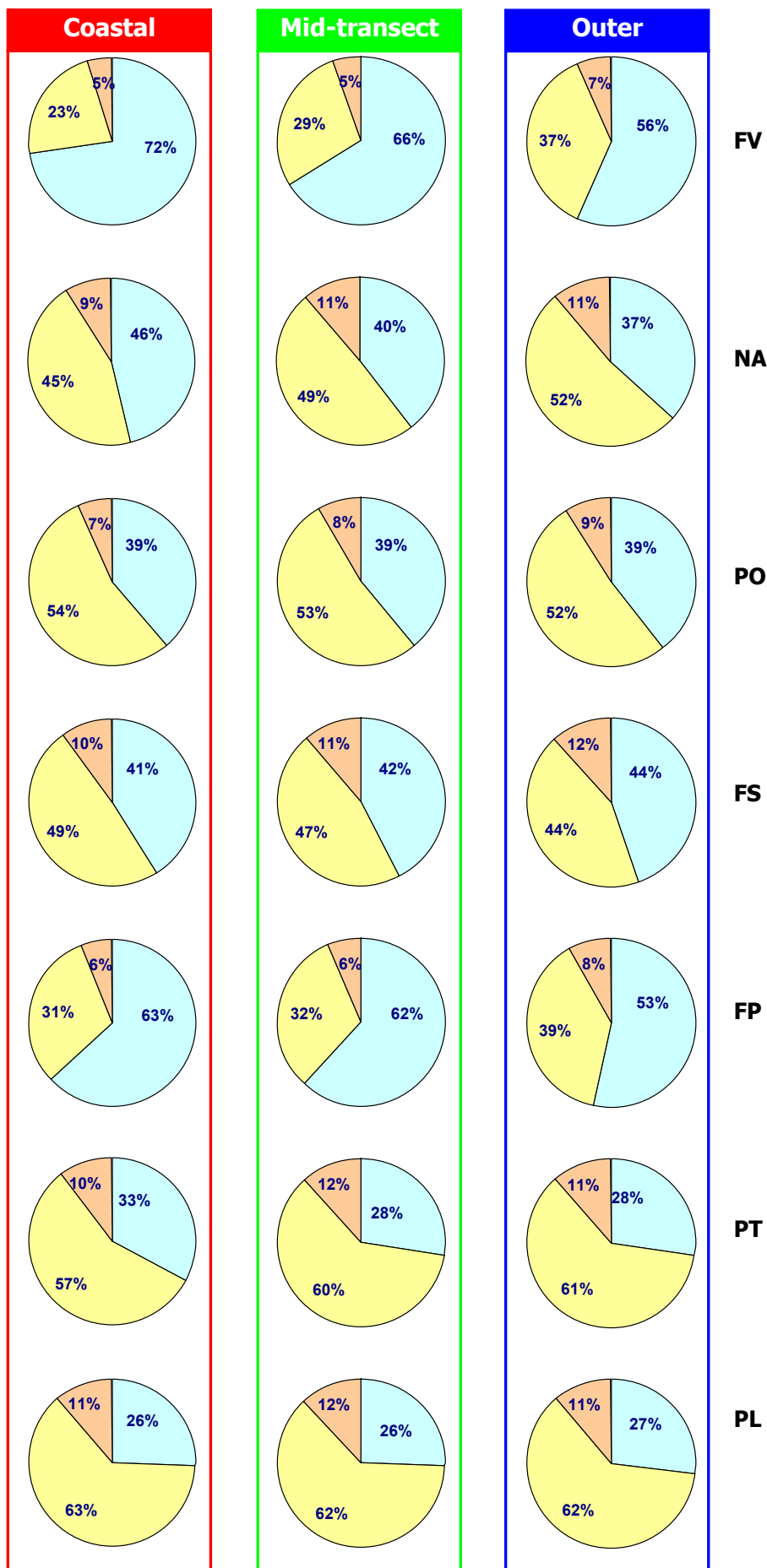


Fig. 3.10 - Percentage composition of DIN (NH_4^+ , NO_3 and NO_2) at each sampling site (for ■ coastal, ■ mid-transect and ■ outer stations).

The composition of DIN was extremely different among the sampling sites (Fig. 3.10). The highest percentages of NO₃ were found in the coastal stations in proximity of the Volturno and Picentino rivers (60-70%) and values greater of 50% were still observed in the offshore stations. In the Gulf of Naples (NA, PO and FS) NH₄ accounted for 50% of DIN. At PT and PL the NH₄ was the major source of DIN (=60%), whereas the contribution of NO₃ was only around 30%.

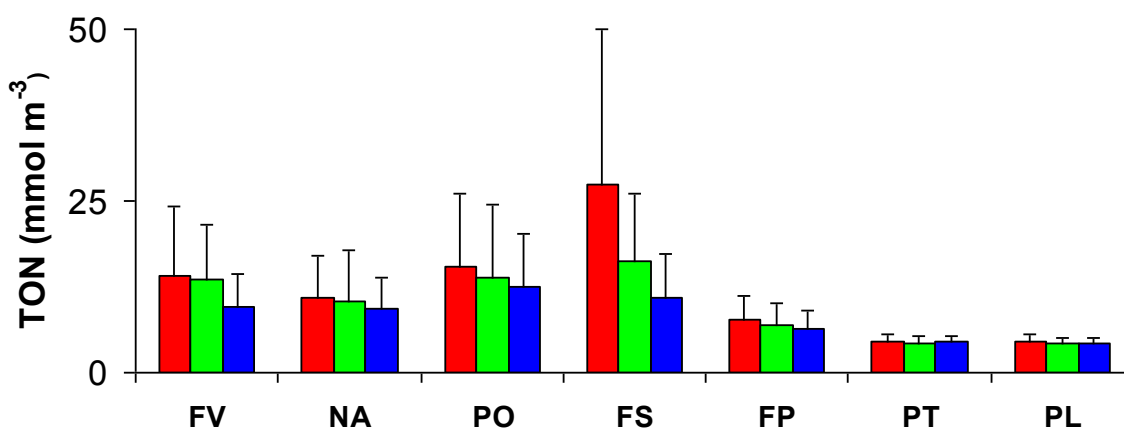


Fig. 3.11- Averaged concentration (2002-2006) and standard deviation of TON at each sampling site (■ coastal, ■ mid-transect and ■ outer stations).

Tab III.6 - Yearly averaged values and standard deviations of TON (mmol m⁻³) at each sampling station.

Transect	Station	2002	2003	2004	2005	2006
FV	coastal	13.88±7.03	11.83±7.5	13.49±10.53	16.4±13.45	14.59±9.29
	mid-transect	12.18±5.01	10.62±5.13	13.04±8.09	17.02±8.88	15.79±11.36
	outer	10.13±3.87	10±4.81	9.91±5.75	9.52±4.84	8.99±5.33
NA	coastal	9.96±5.78	11.77±6.72	10.7±5.68	10.68±6.51	10.54±6.13
	mid-transect	9.74±5.45	10.81±5.19	9.83±5.97	13.27±12.86	9.17±4.52
	outer	9.57±4.5	10.14±5.09	9.49±4.46	9.58±5.42	8.32±3.06
PO	coastal	14.78±9.61	16.48±10.22	13.49±7.28	14.76±9.16	15.65±14.2
	mid-transect	14.79±10.33	14.93±10.59	13.57±15.94	12.94±7.81	13.1±9.28
	outer	12.74±7.66	12.91±8	11.25±6.26	13.1±7.42	12.84±8.98
FS	coastal	26.37±18.16	30.47±28.15	19.23±12.43	23.07±18.46	28.32±24.26
	mid-transect	14.37±7.24	15.11±8.95	15.24±8.52	15.7±9.91	15.8±8.36
	outer	11.54±5.9	11.12±6.81	10.08±5.43	10.75±7.72	10.19±5.76
FP	coastal	7.84±2.02	7.43±2.96	7.17±3.32	7.57±4.28	8.42±5.06
	mid-transect	8.11±2.79	6.55±2.41	6.04±2.69	6.5±3.33	7.75±4.85
	outer	6.47±1.73	6.53±2.78	5.62±2.12	6.39±2.42	7.43±4.2
PT	coastal	4.99±0.92	4.57±0.83	4.62±1.35	4.82±1.13	4.29±0.74
	mid-transect	5.01±0.79	4.64±0.78	3.9±0.87	4.26±0.8	4.12±0.38
	outer	4.97±1.1	4.89±1.11	4.09±0.69	4.25±0.64	4.27±0.62
PL	coastal	4.73±0.68	4.75±0.86	4.64±1.26	4.45±0.8	4.54±0.73
	mid-transect	4.91±0.72	4.46±0.58	4.16±0.81	4±0.63	4.4±0.44
	outer	4.83±0.72	4.6±0.75	3.98±0.7	4.14±0.68	4.3±0.47

The total organic nitrogen (TON) concentrations were calculated as the difference between the TN and the DIN. The TON shows lower spatial variability compared to the total and dissolved inorganic pools. The highest concentrations were observed off the Sarno River and elevated values were

observed near Portici. The lowest TON concentrations were recorded in the southernmost part of the GoS (PT and PL). Moreover, the TON concentrations, as observed for TN and DIN, display a pronounced coastal-offshore gradient, with the only exception of PT and PL (Fig. 3.11).

The yearly concentrations were almost constant during 2002-2006 (Tab. III.6) at all sites, except for some small fluctuations at the coastal stations off the Volturno and Sarno river mouths.

The percentage composition of the TN is highly variable in the investigated stations. The DIN is the major constituent of the TN in the coastal station off the Sarno (=62%) and Volturno (54%) river mouths. At the other stations the total organic form predominates, reaching the highest values (=90%) at PT and PL. The relative contribution of the TON to the TN increases offshore at all the sampling sites, except at PT and PL.

The analysis of the monthly climatological means of N evidenced the presence of different characteristic temporal patterns, depending on the area considered. Two main groups showing different features were identified: the southernmost zone (PT, PL) and the GoN. The FP and FV stations did not display a unique behaviour, falling into one group or into the other depending on the parameter considered. More in details, the TN highest values are found in winter at FV, PL and PT and in spring-early summer in the GoN and at FP stations, while the TON shows the highest values in January-February at FP15, PL and PT and in late spring summer in the other stations (Figure 3.12). At all the stations, the highest concentrations of NO_3 are recorded in late winter-early spring and the lowest in late spring - summer. However, the peaks of NO_3 occur 1-2 months later in the GoN compared to the other sites.

The climatological monthly means of the NH_4 levels reveal a more complex and patchy distribution with respect to the other parameters. At PT, PL and FP15 higher NH_4 concentrations are observed in spring (from March to July) and in September compared to the rest of the year. In the other stations, the highest values are observed from November to June reaching the lowest concentrations from July to October. Looking at the TON/TN ratio, it is evident that the contribution of TON to the total pool of N is generally high from May to September and low in winter- early spring.

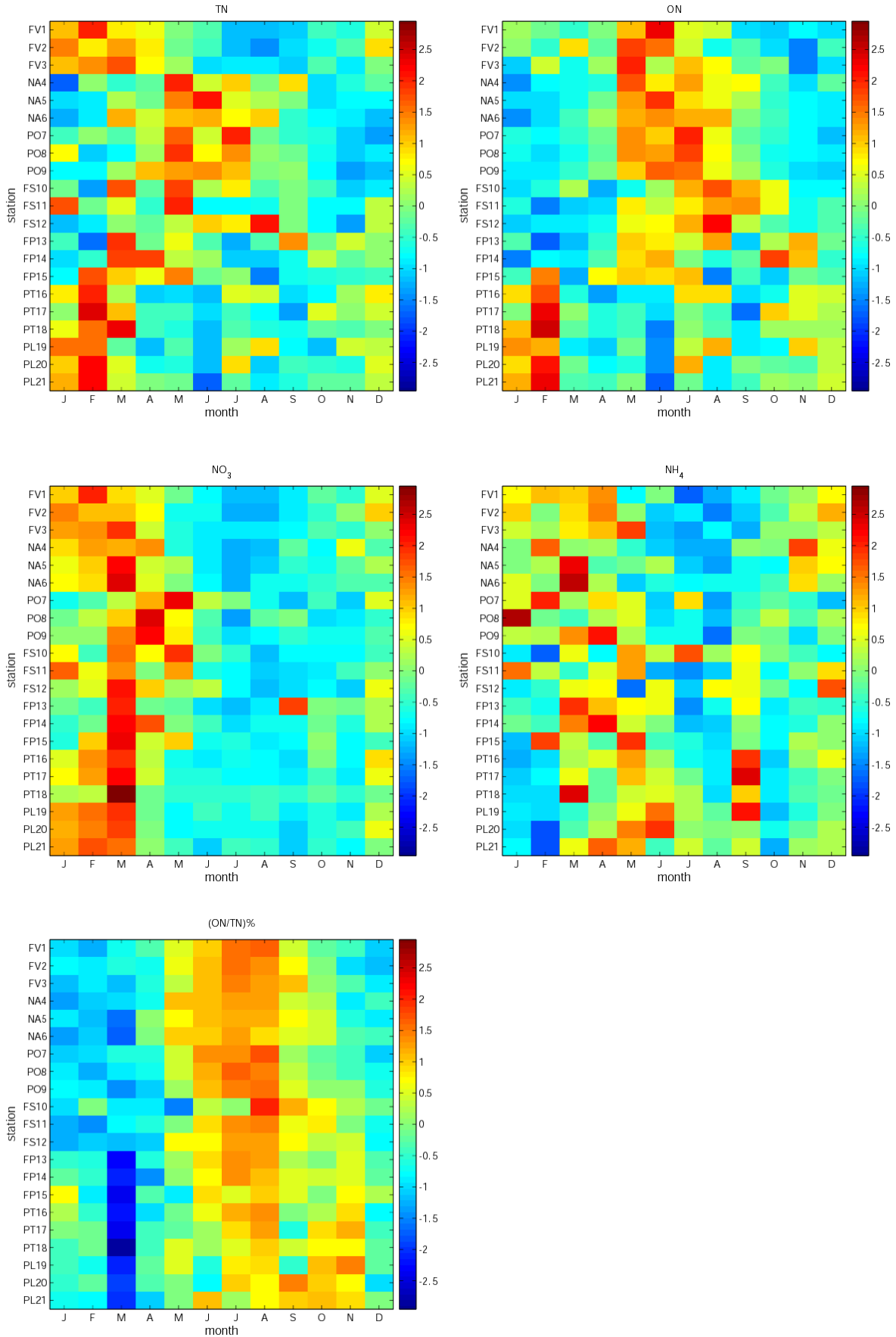


Fig. 3.12- Monthly climatological anomaly (2001-2006), normalized on standard deviation, of the different N pools at each station.

3.3.2.2 Phosphorus

The TP concentrations ranged between 8.12 mmol m⁻³ (02/05/2005) and 0.06 mmol m⁻³ (03/08/2005), recorded at FS10 and PT19, respectively. The highest concentrations were recorded in the northern part of the region (GoG and GoN) and the lowest in the southern (GoS), as shown in figure 3.13. In 2002, the yearly concentrations were lower than the average value (2002-2006) everywhere, whereas in 2004 and 2006 positive anomalies were present in the GoG and GoS, with a less marked signal inside the GoN (Tab. III. 7).

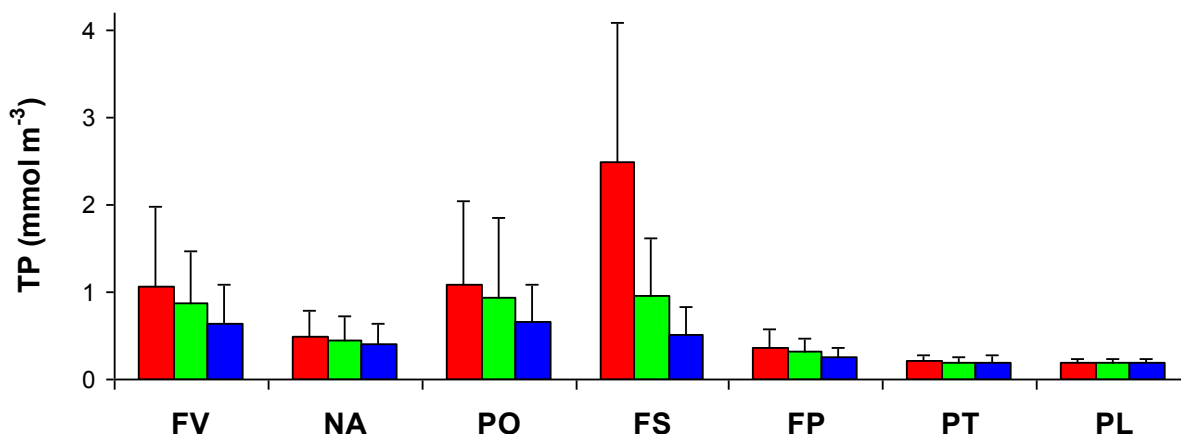


Fig. 3.13 - Averaged concentration (2002-2006) and standard deviation of TP at each sampling site (■ coastal, ■ mid-transect and ■ outer stations).

Tab. III.7 - Yearly averaged values of TP (mmol m⁻³) and standard deviations at each sampling station.

Transect	Station	2002	2003	2004	2005	2006
FV	coastal	0.75±0.49	0.90±0.76	1.28±1.12	0.95±0.70	1.46±1.17
	mid-transect	0.53±0.17	0.84±0.61	1.00±0.57	0.81±0.45	1.15±0.86
	outer	0.43±0.19	0.61±0.55	0.71±0.47	0.67±0.50	0.76±0.38
NA	coastal	0.36±0.17	0.52±0.28	0.52±0.19	0.48±0.31	0.57±0.44
	mid-transect	0.38±0.23	0.49±0.24	0.48±0.19	0.50±0.44	0.42±0.16
	outer	0.31±0.13	0.45±0.20	0.47±0.24	0.44±0.30	0.40±0.14
PO	coastal	0.92±0.78	1.33±0.95	1.40±1.45	0.98±0.62	0.85±0.56
	mid-transect	0.91±0.76	0.91±0.81	0.96±1.00	0.81±0.64	1.05±1.29
	outer	0.59±0.38	0.67±0.45	0.78±0.42	0.65±0.40	0.63±0.37
FS	coastal	2.20±1.58	2.53±1.82	2.42±1.41	2.78±1.91	2.59±1.04
	mid-transect	0.75±0.44	1.00±0.78	1.30±0.70	0.86±0.61	0.93±0.50
	outer	0.43±0.23	0.54±0.36	0.71±0.38	0.44±0.28	0.45±0.23
FP	coastal	0.32±0.16	0.35±0.18	0.43±0.16	0.27±0.08	0.44±0.31
	mid-transect	0.31±0.19	0.30±0.14	0.34±0.12	0.27±0.12	0.35±0.13
	outer	0.24±0.12	0.25±0.08	0.30±0.10	0.20±0.08	0.28±0.08
PT	coastal	0.19±0.06	0.21±0.06	0.24±0.04	0.15±0.05	0.23±0.06
	mid-transect	0.18±0.06	0.20±0.06	0.22±0.04	0.15±0.05	0.23±0.05
	outer	0.19±0.06	0.20±0.06	0.24±0.09	0.15±0.05	0.22±0.05
PL	coastal	0.18±0.06	0.19±0.05	0.21±0.03	0.14±0.05	0.22±0.04
	mid-transect	0.18±0.06	0.19±0.05	0.22±0.04	0.14±0.05	0.21±0.05
	outer	0.17±0.05	0.19±0.05	0.21±0.04	0.14±0.05	0.20±0.05

The PO₄ concentrations ranged between 6.14 mmol m⁻³ recorded at PO7 (02/02/2004) and values near to the detection limit (0.01 mmol m⁻³) recorded several times in different stations. As noticed

for TP, the PO₄ concentrations were sensibly higher in the GoG and GoN compared to the GoS, especially PT and PL (Fig. 3.14). Similarly, a larger variability is present in the yearly average values of PO₄ in the GoG and GoN compared to the GoS. In 2004, a clear negative anomaly was recorded at all sites except FS10 (Tab III.8).

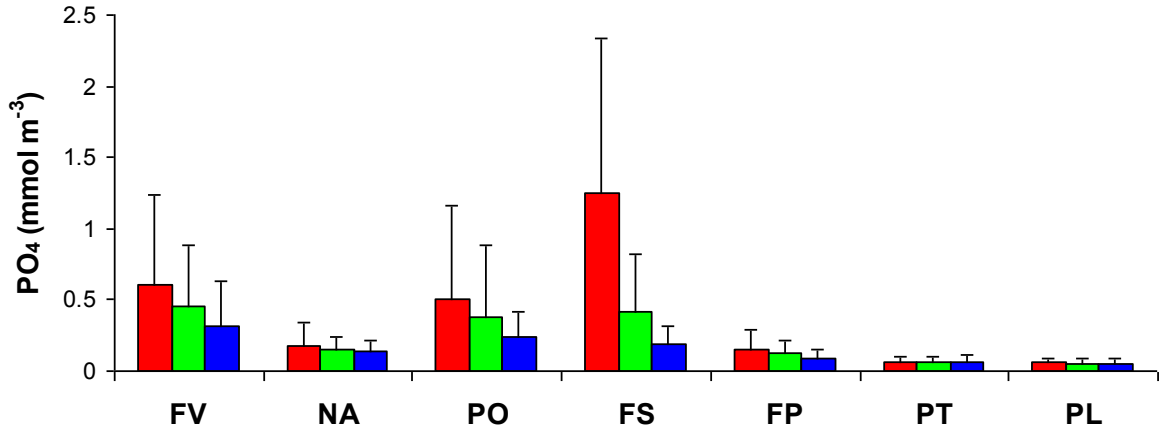


Fig. 3.14 - Averaged concentration (2002-2006) and standard deviation of PO₄ at each sampling site (■ coastal, ■ mid-transect and ■ outer stations).

Tab.III.8 - Yearly averaged values of PO₄ (mmol m⁻³) and standard deviations at each sampling station.

Transect	Station	2002	2003	2004	2005	2006
FV	coastal	0.43±0.29	0.41±0.33	0.69±0.69	0.48±0.41	1.04±0.94
	mid-transect	0.3±0.13	0.36±0.28	0.46±0.32	0.41±0.28	0.78±0.67
	outer	0.23±0.1	0.27±0.34	0.34±0.39	0.28±0.21	0.45±0.38
NA	coastal	0.18±0.09	0.19±0.09	0.16±0.08	0.14±0.08	0.22±0.31
	mid-transect	0.16±0.1	0.17±0.08	0.15±0.07	0.14±0.11	0.14±0.08
	outer	0.14±0.08	0.15±0.07	0.14±0.1	0.11±0.07	0.13±0.08
PO	coastal	0.41±0.45	0.53±0.4	0.74±1.21	0.43±0.4	0.39±0.34
	mid-transect	0.37±0.35	0.34±0.29	0.34±0.38	0.33±0.41	0.52±0.86
	outer	0.23±0.15	0.25±0.18	0.28±0.19	0.22±0.14	0.25±0.17
FS	coastal	0.96±0.96	1.24±1.29	1.04±0.81	1.28±1.22	1.72±0.92
	mid-transect	0.37±0.32	0.41±0.41	0.52±0.42	0.36±0.43	0.46±0.37
	outer	0.19±0.14	0.2±0.17	0.23±0.14	0.13±0.1	0.16±0.11
FP	coastal	0.16±0.11	0.14±0.09	0.16±0.11	0.08±0.03	0.21±0.23
	mid-transect	0.15±0.1	0.12±0.08	0.11±0.09	0.08±0.04	0.14±0.12
	outer	0.12±0.07	0.1±0.04	0.08±0.06	0.05±0.03	0.09±0.06
PT	coastal	0.09±0.04	0.08±0.04	0.06±0.02	0.05±0.02	0.06±0.05
	mid-transect	0.08±0.03	0.08±0.04	0.05±0.02	0.04±0.02	0.05±0.04
	outer	0.08±0.04	0.08±0.05	0.07±0.07	0.04±0.01	0.06±0.04
PL	coastal	0.07±0.03	0.08±0.03	0.05±0.02	0.04±0.02	0.05±0.04
	mid-transect	0.08±0.04	0.07±0.03	0.05±0.03	0.03±0.01	0.05±0.03
	outer	0.07±0.03	0.07±0.03	0.05±0.03	0.04±0.01	0.05±0.04

The TOP concentrations ranged between 0.02 (recorded in several sampling at different stations) and 5.39 mmol m⁻³, observed at FS10 (06/09/2005).

The highest TOP concentrations are found in the highly impacted area of the GoN (Sarno and Portici) and the lowest at PT and PL (Fig. 3.15).

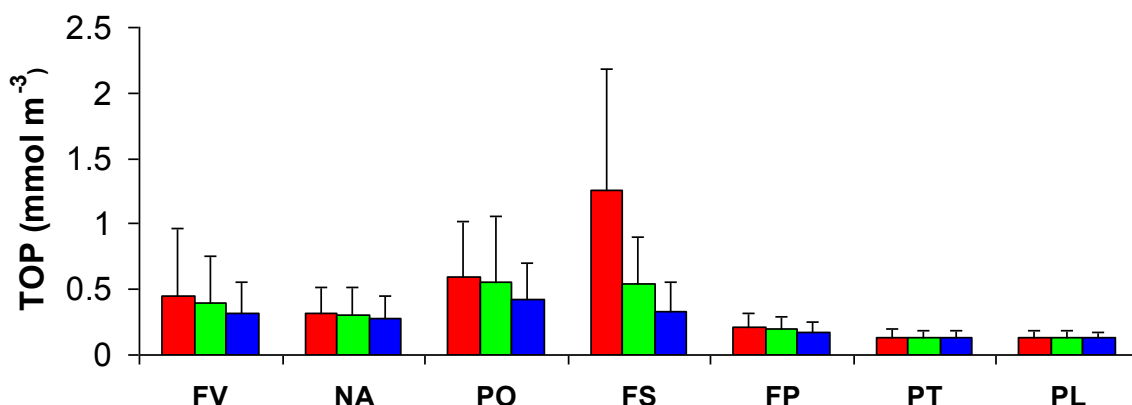


Fig. 3.15 - Averaged concentration (2002-2006) and standard deviation of TOP at each sampling site (■ coastal, ■ mid-transect and ■ outer stations).

Tab.III.9 - Yearly averaged values of TOP (mmol m⁻³) and standard deviations at each sampling station.

Transect	Station	2002	2003	2004	2005	2006
FV	coastal	0.32±0.26	0.49±0.62	0.58±0.74	0.47±0.35	0.41±0.39
	mid-transect	0.23±0.12	0.48±0.49	0.54±0.35	0.4±0.32	0.38±0.28
	outer	0.21±0.12	0.33±0.26	0.37±0.18	0.39±0.34	0.32±0.14
NA	coastal	0.18±0.11	0.33±0.22	0.36±0.16	0.35±0.24	0.34±0.2
	mid-transect	0.21±0.16	0.32±0.19	0.34±0.14	0.36±0.34	0.28±0.11
	outer	0.16±0.09	0.31±0.16	0.33±0.16	0.32±0.24	0.27±0.1
PO	coastal	0.52±0.42	0.8±0.59	0.65±0.35	0.55±0.33	0.46±0.27
	mid-transect	0.55±0.48	0.57±0.55	0.62±0.63	0.49±0.3	0.53±0.47
	outer	0.37±0.28	0.43±0.3	0.5±0.26	0.43±0.28	0.38±0.22
FS	coastal	1.24±0.94	1.29±0.94	1.38±0.86	1.5±1.14	0.87±0.5
	mid-transect	0.38±0.21	0.59±0.45	0.78±0.41	0.51±0.24	0.47±0.24
	outer	0.24±0.16	0.34±0.26	0.48±0.27	0.31±0.21	0.29±0.14
FP	coastal	0.16±0.09	0.21±0.12	0.27±0.09	0.19±0.07	0.22±0.11
	mid-transect	0.16±0.12	0.18±0.09	0.22±0.07	0.2±0.09	0.21±0.09
	outer	0.12±0.07	0.15±0.07	0.22±0.09	0.15±0.07	0.19±0.08
PT	coastal	0.11±0.05	0.13±0.06	0.18±0.04	0.11±0.04	0.17±0.05
	mid-transect	0.1±0.04	0.12±0.05	0.17±0.03	0.11±0.04	0.17±0.04
	outer	0.11±0.04	0.12±0.04	0.18±0.04	0.11±0.04	0.16±0.04
PL	coastal	0.11±0.05	0.11±0.05	0.16±0.03	0.1±0.05	0.17±0.04
	mid-transect	0.11±0.04	0.12±0.04	0.17±0.03	0.11±0.05	0.16±0.04
	outer	0.1±0.04	0.12±0.04	0.16±0.03	0.1±0.04	0.15±0.04

Moreover, the coastal stations that were more affected by terrestrial inputs displayed the highest interannual variability. A common temporal pattern was not observed. However, the highest concentrations were generally found in years 2003, 2004 and 2006 in the GoG and the GoN, and in 2004 and 2006 in the GoS (Tab. III.9).

The composition of P follows the same spatial pattern observed for N: the inorganic fraction is higher at the coastal stations in proximity of Volturno and Sarno rivers (>50%), whereas the

organic fraction is the main source of P at PT and PL (>65%). However, the percentage of the ratio TOP/TP was generally lower and less variable compared to the TON/TN.

The monthly climatological means of TP display different temporal patterns, depending on the area considered (Fig 3.16). At FV, the highest concentrations are recorded from January to March; in the GoN from May to July, except off Sarno River, where enhanced concentrations are observed up to September. In the GoS, two peaks are observed: the first in February-March and the second in June.

The OP seasonality shows a clear maximum in June in the GoS, relatively high concentrations in the period May-July at FV3, NA and PO and a delayed maximum (August-September) off the Sarno. The PO₄ concentrations are generally maximum in February-March, but a considerable increase occurs in the GoN and off the Picentino River also in May- June.

The ratio TOP/TP increases from April to June and reaches the highest values in the period July-September. The lowest values are usually observed from December to March.

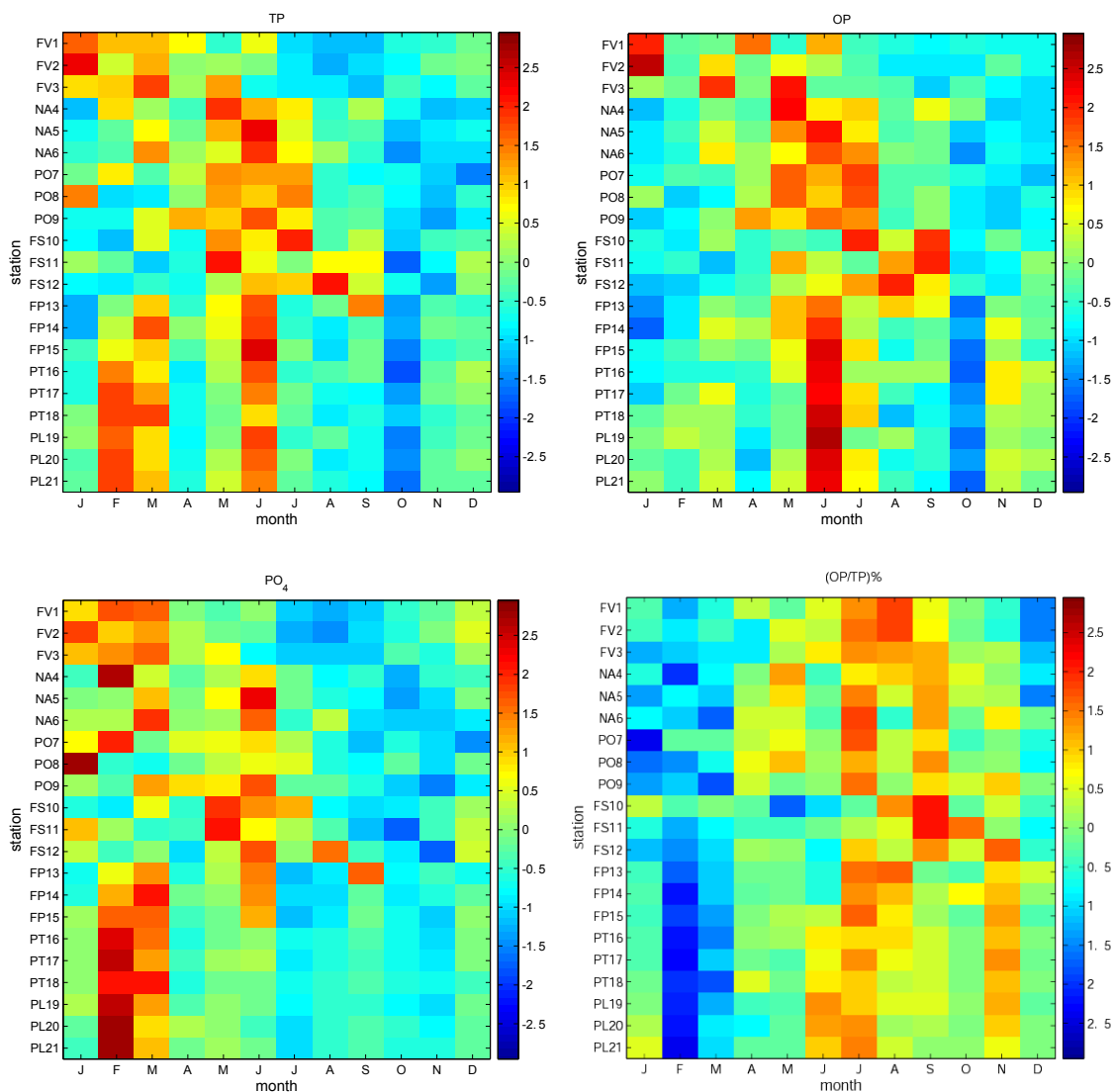


Fig. 3.16 - Monthly climatological anomaly (2001-2006), normalized on standard deviation, of the different P pools at each station.

3.3.2.3 Nitrogen:Phosphorus ratio

The ratios between nitrogen and Phosphorus were analyzed in the total, inorganic and organic inventories. The TN:TP ratio displays one order of magnitude of variability among the sampling sites, ranging from 10 to 126. The average values (2002-2006) are slightly higher close to the rivers (>35) compared to the other stations (≈ 28), as shown in figure 3.17.

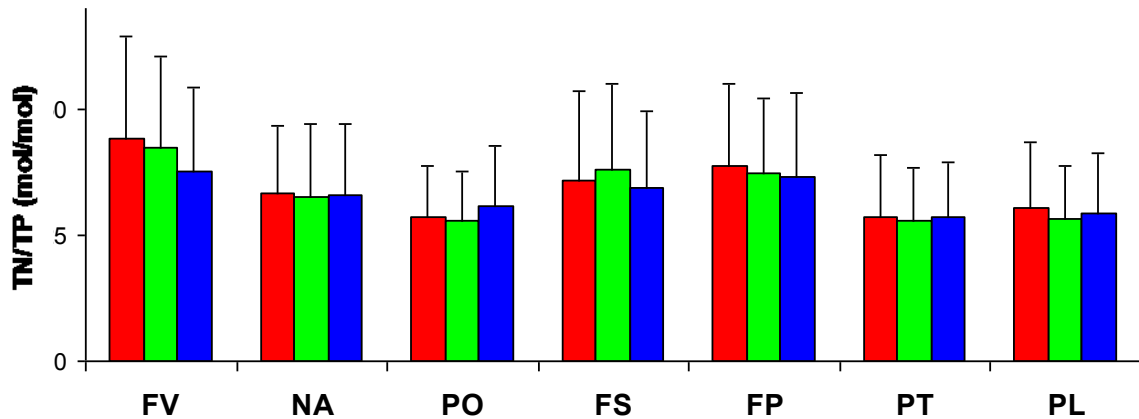


Fig. 3.17- Averaged (2002-2006) value and standard deviation of the TN/TP ratio at each sampling site (■ coastal, ■ mid-transect and ■ outer stations).

The average N:P ratio in the inorganic pool (DIN/PO_4) are highest (>40) near the river mouths and sensibly lowest (≈ 11) in the pristine area (PT and PL). Near the river mouths a remarkable coast-offshore gradient can be observed. At NA and PO the mean DIN/PO_4 ratio assumes values in the range 30-22 (Fig.3.18).

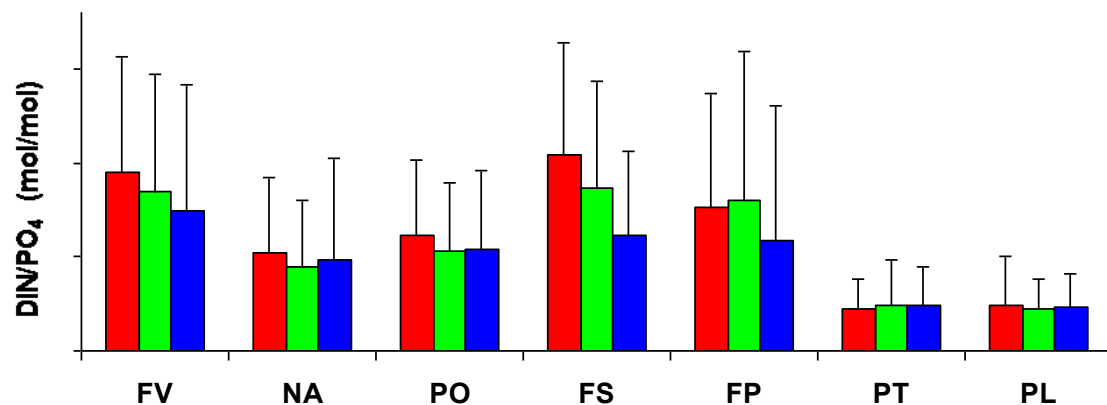


Fig. 3.18- Averaged (2002-2006) value and standard deviation of the NO_3/PO_4 ratio at each sampling site (■ coastal, ■ mid-transect and ■ outer stations).

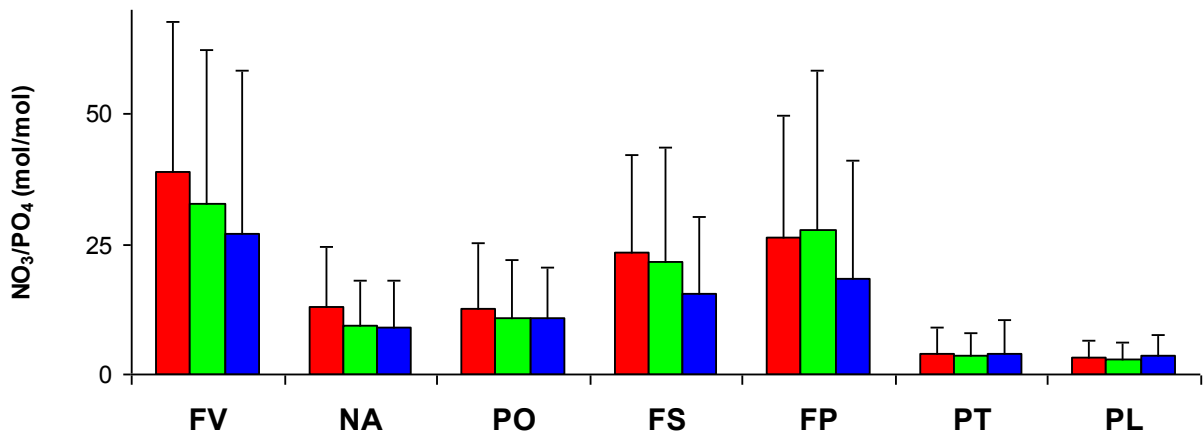


Fig. 3.19- Averaged (2002-2006) value and standard deviation of the NO₃/PO₄ ratio at each sampling site (■ coastal, ■ mid-transect and ■ outer stations).

The spatial differences observed in the DIN/PO₄ ratio are even more pronounced in the NO₃/PO₄. This ratio is greater than 20 near the river mouths, close to 10 at PO and NA and 3-4 at PL and PT (Fig. 3.19).

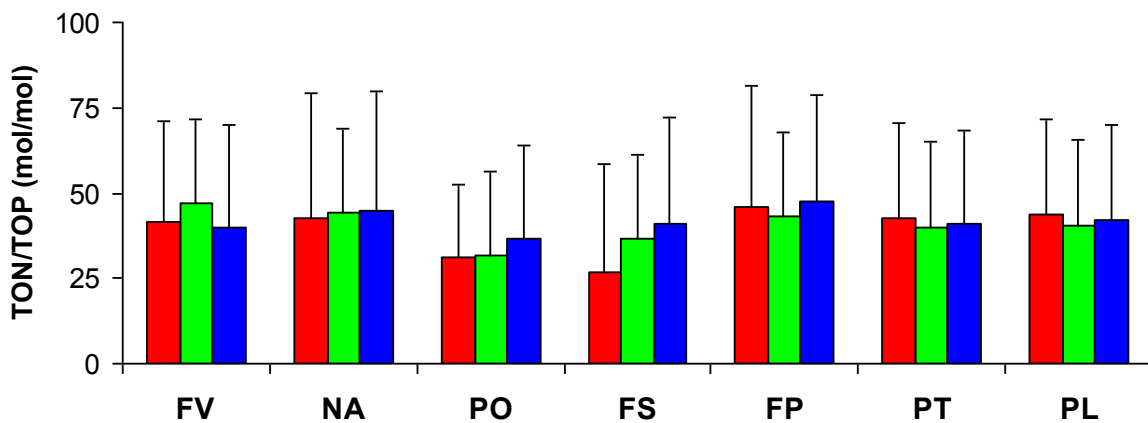


Fig. 3.20- Averaged (2002-2006) value and standard deviation of the TON/TOP ratio at each sampling site (■ coastal, ■ mid-transect and ■ outer stations).

The mean TON/TOP ratios (Fig. 3.20) show a lower variability among the investigated areas compared to that observed in the total and the inorganic pools. The mean TON/TOP ratios observed in the stations off Portici and Sarno River are slightly lower (<40) compared to the other sites (>40). At Sarno River a decreasing gradient from the coastal to the outer station was observed in the TON/TOP ratio.

The monthly climatological mean of the N:P ratio was analyzed in the total (TN/TP), in the dissolved (as DIN/PO₄ and NO₃/PO₄) and in the organic (TON/TOP) pools (Fig. 3.21).

The ratios TN/TP show the lowest values in June at all the investigated stations (average ratio≈25), while the highest values are displayed in October (average ratio≈40).

The N:P ratio in the inorganic pool showed a clear seasonality, more pronounced in the NO₃/PO₄ compared to the DIN/PO₄. The highest values were observed in winter and the lowest in summer.

The average DIN/PO₄ was 38 in March and 16 in June, whereas the average NO₃/PO₄ ratio ranged between 26 and 7 in the same months.

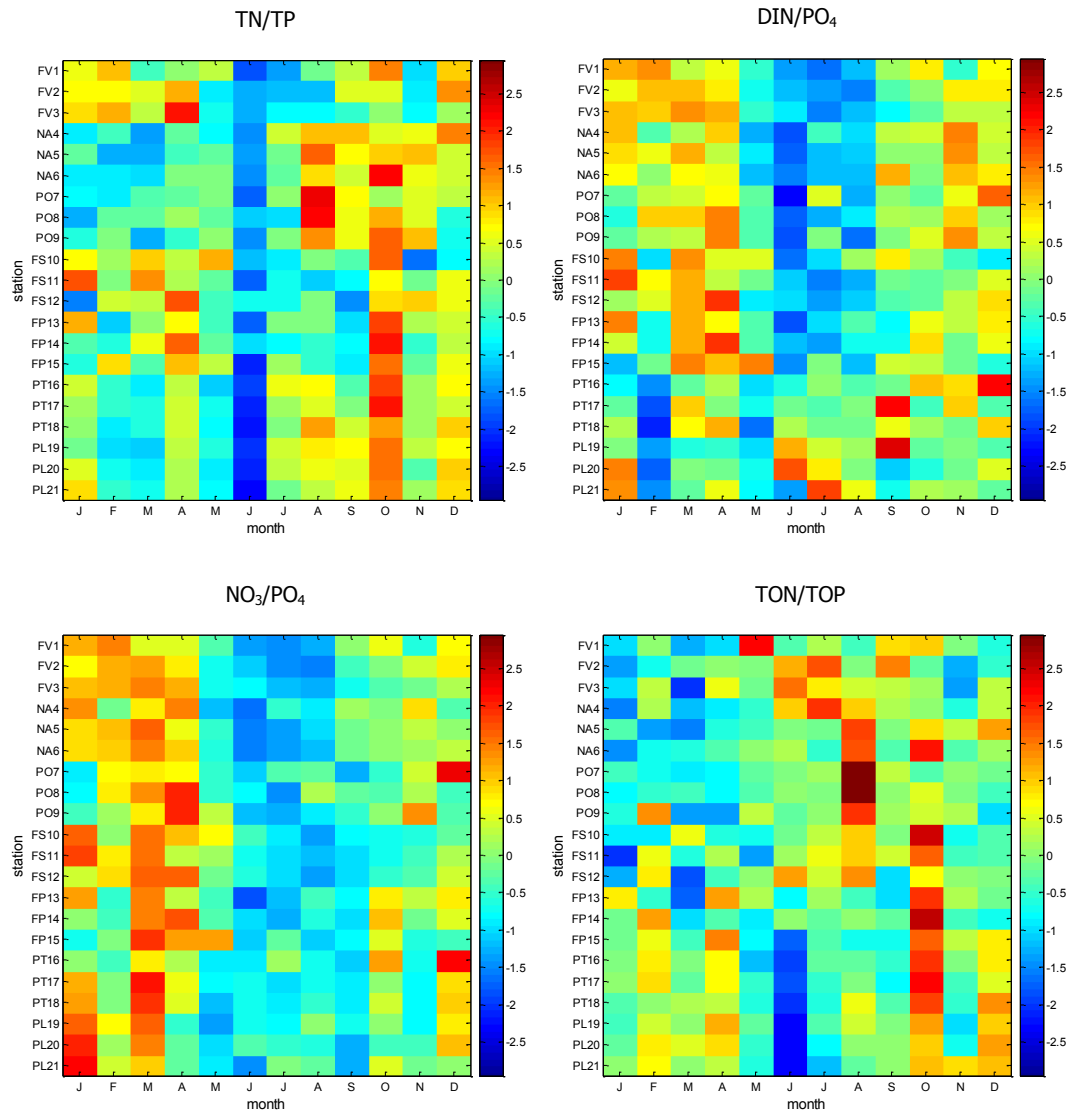


Fig. 3.21 - Monthly climatological mean (2001-2006), normalized on standard deviations, of the N:P ratio in different pools.

The N:P ratio in the organic pool followed different temporal patterns, depending on the area considered. In the GoN the highest ratios are observed in May-June, in the GoN in August and in the GoS in October.

3.3.3 Environmental characterization of the Campania coast

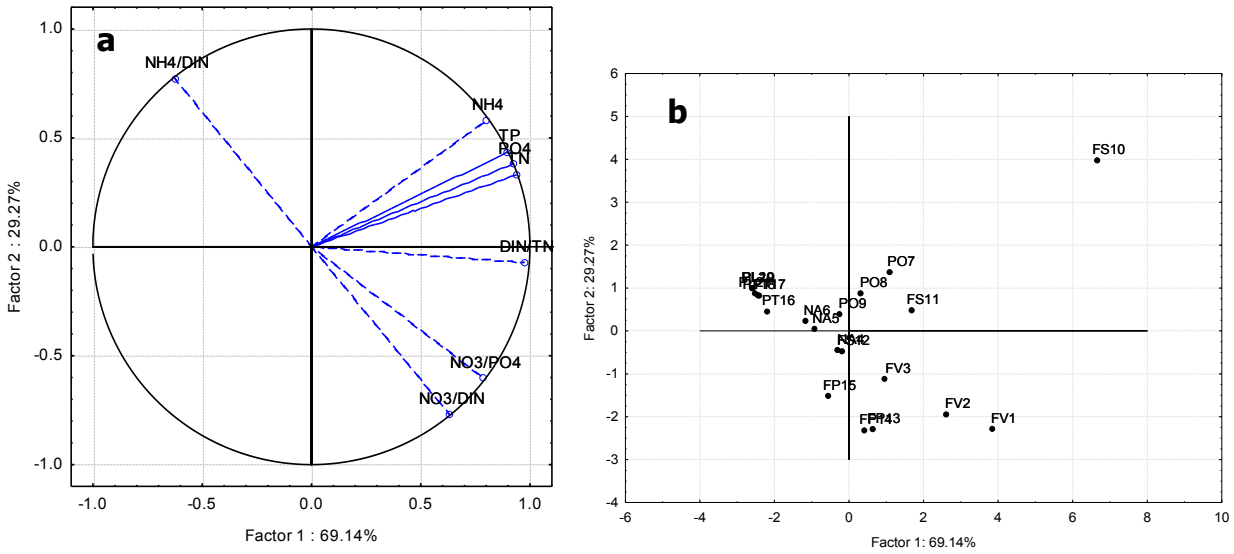


Fig. 3.22 - Results of Principal Component Analysis performed on the averaged chemical properties (2002-2006) of each sampling site. Plot of the projected variables (**a**) and the sampling cases (**b**) on the factor-plane described by the first and second principal factors.

In order to characterize the different environments on the basis of their typical chemical properties, a principal component analysis (PCA) was performed on the averaged values (2002-2006) of TP, TN, NH₄, PO₄, NO₃/PO₄, NO₃/DIN, NH₄/DIN and DIN/TN for each station (Fig.3.22). TP, TN, NH₄, PO₄ have been chosen as proxy of terrestrial loads, while the N ratios have been selected as indicators of different environmental features.

The first axis separates the stations in function of the relative contribution of the dissolved inorganic pool to the total nitrogen and in function of the nutrient loads, while the second basically displays the difference in the nutrient inventories.

The coastal station off the Sarno river mouth (FS 10) is completely separated by the other stations, indicating peculiar chemical features. As shown before, the highest nutrient loads were observed at the stations FS10 and FV1, whereas PT and PL displayed the lowest values. NO₃ was the main source of DIN at the stations located near the river mouths, except at FS10 where NH₄ and NO₃ contributed in the same percentage to the DIN concentrations. In the pristine areas (PT and PL) the DIN was largely composed by NH₄ and very low NO₃ concentrations were noticed.

The differences between the coastal and the outer stations of each sampling site were very pronounced at the Sarno transect and almost negligible at Licosa Cape. The offshore stations of the GoN showed a pronounced similarity in their chemical properties.

The projection of the cases on the factor plane highlighted the presence of four main groups of stations: the coastal station of the Sarno transect (FS10), the stations influenced by rivers (FV1, FV2, FV3, FP13, FP14, FP15), the stations impacted by terrestrial loads located in the GoN (NA4, NA5, NA6, PO7, PO8, PO9, FS10, FS11, FS12) and the oligotrophic stations located in the pristine areas (PT16, PT17, PT18, PL19, PL20, PL21). The main chemical properties and the mean surface salinity of each group are reported in Tab III.10.

Tab. III.10 - Average nutrient concentrations (mmol m⁻³) and average surface salinity (SS) for each group of station as identified by the PCA.

GROUP	STATION	TN	NH₄	NO₃	TP	PO₄	SiO₄	ON	OP	SS
1	<i>FS10</i>	88.56	26.06	31.55	2.51	1.25	76.01	25.50	1.26	34.70
2	<i>FV1, FV2, FV3, FP13, FP14</i>	22.51	2.20	10.17	0.58	0.29	18.07	9.77	0.29	36.71
3	<i>NA4, NA5, NA6, PO7, PO8, , PO9, FS11, FS12</i>	19.85	3.81	3.23	0.69	0.27	6.43	12.28	0.42	37.46
4	<i>PT16, PT17, PT18, PL19, PL20, PL21</i>	5.03	0.31	0.18	0.19	0.06	1.28	4.49	0.13	37.90

An additional PCA was performed for each group of stations in order to link the chemical properties (NO₃, NH₄, PO₄, TON, TOP) to the physical parameters (temperature and salinity). In this analysis, the salinity can be considered as an indicator of the terrestrial origin of the waters, while temperature (though eventually correlated to salinity) can give an idea of the mixing/stratification of the surface layers.

The salinity was negatively correlated to nutrient concentrations on the first axis in all group of stations, but decreasing salinities mainly affected NO₃ and SiO₄ in the second group (rivers), PO₄, NH₄, SiO₄ at the Sarno river mouth and in the GoN (first and third groups), and NO₃ and SiO₄ in the fourth (even if the explained variance was sensibly lower). However, NO₃, PO₄ and SiO₄ concentrations were mainly influenced by temperature in the fourth group of stations.

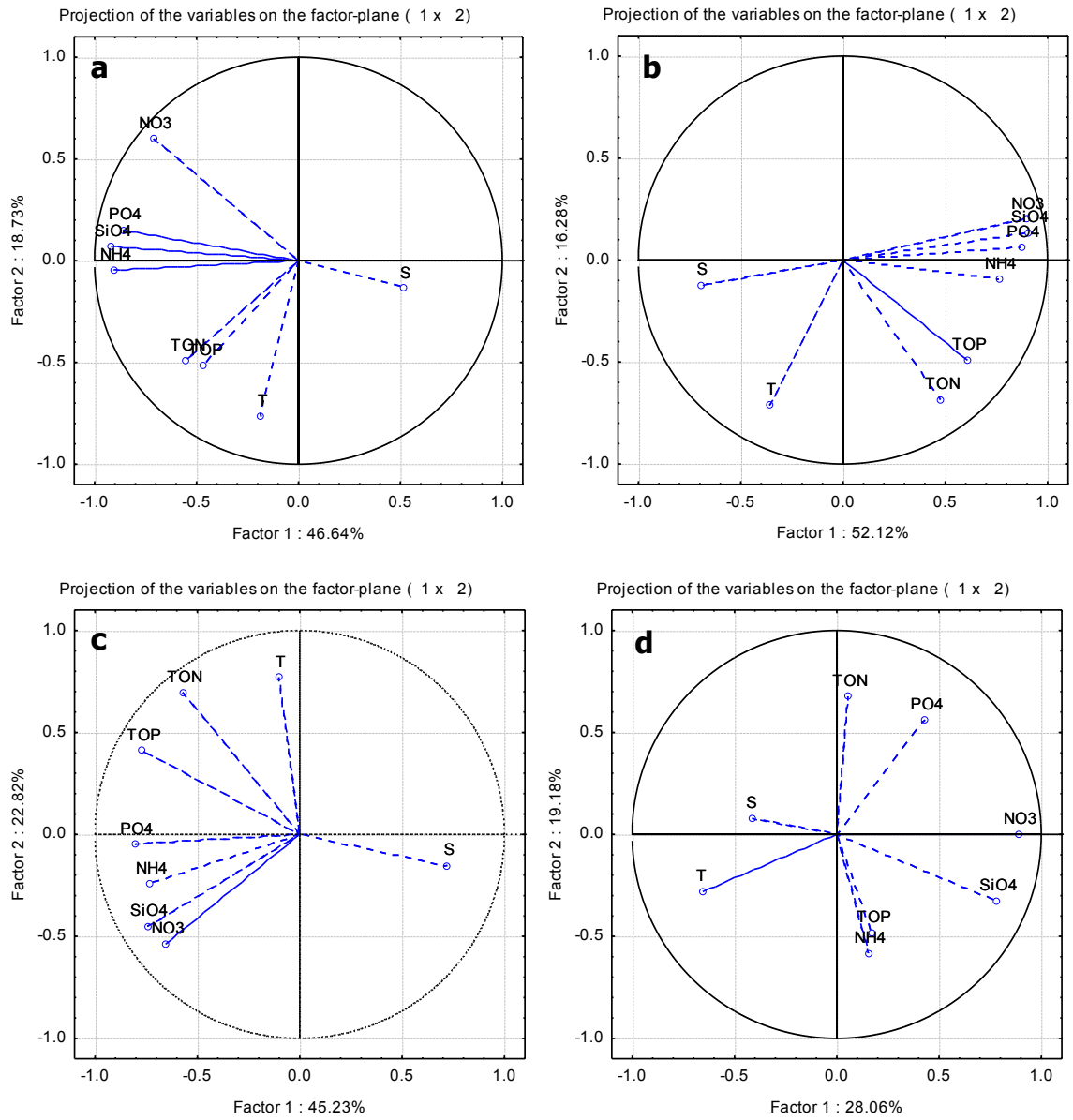


Fig. 3.23 - Factorial maps of the correlation circles of first and second principal components resulting from the PCA performed on the (a) first, (b) second, (c) third and (d) fourth group of stations.

3.4 Discussion

In the previous sections, the seven sites located along the Campania coasts have been characterized in terms of their hydro-chemical properties and corresponding spatial and temporal (interannual and seasonal) variability has been described in detail for each of the parameters considered.

In this following, we will go through these results to give a more synthetic view, identifying the common features observed, and proposing a first interpretation of the characteristic patterns that influence the nutrient dynamics in the coastal areas of the Campania region.

Hydrography

The hydrological features display a pronounced spatial and temporal variability. More in details, the seasonal cycle of temperature is typical of the temperate climate and, even if the stations located off the river mouths are generally affected by the freshwater inputs, the same interannual variability was recognized at all the sampling sites.

Indeed, the lowest temperatures, recorded in the winters 2004/2005 and 2005/2006, were due to basin scale signals. Persistent cold and dry northerly winds, as well as the recurrent arrival of polar fronts (Lopez-Jurado et al., 2005) were observed in winter 2004/2005, several events of dense shelf water cascading (DSWC) were detected in the Gulf of Lions (Canals et al., 2006; Ulses et al., 2008) and the production of anomalously warm, salty deep water in the northwestern Mediterranean Sea during winters 2004/2005 and 2005/2006 was reported (Schroeder et al., 2010). In the Ligurian Sea (at Dyfamed station) low air temperature and high wind speed were recorded for two months in winter 2005/2006. In winter 2004/2005 the lowest temperatures were observed, but it was for a short time and accompanied by less intense wind. As consequence, higher convective events were observed at Dyfamed in 2004, 2005 and 2006, compared to the years 2000-2003, that led to sensibly higher nutrient (nitrate, silicate and phosphate) concentrations at surface (Marty and Chiaverini, 2010).

Similarly, the summer 2003 was the hottest experienced in Europe since 1500 (Luterbacher et al., 2007), and the effects of the heatwave are well documented. Mass mortalities in rocky benthic communities were observed in the Balearic Islands, in the Gulfs of Genoa and Naples, along the Catalan, Provence, Sardinia and Corsica coasts (Garabou et al., 2009), an anomalous mucilage benthic event was detected in the Ligurian Sea (Schiaparelli et al., 2007) and massive mortality events affected the sessile marine invertebrates in all the Mediterranean Sea (Lejeusne et al., 2009).

The salinity was strongly affected by terrestrial inputs: the stations located near the river mouths displayed the highest freshwater content, but low salinity values were recorded in all the GoG (NA and PO). The southernmost stations (PT and PL) displayed negligible freshwater inputs, except in spring 2004, when exceptional low salinity values were recorded at the surface, associated with high nutrient concentrations, especially in the outer station of PT (PT18). This anomaly in salt content could be explained by the strong flow from the Sele River, probably due to heavy rains, as

identified in satellite images of Chl *a* acquired the 27/03/2004 that shows an anomalous high concentration of Chl *a* in all the GoS (<http://gos.ifa.rm.cnr.it/adricosm/index.html>).

The seasonal cycle of surface salinity points out clear differences between the sites located off the rivers mouths and the others. In the former, the lowest values were observed from March to May, whereas in the second they occur in May and June. Boukthir and Barnier, 2000, estimated the minimum of freshwater deficit ($FWD=E-(P+R)$, FWD= fresh water deficit, E=Evaporation, R=River discharge) in May for the Western Mediterranean Sea, whereas remarkable high river discharges were recorded from January to June with the maximum recorded in May. The delay observed in the sites not affected by the river mouths could be ascribable to the minima in FWD, that are shifted with respect to the river peak.

The interannual variability observed along the Campania Region coasts was recorded also in other Mediterranean sampling sites. At Dyfamed station the salinity in the layer 0-100m was higher in the period 2004-2006 compared to the years 2001-2003 (Grignon et al., 2010). A similar pattern in surface salinity was observed in the Corsica Channel (Schroder et al., 2006): the authors reported decreasing values of salinity till 2003 and increasing value starting from April 2004.

Summarizing, notwithstanding the pronounced spatial variability observed in the hydrographic features, basin scale signals dominated the interannual variability observed in both temperature and salinity. This feature reveals the importance of coastal monitoring programs also for the study of larger scales processes with reduced efforts with respect to offshore programs.

N and P inventories

The nutrient concentrations highlighted the presence of different trophic regimes along the Campania coastal waters. The northern area resulted more affected by terrestrial inputs and displayed the highest concentrations of all nutrients. The stations off the Volturno Rivers (FV1, FV2 and FV3), as well as the coastal and mid-transect stations off Portici and Sarno River (PO7, PO8, FS10 and FS11), displayed eutrophic characteristics (average concentrations of DIN $>8 \text{ mmol m}^{-3}$ and $\text{PO}_4 >0.3 \text{ mmol m}^{-3}$). Naples (NA4, NA5, NA6), Picentino River (FP13, FP14, FP15) and the outer station of Portici and Sarno (PO9 and FS12) showed mesotrophic features (average concentrations of DIN $>2 \text{ mmol m}^{-3}$ and $\text{PO}_4 >0.09 \text{ mmol m}^{-3}$). The station in the southernmost part of the GoS (PL and PT) were characterized by oligotrophic conditions, in fact in these stations the average concentrations of DIN were $< 0.6 \text{ mmol m}^{-3}$ and $\text{PO}_4 < 0.07 \text{ mmol m}^{-3}$.

A strong coastal-offshore gradient was observed in all monitoring sites, except for the southern zone (PT and PL), supporting the hypothesis that the main source of nutrients is of terrigenous origin in the northern part of the Campania Region coastline. These results are in good agreement with the previous studies conducted in this area. Marino and co-authors (1984) highlighted pronounced differences between the GoN and the GoS: the GON displays pronounced gradients in hydrographical and biological parameters from the coast to the open sea, with a very evident spatial variability, mainly related to the presence of several terrestrial inputs. In contrast, inside the GoS, coastal waters are generally restricted to nearshore areas and very often offshore waters

almost reach the coast line. Finally, the strong influence of irregular pulses of freshwater nutrient-enriched waters, which determines hydrographic and biological properties peculiar of coastal eutrophic systems in the inner part of the GoN, is well documented in several studies (Carrada et al., 1980; Zingone et al., 1990; A. Zingone et al., 1995, Modigh et al., 1996).

As papers focused on nutrient dynamics at Mediterranean coastal sites are relatively scarce and mainly related to occasional cruises, rather than to time-series projects, comparing our results to other sites could give only a partial view. Multiyear studies at coastal site of the Mediterranean Sea have been conducted in the Bay of Blanes (Lucea et al., 2005), in the Gulf of Trieste (Lipizer et al., 2011) and along the Catalan coast (Flo et al., 2011). The inorganic N and P concentrations observed in the GoN and in the GoG are comparable with those recorded in the Catalan coast, highly influenced by the discharge of the Ebro River, which is one of the largest European river (watershed of 84,230 km² and mean water discharge at the river's mouth of 416 m³s⁻¹ (Ludwig et al., 2009)). The mean DIN and PO₄ concentrations in the Gulf of Trieste, influenced by the Isonzo River, are lower compared to the GoG and GoG, but higher than those observed in the southern part of the GoS. The mean concentrations of inorganic nutrients observed in the Bay of Blanes, which is located in an oligotrophic coastal area, are comparable to the mean values of PL and PT. Moreover, to the best of our knowledge, the concentrations recorded at PO7 and PO8 were sensibly higher than those observed in other Mediterranean coastal sites not located in proximity of the river mouths or not directly affected by submarine groundwaters. Higher concentrations were reported (Bizsel and Uslu, 2000) only in the inner part of the Izmir Bay (1993-1994), whereas in Kaštela Bay in the years 1972-2000 (Marasovic et al., 2005), in Venice Lagoon in 1985-1986 (Sfriso et al., 1988) and in Thau Lagoon (Picot et al., 1990; Souchu et al., 1998) the DIN and PO₄ concentrations were comparable or lower. Thus, the inorganic loads of N and P in the inner part of the GoN are sensibly high also in stations not directly affected by river discharges, indicating a poor water quality in these coastal waters. On the contrary, the concentrations recorded at PT and PL stations, always near to the detection limits, not significantly differed from those reported for the open Mediterranean surface waters (Puyo-Pay et al., 2011; Marty et al., 2002) because of the low population density, the poor industrial and agricultural exploitation and the high exchange rates with the open Tyrrhenian waters (Marino et al., 1984).

Looking more in details to the nutrient loads at the three investigated river mouths, diverse features have been observed, due to the differences in terms of flow rate, size of the basin and land use. The highest concentrations were recorded off Sarno River, high values were observed in proximity of the Volturno, while sensibly lower nutrient values were recorded at FP.

The DIN/TN ratio in the coastal stations in proximity of the river mouths (FV1, FS10 and FP13) shows the highest value (64%) off Sarno, the lowest (35%) off Picentino, whereas off Volturno the DIN/TN ratio was 56%. On global scale, the TN exported by the rivers is composed by approximately 38% of DIN, 46% of PON and 18% of DON; the DIN export is highest in regions with high rate of human activity, the PON increase in the mountainous zones, such as in the Asian rivers draining the Himalaya region, whereas the highest percentage of N exported as DON occurs

at arctic latitude (Seitzinger and Harrison, 2008). The DIN fraction observed in the coastal waters off the Picentino River is very close to the global mean, whereas the highest DIN percentages observed off Volturno and Sarno Rivers are similar to the North-European rivers, where, due to the highly density of population, the DIN is the dominant form in the TN fluxes (Ludwig et al., 2009). The NO_3 is by far the dominant form in the TN for the most of the rivers flowing in the Mediterranean Sea and the high nitrate load is typical where agricultural land use is densely developed, whereas NO_2 and NH_4 are abundant only when rivers suffer from organic pollution (Ludwig et al., 2009). Near the Volturno and Picentino river mouth the NO_3 dominates the DIN fluxes (>60%), whereas off Sarno the sum of NO_2 and NH_4 concentrations accounts for the 60% of the DIN. The dissimilarity observed in the composition of the DIN reflects the differences in the waters pouring into the rivers: reasonably the Volturno and Picentino Rivers watersheds are mainly agricultural, whereas industrial and domestic wastewaters are collected into the Sarno basin. A simplified mass balance was performed in order to achieve a roughly estimate of the Sarno and Volturno Rivers nutrient loads on the coastal ecosystems. The total load, for each nutrient, was calculated multiplying the average concentration (2002-2006) of the nutrient by the mean flow of the river, whereas the load for basin unit (yield) was the total load divided the basin area. For the Sarno River, a mean flow of $13 \text{ m}^3 \text{ s}^{-1}$ was assumed, with a basin area of 500 Km^2 (Celico et al., 1991). Corresponding values for the Volturno attained around $83.1 \text{ m}^3 \text{ s}^{-1}$ and 5550 Km^2 (De Blasio, 1993). A conservative (low) estimate has been computed, assuming the average nutrient concentration in the coastal station as representative of the nutrient concentration in the river. Notwithstanding this assumption clearly lead to underestimated values, the loads for basin unit for the Sarno River were extremely high, supporting once again the low quality of the waters pouring into the river (Tab. III.11). For instance, the yields reported for the Arno River ($\text{NO}_3 = 609 \text{ Kg N Km}^{-2} \text{ yr}^{-1}$ and $\text{PO}_4 = 38 \text{ Kg N Km}^{-2} \text{ yr}^{-1}$), calculated using the river concentrations (Ludwig et al., 2009), are respectively lower and similar compared to those observed for the Sarno River, calculated using the concentrations at sea.

Tab.III.11- Estimates of DIN, TN PO_4 and TP load and yield for Volturno and Sarno Rivers

	LOAD (ton y^{-1})				YIELD (Kg $\text{Km}^{-2} \text{ yr}^{-1}$)			
	N-DIN	N-TN	P- PO_4	P-TP	N-DIN	N-TN	P- PO_4	P-TP
Volturno	1115	1626	49	86	201	293	9	15
Sarno	362	508	16	32	723	1017	32	64

The nutrient inventories highlighted different features in the investigated sites. The organic fractions are the main source of N and P at all sampling sites, except at the coastal stations off Sarno and Volturno Rivers, where the inorganic forms preponderate over the organic pool. The DIN is composed mainly by nitrate near the Volturno and Picentino river mouths (up to 73%), in the GoN ammonia and nitrate equal contribute to the DIN pool, whereas in the in the pristine area of the GoS (PT and PL) the main source of DIN is NH_4 . The N:P ratio in the dissolved inorganic pool is highest near the rivers (>40), lowest at PT and PL (~11), and near 25 in the highly impacted GoN

(NA and PO). The N:P ratio in the total pool displayed higher values near the river (>35) compared to the other stations (~28).

Unfortunately, as the particulate values are missing, it is not possible to totally characterize the N and P pools in the investigated area. The particulate fraction is highly variable in marine environments, ranging from values <10% of the TON and TOP in oligotrophic open waters (eg, Karl et al., 2001) up to values > 50% of the total N and P pools in riverine discharges (Seitzinger et Harrison, 2008).

It is possible to roughly estimate the mean PN (particulate nitrogen) and PP (particulate Phosphorus) concentrations at the coastal stations using the phytoplankton biomass values measured in the same period (Siano, 2007), assuming that the totality of particulate matter is given by phytoplankton and using the ratio C:N:P=163:20.7:1, as reported by Puyo-Pay and coauthors (2011) for the Mediterranean Sea. The DON and DOP concentrations were then estimated from the difference between TON and PON and TOP and DOP, respectively.

PN and PP account for a large fraction of the organic pool at NA4 and PO7, while at the other sites the dissolved fraction predominates. The DON is the main source of dissolved nitrogen in all the sampling sites, except near the rivers where the DIN concentrations account for more than 75% of the TDN. The composition of the TDP follows a spatial gradient: the inorganic forms predominate in the GoG and the GoN, whereas the organic in the GoS (Tab III.12).

Tab III.12 - Concentrations of carbon biomass in phytoplankton (PhytoC) and estimated PON, POP, DON and DOP (mmol m^{-3}), relative contribution of DON on total dissolved nitrogen (TDN) and DOP on total dissolved Phosphorus (TDP), at the coastal stations of each transect (2002-2006).

	PhytoC	PON	POP	DON	DOP	%DON/TDN	%DOP/TDP
FV1	28.16	3.58	0.17	10.47	0.28	25	32
NA4	41.20	5.23	0.25	5.50	0.09	58	34
PO7	60.14	7.64	0.37	7.40	0.23	38	31
FS10	32.43	4.12	0.20	11.13	1.06	15	46
FP13	8.51	1.08	0.05	5.91	0.16	52	51
PT16	1.08	0.14	0.01	4.26	0.13	88	66
PL19	0.58	0.07	0.004	4.56	0.13	90	69

N and P dynamics

The investigated sites differ both for the 'quantity' and 'quality' of nutrients, and four main characteristic groups (classes) with different features and dynamics were identified.

The coastal station off the Sarno River mouth displays peculiar features. The high pollution levels of the waters pouring into the rivers determine sensibly higher concentrations of all nutrients, compared to the other stations. The DIN is mainly composed by ammonia, and the inorganic

nutrient concentrations are mainly driven by salinity. However, lowest salinities mostly determine increasing NH_4 concentrations.

The second group is composed by the station strongly influenced by the rivers (FV1, FV2, FV3, FP13, FP14, FP15). In these stations the DIN is composed mainly by nitrate, and lowest salinities mostly determine increasing concentrations of nitrate and silicate. NO_3 , PO_4 , NH_4 , TN and TP are delivered by the river outflow, thus the maxima values of these nutrients are recorded in the period of highest river discharge (winter-early spring) and the lowest in summer. On the other hand, ON and OP, mainly linked to the biological activity rather than to the river outflow, showed the highest concentration in summer.

The third group, collect the stations located in the GoN, strongly impacted from terrestrial loads. The terrigenous impact is more pronounced at stations PO7, PO8 and FS11, compared to NA4, NA5, NA6, PO9 and FS12. The analysis of the seasonal cycles of the N and P inventories at all these stations reveals the presence of decoupling features compared to the GoS and the GoG, probably due to different mechanisms in nutrients enrichment. In the GoN NH_4 account for 50% of the DIN and high level of P loads (both in organic and inorganic forms) were observed. The terrestrial inputs essentially determine increasing concentrations of PO_4 , NH_4 , SiO_4 , TN and TP, probably originated by sewages and industrial wastewaters.

In the fourth group there are the stations located in the southernmost area of the GoS, characterized by pristine environmental conditions. The main source of N and P is the organic matter (TON and TOP). Considering that in coastal stations of PT and PL the particulate organic fraction is negligible (Tab III.12) and no differences at all were observed from coast to offshore, it seems reasonable to hypothesize that TN and TP are mainly composed by DON and DOP also in the mid transect and in the outer stations. The high contribution of the DON and DOP to the TN and TP has been reported also for the oligotrophic open Mediterranean waters, depleted in nutrient at surface (Lucea et al., 2003; Moutin and Raimbault, 2002; Pujo-Pay et al., 2011).

Moreover, in these stations the main source of DIN is ammonia, but due to the scant concentrations and the high percentage of the DOM, the high ammonia fraction could be due to the ecosystem functioning (regenerated production) rather than local terrestrial sources. In fact, the high grazing pressure observed in this area (Di Capua and Mazzocchi, 2005) and the relative excretion products may support this hypothesis and could explain the high NH_4 and DOM percentages observed. In the pristine areas, NO_3 and SiO_4 concentrations are mainly influenced by temperature rather than salinity, indicating the supply of nutrient is related to the winter mixing processes rather than to terrestrial inputs. Thus, in the last years of the time-series, characterized by lower winter temperatures, the mean yearly concentrations of DIN were higher compared to the first two years.

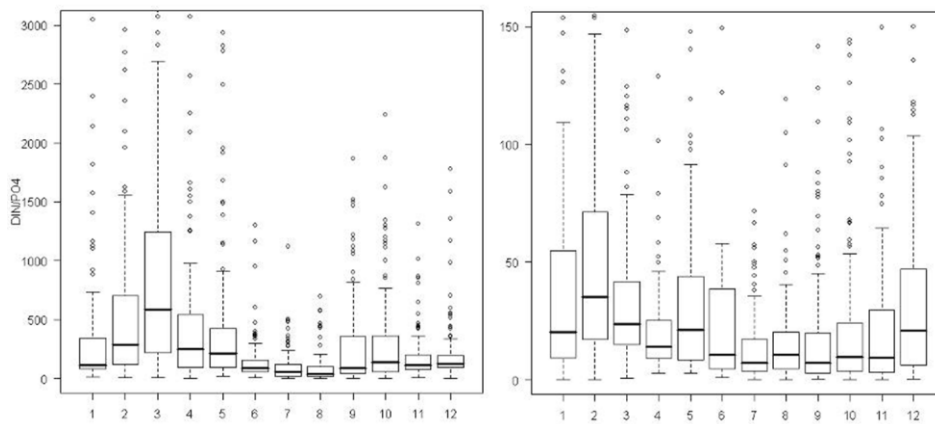


Fig.3.24 - Seasonal cycle of the DIN/PO₄ ratio at **a)** Emilia Romagna and **b)** Liguria Regions coastal station sampled during the Si.Di.Mar Project (2001-2006), box-plot by month.

Finally, despite the pronounced variability observed in terms of N and P inventories and dynamics, a strong seasonal signal in the N/P ratios in the dissolved inorganic pool has been recorded at all the sampling sites, which seems to be related mainly to the NO₃ seasonality.

This ratio is sensibly higher in the winter period compared to the summer values. The same seasonality has been observed analysing the data collected in the framework of Si.Di.Mar. project along other coastal stations (<http://www.sidimar.tutelamare.it/AreaDownload/acegilogin.jsp>). As an example, the seasonality of the DIN/PO₄ at the coastal stations of Emilia-Romagna and Liguria has been reported in figure 3.24.

Moreover, the same signal has been observed also at other coastal sites: in the English Channel (Jordan and Joint, 1998), in the Gulf of Trieste (Lipizer et al., 2011), and in the Bay of Blanes (Lucea et al., 2005).

**Chapter 4: Water column distribution and
time evolution of N and P at a coastal site
of the Gulf of Naples (2002-2009)**

4.1 Specific aims of the chapter

In this chapter, the dissolved inorganic N and P were analyzed in detail, in order to describe their vertical and temporal distribution at LTER-MareChiara (MC) station.

The influence of the some physical (temperature and salinity), as well as meteorological (precipitations) forcings has been investigated in order to estimate their role in modulating the N and P dynamics.

Finally, the phytoplankton biomass distribution has been characterized, aiming to elucidate its relation and eventual feedback on the inorganic dissolved N and P variability.

Our results have been compared to:

- the results illustrated in the previous chapter, in order to contextualize the MC analyses in a larger spatial scale and wider range of processes;
- the previous data recorded at LTER-MC, in order to evaluate possible temporal changes in the seasonal dynamics and the trophic characteristics of the investigated area.

4.2 Study area

4.2.1 Gulf of Naples

The Gulf on Naples is a wide semi-enclosed embayment of the central Tyrrhenian Sea, limited by the islands of Procida and Ischia and by the Campi Flegrei in the northern part, and by the island of Capri and by the Sorrento peninsula in the southern part (Figure 4.1). The basin is located over the continental shelf of the southern Italy, and is characterized by an average depth of 170 m and an area of approximately 870 km² (Carrada et al., 1980). Three marginal sub-basins can be identified inside the GoN: the Bay of Pozzuoli in the northern part, the Bay of Naples in the northeastern sector of the region, the Gulf of Castellammare in the southeastern part of the basin (Uttieri et al., 2011).

The main opening, Bocca Grande (between Capri and Ischia), allows the direct communication between the inner waters of the GoN and the open Tyrrhenian Sea. The exchanges with the neighbouring basins occur along the Procida and Ischia channels and Bocca Piccola (between Capri and the Sorrento Peninsula), connecting the GoN to the GoG and the GoS , respectively.

From the hydrographic point of view, the outer part of the GoN is more directly influenced by Tyrrhenian open waters (e.g., Povero et al., 1990), whereas its inner part is mostly influenced by the land runoff from a very densely populated region. However, differently from other coastal sites, river discharges are limited and highly intermittent (Adriana Zingone et al., 2010b). The location of the boundary between these two subsystems exhibits a strong seasonal variability (Carrada et al., 1980; Carrada et al., 1981; Marino et al., 1984). In fact, the exchanges between the coastal area and the open Tyrrhenian waters are driven by complex circulation patterns, with five main circulation schemes (Cianelli et al., 2011). Two of them are driven by the offshore Tyrrhenian currents: when they are oriented towards the north-west, an intense flux enters the GoN from the Bocca Piccola and the freshwaters coming from the Sarno river and from the city of Naples are

advected offshore (De Maio et al., 1983). When the Tyrrhenian current reverses, the offshore waters are isolated from the coastal area, leading to a substantial stagnation of surface waters (De Maio et al. 1983). The three remaining scenarios can be assumed as purely wind-driven. When winds blow from the north-east (typical winter conditions), a rapid renewal of the surface waters occurs (Grieco et al., 2005; Menna et al., 2007). In presence of low atmospheric pressure systems, intense southwesterly winds are generally recorded and the currents are mostly coastward. Under these conditions, surface waters are retained in the littoral area (Gravili et al., 2001 ; Grieco et al. 2005; Menna et al. 2007). Finally, in the typical summer condition, breeze regimes become the dominant local forcings, the renewal times are very long and the exchanges between coastal areas and open waters are hampered (Buonocore et al., 2010).

Biological studies have been carried out in the Gulf of Naples since the end of the nineteenth century at the Zoological Station "A. Dohrn, yet it was not until the 1980's that an ecological approach was applied, essentially focused on plankton communities (e.g. Carrada et al., 1981; Marino et al., 1984, Ianora et al., 1985; A. Zingone et al., 1990; Modigh, 2001). The presence of different water masses in the GoN explains differences in the zooplankton communities (Carrada et al., 1980), in phytoplankton assemblages (Carrada et al., 1981; Casotti et al., 2000) and bacteria (Casotti et al., 2000). Moreover, the Long-Term Ecological Research Station MareChiara, is regularly sampled since January 1984 (Ribera d'Alcalà et al., 2004, Zingone et. al, 2010, Mazzocchi et al., 2011) for plankton and associated environmental variables.

This station has also been chosen for the present investigation in order to exploit the base of knowledge accumulated over the years and better interpret the data obtained in this project.

4.2.2 Sampling strategy

The surveys have been carried out at the Long Term Ecological Research Station MareChiara (st. LTER-MC, 40°48.5' N, 14°15' E), located two nautical miles far from the coastline, in proximity of the 75 m isobath (Fig. 4.1), in an area where the influence of the coast is still pronounced over most of the year.

Sampling was carried out weekly between January 2002 and December 2009. Profiles of physical parameters (temperature, salinity) were determined with a CTD (see section 2.1), while water samples for nutrient determinations were collected at ten depths (0, 2, 5, 10, 20, 30, 40, 50, 60, 70 m). All analytical procedures are reported in section 2.2 of the previous chapter.

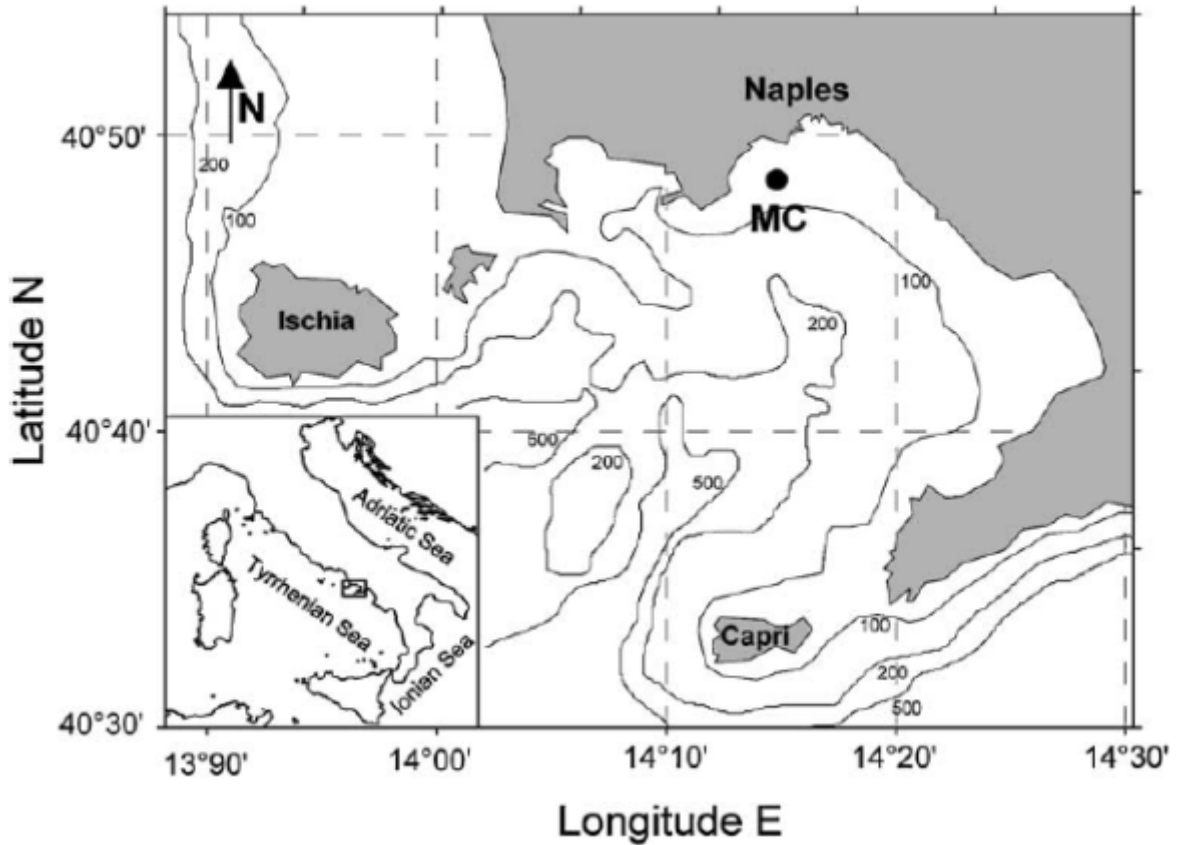


Fig. 4.1 – Map of the Gulf of Naples and position of the LTER-MareChiara station

4.3 Results

The following section is focused on the analysis of the hydrographic features (temperature and salinity), dissolved nutrient pools (nitrogen and Phosphorus) and phytoplankton biomass (as Chl *a*), as measured at LTER-MareChiara (MC) station in years 2002-2009. More in details, for each variable, the vertical distribution, the interannual variability and the seasonality have been investigated. In order to discriminate the presence and the relative importance of interannual, seasonal, and single event in the time-series, a multiplicative decomposition was applied to temperature, salinity, NO_3 , NH_4 , PO_4 and Chl *a*. The decomposition was performed using the 'wq' package in R (details on the theoretical background can be found in the 'Materials and methods Chapter'). The depths (0, 20, 60) have been first selected for this analysis, as they can be considered representative of quite different layers. Then the decomposition has also been applied to the average values (integrated from the surface to the deepest sampled depth), to characterize the variability in the bulk properties of the water column. Moreover, the N/P ratio in the dissolved organic pool has been analysed as NO_3/PO_4 and as well as DIN/PO_4 .

Finally, the precipitation data has been reported as cumulative values at daily, monthly and annual scale in order to discern the effect of the rainwaters on the physical and chemical features at LTER-MC station.

4.3.1 Temperature

In 2002-2009, the temperature ranged between 12.36°C (8/3/2005 at 6m depth) and 28.55 °C. (18/08/2003 at the surface).

The time-series of temperature profiles (Fig.4.2) shows the typical seasonal cycle of temperate areas: the thermal stratification begins in spring (usually April) and ends in late autumn-early winter (November-December).

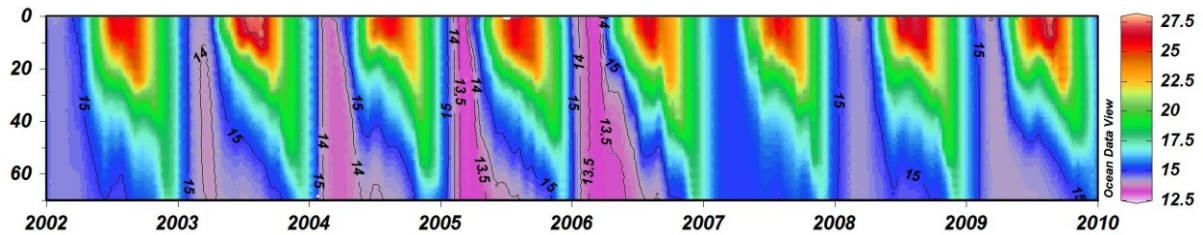


Fig. 4.2 - Time-series of temperature profiles at LTER-MC (2002-2009).

Tab 4.I- Annual minimum and maximum temperature values at surface and as mean value (0-70m) in the years 2002-2009.

Surface Temperature	2002	2003	2004	2005	2006	2007	2008	2009
Min	14.10	13.75	12.92	12.36	12.56	14.74	13.46	13.55
Max	27.09	28.55	26.65	27.41	27.49	27.61	28.15	28.42
Mean Temperature	2002	2003	2004	2005	2006	2007	2008	2009
Min	14.27	13.80	13.43	12.95	13.01	14.98	14.00	14.03
Max	20.82	19.73	20.21	19.86	20.64	20.38	19.83	19.98

The interannual variability of winter temperatures evidenced a general decrease, starting from 2002 till 2006. The lowest temperature (both at surface and mean) were recorded in 2005, even though low values lasted for a shorter time compared to 2006. In winters 2004, 2005 and 2006 the water column displayed mean temperatures lower than 13.5°C. In contrast, the winter 2007 was extremely warm, and showed temperatures always greater than 15°C, except for the survey carried out in the 27th of March. In this cruise, a mean temperature of 14.88 °C was observed in the first 37 m of the water column.

The summer 2003 displayed the highest temperatures of the investigated period, as well as the highest peak (28.55 °C) of the entire long term series (1984-2009). However, temperatures higher than 28°C were also recorded in summer 2008 and 2009. The annual maxima of the mean temperatures (in the layer 0-70m) showed the lowest value (19.73°C) in 2003, notwithstanding the high temperatures recorded at surface (Tab.4.I). As mean values are representative of the heat content along the water column, this means that a strong stratification was present. Conversely,

the highest mean value was observed in 2002 (20.82°C) although the surface temperature were not particularly high, thus indicating the warm anomaly was distributed all along the water column. The multiplicative decomposition at the selected depth (surface, 20m, 60m) and for the mean value in the layer 0-70m is presented in Fig. 4.3-4.6.

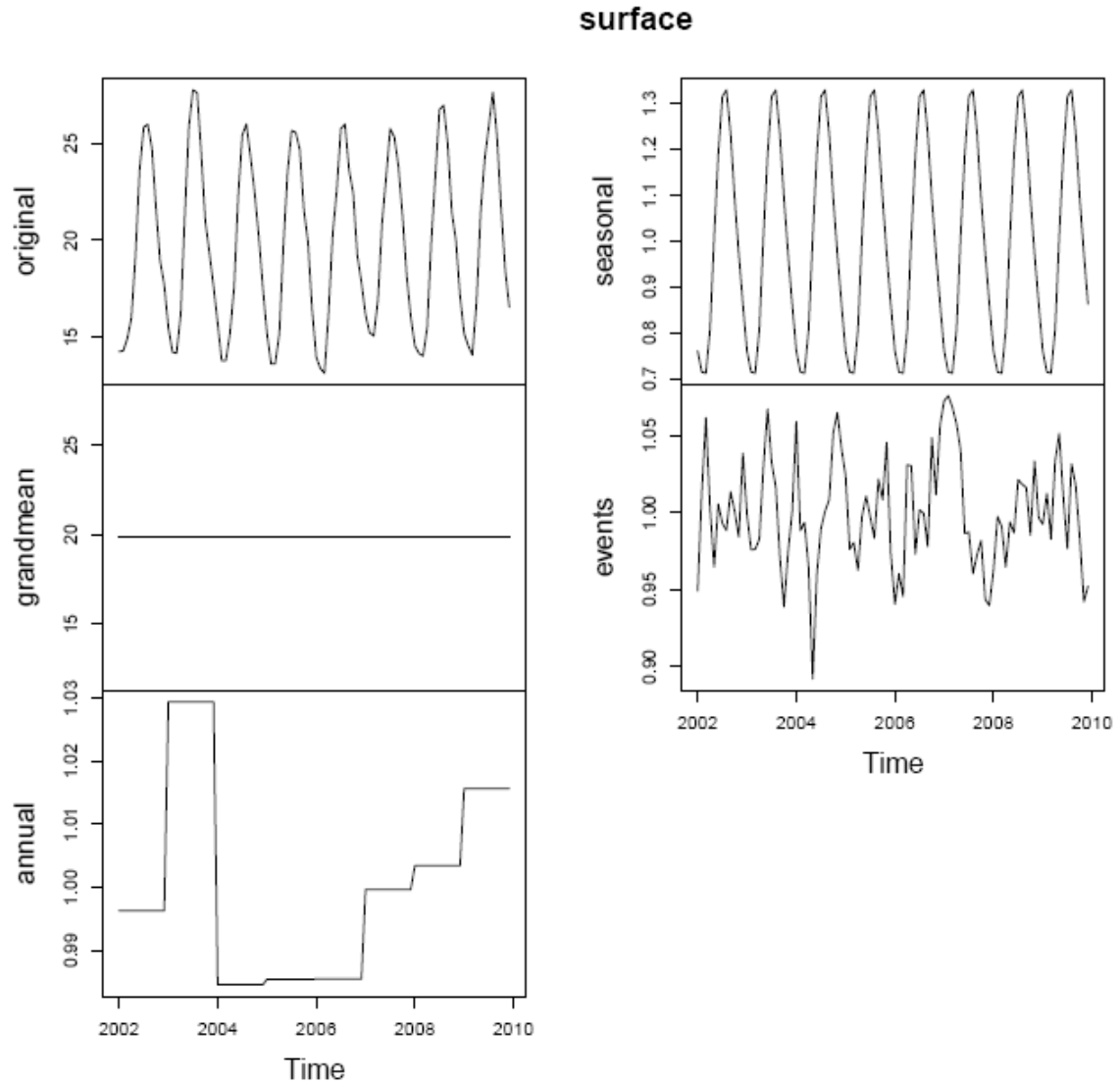


Fig. 4.3– Multiplicative decomposition of temperature at surface at LTER-MC (2002-2009).

The decomposition of temperature at surface pointed out the presence of a strong seasonal signal, characterized by an almost perfect sinusoidal pattern (Fig.4.3). The monthly minima are observed in March (14.11°C), whereas the maxima in August (26.37°C). The average mean of surface temperature in the period 2002-2009 was 19.83°C, the annual effect showed high temperatures in 2003 and low values in 2004, 2005 and 2006. The analysis of the events pointed out the presence of two main anomalies: in May 2004 the surface temperature was more than 2°C below the average value for the month, and for a long time (December 2006-May 2007) the temperature was higher than the seasonal mean.

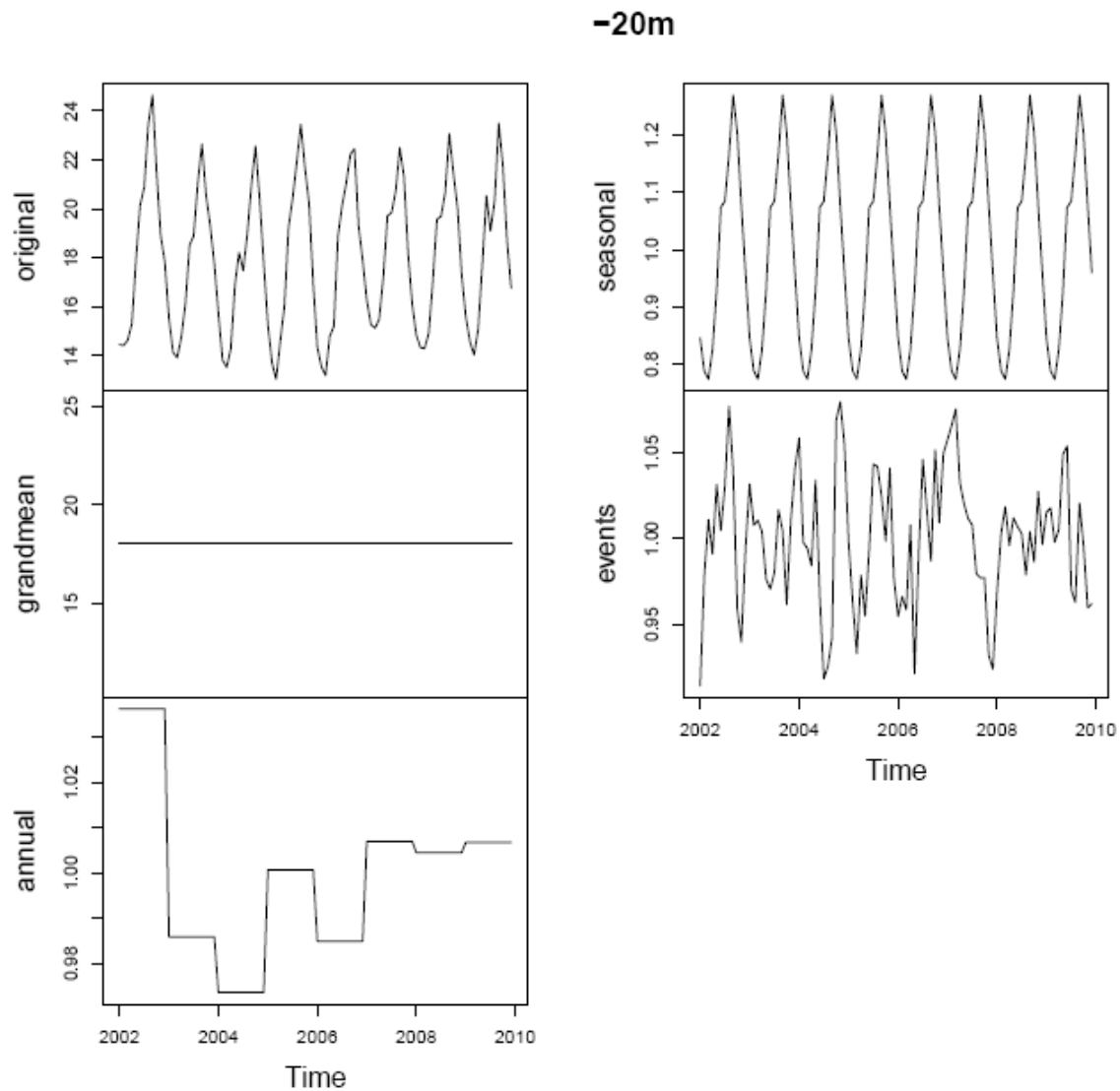


Fig.4.4 – Multiplicative decomposition of temperature at 20m depth at LTER-MC (2002-2009).

The decomposition of temperature at 20m depth showed an average value of 18.02°C, an annual effect maximum in 2002 and minimum in 2004 (Fig.4.4).

The seasonal cycle displays a more complex pattern with respect to the surface, with a more regular increase between March and June, a sort of plateau between June and July, a new warming between July and September, followed by a steep decrease starting in October. This behaviour clearly depends on the combination of diffusion, mixing and radiative heating on the temperature variability. The highest temperatures are recorded in September (22.87°C) and the lowest in March (13.97°C).

The highest events (>1.06) were observed in August 2002, October and November 2004 and in February –March 2007. More in details, for the all period December 2006 - June 2007 events >1 were observed. The lowest events (< 0.93) were detected in January 2002, July 2004, May 2006 and December 2007.

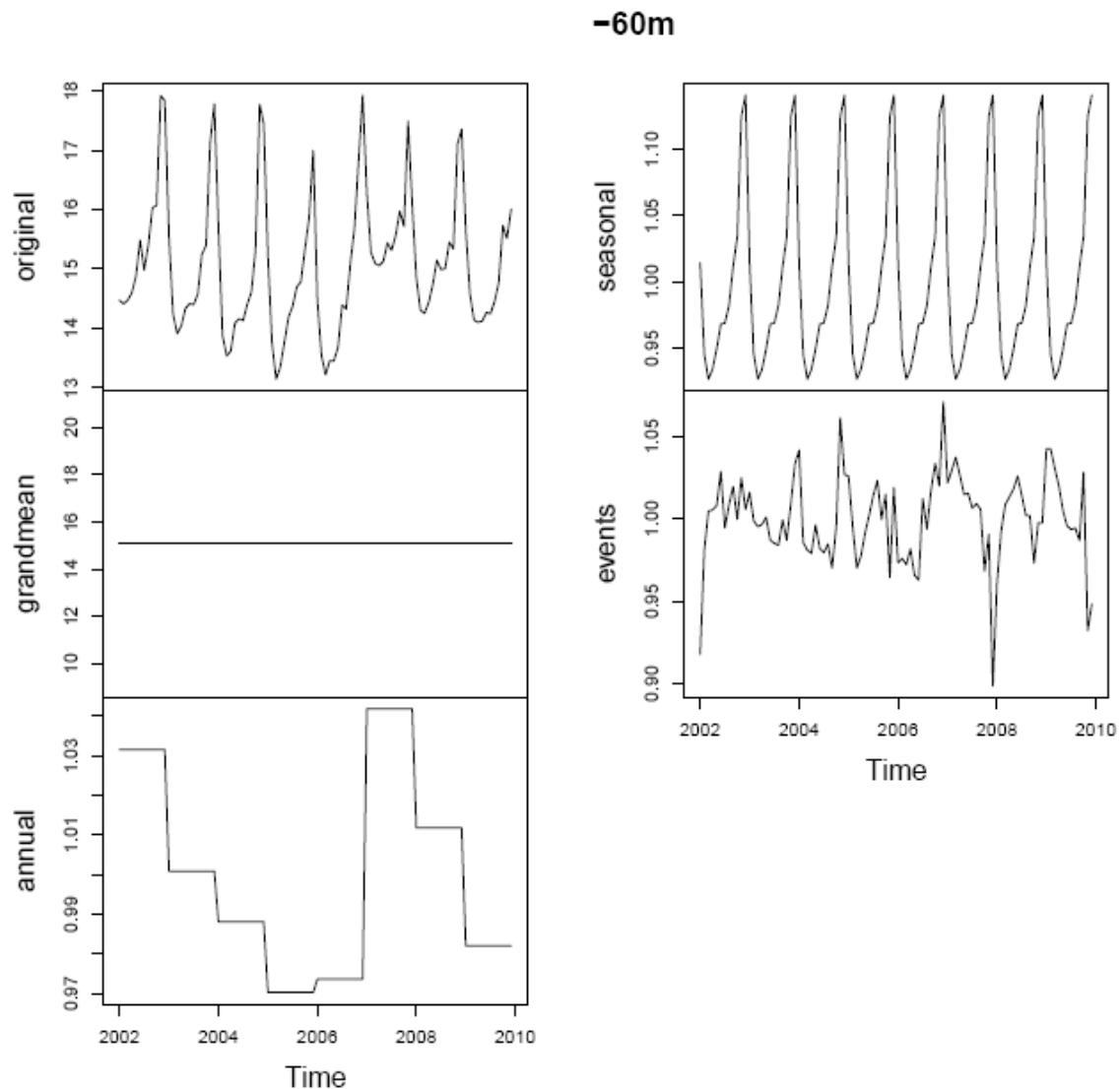


Fig.4.5 – Multiplicative decomposition of temperature at 60m depth at LTER-MC (2002-2009).

The average temperature (2002-2009) at 60m depth was 15.07 °C. The seasonal cycle again significantly departs from a sinusoidal pattern, with a more regular increase between March and June, a sort of plateau between June and July, a new gradual warming between July and October, followed by a more pronounced increase up to December, when temperature starts decreasing again. As said, this behaviour reflects the different role of diffusion, mixing and radiative heating on the temperature variability, with a predominant role of mixing starting in October, possibly dominating until March. The lowest monthly value occurs in March (13.97°C) and the highest in December (17.19 °C).

The interannual variability showed a decreasing trend from 2002 till 2006, with an abrupt discontinuity in 2007, when the highest annual effect was observed, and a new decrease from 2007 to 2009 (Fig.4.5).

All the events with the highest amplitudes were observed in late autumn-winter. The lowest events (<0.93) were recorded in winter January 2002, December 2006 and November 2009, whereas

the .the highest (>1.04) occurred in January and November 2004, December 2006 and February 2009.

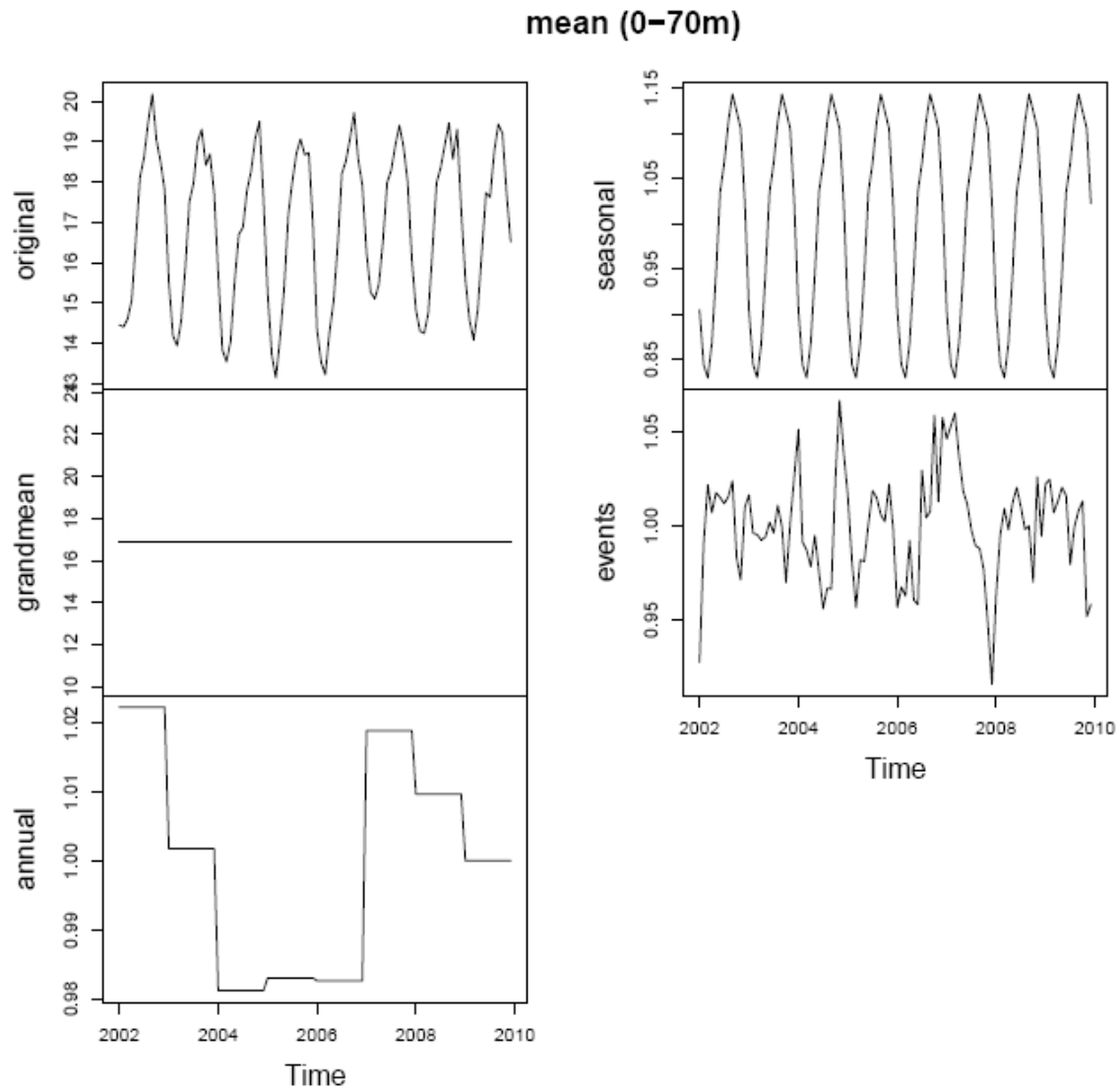


Fig.4.6 – Multiplicative decomposition of the mean temperature in the layer 0-70m at LTER-MC (2002-2009).

The mean temperature in the layer 0-70m was 16.86°C (Fig.4.6). The annual cycle displayed the lowest values of monthly temperature in March (13.98°C) and the highest in September (19.27°C). Two main lowest events were detected: in January 2002 and December 2007. The highest events were observed in January 2004, in November 2004 and for all the period July 2006 - June 2007, when events>1 were recorded, peaking in March.

4.3.2 Salinity

The salinity, in the years 2002-2009, ranged between 36.20 (14/10/2004 at surface) and 38.36 (24/10/2006 at -39m depth).

The time-series of salinity profiles (Fig.4.7) indicates the recurrence of fresh water input, usually confined in the first 10m of the water column, eventually reaching deeper layers. In spring-summer the vertical gradients of salinity are generally more pronounced compared to the rest of the year due the presence of lower salinity water in the surface layers. On contrary, the water column usually displays highest salinities and a more homogenous vertical distribution in late autumn-winter.

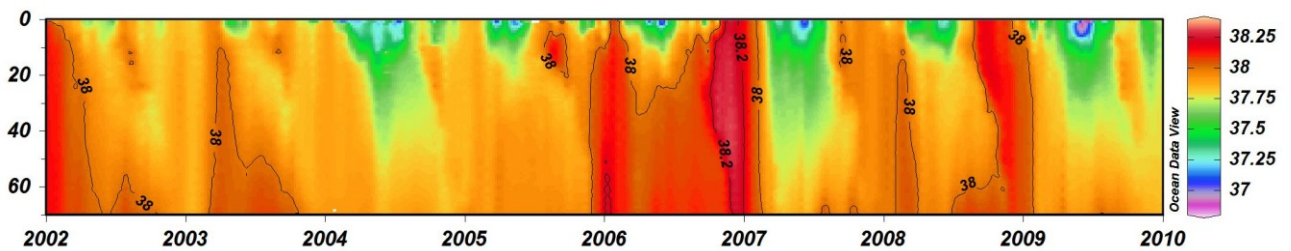


Fig. 4.7- Time-series of salinity profiles at LTER-MC (2002-2009).

The salinity variability seems to be dominated by both interannual signals and single events. Starting from 2002, a salinity decrease was observed till spring 2004. From October 2003 up to August 2005 the isoaline of 38 completely disappeared. Starting from April 2005, salinity increased again, ranging noticeable values in 2006 (>38.2). Afterwards, a new decrease in salt content was observed and the high values detected in 2006 were not recorded anymore.

Tab 4.II - Annual minimum and maximum salinity values at surface and mean (0-70m), in the years 2002 – 2009.

Surface Salinity	2002	2003	2004	2005	2006	2007	2008	2009
Min	37.25	37.29	36.20	36.76	36.65	36.86	36.93	36.63
Max	38.10	38.05	37.94	38.22	38.32	38.17	38.23	38.05
Mean Salinity	2002	2003	2004	2005	2006	2007	2008	2009
Min	37.81	37.77	37.51	37.76	37.86	37.58	37.75	37.61
Max	38.16	38.06	37.91	38.07	38.32	38.17	38.15	38.06

To investigate the relative importance of interannual, seasonal signals and the impact of single events on salinity distribution, the multiplicative decomposition was applied for the surface, 20m, 60m, and for the mean value in the layer 0-70m (Figg. 4.8-4.11).

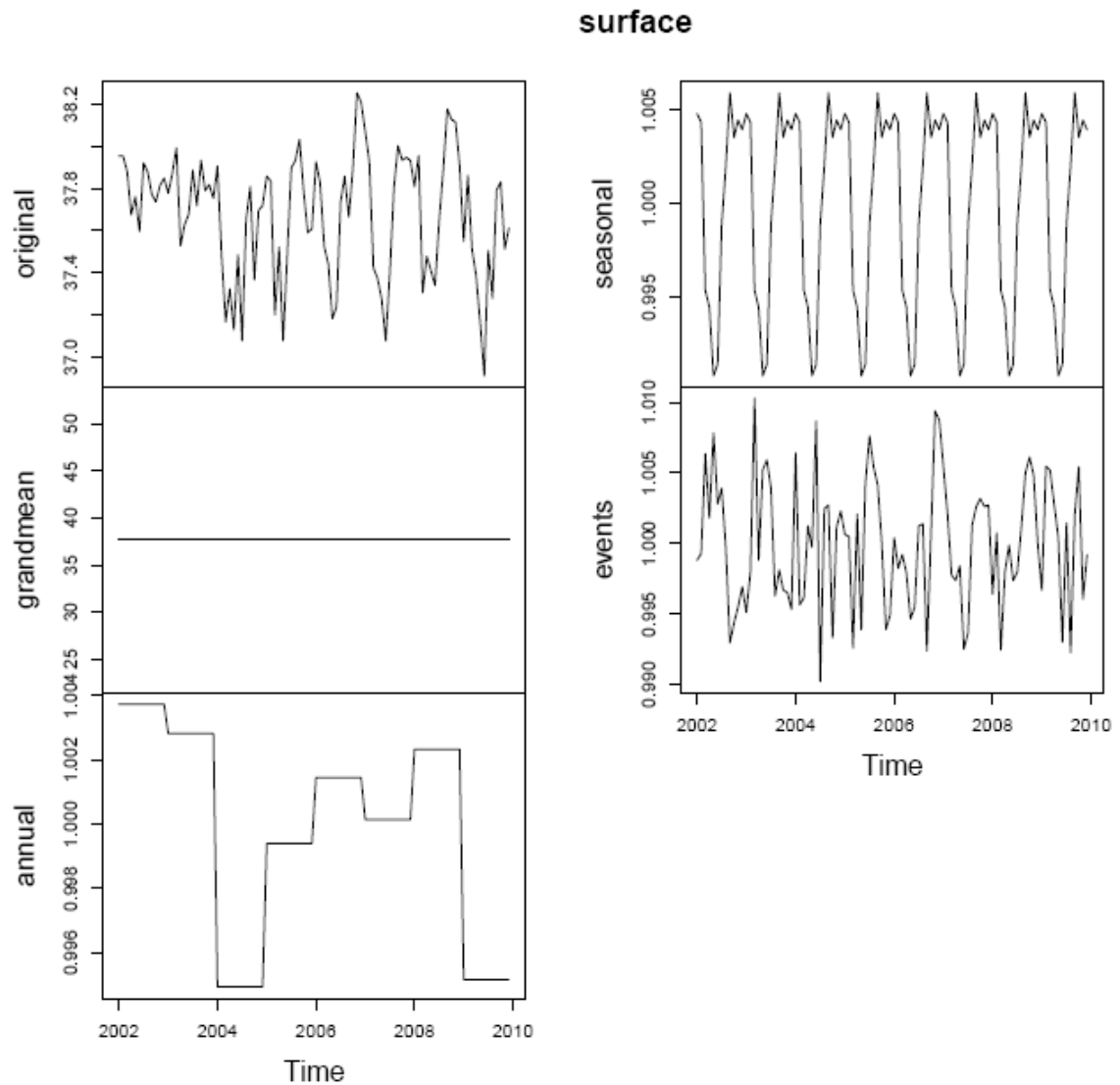


Fig. 4.8 – Multiplicative decomposition of salinity at surface at LTER-MC (2002-2009).

The average value of surface salinity was 37.66 and the monthly values ranged between 37.16 (May 2009) and 38.25 (November 2006). The seasonality was characterized by salinities lower than the grandmean from March to July and higher, rather constant, values from August to February. The lowest and highest monthly salinities were observed in May (37.33) and September (37.90), respectively. Surface salinity displayed the highest annual effects in 2002-2003 and the lowest in 2004 and 2009 (Fig.4.8).

The amplitude of the events displays higher values with respect to both the seasonal and annual effects, with the annual effect playing the less important role. The highest events (>1.008) were detected in March 2003, June 2004 and from October to December 2006. The lowest event was observed in July 2004.

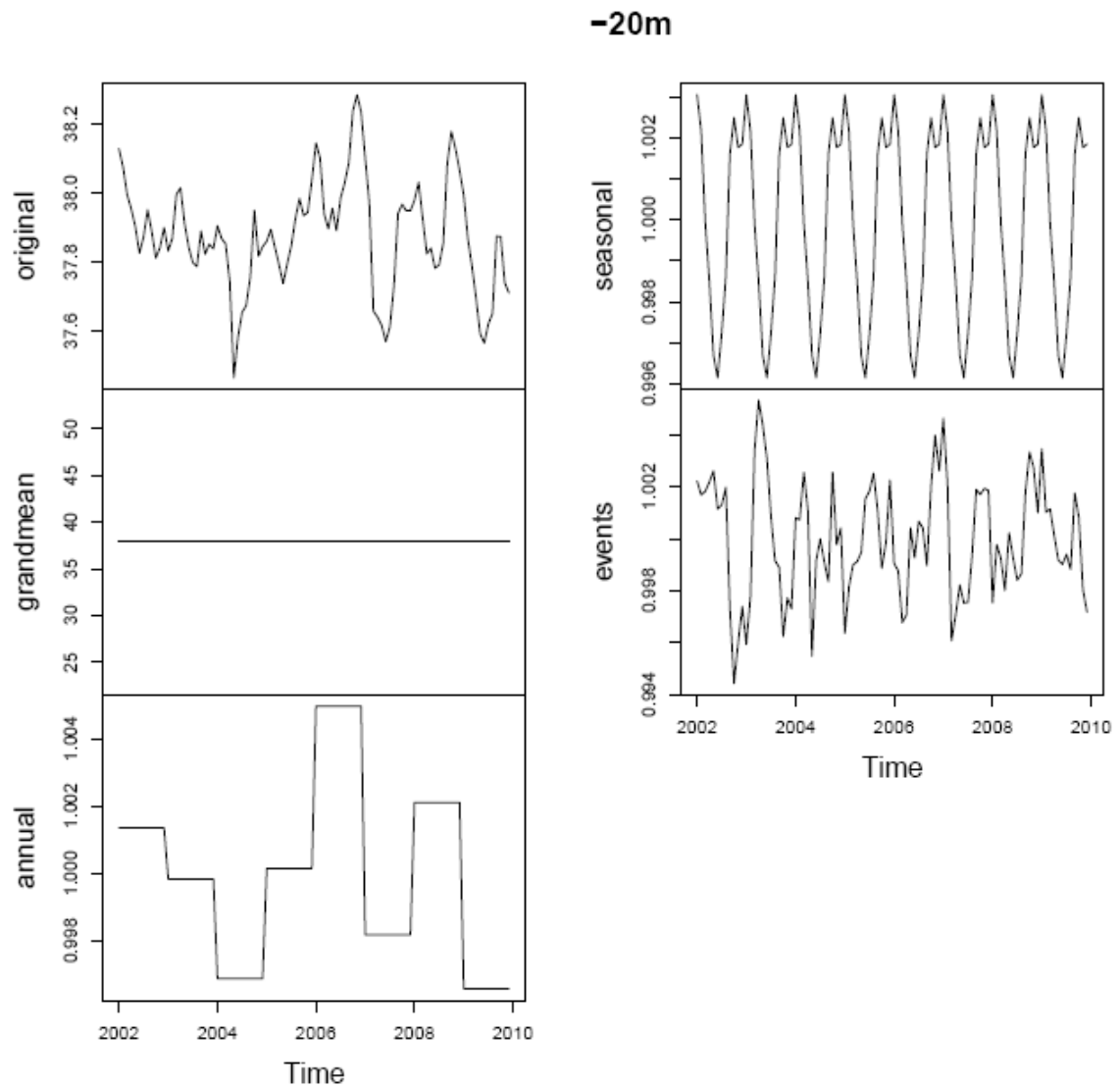


Fig. 4.9 – Multiplicative decomposition of salinity at 20m depth at LTER-MC (2002-2009).

The average salinity at 20m depth was 37.88 and ranged between 37.45 (May 2004) and 38.29 (November 2006). The annual effects showed the highest value in 2006 and lowest in 2009. The seasonal cycle displayed values lower than 37.88 from March to August and higher from September to February. The monthly minimum value was recorded in June (37.73), the maximum in January (37.99) and a second peak was observed in October (38.97).

Four high events (>1.004) were observed: April-May 2006, November 2006, January 2007. The lowest events occurred in October 2002, April 2004 and March 2007. Once again, the events present the highest multiplicative deviations with respect to both the annual and seasonal effects (Fig.4.9).

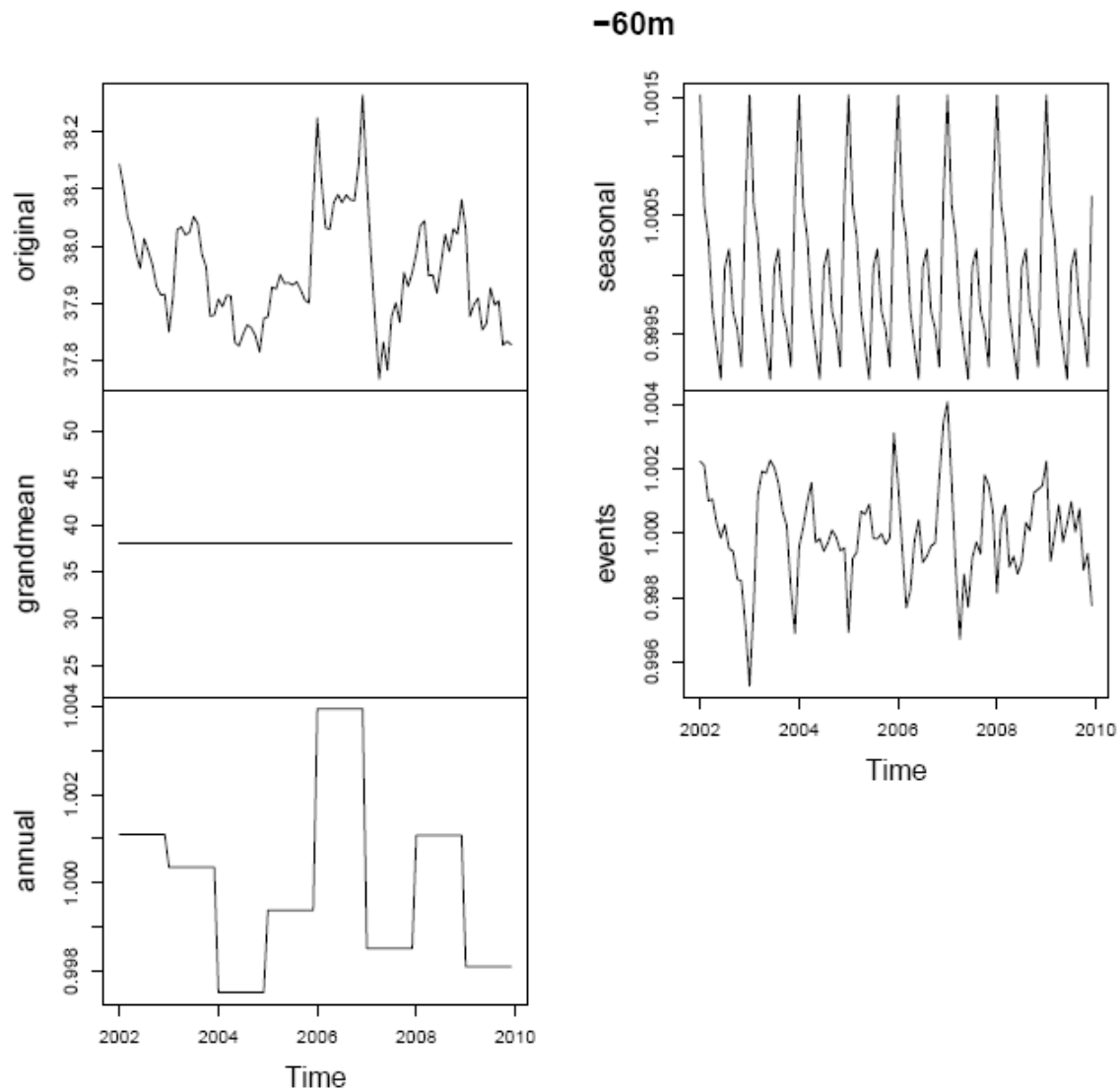


Fig. 4.10 – Multiplicative decomposition of salinity at 60m depth at LTER-MC (2002-2009).

At 60m depth, the monthly salinity ranged between 37.77 (April 2007) and 38.27 (December 2006) and displayed a mean value of 37.96. The annual effect was highest in 2007 and lowest in 2004. The seasonal cycle showed a decrease in salt content from January (38.02) till June (37.92). Afterwards, salinity increases, and a second peak is observed in August (37.97). Starting from August, salinity decreases and reaches a relative minimum in November (37.92), followed by a steep increase in December (Fig. 4.10).

The highest events were detected in December 2005, December 2006 and January 2007, whereas the lowest were observed in November and December 2002, December 2003, January 2005 and April 2007. At this depth, the events and annual effects show the highest multiplicative deviations with respect to the seasonal effect, whose amplitude is almost one order of magnitude lower.

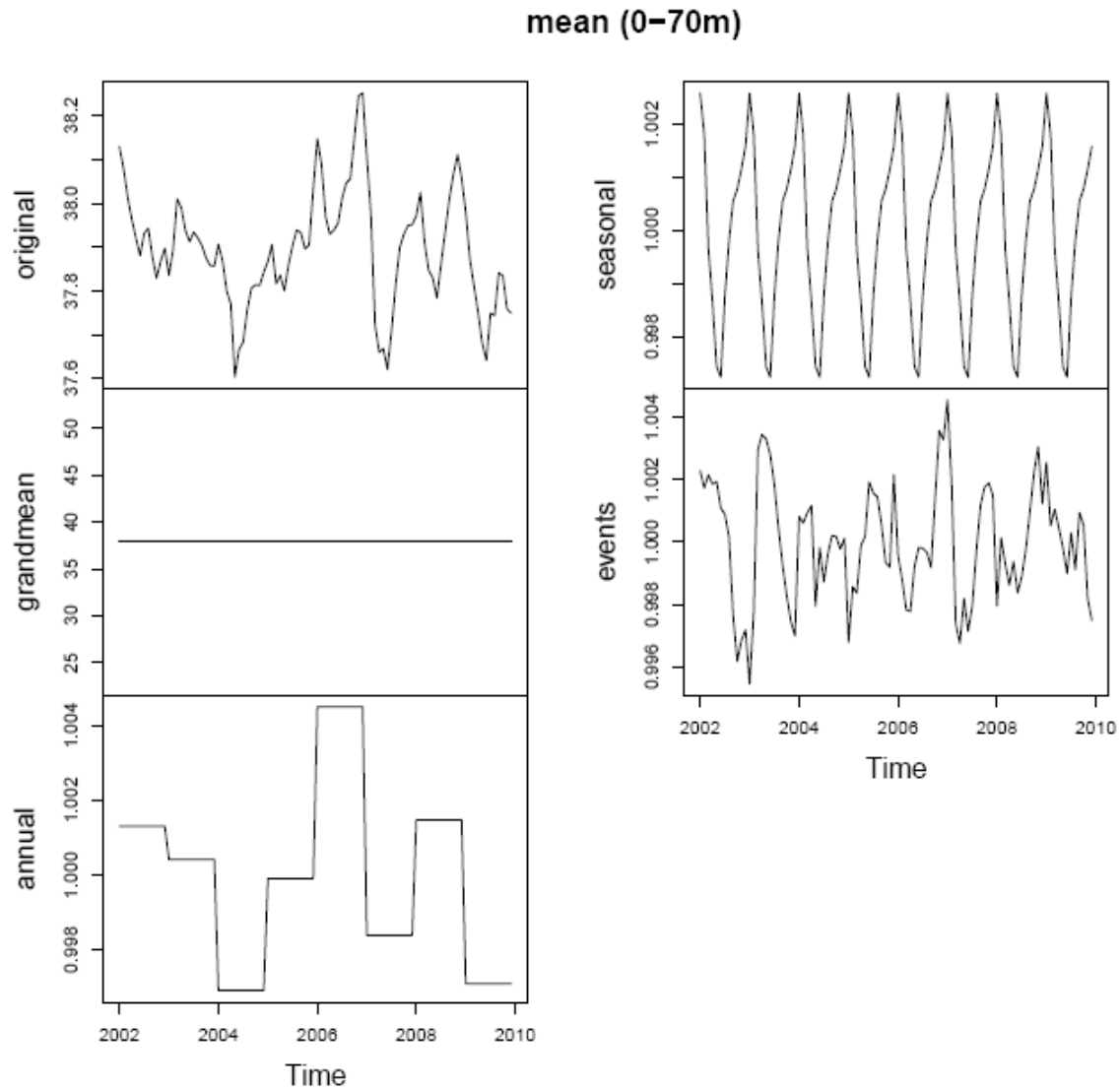


Fig. 4.11 – Multiplicative decomposition of mean salinity (0-70m) at LTER-MC (2002-2009).

The average salinity in the layer 0-70m was 37.89. The monthly salinity in years 2002-2009 displays the lowest value in May 2004 (37.70) and the highest in December 2006 (38.25). The seasonality shows a decrease from January, which is the annual maximum (37.99) till June (37.90), which is the annual minimum. From June to December the salinity increases again, with a higher slope in the period June-August compared to August-December (Fig 4.11).

The highest events were observed from March to June 2003 and from November 2006 to January 2007. The lowest events were detected October-November 2002, January 2005 and April 2007.

On the mean values, seasonality seems to play a slightly less important role with respect to events and annual effects.

4.3.3 Dissolved Inorganic Nitrogen (DIN)

The DIN at LTER-MC station ranged between 0.02 mmol^{-3} and 21.93 mmol^{-3} , recorded at 5m depth (04/08/2003) and at surface (28/03/2006), respectively.

The highest DIN concentrations were generally observed in the upper part of the water column (0-10m) and the lowest in the intermediate layer (20-40m). The DIN in the deeper layer (50-70m) exhibited higher concentrations compared to the intermediate, but did not reached the values observed in the upper layer (Fig 4.12).

The three layers show different seasonal patterns: in the upper layer the highest concentrations are generally recorded in winter or spring (mainly in March), in the intermediate layer in winter (January-February), whereas in the deeper layer two distinct maxima are observed, the first in winter (January-February) and the second in late spring (mainly in May).

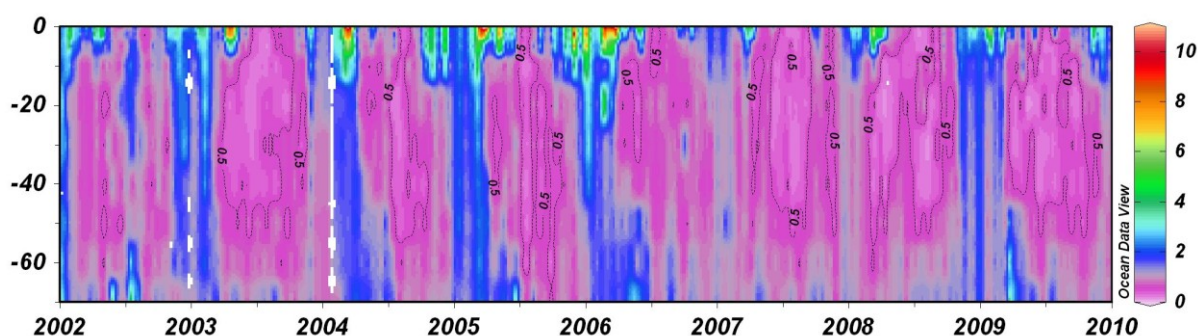


Fig. 4.12– Time-series of DIN profiles (mmol m^{-3}) at LTER-MC (2002-2009).

Tab 4.III - Annual minimum, maximum and average DIN concentrations (mmol m^{-3}) at surface and mean integrated (0-70m) at LTER-MC (2002-2009).

Surface DIN	2002	2003	2004	2005	2006	2007	2008	2009
Min	0.22	0.05	0.11	0.13	0.19	0.08	0.08	0.08
Max	9.59	13.56	13.29	18.87	21.93	6.36	9.73	9.29
AVG	1.40	1.04	1.37	1.68	1.58	0.87	1.10	1.14
Mean integrated DIN	2002	2003	2004	2005	2006	2007	2008	2009
Min	0.39	0.30	0.26	0.22	0.50	0.24	0.35	0.32
Max	2.61	2.83	2.61	3.74	3.87	1.82	2.26	2.60
AVG	1.20	0.82	1.10	1.26	1.24	0.78	0.92	0.92

A remarkable interannual variability is evidenced by the data reported in Tab.4.III More in details, 2005 and 2006 were characterized by highest DIN concentrations at the surface, as well as in the whole 0-70m layer. In 2008, the maximum and mean concentrations were sensibly lower than in the other years.

The composition of DIN differs in the three different layers: ammonia predominates in the upper and intermediate layers, whereas nitrate is the main constituent in the deeper layer. The relative contribution of nitrite increases with depth, even if it constitutes a relatively small fraction of the DIN in each layer (Fig 4.13).

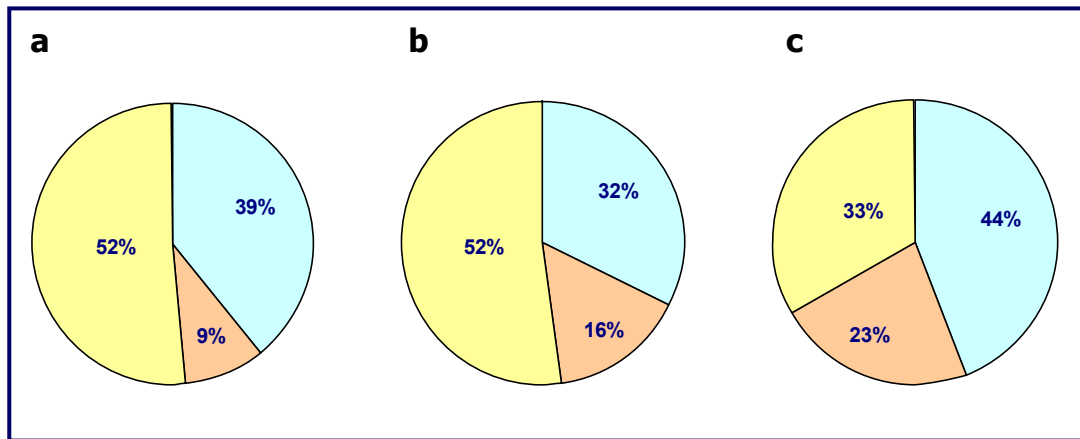


Fig. 4.13– Composition of DIN (NH_4 , NO_3 and NO_2) in the **a**) upper (0-10m), **b**) intermediate (20-40m) and **c**) deeper layer (50-70m) at LTER-MC (2002-2009).

In order to characterize the seasonality and the dynamics of the DIN, its two major forms (nitrate and ammonia) were analyzed in depth in the following sections.

4.3.3.1 Nitrate

Nitrate concentrations at LTER-MC station ranged between values below the detection limit (0.01 mmol^{-3}) and 9.92 mmol^{-3} , recorded at surface (28/03/2006).

The NO_3 concentrations displays a pronounced vertical gradient: the highest concentrations are detected at surface (mainly in late winter-early spring) and sharply decrease with depth, even if the bottom layer (60-70m) often shows high concentrations, mainly during spring, with values eventually higher than those measured at the surface. To get an idea of the number of times the concentrations at 70m depth were significantly higher than those at the surface, we fixed threshold difference of 0.25 mmol^{-3} between the two values (chosen empirically). The deep maximum was observed in 130 surveys (35% of the total observations). In winter, due to the vertical mixing, the surface NO_3 is diluted along the water column and high concentrations are detected at all depths.

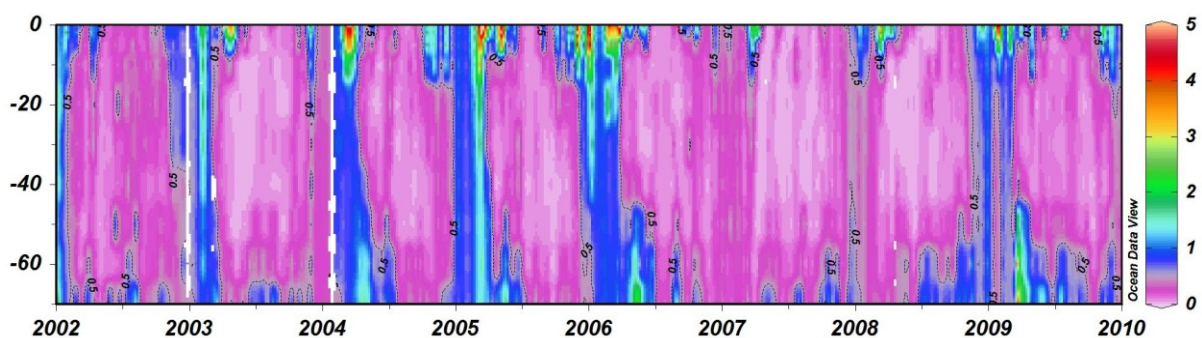


Fig. 4.14 – Time-series of NO_3 profiles (mmol m^{-3}) at LTER-MC (2002-2009)

The surface annual maxima of NO_3 increased considerably from 2002 till 2006, then suddenly decreased in 2007, slightly increasing again afterwards (Tab. 4:IV)

The mean integrated concentrations displayed the highest value in 2005 and the lowest in 2007.

Tab 4.IV - Annual minimum and maximum NO₃ concentrations (mmol m⁻³) at surface and mean integrated values (0-70m) in the years 2002-2009.

Surface NO₃	2002	2003	2004	2005	2006	2007	2008	2009
Min	0.03	<0.01	0.02	0.01	0.01	<0.01	<0.01	<0.01
Max	2.10	5.31	6.18	8.62	9.92	4.98	5.48	5.70
Mean integrated NO₃								
Min	0.04	0.03	0.05	0.01	0.04	0.02	0.03	0.07
Max	1.44	1.67	1.34	2.55	1.64	0.70	1.16	1.83

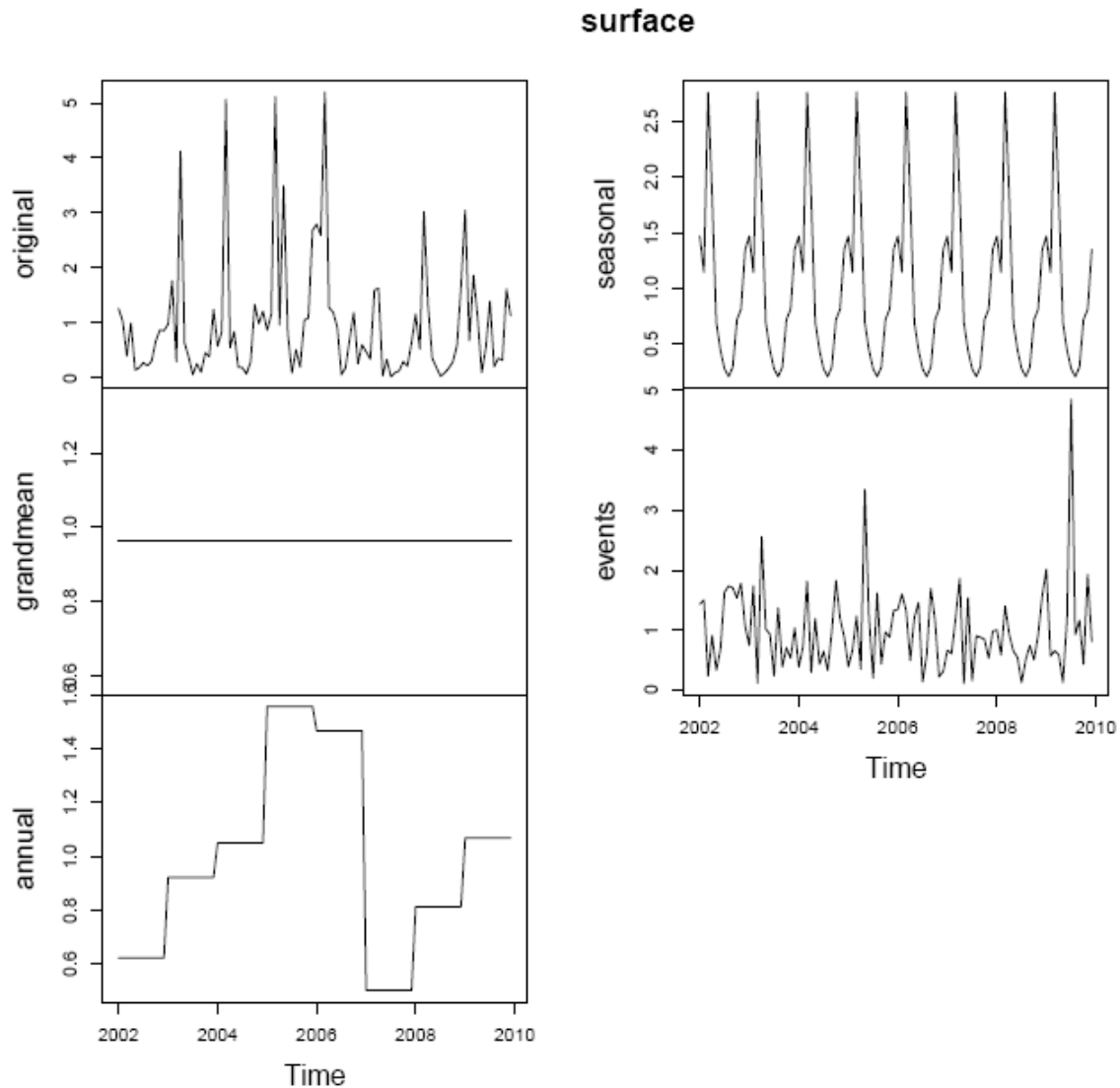


Fig. 4.15 – Multiplicative decomposition of NO₃ monthly concentrations at surface at LTER-MC (2002-2009).

The mean NO₃ concentration at surface was 0.96 mmol⁻³ and the monthly values ranged between 0.021 (July 2007) and 5.19 (March 2006) mmol⁻³. The annual effect was highest in 2005 and 2006 and lowest in 2007. The concentrations were highest from January to April, reaching the maximum in March (2.65 mmol⁻³). NO₃ concentration declined from March to August (0.02 mmol⁻³) and then raised again till December(Fig. 4.15).

Annual effects appear to be less important with respect to seasonality and events, with the latter significantly exceeding the seasonal amplitude in three cases (April 2003, May 2005 and July 2009).

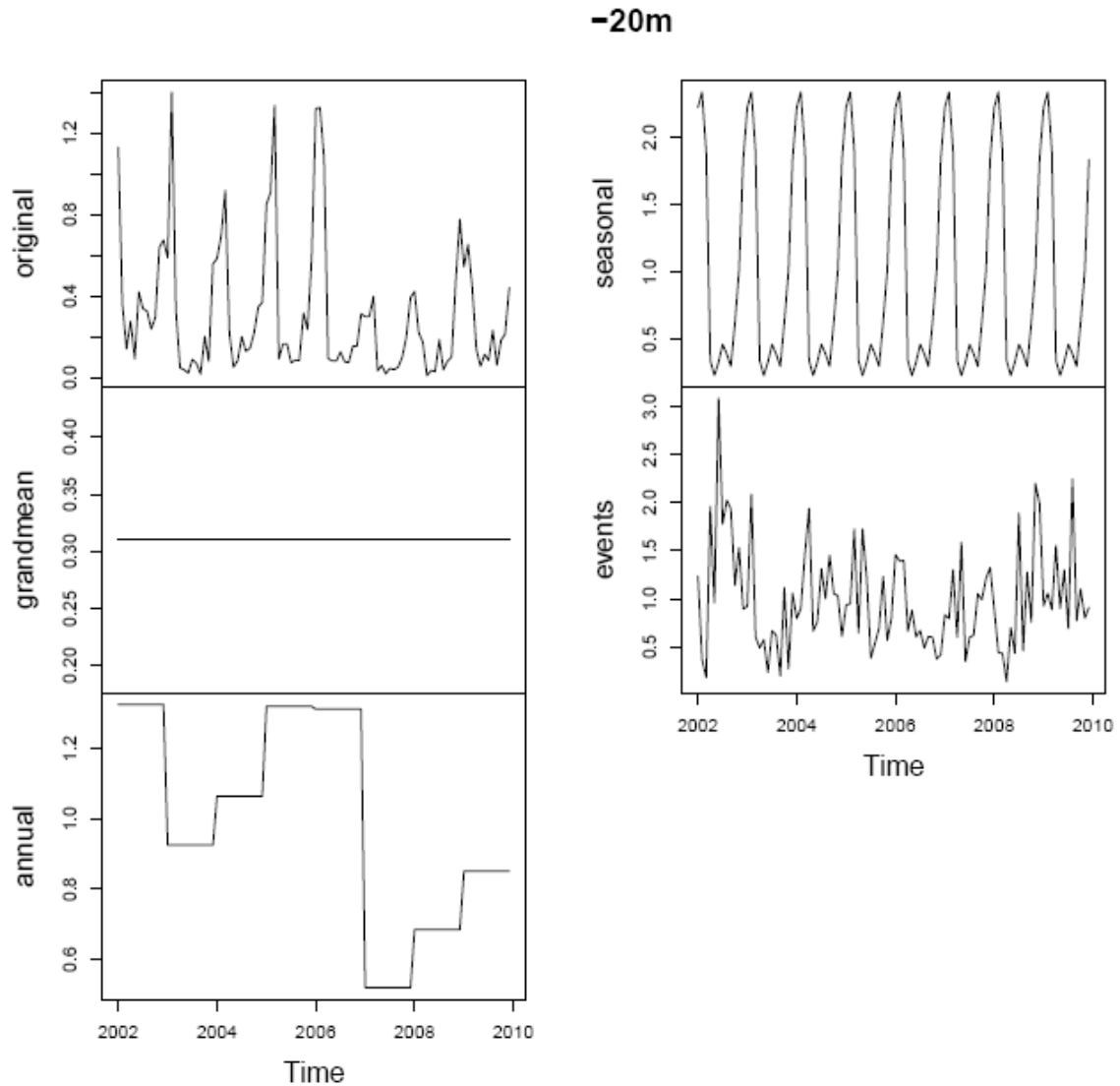


Fig. 4.16 – Multiplicative decomposition of NO_3 monthly concentrations at 20m depth at LTER-MC (2002-2009).

The mean concentration of NO_3 at 20 m depth was 0.31 mmol^{-3} , and the monthly values were in the range 0.01 mmol^{-3} (April 2008) and 1.40 mmol^{-3} (February 2003).

The annual effect was very high in 2002, 2005 and 2006 and sensibly low in 2007.

The seasonal effect leads to NO_3 concentrations greater than 0.5 mmol^{-3} from January to March, and lower than 0.15 mmol^{-3} from April to September. Afterwards increasing concentrations are observed up to December. The minimum is observed in May (0.07 mmol^{-3}) and the maximum in February (0.73 mmol^{-3}).

Events and seasonality again play a comparable role, while annual effects are less relevant (Fig. 4.16).

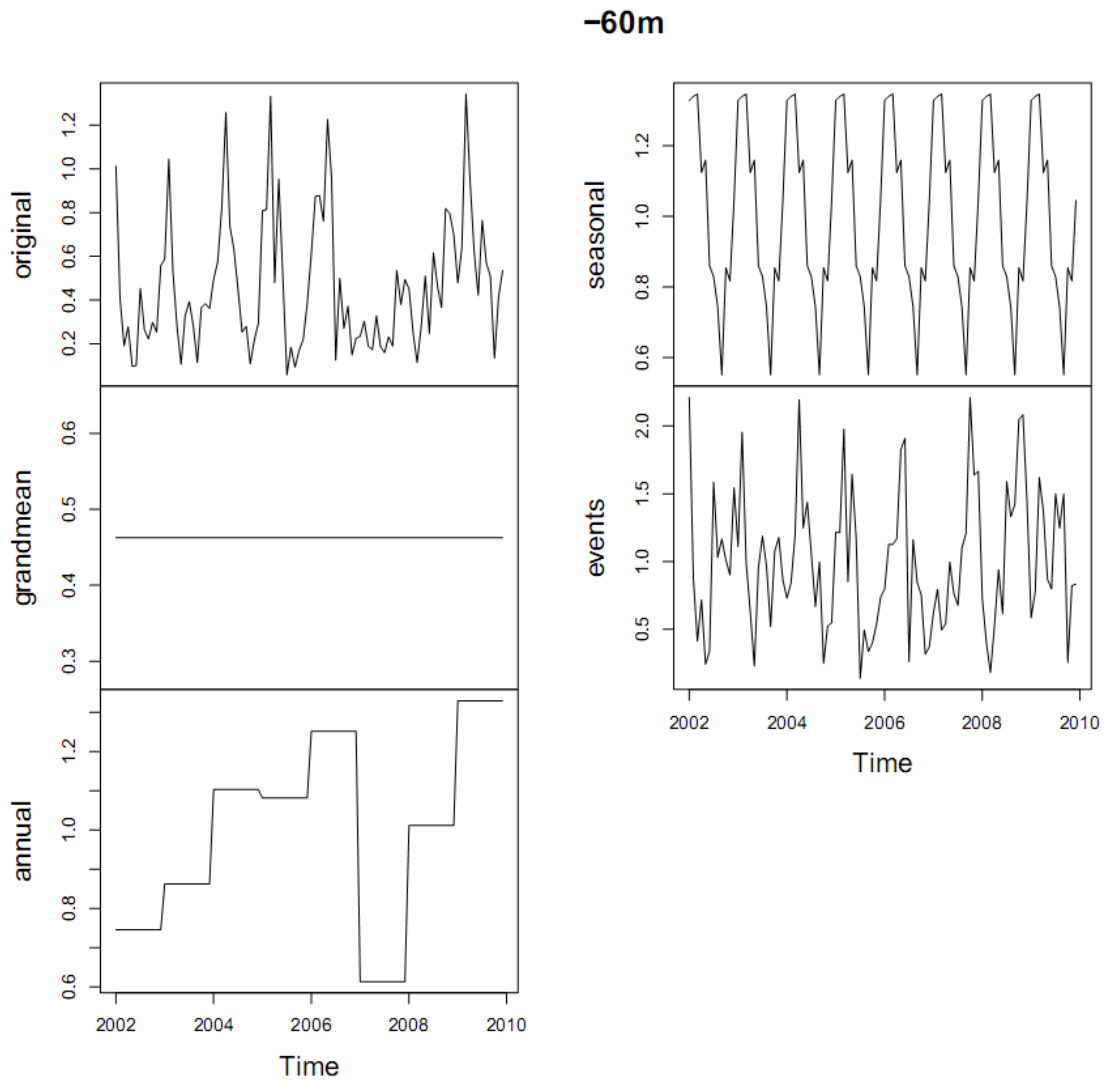


Fig. 4.17 – Multiplicative decomposition of NO_3 monthly concentrations at 60m depth at LTER-MC (2002-2009).

The average concentration at 60m depth in the period 2002-2009 was 0.46 mmol m^{-3} , the monthly values were in the range 0.58 mmol m^{-3} (July 2005) and 1.34 mmol m^{-3} (March 2009). The annual effects pointed out an increasing concentration from 2002 to 2006, a strong decrease in 2007 and then a new increase up to 2009, when the strongest annual effect was observed.

Seasonally, the highest mean concentrations are observed from January to March ($> 0.6 \text{ mmol m}^{-3}$), and the lowest mean monthly value (0.25 mmol m^{-3}) is recorded in September.

The amplitude of the events exceeds the annual and seasonal effects. Five main high events were identified: January 2002, April 2004, October 2007, October-November 2008. The main low events were observed in October 2004 and March 2008 (Fig.4.17).

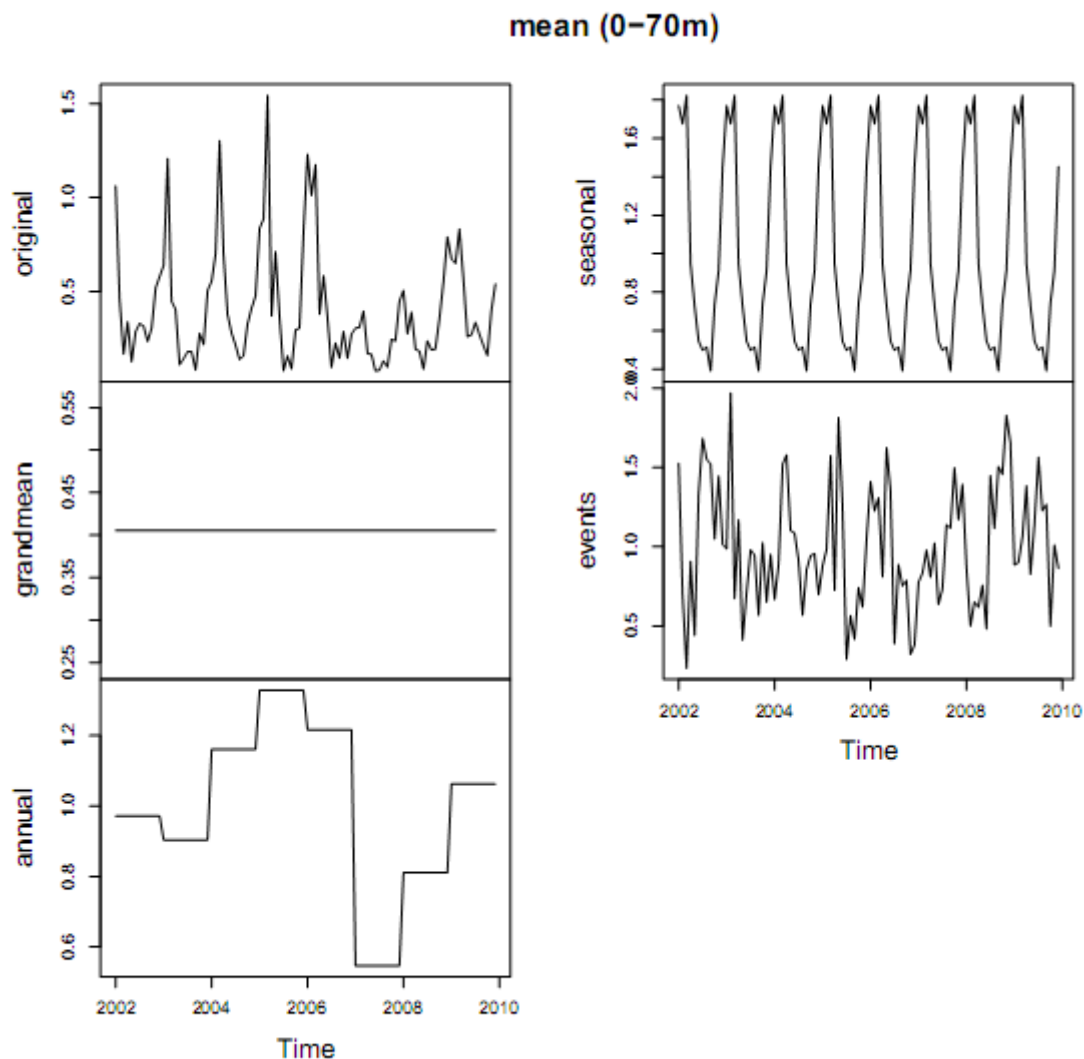


Fig. 4.18 – Multiplicative decomposition of monthly integrated NO_3 means in the layer 0-70m at LTER-MC (2002-2009).

The values of monthly integrated mean in the layer 0-70m ranged between 0.08 mmol m^{-3} (July 2005) and 1.54 mmol m^{-3} (March 2005) and the average value was 0.41 mmol m^{-3} (Fig. 4.18).

The years 2004, 2005 and 2006 show the highest annual effects, whereas the 2008 presents the lowest. The seasonal pattern was characterized by high values from January to March, when the annual maximum (0.74 mmol m^{-3}) is reached, afterwards NO_3 concentrations steeply declines and remains lower than the grandmean till November. The annual minimum is September (0.16 mmol m^{-3}), even if sensibly low concentrations are detected in all the period June-September. Starting from September NO_3 concentrations raise again.

Events and seasonality play a comparable role, while annual effects are less relevant in modulating the NO_3 concentrations, as mean values integrated over the 0-70m layer. The highest events were observed in February 2003, May 2005 and November 2008, the lowest in March 2002, July 2005 and November 2006.

4.3.3.2 Ammonia

The ammonia concentration ranged between values below the detection limit (0.01 mmol m^{-3}) and $13.12 \text{ mmol m}^{-3}$, recorded at surface (30/03/2005). A strong vertical gradient was present, more pronounced than that observed for nitrate. In fact, the differences between the NH_4 concentrations at surface and at 70m depth were lower than $-0.25 \text{ mmol m}^{-3}$ only in 12 sampling stations (3% of the total observations).

The highest concentrations were generally detected in the upper layer of the water column (0-10m), whereas a drastic decrease was observed below 10m (Fig. 4.19).

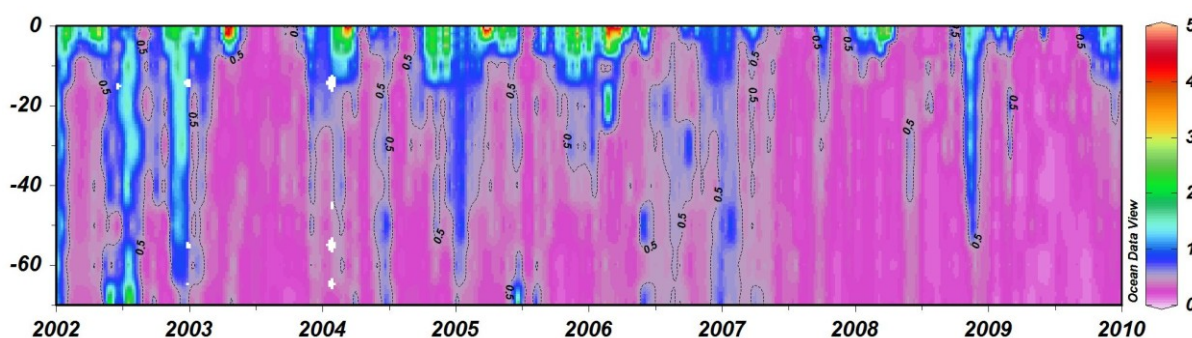


Fig. 4.19– Temporal variability of NH_4 concentrations (mmol m^{-3}) at LTER-MC (2002-2009)

The surface annual maxima of NH_4 were sensibly higher in 2005 and 2006 ($>11 \text{ mmol m}^{-3}$), whereas, starting from 2007 a drastic reduction was observed ($<4.5 \text{ mmol m}^{-3}$). The annual maxima of the mean integrated values (0-70m) did not display the same temporal pattern: the maximum in 2005 was similar to that observed in 2008, despite the strong differences recorded at surface (Tab. 4.V).

Tab. 4.V - Annual minimum and maximum NH_4 concentrations (mmol m^{-3}) at surface and mean integrated values (0-70m) in the years 2002-2009.

Surface NH_4	2002	2003	2004	2005	2006	2007	2008	2009
Min	0.17	0.05	0.14	0.05	0.16	<0.01	0.04	0.06
Max	7.72	8.25	6.89	13.12	11.21	3.41	4.49	3.46
Mean integrated NH_4	2002	2003	2004	2005	2006	2007	2008	2009
Min	0.20	0.10	0.15	0.14	0.23	0.10	0.10	0.07
Max	2.05	1.19	1.18	1.36	1.94	0.94	1.28	0.97

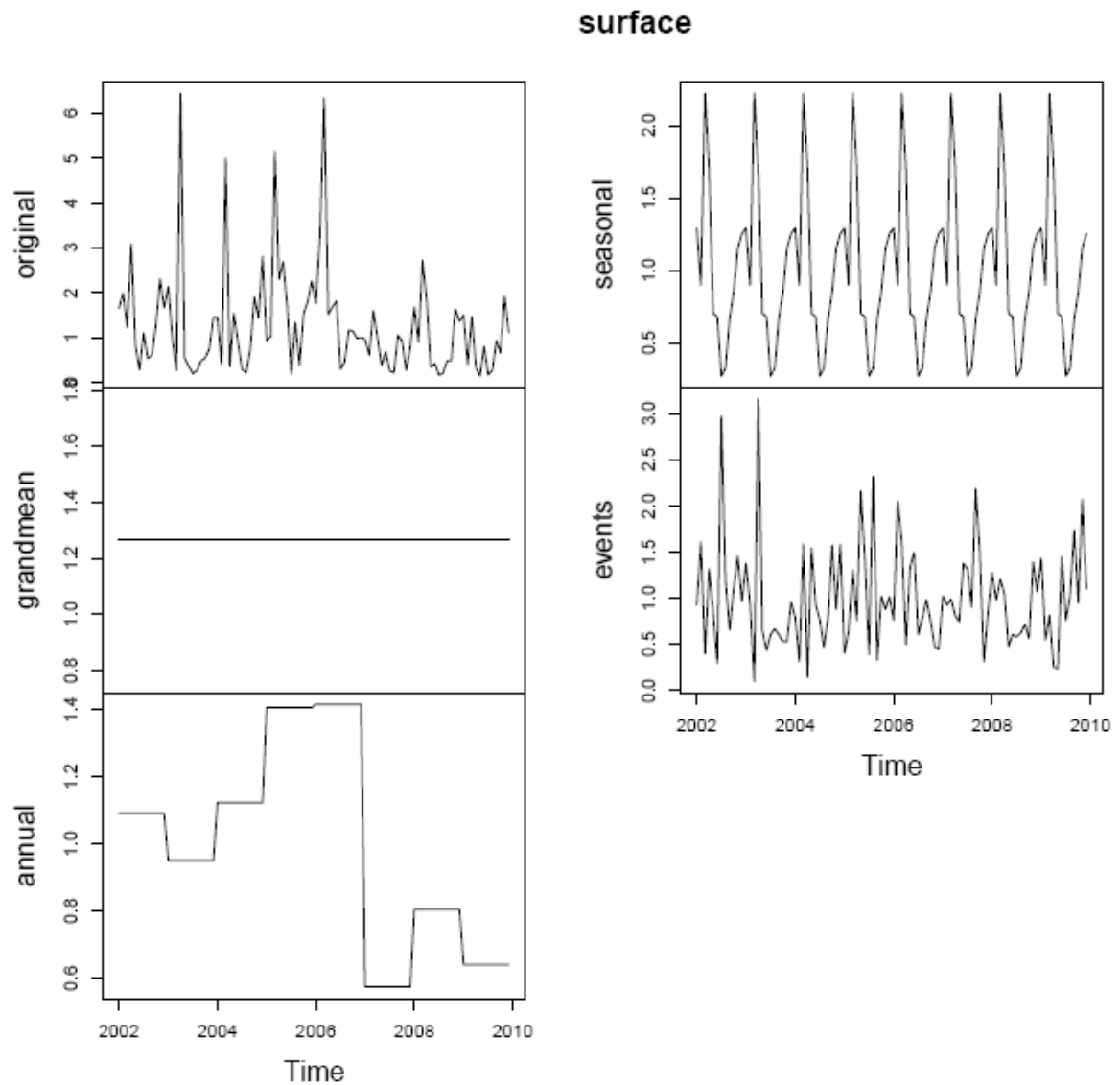


Fig. 4.20 – Multiplicative decomposition of NH_4 monthly concentrations at 60m depth at LTER-MC (2002-2009).

The monthly concentrations of ammonia at surface were within the range $0.13 - 6.45 \text{ mmol m}^{-3}$, recorded in May 2009 and April 2003, respectively. The mean value 2002-2009 was 1.26 mmol m^{-3} and the annual effects were more evident in 2005 and 2006 (high values) and 2007 and 2009 (low values).

The seasonality is characterized by low concentrations from May to October and by high values from November to April. The maximum annual value (2.81 mmol m^{-3}) is observed in March and the minimum (0.33 mmol m^{-3}) in July.

Two high-intensity events were observed in July 2002 and April 2003. The lowest events were detected in March 2003, April 2004 and April-May 2009 (Fig. 4.20).

All effects seem to play a comparable weight in modulating ammonia concentrations at the surface (Fig.4.20).

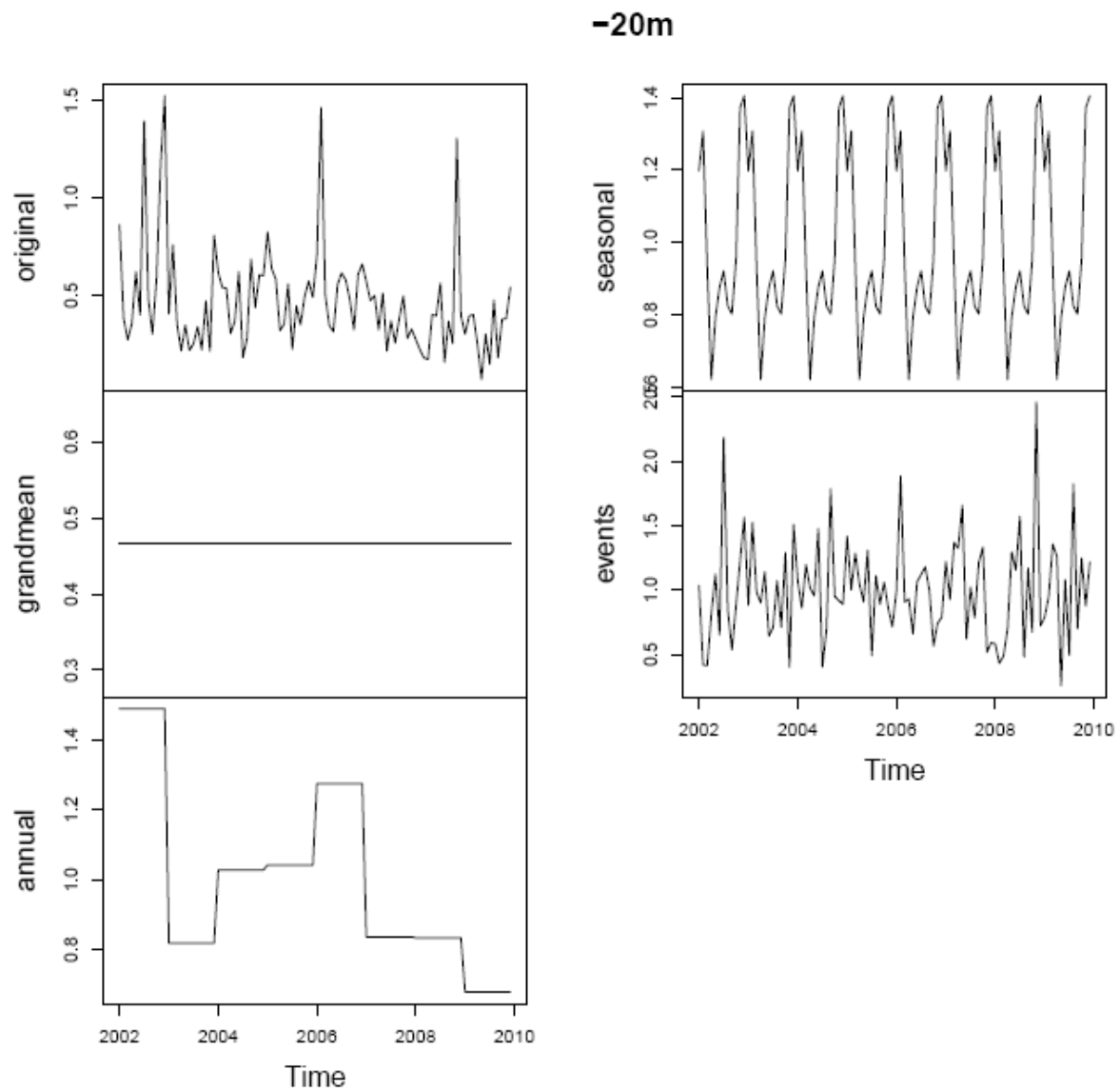


Fig. 4.21 – Multiplicative decomposition of NH_4 monthly concentrations at 60m depth at LTER-MC (2002-2009).

The grandmean for the period 2002-2009 was 0.47 mmol m^{-3} and the minimum and maximum values were $0.064 \text{ mmol m}^{-3}$ (May 2009) and 1.52 mmol m^{-3} (December 2002), respectively.

The annual effect was high in 2002 and low 2003 and 2009 (Fig. 4.21).

The seasonal cycle is smoother compared to the surface and displays values lower than the grandmean from March till November and higher from November up to February. The monthly highest concentration occurs in December (0.65 mmol m^{-3}) and the lowest in April (0.29 mmol m^{-3}). Events present the highest amplitude compared to seasonal and annual effects.

The highest events were observed in July 2002 and November 2008, whereas the lowest in November 2003, July 2004 and May 2009 (corresponding to the minimum monthly value in the investigated period).

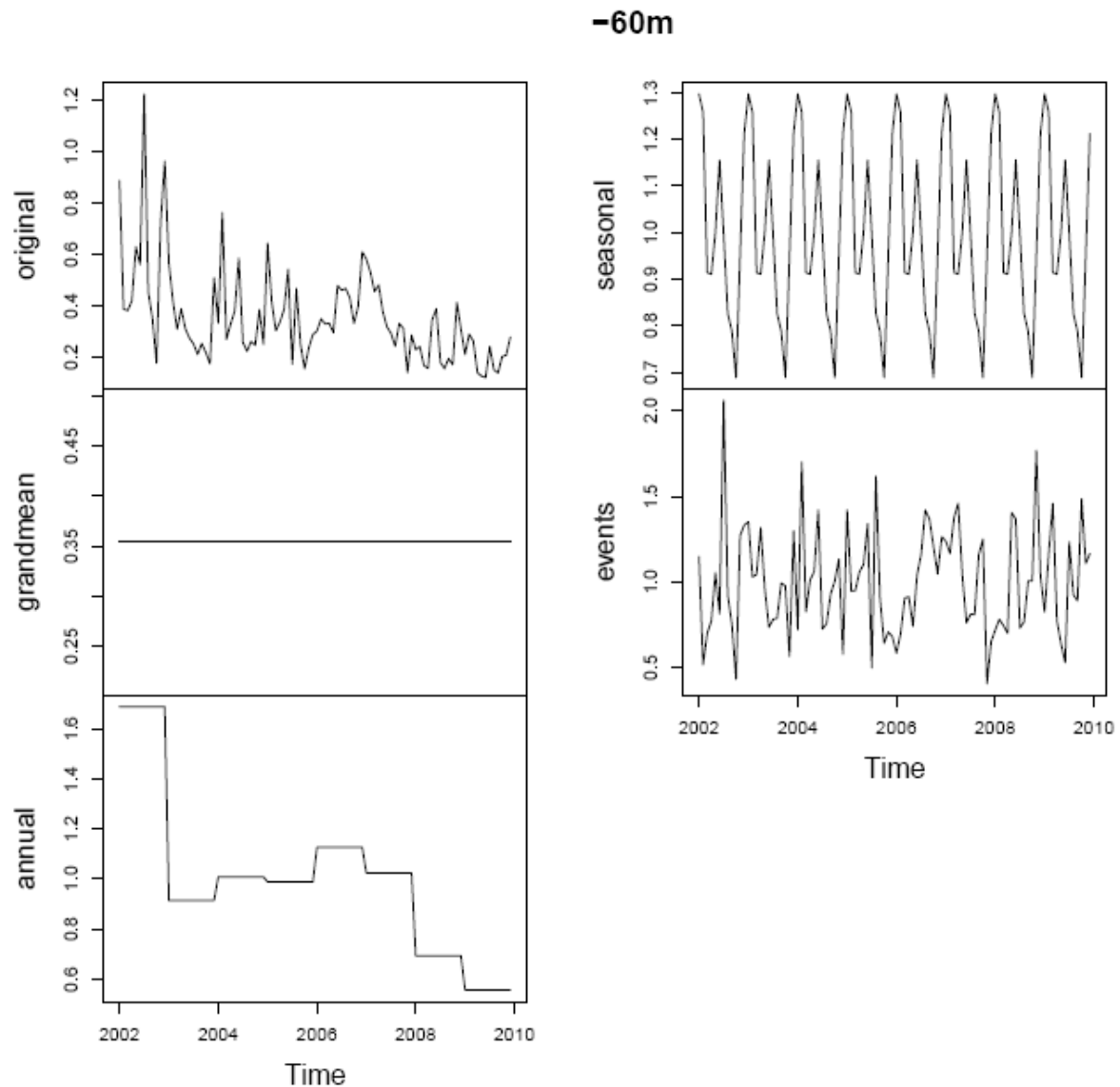


Fig. 4.22 – Multiplicative decomposition of NH_4 monthly concentrations at 60m depth at LTER-MC (2002-2009).

The concentrations of NH_4 at 60m depth ranged between 0.12 mmol m^{-3} (May 2009) and 1.23 mmol m^{-3} (July 2002), with an average value of 0.35 mmol m^{-3} . The annual effect was high in 2002, quite constant from 2003 till 2007, and drastically decreased in 2008 and 2009 (Fig. 4.22).

The seasonality is less pronounced than the annual and event effects. It displays decreasing values from December till March. Afterwards, rising concentrations are observed up to June, which presents a relative maximum. From June till October, NH_4 levels decrease again, whereas increasing concentrations are observed from November up to December. The seasonal maximum is recorded in January (0.46 mmol m^{-3}) and the minimum in October (0.24 mmol m^{-3}).

The two highest events occurred in July 2002, corresponding to the highest monthly observed value, and in May 2009. The lowest events were observed in October 2002, July 2005 and November 2007.

mean (0-70m)

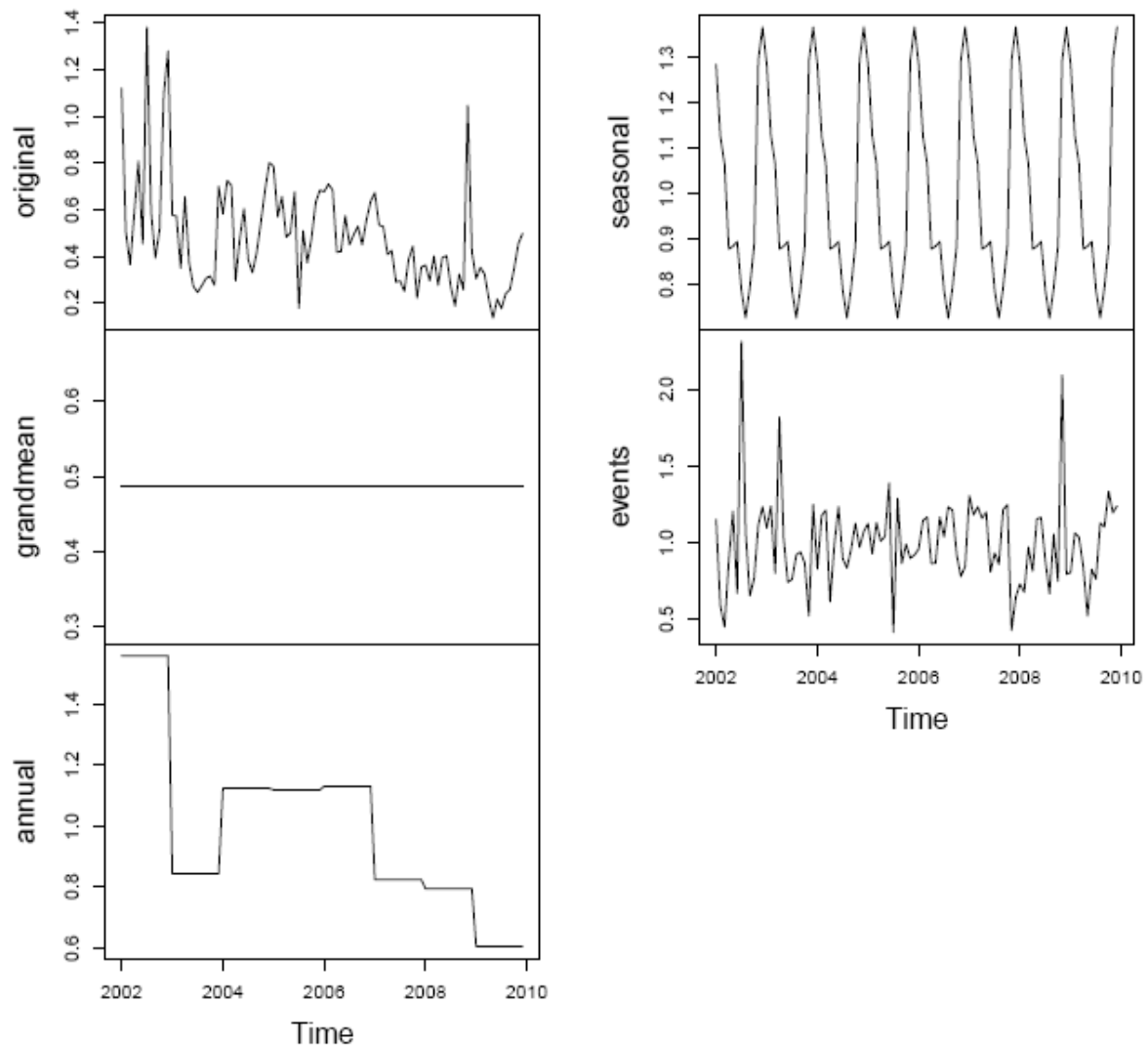


Fig. 4.23 – Multiplicative decomposition of monthly integrated NH_4 means in the layer 0-70m at LTER-MC (2002-2009).

The monthly integrated NH_4 values were within the range 0.14 - and 1.38 mmol m^{-3} , observed in May 2009 and July 2002, respectively. The average concentration for the entire period of study was 0.49 mmol m^{-3} . The annual effects were extremely pronounced in 2002 and 2009 (Fig.4.23).

The seasonality shows decreasing concentrations from January to August. In this latter month, the minimum annual value (0.35 mmol m^{-3}) is observed. From August up to the end of the year, the ammonia levels raise, reaching the maximum (0.66 mmol m^{-3}) in December.

In July 2002, April 2003 and November 2008 the highest events were observed, whereas the lowest were observed in March 2002, July 2005 and November 2007.

The strongest variations on the mean integrated values of ammonia are related to single events. However, interannual changes are clearly observed, while seasonality appears to play a role comparable to the average events.

4.3.4 Phosphate

The phosphate data are available only from 2003.

The phosphate concentration ranged between values below the detection limit (0.01 mmol m^{-3}) and 0.55 mmol m^{-3} , recorded at surface(07/06/2006).

The vertical distributions of phosphate was characterized by higher concentrations in the upper (0-10m) and lower (60-70m) parts of the water column, compared to the intermediate layer (10-60 m). However, as already observed for nitrate and ammonia, the highest concentrations were generally recorded at surface (Fig.4.24). Choosing $0.025 \text{ mmol m}^{-3}$ as threshold value, the difference between phosphate concentration at surface and at 70m was lower than this value only in 7 samples, corresponding to 2% of the total observations.

Over the years, a clear reduction of the phosphate concentration in the intermediate layer was recorded. Values below $0.025 \text{ mmol m}^{-3}$, rarely observed in 2003, were measured more and more frequently starting from 2007.

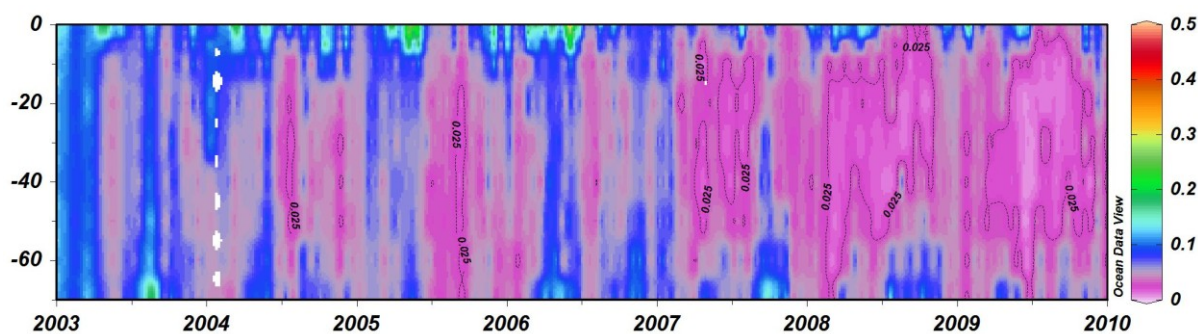


Fig. 4.24– Time-series of PO_4 profiles (mmol m^{-3}) at LTER-MC (2003-2009)

The annual surface maxima were significantly higher in 2005 and 2006, whereas the maximum values of the integrated mean did not display a pronounced interannual variability; the only exception was year 2008, which displayed a sensibly lower maximum (Tab.4.IV).

Tab 4.VI - Annual minimum and maximum PO_4 concentrations (mmol m^{-3}) at surface and mean integrated values (0-70m) in the years 2003-2009.

Surface PO_4	2003	2004	2005	2006	2007	2008	2009
Min	<0.01	<0.01	<0.01	<0.01	<0.01	<0.01	<0.01
Max	0.31	0.26	0.43	0.55	0.26	0.22	0.27
Mean integrated PO_4	2003	2004	2005	2006	2007	2008	2009
Min	0.02	0.02	0.01	0.03	0.02	0.01	0.01
Max	0.13	0.12	0.11	0.13	0.11	0.06	0.09

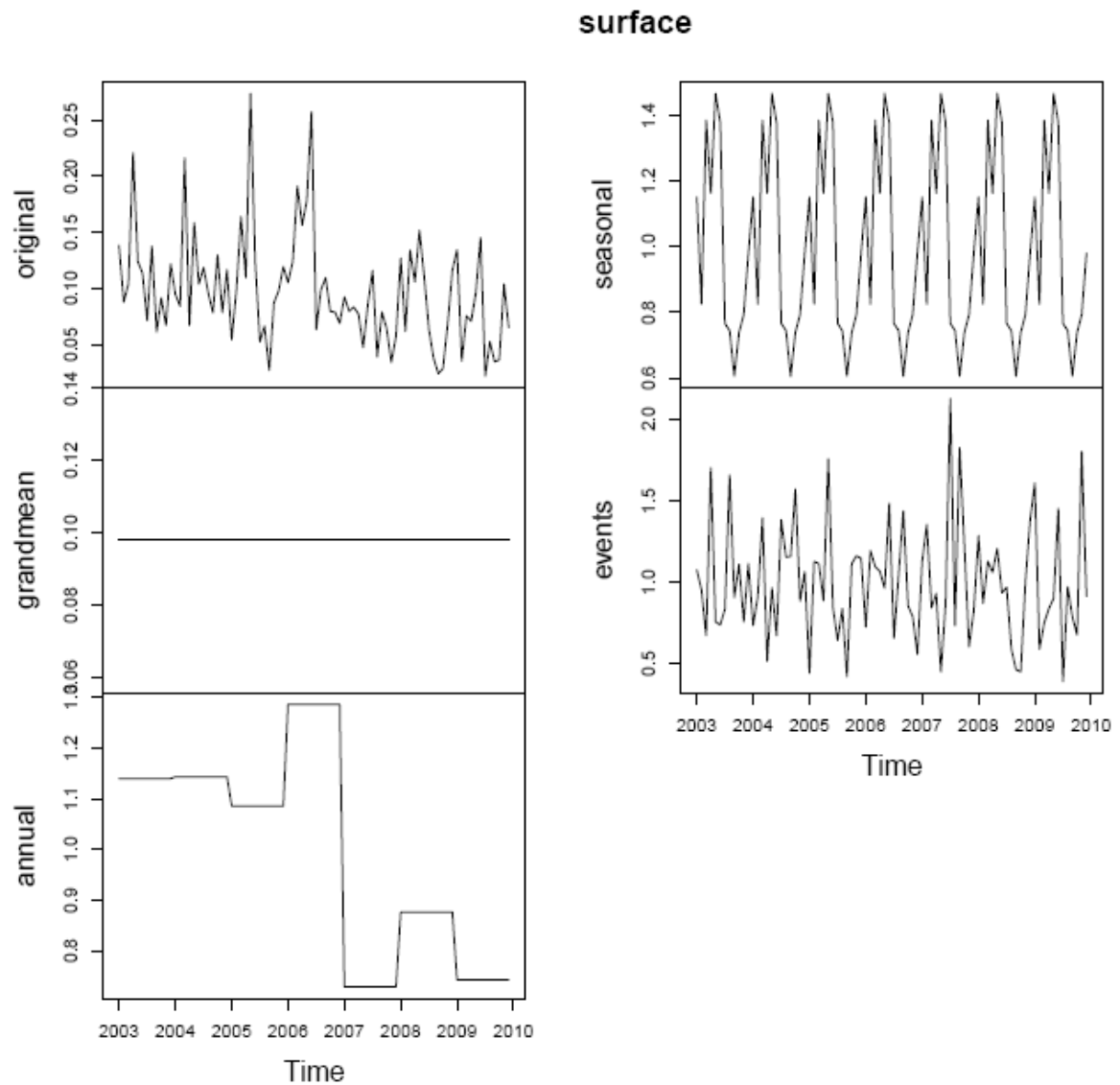


Fig. 4.25 – Multiplicative decomposition of PO_4 monthly concentrations at surface at LTER-MC (2003-2009).

The monthly PO_4 concentrations in 2003-2009 were observed in the range $0.027\text{-}0.27 \text{ mmol m}^{-3}$ and showed a mean value of 0.98 mmol m^{-3} . The highest value was observed in May 2005 and the lowest in September 2005. The annual effect displayed a drastic discontinuity in 2007: from 2002 till 2006 the higher annual values were recorded, whereas starting from 2007 sensibly lower concentrations were detected (Fig. 4.25).

The seasonality displays the highest values in the first six months of the year and the lowest from July to December. The highest monthly value (0.14 mmol m^{-3}) is observed in May and the lowest (0.06 mmol m^{-3}) in September.

The highest effects were observed in July and September 2007 and the lowest in September 2005 (minimum value 2003.2009) and July 2009. The events amplitude ranges among higher values than both the annual and seasonal effects.

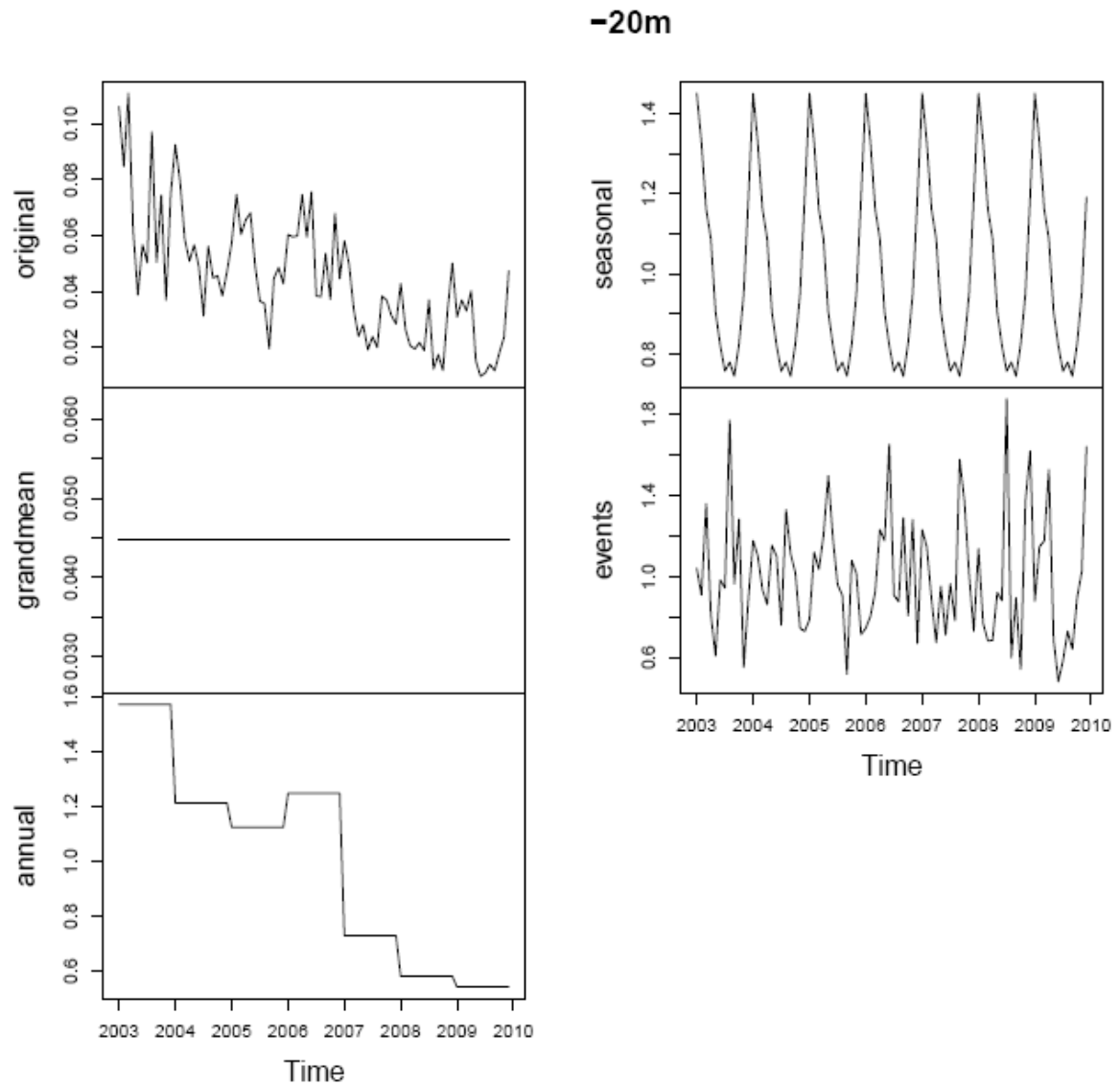


Fig. 4.26 – Multiplicative decomposition of PO_4 monthly concentrations at 20m depth at LTER-MC (2003-2009).

The original monthly concentration of PO_4 were within the range $0.01\text{-}0.11 \text{ mmol m}^{-3}$, recorded in March 2003 and April 2009, respectively. The average value was $0.04511 \text{ mmol m}^{-3}$.

The phosphate concentrations at 20m depth displayed a clear decreasing trend, clearly emerging in the annual effect values, which attained at 1.57 in 2003, around 1.2 in the years 2004-2005-2006 and sensibly <1 starting from 2007 (Fig. 4. 26).

The seasonal cycle presents decreasing values starting from January, which represents the annual maximum (0.65 mmol m^{-3}), up to July. From July till September the monthly concentrations are almost constant and display low values. From September, which is the annual minimum ($0.033 \text{ mmol m}^{-3}$) the PO_4 levels increase till the December.

The two highest effects were both detected in summer (August 2003 and July 2008), the lowest in September 2005 and June 2009.

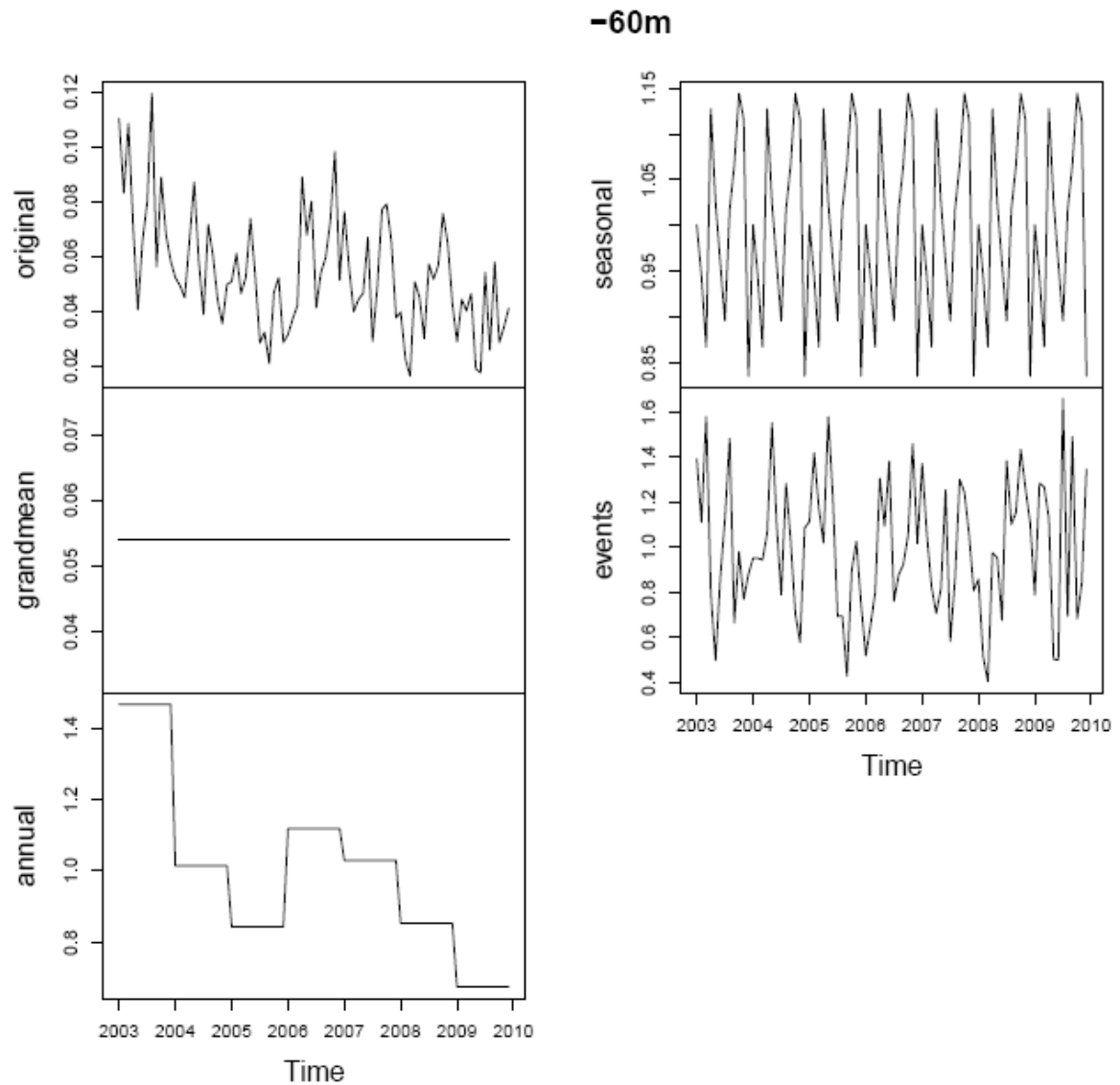


Fig. 4.27 – Multiplicative decomposition of PO_4 monthly concentrations at 60m depth at LTER-MC (2003-2009).

The concentrations of PO_4 at 60m depth ranged between 0.16 mmol m^{-3} (March 2008) and 0.12 mmol m^{-3} (August 2003), whereas the mean value was $0.054 \text{ mmol m}^{-3}$ (Fig.4.27).

The highest annual effect was observed in 2003 and the lowest in 2009.

The annual effect displays higher values than the seasonality, meaning that the interannual variability influenced the PO_4 concentrations sensibly more than the seasonal cycle. The seasonal signal is characterized by very low amplitudes with two relative maxima (April and September-October) and three minima (March, July and December). The annual minimum and maximum were observed in December ($0.045 \text{ mmol m}^{-3}$) and October ($0.062 \text{ mmol m}^{-3}$), respectively.

The highest events were observed in March 2003, May 2009 and July 2009. The lowest events were detected in July 2005 and March 2008, which was the minimum monthly value observed. Events and interannual effects dominate the phosphate variability in the lower layer.

mean (0-70m)

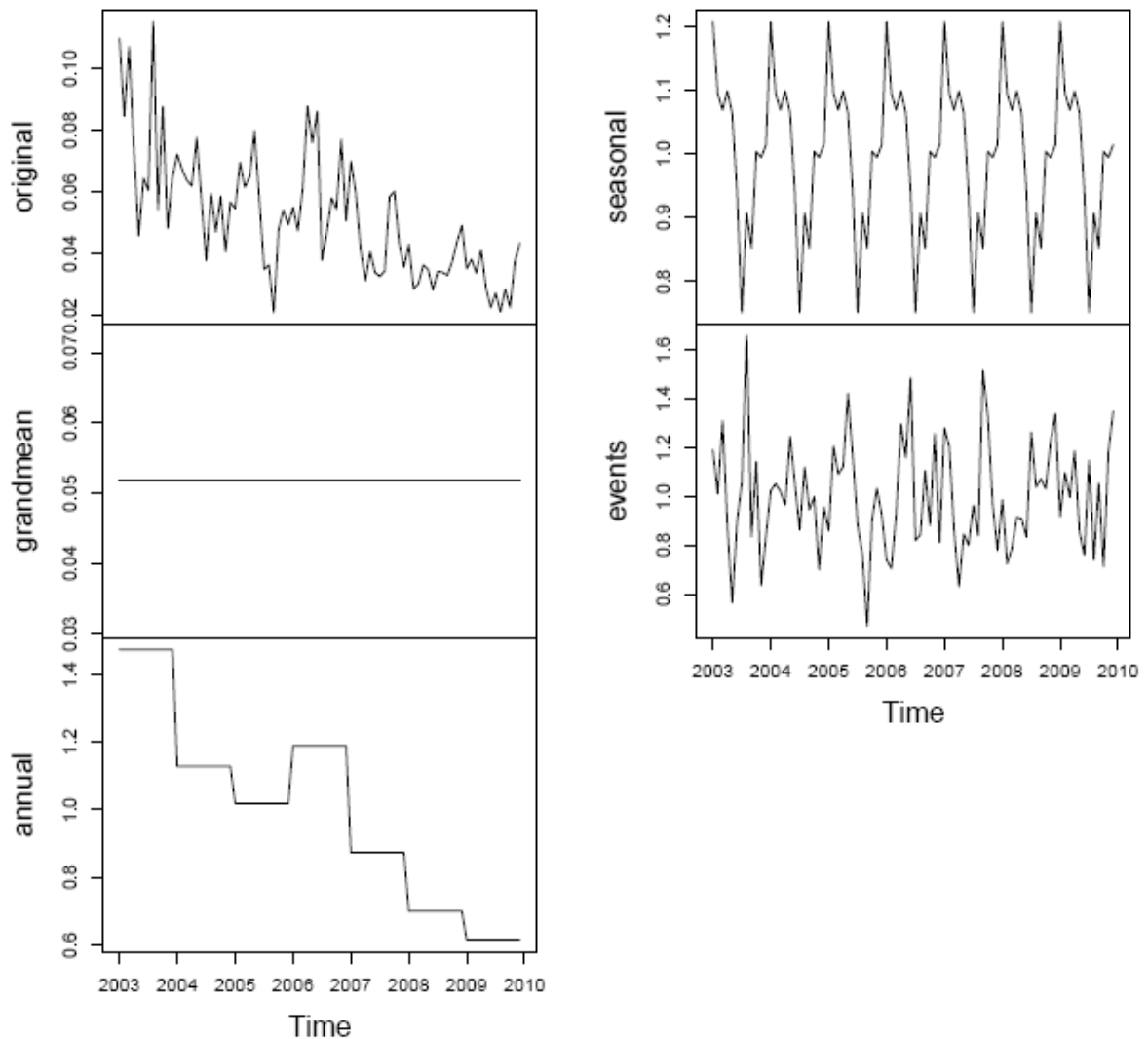


Fig. 4.28 – Multiplicative decomposition of PO₄ monthly integrated means in the layer 0-70m at LTER-MC (2003-2009).

The integrated mean of PO₄ in the layer 0-70m showed decreasing values over the years, ranging from 0.021 mmol m⁻³ (September 2005) and 0.12 (August 2003) mmol m⁻³. The long-term mean was 0.052 mmol m⁻³ and the annual effects pointed out decreasing values during 2003-2009 (Fig. 4.28).

The seasonal cycle displays decreasing value from the maximum (0.062 mmol m⁻³), observed in January, up to the minimum value (0.039 mmol m⁻³), recorded in July. After that the PO₄ concentrations started to raise again.

The most intense events overlapped with the maximum (August 2003) and the minimum (September 2005) monthly values.

4.3.5 N/P ratio in the inorganic dissolved pool

The Nitrogen to Phosphorus ratio in the dissolved inorganic pool has been analyzed for the years 2003-2009. More in details, the vertical distribution, the seasonality and the interannual variability of the DIN/PO₄ and NO₃/PO₄ ratios have been studied.

The DIN/PO₄ ratio in the dissolved inorganic pool, during the seven years under studies, was in the range 0.63-337; while the NO₃/PO₄ ranged between 0 (NO₃ < of the detection limit) up to 235. The DIN/PO₄ shows sensibly higher value compared to the NO₃/PO₄ ratio, especially at the surface (Fig 4.29). The mean values of the DIN/PO₄ ratio do not change significantly with depth and shows values slightly higher than 20 (\approx 24). On the contrary, the NO₃/PO₄ ratio displays a clear vertical pattern: the ratio is \approx 9 in the first 10m of the water column, it decreases in the layer 10-40m (\approx 7), and then increases again from 50m up to 70m, where it reaches a value close to 13. The N/P ratio in the inorganic pools increases during winter, over the whole depth.

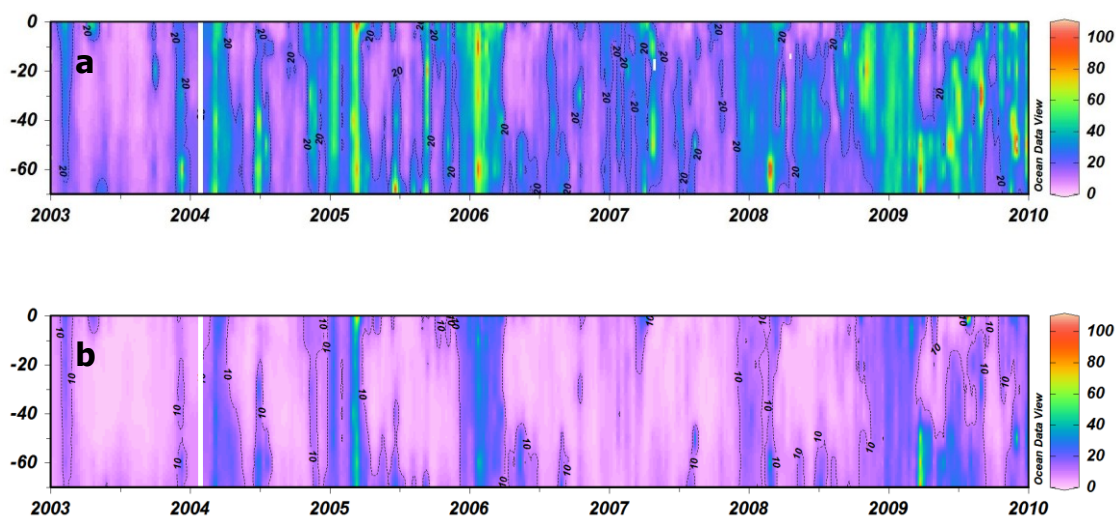


Fig. 4.29 –Contour plot of (a) DIN/PO₄ (mol/mol) and (b) NO₃/PO₄(mol/mol), in the years 2003-2009.

The monthly climatological statistics of the two ratios have been computed for the surface, 20m and 60m depth, as well as for the mean integrated value in the layer 0-70m.

The seasonal cycle at the surface is very pronounced for both ratios (Fig. 4.30). Median values greater than 20 for the DIN/PO₄ and greater than 10 for NO₃/PO₄ are observed in the first three months of the year. Starting from April, a clear decrease of the two ratios is observed, and considerably low values are recorded in the period July-August. Starting from August till December, both ratios increase again. To summarize, the median DIN/PO₄ ratios are < 10 from May to August, and >10 in the other months. The median NO₃/PO₄ values in the months July-August are <3.

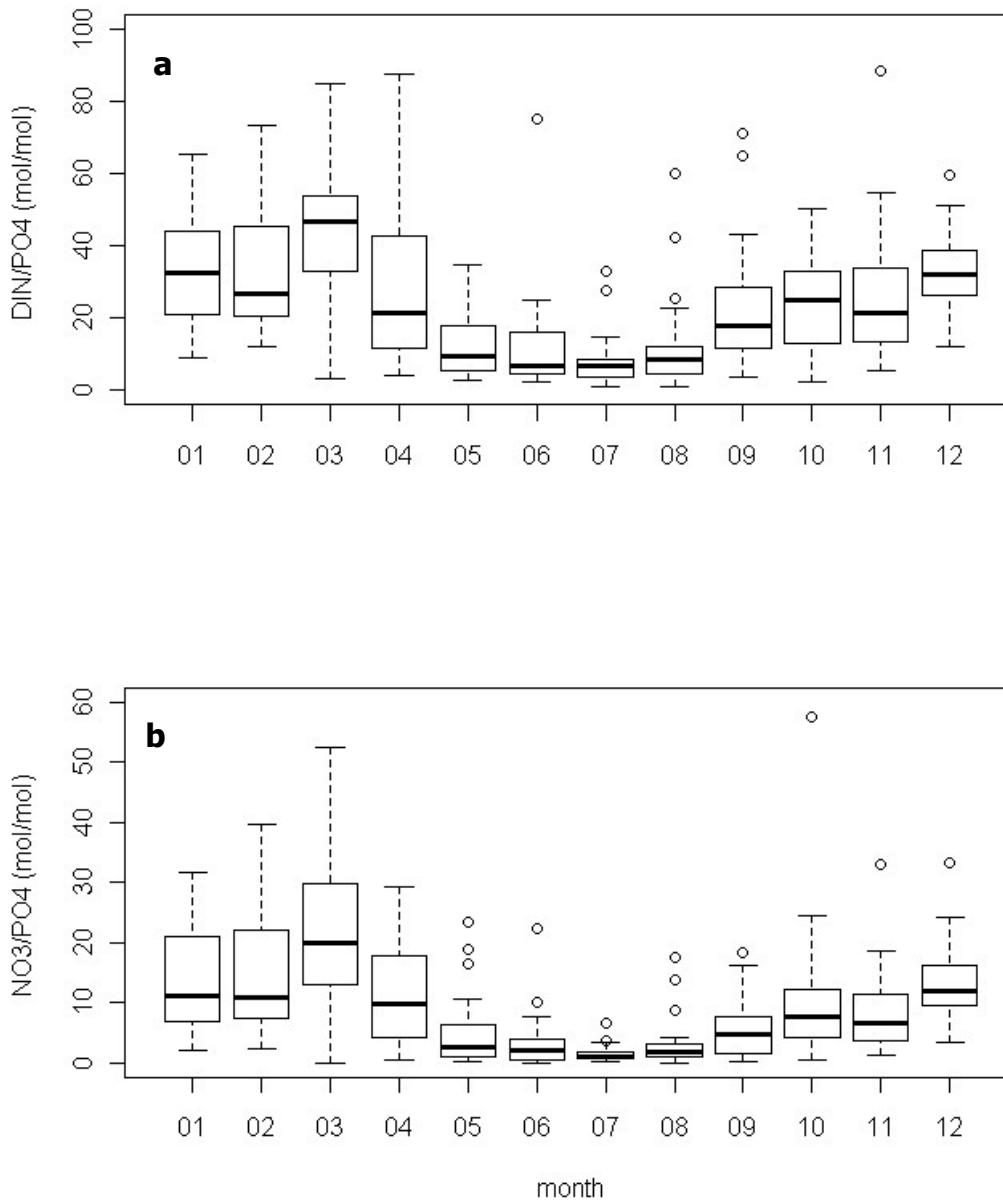


Fig. 4.30–Seasonal cycle of (a) DIN/PO₄ (mol/mol) and (b) NO₃/PO₄(mol/mol) at the surface in the years 2003-2009 (box-plot by month).

At 20m depth, a clear seasonality is still recognizable, however the pattern differs from that observed at the surface (Fig 4.31). The highest ratios are still observed from January to March, whereas in April an abrupt reduction of both ratios is observed. In April and May the DIN/PO₄ and NO₃/PO₄ ratios show the lowest annual values. From June to September a slight increase of the two ratio, compared to the previous months, is observed, whereas from October to December the ratios significantly increase.

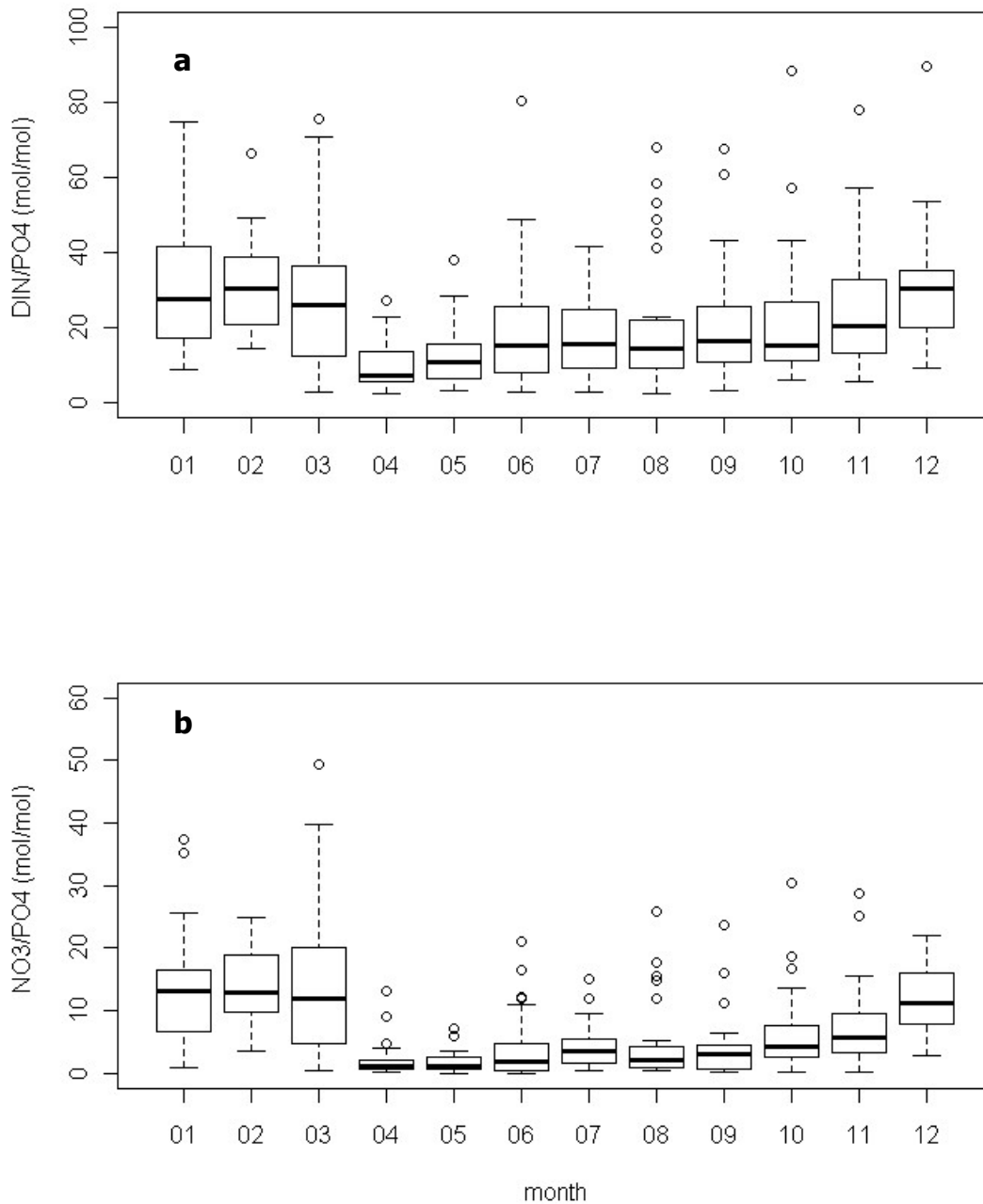


Fig. 4.31– Seasonal cycle of (a) DIN/PO₄ (mol/mol) and (b) NO₃/PO₄(mol/mol) at 20m depth in the years 2003-2009 (box-plot by month).

The seasonal cycles at 60m depth (Fig. 4.32) show decreasing median values of the two ratios from January up to October, and a subsequent rise starting from October up to December. The minimum annual median values occur in autumn (September-October) and the maxima in winter (January-March). Moreover, the variability observed is lower compared to the surface and to 20m.

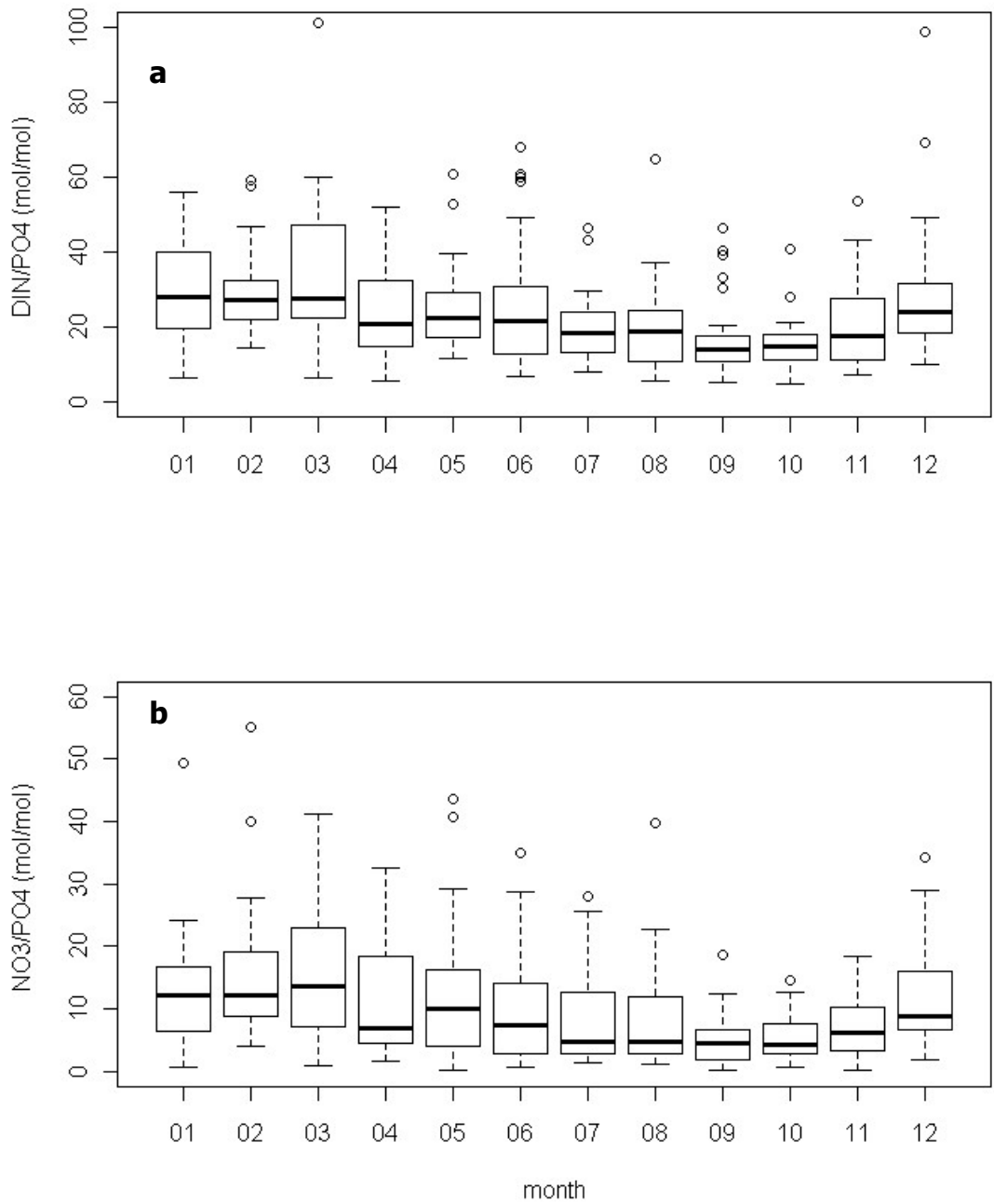


Fig. 4.32— Seasonal cycle of **(a)** DIN/PO₄ (mol/mol) and **(b)** NO₃/PO₄(mol/mol) at 60m depth in the years 2003-2009 (box-plot by month).

The mean integrated values (0-70m) of the N/P ratios display a seasonality similar to that observed at the surface (Fig. 4.33). The highest values are recorded from January to March and the lowest in April-September. However, the variability observed in the integrated mean values is sensibly lower compared to the surface. Moreover, both the DIN/PO₄ and the NO₃/PO₄ in June-August integrated mean ratios present higher values compared to the surface.

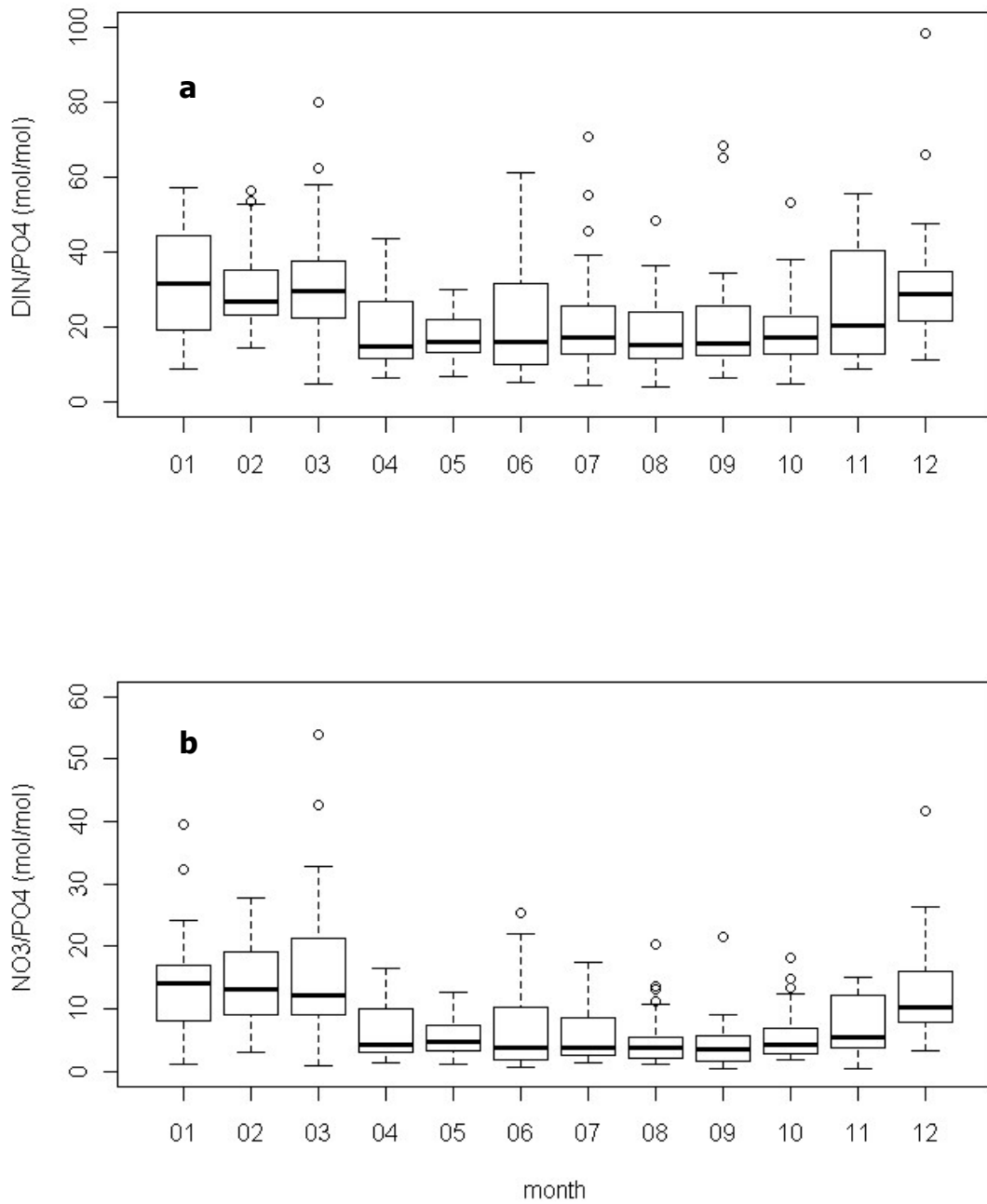


Fig. 4.33–Seasonal cycle of **(a)** DIN/PO₄ (mol/mol) and **(b)** NO₃/PO₄(mol/mol) as mean integrated values (0-70m) in the years 2003-2009 (box-plot by month).

Finally, the interannual variability of the N/P ratio has been analyzed by means of yearly box plot.

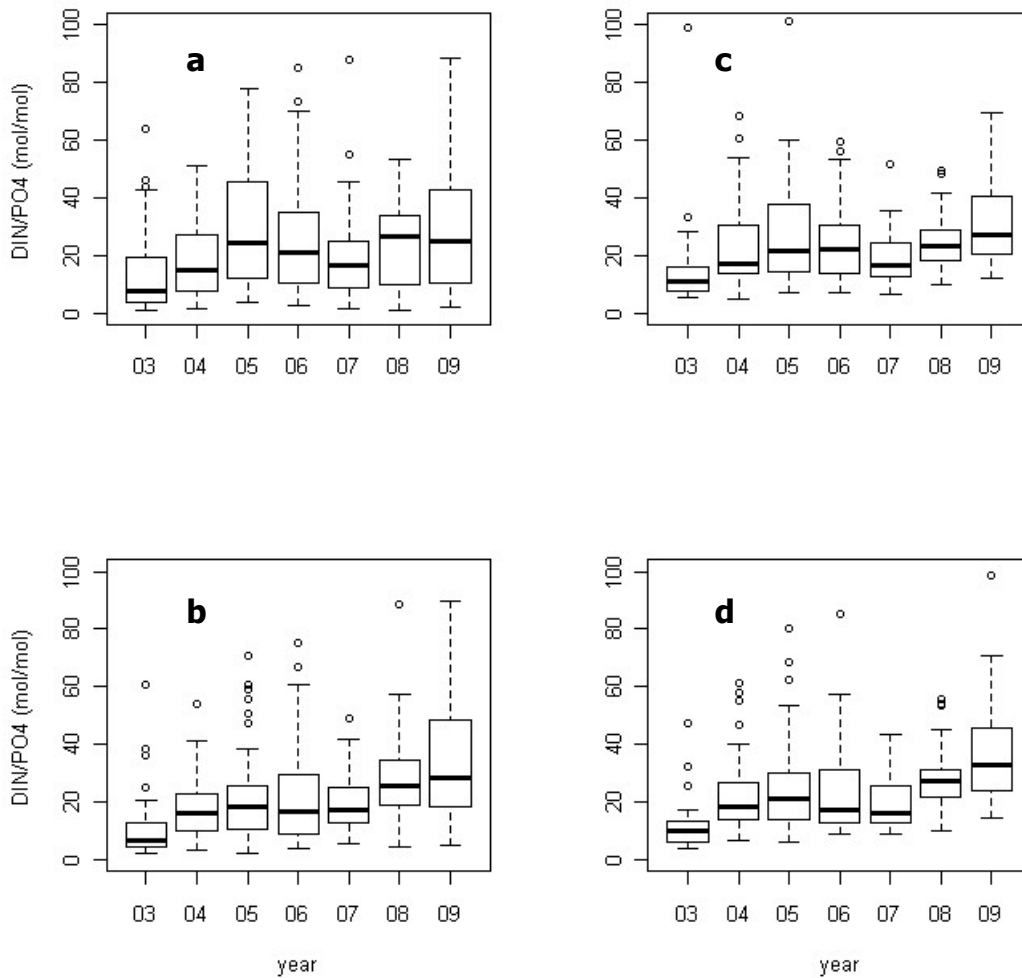


Fig. 4.34—Interannual variability of DIN/PO_4 (mol/mol) at the surface(**a**), at 20m depth (**b**), at 60m depth (**c**) and as integrated mean value (0-70m) (**d**) in the years 2003-2009 (box-plot by year).

The DIN/PO_4 ratio at the surface seems to be characterized more by interannual fluctuations than by a clear trend. In 2005 and 2009 the highest ratios were observed, while the lowest occurred in 2003 and 2007 (Fig.4.34 a).

On the contrary, at 20m, at 60m and as mean integrated values, the interannual variability displays a progressive increase of the DIN/PO_4 , ratio during the seven years of studies (Fig. 4.34, b-c-d).

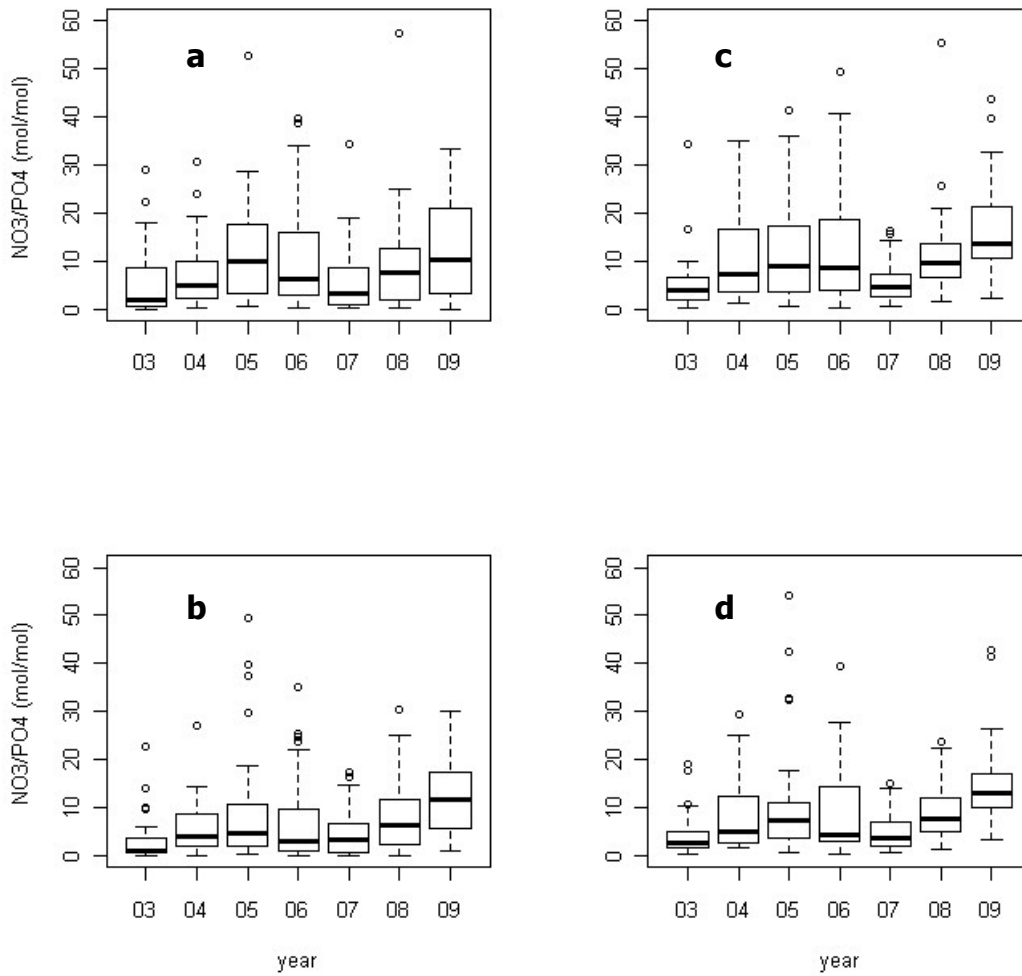


Fig. 4.35– Interannual variability of NO_3/PO_4 (mol/mol) at the surface(**a**), at 20m depth (**b**), at 60m depth (**c**) and as integrated mean value (0-70m) (**d**) in the years 2003-2009 (box-plot by year).

The NO_3/PO_4 ratio at the surface displays the same interannual variability observed for the DIN/PO_4 : the highest values were observed in 2005 and 2009 and the lowest in 2003 and 2007. Similarly, an increasing trend in the median value of the NO_3/PO_4 is detectable at 20m, 60m and in the mean integrated value during the period 2003-2009. Despite the clear trend observed in the interannual variability, the 2007 displays peculiar features, being characterized by low N/P ratios.

4.3.6 Phytoplankton biomass (Chl *a*)

The chlorophyll *a* (Chl *a*) is generally used as proxy of phytoplankton biomass. During the 2002-2009 period, Chl *a* ranged between 0.04 mg m⁻³ and 8.64 mg m⁻³, recorded at 60m (25/10/2002) and 2m (20/07/2004), respectively.

The vertical distribution of Chl *a* exhibited a strong gradient: significantly higher concentrations were observed in the first 10 m of the water column. On the contrary, in the layer 20-60m the Chl *a* values were lower (mostly smaller than 0.5mg m⁻³), and enhanced concentrations were observed only in winter/early-spring and autumn, in the absence of strong stratification (Fig. 4.36). Moreover, only in 30 surveys (7% of the total observations) the difference between the Chl *a* at 60m depth and at the surface was greater than 0.025 mg m⁻³.

The highest concentrations of phytoplankton biomass were generally observed in late-spring/early-summer at the surface, and in late-winter/early-spring as mean integrated value in the layer 0-60m.

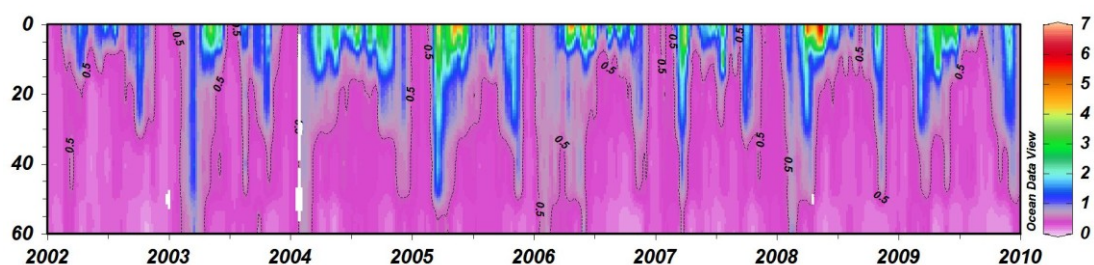


Fig. 4.36– Time-series of Chl *a* profiles (mg m⁻³) at LTER-MC (2002-2009).

The maximum concentration recorded at the surface did not dramatically differ through the years (Tab4.7), whereas the thickness and the number of blooms varied from year to year, thus intensely affecting the yearly integrated values of Chl *a*. The maximum integrated value was recorded in 2005 and the minimum in 2003.

Tab 4.VII - Annual minimum and maximum Chl *a* concentrations (mg m⁻³) at surface and mean integrated values (0-60m) in the years 2002-2009.

Surface Chl <i>a</i>	2002	2003	2004	2005	2006	2007	2008	2009
Min	0.09	0.15	0.29	0.22	0.17	0.15	0.11	0.16
Max	4.97	5.60	7.77	6.62	7.75	6.27	6.95	7.06
Mean integrated Chl <i>a</i>	2002	2003	2004	2005	2006	2007	2008	2009
Min	0.15	0.19	0.30	0.19	0.18	0.21	0.23	0.18
Max	1.19	1.82	1.43	3.06	1.39	2.13	1.83	1.97

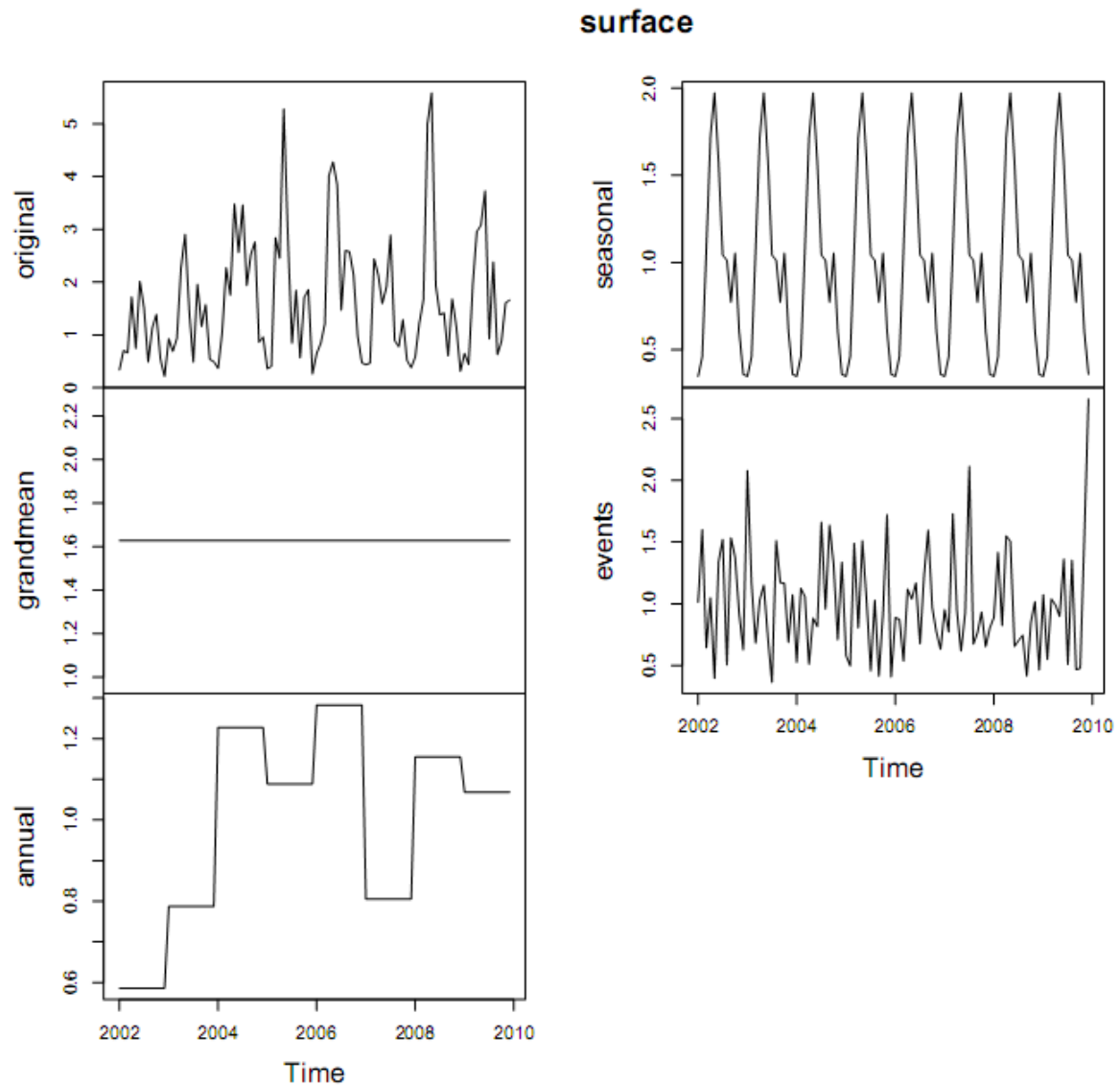


Fig. 4.37 – Multiplicative decomposition of Chl *a* monthly concentrations at the surface at LTER-MC (2002-2009).

Moving to the analysis of the multiplicative decomposition (Fig.4.37), we found that, the monthly Chl *a* values ranged between 0.21 mg m^{-3} (December 2002) and 5.59 mg m^{-3} (May 2008) and showed a mean value of 1.63 mg m^{-3} . In 2004, 2005, 2006, 2008 and 2009 annual effects >1 were observed, while the years 2002, 2003 and 2007 exhibited annual effects <1 .

A marked seasonality has been identified: the concentrations increase from January, which represents the annual minimum (0.57 mg m^{-3}), till May, when the annual maximum (3.21 mg m^{-3}) is recorded. From May up to September, the Chl *a* starts decreasing. A new peak is finally detected in October and a subsequent reduction of Chl *a* values is then generally observed up to December. The most relevant effects were detected in January 2003, July 2007 and December 2009, when unusual high concentrations were measured. May 2002 and July 2003 displayed the lowest effects.

Except for a few single events, seasonality plays a major role in the modulation of the Chl *a* concentrations at the surface.

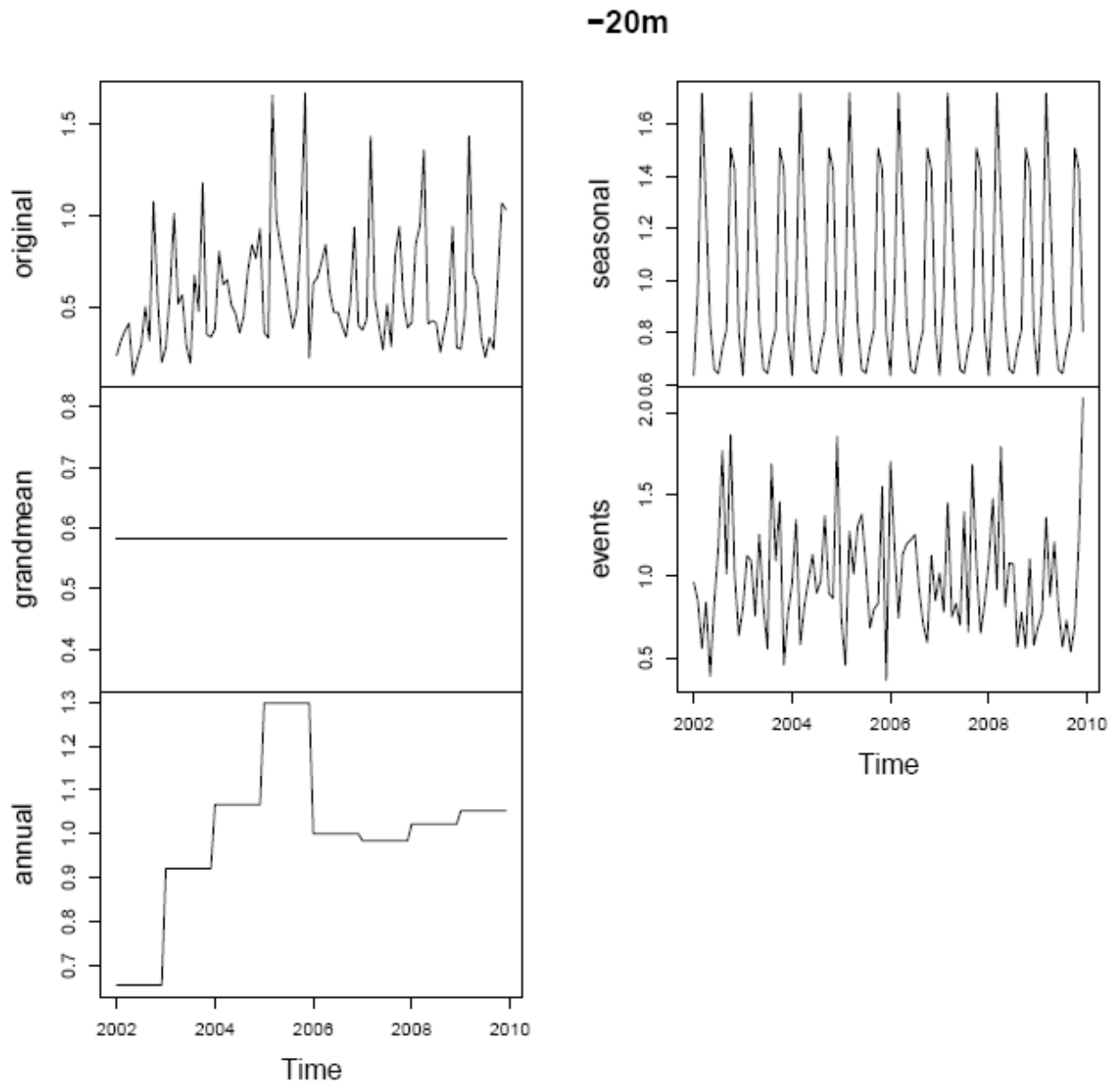


Fig. 4.38 – Multiplicative decomposition of Chl *a* monthly concentrations at 20m depth at LTER-MC (2002-2009).

At 20m depth, the Chl *a* concentrations were within the range 0.12-1.67 mg m⁻³, recorded in May 2002 and November 2005, respectively. The mean value during the eight years was 0.58 mg m⁻³. The highest annual effect was observed in 2005, while the lowest occurred in 2002 (Fig. 4.38). The annual effect increased from 2002 till 2005, whereas starting from 2006 till 2009 it was almost constant.

The seasonality exhibits incrementing concentrations from January, when the minimum annual value (0.37 mg m⁻³) is observed, till March, when the maximum annual concentration (1 mg m⁻³) is reached. Elevated levels of biomass are still present in April, whereas starting from June up to

September quite stable and reduced concentrations of Chl *a* are observed. In autumn (October and November), a rapid enhance of biomass is observed, reaching almost the same level than the spring maxima, which abruptly declines in December.

The highest event effects were due to positive anomalies in the autumn bloom (October 2002, December 2004 and December 2009), whereas the lowest were detected in May 2002 (corresponding to the minimum monthly value) and in December 2005.

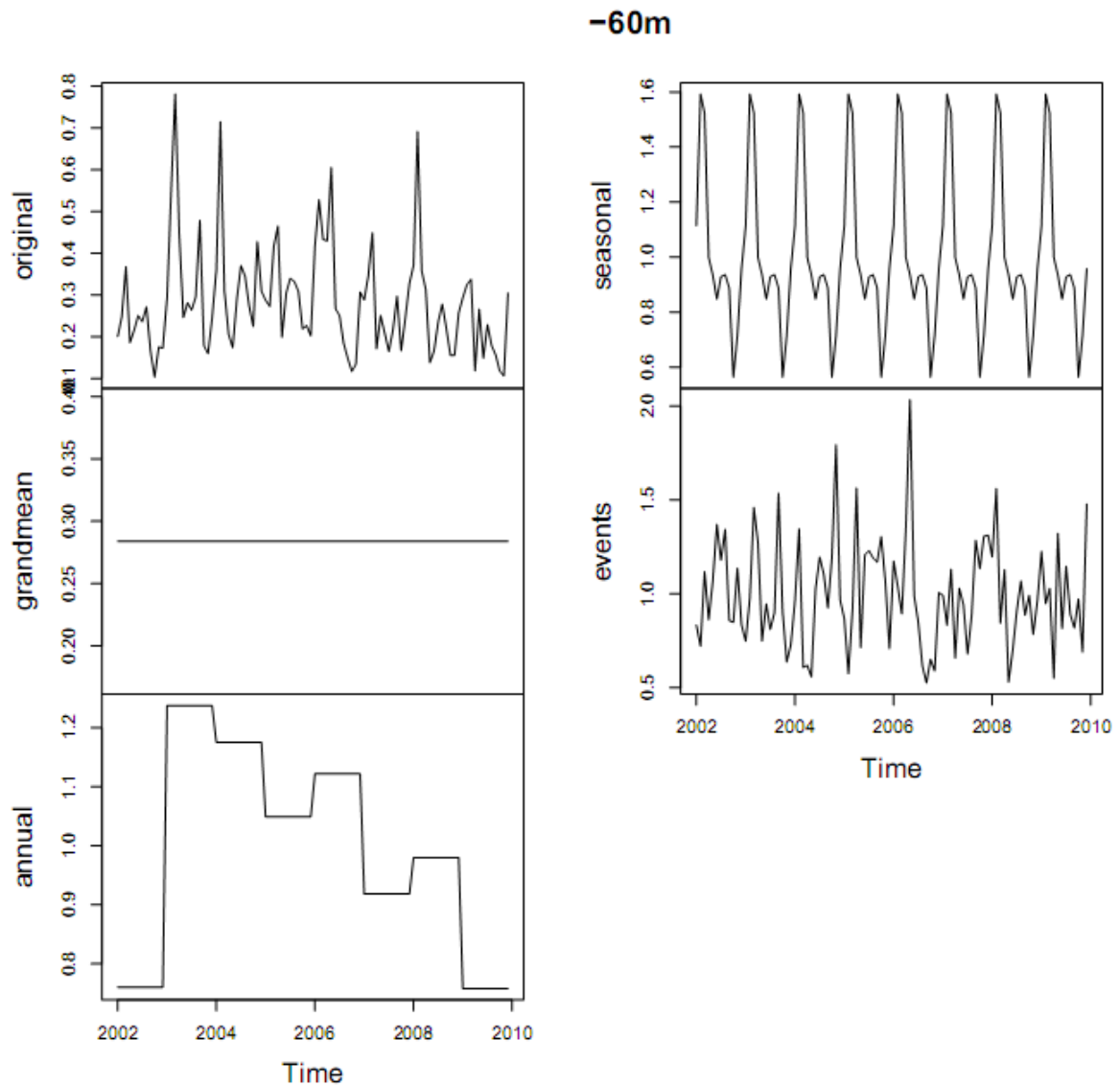


Fig. 4.39 – Multiplicative decomposition of Chl *a* monthly concentrations at 60m depth at LTER-MC (2002-2009).

The Chl *a* concentrations at 60m depth displayed values in the range 0.16-0.78 mg m⁻³, recorded in September 2002 and March 2003, respectively (Fig. 4.39). The mean over the entire sampling period was 0.28 mg m⁻³. The annual effects were higher than 1 starting from 2003 up to 2006, and sensibly lower in 2002 and 2009.

The seasonal cycle is characterized by concentrations higher than the mean from January up to March. From May up to September the Chl *a* values fluctuate around the mean value, whereas in October and November they are sensibly lower. The maximum annual value is generally found in February (0.45 mg m⁻³) and the minimum in October (0.20 mg m⁻³). Extremely high events were detected in November 2004 and May 2006, while the lowest events occurred in September 2006 and May 2008. By the way, events seem to have a role comparable to seasonal effects, with minor impact of the annual effects.

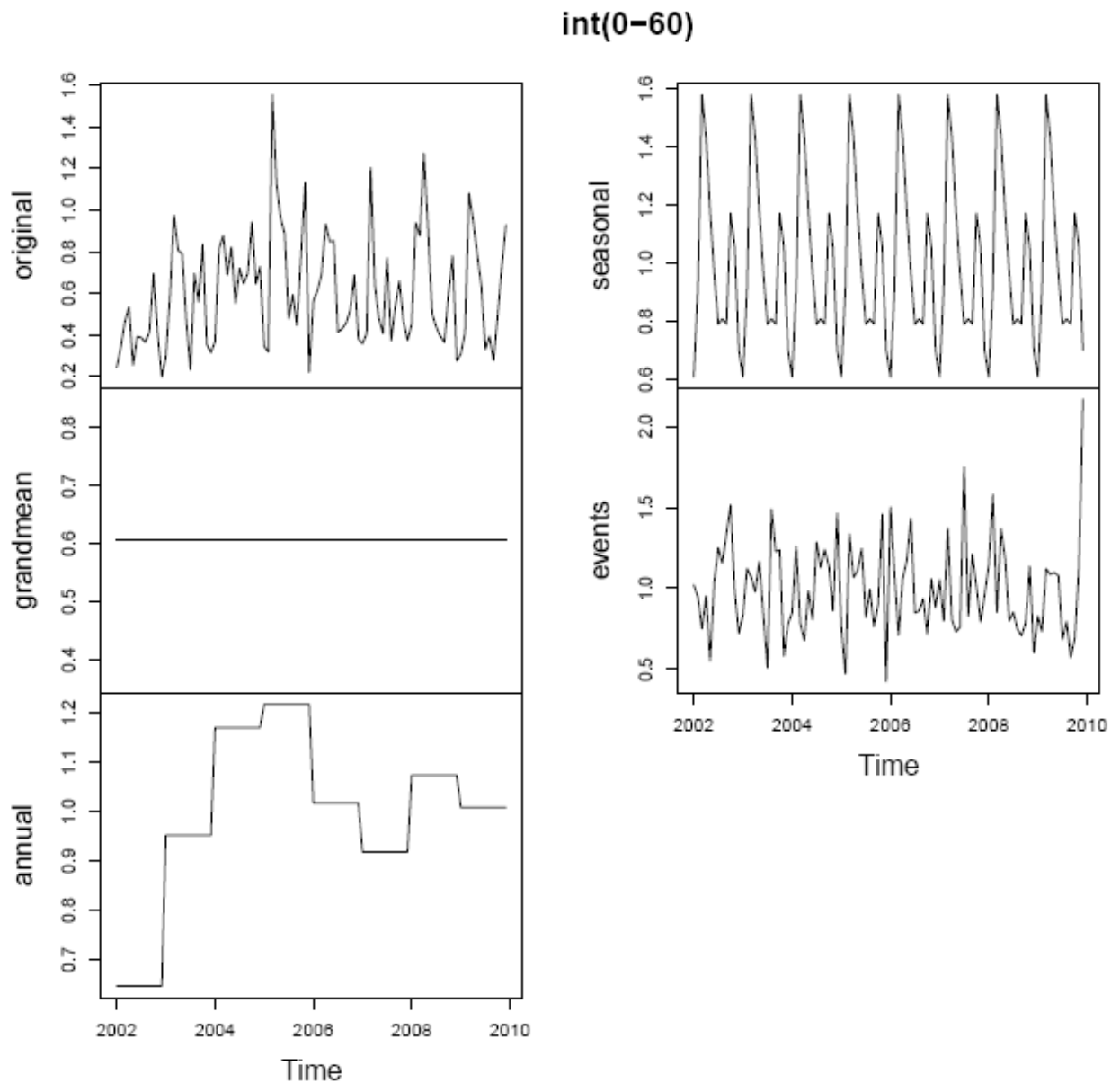


Fig. 4.40 – Multiplicative decomposition of monthly Chl *a* (mg m⁻³) integrated means in the layer 0-60m at LTER-MC (2002-2009).

The Chl *a* as integrated mean value in the layer 0-60m varied between 0.2 mg m⁻³ (December 2002) and 1.6 mg m⁻³ (March 2005), with a mean value of 0.61 mg m⁻³. The interannual variability

evidenced a strong increase starting from 2002 (lowest annual effect) till 2005 (maximum annual effect) , from 2006 up 2010 the Chl *a* remained quite stable (Fig. 4.40).

The seasonal cycle follows the typical pattern of the temperate areas characterized by two main blooms (spring and autumn), with the former reaching higher values than the latter. The phytoplankton biomass increases from January, which is the annual minimum (0.37 mg m^{-3}), to March, reaching the annual maximum (0.96 mg m^{-3}), while elevated values are still recorded in April. From April, the biomass declines till July. During summer (July-September), the Chl *a* concentrations are steadily low, whereas in autumn (October-November) they raise again. In July 2007 and December 2009 the highest event effects were observed, while in February and December 2005 the lowest one were detected. Seasonal and events multiplicative deviations display the higher range, even if events show an extremely anomalous peak in December 2009. Year to year variations seem to have a smaller impact on mean integrated Chl *a* variations.

4.3.7 Precipitations

The daily precipitations measured at the DISAM, displayed an intense variability during the years 2002-2009. In 2002, the raining events were distributed all over the year, whereas in the last three years of the time-series (2007-2009) the precipitations were practically absent during summer (July-August).

The more intense daily events were observed on 3/01/2009, when 69.6 mm of rain were recorded.

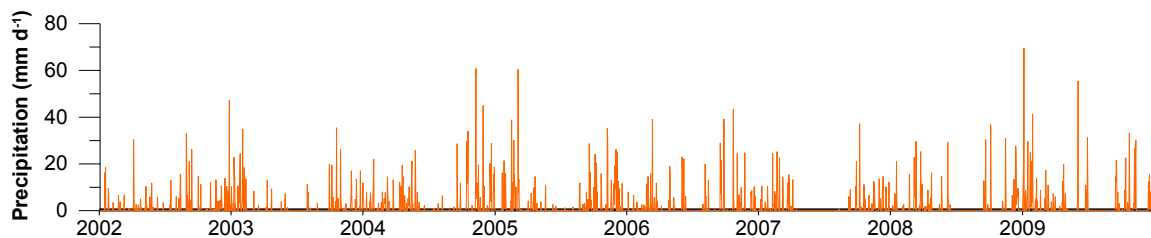


Fig. 4.41– Cumulative daily precipitation values recorded at Naples (2003-2009).

At monthly scale, the cumulative precipitations ranged between 0 (recorded in 4 occasions: July 2007, July and August 2008, August 2009) and 279 mm (January 2009) and shows a mean value of 58.25 mm. The annual cycle of precipitations is characterized by high values from January up to March and from September up to November. In spring (April, May and June), the precipitation are sensibly lower than those observed in winter and autumn, while July and August are the driest months of the year. The maximum and minimum mean monthly values are recorded in January (95.77 mm) and July (7.15mm), respectively (Fig. 4.42).

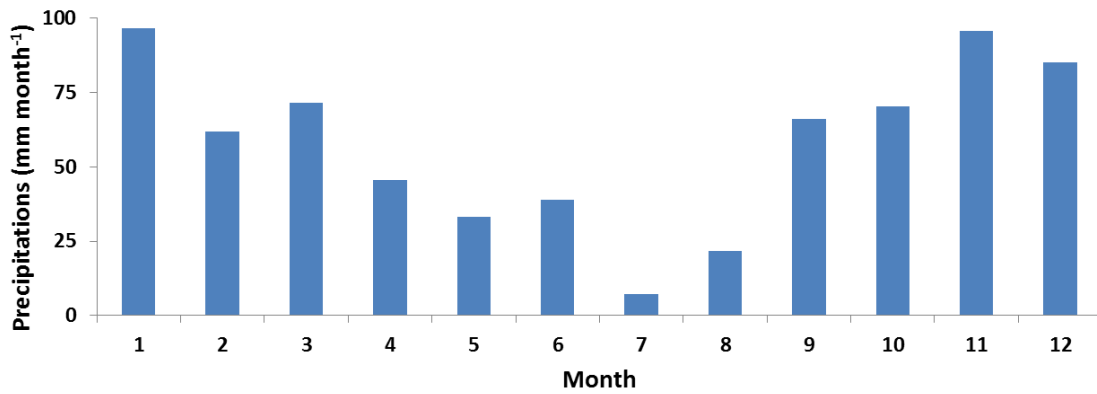


Fig. 4.42– Mean cumulative monthly precipitations at Naples (2002-2009).

The yearly cumulative precipitations ranged between 546 mm (2003) and 889 (2009). In 2004, 2005 and 2009 the highest cumulative annual precipitations were recorded, whereas in 2002 and 2003 the lowest were observed (Fig.4.43).

In Fig. 4.43, the precipitations value of the 2007 was not reported, because of the missing data in May and June, which represent ~10% of the yearly values. However, increasing of the 10% the value recorded in 2007, we can estimate the precipitations occurred in 2007. The obtained value (571 mm yr⁻¹) was similar to the low values recorded in 2002 and 2003.

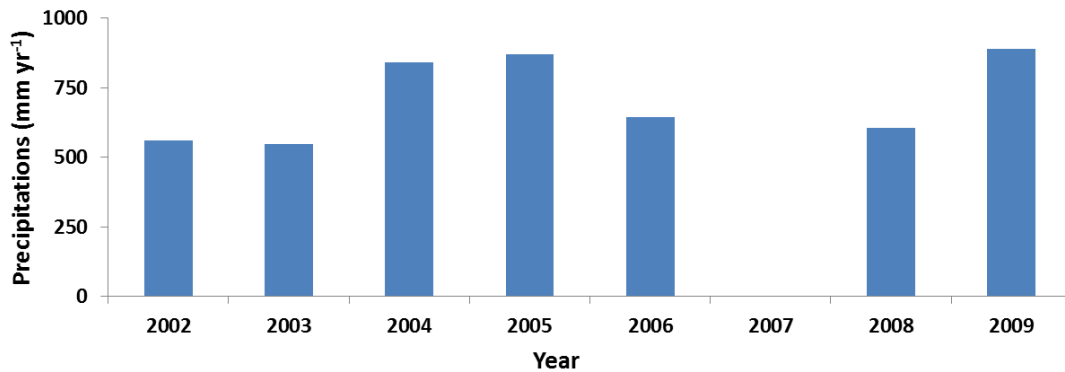


Fig. 4.43– Yearly cumulative precipitations recorded at Naples (2002-2009).

4.4 Discussion

In the previous section, a detailed investigation on the physical (temperature and salinity), meteorological (precipitations), chemical (dissolved inorganic N and P) and biological (phytoplankton biomass) features has been reported. In the following, we aim to elucidate the mechanisms that affect the N and P dynamics at LTER-MC station. In fact, even if LTER-MC has been sampled since 1984, studies focused on the nutrient dynamics have never been conducted. Previous works have mainly investigated the role of nutrients in triggering/limiting the phytoplankton dynamics (Ribera d'Alcalà et al., 2004; Zingone et al., 2010), and only the analysis of the first year of sampling described more exhaustively the nutrient distribution and variability, also investigating its relation to some physical parameters (Scotto di Carlo et al., 1985).

Hydrography

The hydrographic features at LTER-MC station display the presence of pronounced seasonal and interannual signals.

Using the multiplicative decomposition provided by the 'wq' package, we observed that the seasonality is the strongest signal for temperature at all depths. Moreover, the temperature seasonal cycle is characterized by the highest values at surface in summer and the lowest in winter, over the whole water column. However, a strong interannual variability was recorded, characterized by decreasing winter temperatures from 2002 till 2006, and by an exceptionally warm winter in 2007. The highest temperatures were recorded in summers 2003, 2008 and 2009. The same interannual signals were observed along the whole Campania Region coastline in 2002-2006, as reported in the previous chapter, and it was clearly related to basin scale processes.

The mean monthly values of the water column in 2002-2009 are comparable with those reported for the same stations in the years 1984-2000 (Ribera d'Alcalà et al., 2004), highlighting the absence of significant trends in temperature throughout the 1984-2009. Despite the stability observed in the mean monthly temperatures, the amplitude of the temperature signal was higher in the last years of the time-series, with respect to the period 1984-2001, and several anomalous events were detected. More in details, mean temperatures (0-70m) lower than 13°C were observed for the first time at LTER-MC in 2005 and 2006, while temperatures higher than 28.4 °C were observed in summer 2003 and 2009. The intensification of extreme anomalies is recognized as a direct effect of the ongoing global change (e.g., Schär et al., 2004) and can have a large impact on the marine organisms. For instance, mass mortalities events caused by heat waves recorded in 2003, 2008 and 2009 are well documented in several studies (Lejeune et al., 2009; Garrabou et al., *Glob. Change Biol.*, 15: 1090-1103, Gambi et al., 2010,).

Contrary to what we found for temperature, the multiplicative decomposition reveals a strong dependence of salinity from the annual effect and the 'events'. More in details, the role of the events is stronger in the upper part of the water column (0 and 20m), while the interannual variability seems to play a major role in the deeper one (60m). Looking at the bulk properties of the water column, the mean values (0-70m) of salinity are driven by both annual effects and events.

The mean surface salinity at LTER-MC in the period 2002-2009 was 37.70. Comparing this value with those observed in the coastal stations described in the previous chapter, it is higher than the mean salinity of the stations affected by high terrestrial load (37.53 - Group III), but it is lower than the salinity of the pristine area (37.90 - Group IV). Therefore, the terrigenous loads are still evident at LTER-MC. On the other hand, comparing the salinity data recorded in 2002-2009 with those of the period 1984-2000 (Ribera d'Alcalà et. al, 2004), no significant differences on the mean values have been recorded, indicating the absence of trends in salinity, as already observed for the temperature.

Despite the observed dependence from interannual variability and single events, a recurrent seasonality at surface was also detected. This observed seasonal cycle displays the lowest values in May-June and the highest in September-October. This feature agrees with the observations presented in the previous chapter (at the stations not directly influenced by the rivers), with the previous studies carried out at LTER-MC (Ribera d'Alcalà et. al, 2004). It can thus be related to the seasonal dynamics of the 'fresh water budget' in the Western Mediterranean Sea, which reach its maximum annual value in May (Boukthir and Barnier, 2000; Mariotti et al., 2002).

Finally, the salinity throughout the years 2002-2006, displays the same interannual variability observed at the coastal stations of the Campania Region, sampled in the framework of the Si.Di.Mar Project (2001-2006).

The observed salinity variations cannot be explained only by the precipitations. For instance, in 2005 precipitations were high, but they were not coupled to sensibly lower salinities at the surface or in the mean (0-70m) values. For sure salinity is strongly affected by the local precipitations, but evaporation, river discharge and local advection also contribute to modulate it, leading to a more complex budget. Reasonably, precipitations are expected to play a more important role in driving anomalous events, whereas global scale processes (such as basin scale circulation, winter deep convection events etc.) are mainly responsible for the observed interannual variability.

Summarizing, in this study we observed a strong dependence on large scale processes of temperature and salinity interannual variability in the coastal waters. Therefore, monitoring programs, as well as long time-series studies, are powerful tools in identifying basin scale signals, and can be used as proxy of larger spatial scale processes, with sensibly reduced efforts.

Nutrients

At coastal sites, the nutrient dynamics is driven by a combination of river discharges, direct inputs from land, exchange with the open waters, groundwater fluxes and atmospheric depositions (Jickells et al, 1998). In this study, we analyzed the distribution and temporal variation of nutrients and nutrient ratios at different depths in order to discern the mechanisms that modulate their concentrations in the different layers of the water column.

First of all, the surface inorganic nutrients at LTER-MC display intermediate concentrations compared to the stations of the Groups III and IV, as defined in the previous chapter. Moreover, the composition of the DIN at the surface is similar to the percentage observed in the GoN,

especially at the station NA6, confirming a strong influence of terrestrial loads on the abiotic properties at LTER-MC.

Comparing our data to the previous surveys (Scotto di Carlo et al., 1985; Ribera d'Alcalà et al., 2004), it is possible to observe a clear reduction relative to the first years of the time-series (1984-1988). Moreover, throughout our investigated period, a clear reduction of PO_4 concentrations in the subsurface layer has been observed. Recently, declining nutrient concentration, notably declining phosphorus concentration, was also noted in several systems (Borkman et al., 2009).

Comparing the median surface values with those recorded in the coastal offshore waters ($1500\text{m} < \text{distance from the coast} < 5000\text{m}$) of the Catalan coast (Flo et al. 2011), LTER-MC display similar DIN and PO_4 concentrations. While comparing our result with those obtained in the Gulf of Trieste (Lipizer et al., 2011), LTER-MC displays similar PO_4 values, but halved DIN concentrations.

The multiplicative decompositions indicated that the NO_3 concentrations are mainly driven by seasonality and events; NH_4 values are modulated in a comparable way by the three effects, while PO_4 is affected more by the annual effects and by the events, thus indicating different dominating supply mechanism for each of the three inorganic nutrients. Moreover, various features have been observed within the dissolved inorganic N pool, related to the vertical distribution of its speciation. Nitrate displays the highest concentrations in the upper part of the water column (0-10m) and the lowest in the intermediate layer (20-40m); while in the deepest layer (50-70m) it assumes intermediate values. Ammonium and nitrite display opposite vertical distributions: NH_4 increases its relative contribution in the upper layer, whereas NO_2 is higher in the deep layers. Generally, in the open oceans, NO_2 and NH_4 concentrations are depleted at the surface, show a maximum around 50 to 80m, and rapidly decrease below that depth (e.g. Gruber, 2008). The noticeable ammonium concentrations at surface thus clearly indicate the presence of terrestrial inputs.

The phosphate vertical distribution displays the same pattern observed for nitrate: the highest concentrations were observed in the first 10m, the lowest in the layer 20-40, and intermediate values in the deeper part (50-70m).

The presence of elevated ammonium and phosphate concentrations at the surface is an indicator of anthropogenic pressure mainly due to urban influence (Flo et al., 2001, Mozetic et al., 2008) and thus confirms the strong impact of the terrestrial loads also in the outer part of the GoN.

The strong vertical gradient and the absence of deep maxima let us hypothesize mainly terrestrial sources as driving factor of ammonium. On the contrary, in the case of nitrate and phosphate the two relative maxima observed (at surface and at the bottom), allow us to identify different sources. The terrestrial inputs dominate at the surface, whereas the enhanced concentrations observed at the bottom, could be explained by the exchanges with the open waters and/or by remineralization processes occurring *in situ*.

The occurrence of higher nitrate concentrations over the whole water column and in the deeper layer, during winter and early-spring of the coldest years (2004, 2005, 2006 and 2009), could be related to the NO_3 supply deriving from the vertical mixing in the open waters, which is subsequently transported in the inner part of the GoN. In fact, winter mixing may also supply

nutrients entrained from deeper offshore waters to the coastal zone of temperate region (Lucea et al., 2005). In 2007, an exceptional warm winter occurred and mixing was almost negligible in the southern-central Tyrrhenian Sea (VECTOR cruises). Meanwhile, a complete absence of the typical winter-spring nitrate increase in the sub-surface layers at our coastal site seems to further confirm our thesis. The fact that the exchange between coastal and offshore waters after winter-mixing events plays a key role in fueling nitrate at LTER-MC is an important outcome of this study.

The strong variability related to interannual signals and to events did not allow us to recognize a clear source for the PO_4 enrichments along the water column. However, due to the high frequency of events in the deeper layer and to the low seasonal signal observed at 60m, it is reasonable to hypothesize that the remineralization processes play an important role in modulating the phosphate dynamics in the bottom layer.

As a further analysis, we tried to relate the different nutrient supplies at the surface to the physical and meteorological forcing. As observed before, it is not possible to obtain a simple linear regression between surface salinity and precipitations, and the same generally holds for surface nutrients. However, the highest nutrients concentrations were generally detected in the period of more intense rain events (September-March). More in details, in correspondence of strong rain events it is possible to observe either a simultaneous increase of all nutrients, or only of some of them, or of none. Conversely, high nutrients concentrations can be recorded even without precipitations.

To better understand of the role of the precipitations in modulating the nutrient dynamics at LTER-MC, we selected some specific cases, which can be considered representative of different regimes. In 2005, three consecutive surveys were carried out on the 8th, 15th and 22nd of March. The cumulative precipitations in the four days before each survey and the relative chemical features have been reported in Tab. 4.VII. It is quite evident that the high nutrient concentrations found during the second and third surveys cannot be explained by the precipitations data. Moreover, the nutrient concentrations strongly differed in the three surveys. We can try to explain this discrepancies looking at ocean colour satellite images. In particular, we will look at satellite derived Chl *a* concentration images (<http://gos.ifa.rm.cnr.it/adricosm/index.html>). Even if Chl *a* cannot be considered a purely *passive* tracer, its spatial distribution is clearly related to surface circulation, and might be used to identify different dynamical conditions (Fig. 4.44).

The image corresponding to the first survey does not indicate the presence of any particular structure in the GoN (Fig. 4.44 a). Coherently, the nutrient concentrations observed at MC seem to be related to the local precipitations occurred in the previous days. The ratio NH_4/NO_3 was ~ 0.4 , while the DIN/PO_4 was 74. These values are in agreement with those reported by Kocak et al., 2010, who analyzed nutrient concentrations in Mediterranean aerosol and rainwater, looking at a long time series (1999-2007). The authors reported a high N/P ratio and similar NH_4/NO_3 ratios in rainwater, even if a strong variability in nutrients concentrations and in their relative ratios can occur, mainly depending on the origin of the airflow associated with the deposition.

Tab. 4.VIII – Cumulative precipitations in the four days before each survey and chemical characteristics observed at LTER-MareChiara on the 8th, 15th and 21st of March.

Date	Cumulative precipitation (mm)	NO ₃ (mmol m ⁻³)	NH ₄ (mmol m ⁻³)	PO ₄ (mmol m ⁻³)	DIN/PO ₄ (mol/mol)	NH ₄ /NO ₃ (mol/mol)
8/3/2005	84.2	5.6	2.2	0.1	74	0.4
15/3/2005	0.6	8.6	1.2	0.1	159	0.1
22/3/2005	0	4.5	8.2	0.3	42	1.9

During the second survey, the nutrients originated from the large outflow of the Volturno River, which is spreading in the adjacent waters. The satellite image acquired on the 15th of March, clearly describes this event (Fig. 4.44 b). Moreover, the low NH₄/NO₃ is similar to that observed at the coastal station off the Volturno River mouth (FV1), described in the previous chapter.

In the third case, the satellite images corresponding to the exact date of the survey were cloudy (or masked due to satellite algorithm failure). However, the image acquired one day before (March 21st) seems to indicate a water transport from the eastern part of the GoN to LTER-MC station (Fig. 4.44 c). The NH₄/NO₃ was much higher (1.8), close to the values typically observed at the coastal stations off Portici (PO7) and Sarno River mouth (FS10), as described in the previous chapter. Moreover, the wind recorded during the 4 days before the sampling was mainly from SW (data not shown). Under such conditions, the circulation pattern is characterized by a complex circulation inside the GoN (Gravili et al., 2001; Grieco et al., 2005; Menna et al., 2007), currents are mostly coastward and surface waters are retained in the littoral area (Uttieri et al., 2011).

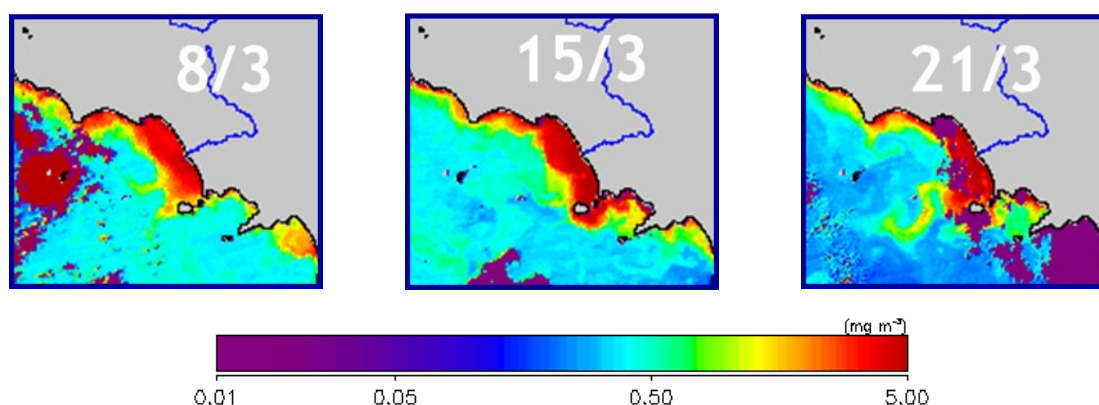


Fig. 4.47 - Ocean colour satellite images of Chl *a* acquired on **a)** the 8th, **b)** 15th and **c)** 21st of March

In conclusion, the surface nutrient dynamics in the GoN is highly dependent from several factors (local and large scale circulations, meteorological forcing, river discharges etc.) and it cannot be explained by a simple correlation between nutrient and salinity and/or precipitations. In order to understand the processes that drive the nutrient dynamics in coastal waters, the long term-series of a single stations can provide only limited information, because of the lacking knowledge of the dynamical conditions and associated advection regimes. New technologies, such satellite imagery or HF radars, in combination with *in situ* measurements, represent useful tools to fill this gap. However, as shown in the previous examples, the knowledge of the chemical features of the area

can help in determining the source of nutrients: the relative contribution of the NH_4 and NO_3 to the DIN can be used as a signature of the origin of the water masses at the surface.

More in details, in the GoN, the presence of high nitrate concentrations associated to relative low ammonia is an indicator of waters originated from the GoG (Volturno River). On the contrary, high levels of both NO_3 and NH_4 , combined with a relative dominance of ammonia, are indicators of waters originated in the eastern part of the GoN.

To further characterize the nutrient dynamics at LTER-MC, we analyzed the N/P ratios in the dissolved inorganic pool. The N/P ratio displayed a clear seasonality at the surface: both the DIN/PO_4 and the NO_3/PO_4 ratios are characterized by higher values in autumn-winter and lower values in spring-summer. The same feature has been described in the previous chapter, for all the coastal sites of the Campania Region, sampled in the framework of the Si.Di.Mar project. As shown in the previous chapter, it has been found also in other Italian Regions. Moreover, it has been reported also for a site in the English Channel (Jordan and Joint, 1998), in the Gulf of Trieste (Lipizer et al., 2011) and in the Bay of Blanes (Lucea et al., 2005), whereas the opposite pattern has been observed in the open waters of the Mediterranean Sea (Dyfamed station) by Marty et al., 2002. Thus, the observed seasonality seems to be a characteristic trait of the temperate coastal waters. Moreover, the amplitude of the oscillations between the winter and summer values seems to be related to the trophic status of the area. In fact in the stations located off the river mouth, where the nutrients load is high (eutrophic conditions) the N/P ratio shows the highest differences between winter and summer values (eg. Volturno and Sarno River mouth described in the previous chapter, Isonzo River mouth in Lipizer et al., 2011). On the contrary, the oligotrophic stations (such as PT and PL described chapter 3, or Bay of Blanes illustrated by Lucea et al., 2005) present the smallest differences.

The observed seasonality in the N/P ratio could be strongly affected by the seasonal variations in the terrestrial inputs. In fact, as shown previously, the nutrient concentrations at the surface are driven by the terrestrial sources (mainly river outflow, local discharge and atmospheric depositions) which increase their loads in the period of more intense rains. Both the river outflow and the depositions are characterized by high N/P ratio in the dissolved pool. Consequently, the enhancements of the N/P ratio seem to be triggered by the terrestrial loads.

Phytoplankton biomass

The multiplicative decomposition displays a stronger dependence of Chl *a* from the seasonality and events compared to the interannual variability.

Comparing the data acquired in 2002-2009 with the previous data reported by Ribera d'Alcalà and coauthors (2004), we found the same annual average of integrated value in the layer 0-60m (0.61 mg m^{-3} in our study, 0.62 mg m^{-3} in 1984-2000). Moreover, as already reported in previous studies a clear decrease in phytoplankton biomass, with respect to the first years of the time-series, has been detected (Ribera d'Alcalà et al., 2004, Zingone et al., 2010b). The lower concentrations have been ascribed to a decline in terrestrial input, which mainly affected the spring-summer blooms, as

well as to a change in the meteorological forcing, which influenced the vertical stability and thus the winter bloom intensity.

The observed Chl *a* seasonality (integrated mean 0-60) is characterized by two annual peaks, the late-winter (February to March) and the autumn blooms, which are a typical trait of the Mediterranean Sea (C. M. Duarte et al., 1999 and references inside). In fact, nutrient depletion and increasing zooplankton grazing cause the decline of the spring blooms and determine low concentrations of biomass during summer (Winder and Cloern, 2010), whereas enhanced nutrient deriving from the erosion of the thermocline, in light conditions still favourable for net growth, mainly trigger the secondary bloom in temperate areas (Margalef, 1969). However, inside the GoN, nutrients supporting the autumn blooms derive from terrestrial sources, while meteorological large scale factors (such as vertical mixing, circulation and light availability) modulate the intensity of this bloom (Zingone et al., 1995, Ribera et al., 2004). The autumn bloom occurs under favourable weather conditions, known as 'St Martin Summer', which are recurrent in October and November (A. Zingone et al., 1995).

In our study, a shift in the timing of secondary peak has been detected with respect to the 1984-2000 period. It occurs mainly in October-November than in the period September-October, reported by Ribera et al., 2004. Moreover, the seasonality observed over the whole water column (0-60m), presents a more defined pattern compared to the mean seasonal cycle observed in 1984-2000 by Ribera et al. (2004). Winder and Cloern (2010), analyzing 125 time-series of phytoplankton biomass from temperate and subtropical zones, found nearly half of time-series had only one peak per year, while two peaks are less frequent (20%) and occur more in lake and oceanic sites, than in coastal and estuarine ecosystems. Therefore, the presence of an enhanced seasonality, the decrease in phosphate concentrations observed in this study, coupled with the decrease in phytoplankton cell size (Ribera d'Alcalà et al., 2004) could be indicators of slow changes of the trophic state of the GoN, even if the temporal scale of this study is still too short to assess the ongoing changes.

**Chapter 5: Detailed vertical distribution
and seasonality of N and P as related to
microbial activity (2008-2009)**

5.1 Specific aims of the chapter

During 2008-2009, in the framework of these Ph.D., additional N and P measurements have been carried out for the first time at LTER-MC. In this chapter, these new measurements are analyzed and discussed. More in details, the total, particulate and dissolved organic N and P pools have been investigated in order to characterize their vertical and temporal distribution in terms of:

- concentration
- partition
- stoichiometry

among the different pools.

Besides that, the abundance of the heterotrophic bacteria, their relative contributions to the total C (phytoplankton plus heterotrophic bacteria) and the enzymatic activities (aminopeptidase and alkaline phosphatase) have been analyzed in order to elucidate the role of the microbial communities in the N and P cycles in coastal waters.

5.2 Sampling strategies

The surveys have been carried out at the Long Term Ecological Research Station MareChiara, described in the previous Chapter, from January 2008 up to December 2009. The sampling strategies differed in relation to the investigated parameters. The TN and TP and the heterotrophic bacteria abundances have been determined at 10 depths (0, -2, -5, -10, -20, -30, -40, -50, -60 and -70m), on weekly time scale. The samples for the analyses of PON, POP, DON and DOP concentrations have been collected at 7 depths (0, -2, -5, -10, -20, -40, and -60m). The enzymatic activities (aminopeptidase, and alkaline phosphatase) have been measured at seven depths (0, -2, -5, -10, -20, -40, and -60m), at least twice per month (June 2008-December 2009) All the analytical protocols have been reported in Chapter 2.

5.3 Results

Because of the limited length of the investigated period, it was not possible apply the multiplicative decomposition as in Chapter 4. Thus, to identify and interpret the variability in the parameters analysed, the time evolution and the vertical distribution have been investigated over the whole water column and computing monthly and yearly statistics at selected depths (0m, 20m, 60m and as integrated mean value in the layer 0-60m).

5.3.1 Total N and P

5.3.1.1. Total Nitrogen

The Total Nitrogen (TN) concentrations at LTER-MC station, during the years 2008-2009, ranged between 3.00 mmol m⁻³ and 31.50 mmol m⁻³, recorded at 60m depth (17/12/2008) and at the surface (3/6/2009), respectively. The temporal variability of the TN (Fig 5.1) displays the highest concentrations in the upper layer of the water column (0-10m), generally from March to June.

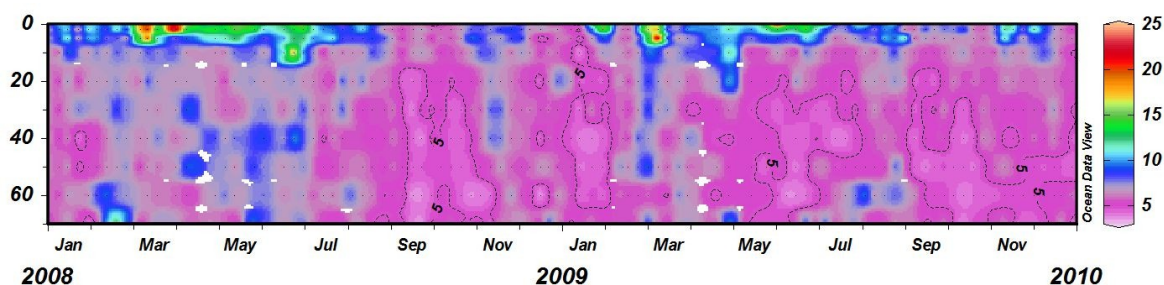


Fig. 5.1 – Temporal variability of the TN concentrations (mmol m⁻³) at LTER-MC station (2008-2009).

The vertical distribution of the TN does not show increasing concentrations in the deepest layer (50-70m), as observed for NO₃ in the previous chapter, except for very limited spotted events. The difference between the concentrations observed at 70m depth and at the surface and were >0.5 mmol m⁻³ only in 12 samples, that means in the 12.5% of the total observations.

The mean integrated concentrations of TN in the layer 0-60m were in the range 3.88-9.61 mmol m⁻³ and showed a mean value of 6.43 mmol m⁻³.

Tab. 5.I – Yearly averaged values and standards deviations, minima, maxima of the TN concentrations at LTER-MC station (2008-2009).

Year	TN (mmol m ⁻³)	Surface	-20m	-60m	Integrated mean value (0-60)
2008	AVG±SD	10.11±4.98	6.27±1.25	6.00±1.48	6.69±1.15
	MIN	3.59	3.74	3.00	4.63
	MAX	27.22	10.11	9.96	9.51
2009	AVG±SD	10.23±5.33	6.02±1.33	5.43±1.30	6.16±1.08
	MIN	3.81	4.05	3.62	3.88
	MAX	31.50	12.16	10.35	9.61

The average yearly values, as well as the minima and maxima, did not change significantly in the two years at all depths. The yearly average and the maximum values display a marked vertical gradient (Tab. 5.I).

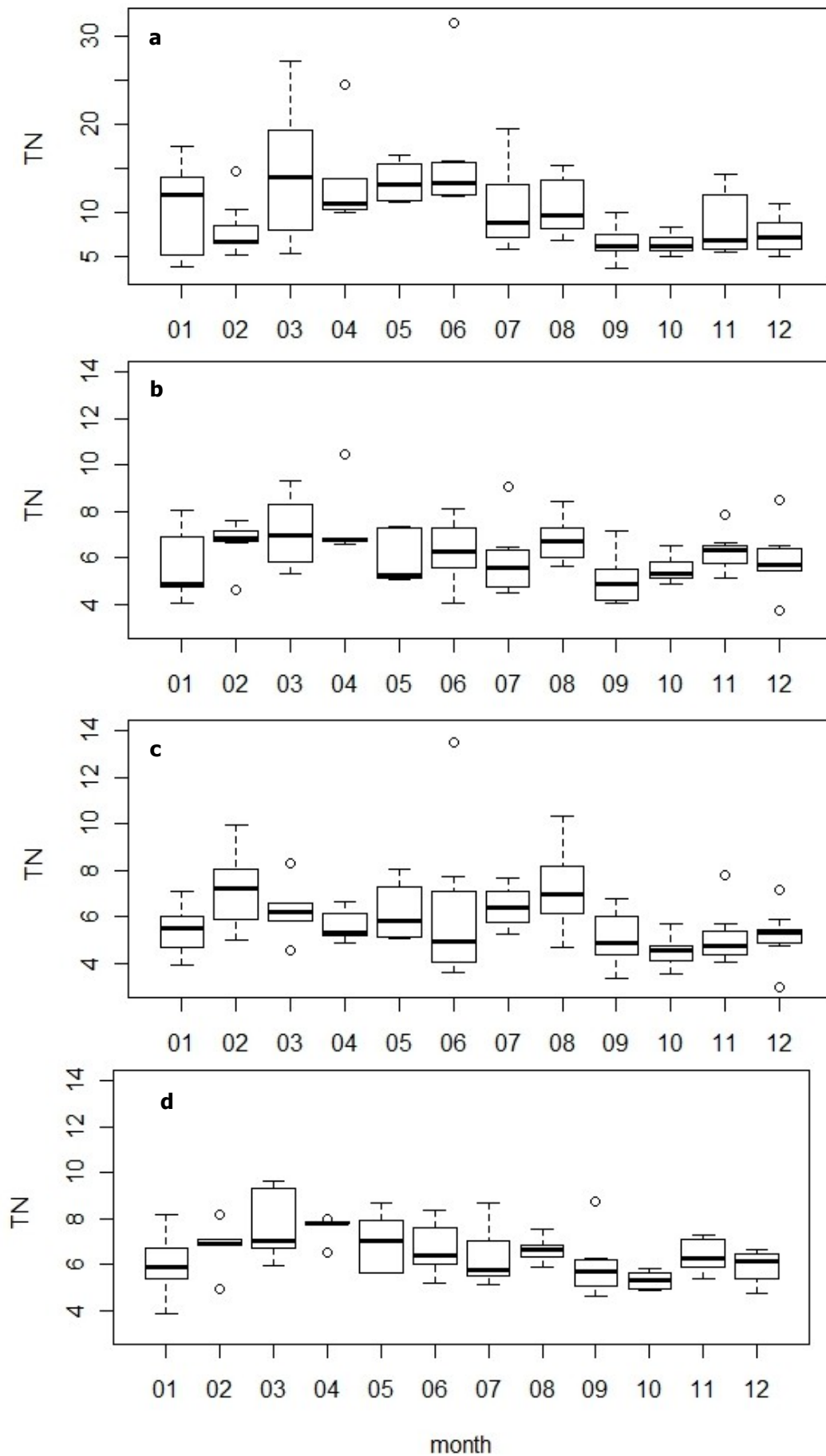


Fig. 5.2 – Seasonal cycle of TN (mmol m^{-3}) at the surface **a**), 20m depth **b**), 60 m depth **c**) and as mean (0-60m) integrated value **d**), box-plot by month.

The monthly statistics present a very pronounced seasonal cycle at the surface (Fig. 5.2 a): the TN increases starting from January up to June, and decreases from July till December. A drastic reduction in TN concentrations is particularly clear in September-December. The highest monthly value ($15.62 \text{ mmol m}^{-3}$) is observed in June, and the lowest (6.39 mmol m^{-3}) in October.

At 20m and 60m, the seasonality of the TN is less pronounced compared to the surface (Fig 5.2, b-c). Generally, from February up to August the TN displays higher concentrations compared to the rest of the year.

The mean monthly values (not shown) reach their maximum in April (7.49 mmol m^{-3}) and the minimum in September (5.09 mmol m^{-3}) at 20m depth. On the other hand, at 60m the maximum of the mean monthly values is recorded in August (7.19 mmol m^{-3}) and the minimum in October (4.51 mmol m^{-3}).

The mean integrated values show a seasonal pattern similar to that of the surface, but characterized by a lower variability (Fig. 5.2, d). The TN concentrations increase from January up to April, then decrease till October and finally increase again afterwards. The highest average monthly value occurs in March (7.72 mmol m^{-3}) and the lowest in October (5.32 mmol m^{-3}).

5.3.1.2. Total Phosphorus

The Total Phosphorus (TP) concentrations in 2008-2009 were in the range 0.04 mmol m^{-3} and 1.74 mmol m^{-3} , observed at 50m (01/07/2008) and at the surface (03/06/2009), respectively.

The highest TP concentrations are observed at the surface, but the vertical gradients are less pronounced compared to the TN (Fig.5.3). An intriguing feature of the TP is the enhancement of the concentrations over the entire water column in periods of strong thermal stratification (June-September), which is coupled to quite high values in 2008.

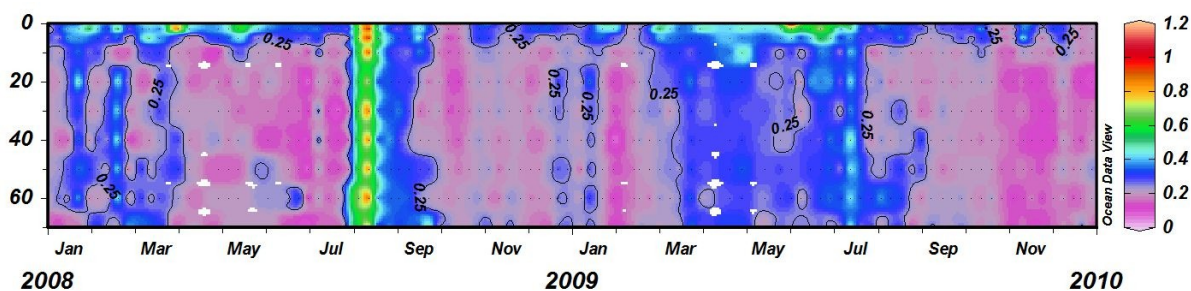


Fig. 5.3 – Temporal variability of the TP concentrations (mmol m^{-3}) at LTER-MC station (2008-2009).

However, the difference between the TP concentrations at 70m and at the surface was higher than 0.05 mmol m^{-3} in 12 observations (12.5% of the total samples), possibly indicating that the main source of TP is of terrestrial origin.

The mean integrated (0-60m) concentrations were in the range 0.09 - 0.97 mmol m^{-3} , and displayed a mean value of 0.25 mmol m^{-3} .

The average and minimum values of TP were similar during the two years (Tab 5.II) at all the investigated depths, and as did the mean integrated (0-60m) values. On the contrary, as

anticipated above, the maxima at 20m, 60m and of the integrated mean were sensibly higher in 2008, due to an exceptional increase of TP over the whole water column occurred on the 12th of August.

Tab. 5.II – Yearly averaged values and standards deviations, minima, maxima of the TP concentrations at LTER-MC station (2008-2009).

Year	TP (mmol m ⁻³)	Surface	-20m	-60m	Integrated mean value (0-60)
2008	AVG±SD	0.38±0.20	0.23±0.13	0.26±0.15	0.26±0.14
	MIN	0.12	0.04	0.06	0.09
	MAX	1.23	0.81	0.99	0.97
2009	AVG±SD	0.39±0.26	0.23±0.09	0.24±0.08	0.24±0.07
	MIN	0.12	0.10	0.11	0.14
	MAX	1.74	0.48	0.46	0.48

The seasonality of the TP is less pronounced compared to the TN at all investigated depths (Fig. 5.4).

At the surface, from March up to August, the TP displays higher concentrations compared to the rest of the year, and shows several outliers. The monthly maximum value is June (0.63 mmol m⁻³), while the minimum is October (0.23 mmol m⁻³).

At 20m and 60m, the concentrations observed from January till August are higher compared to the second part of the year (September-December). At these depths, the highest monthly average values were observed in August (0.36 mmol m⁻³ at 20m and 0.45 mmol m⁻³ at 60m) and the lowest in November (0.17 mmol m⁻³ at both depths).

The mean integrated concentrations (0-60m) display the highest values from March up to September. The average monthly maximum value is August (0.41 mmol m⁻³) and the minimum November (0.19 mmol m⁻³).

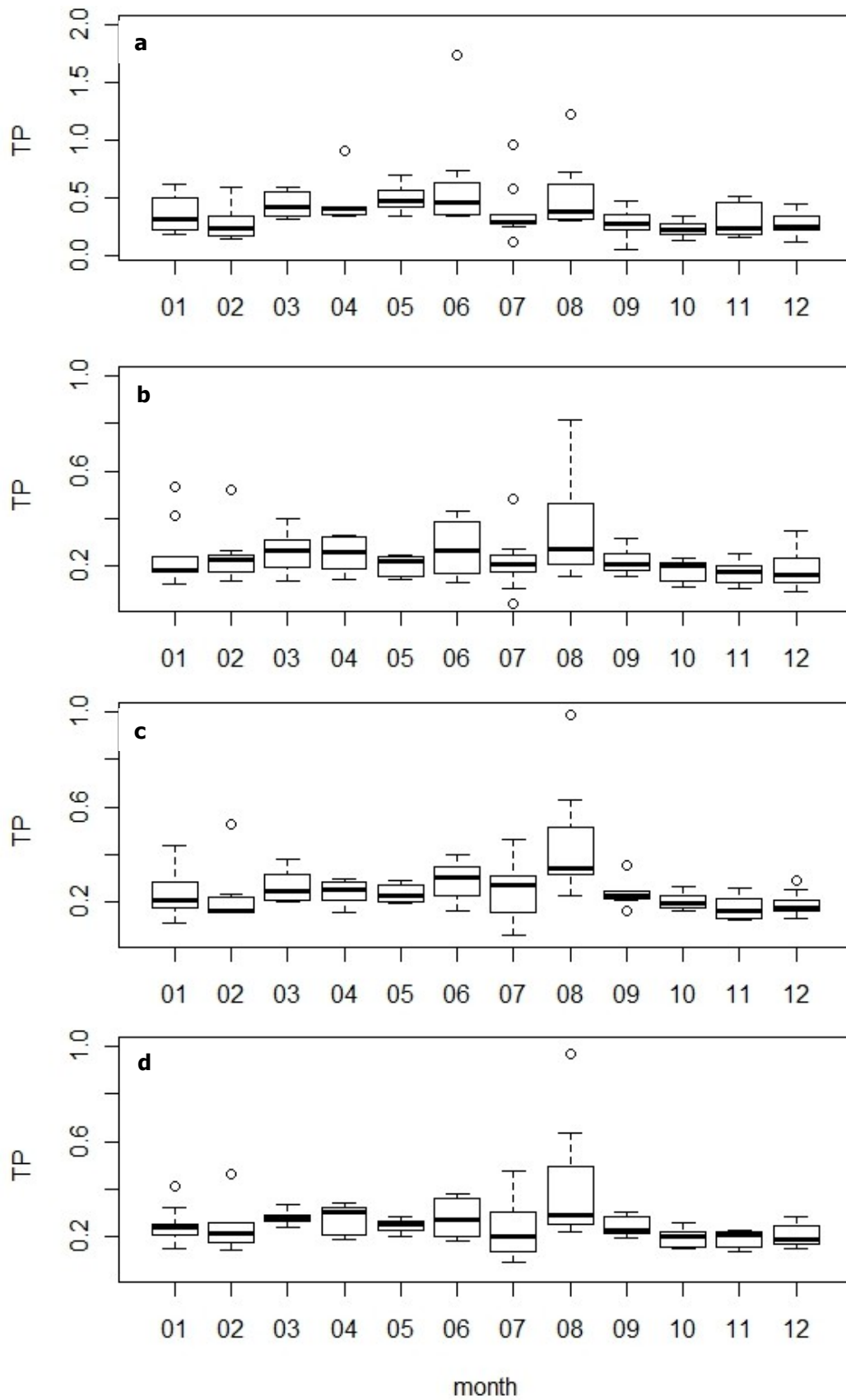


Fig. 5.4 –Seasonal cycle of TP (mmol m^{-3}) at the surface **a**), 20m depth **b**), 60 m depth **c**) and as mean (0-60m) integrated value **d**), box-plot by month.

5.3.2 Particulate N and P

5.3.2.1 Particulate Nitrogen

The Particulate Nitrogen (PN) concentrations at LTER-MC were comprised in the range 0.19-10.93 mmol m^{-3} , recorded at 40m depth (13/5/2008) and at the surface (23/06/2009), respectively.

The PN concentrations displayed the highest values in the upper part of the water column (0-10m), whereas in the lower part (40-60m) the PN concentrations were sensibly lower ($<0.5 \text{ mmol m}^{-3}$) in the most of the surveys (Fig. 5.5). The highest surface concentrations were generally detected in spring (March-June).

The differences between the PN concentrations at 60m and at the surface were greater than 0.2 mmol m^{-3} in only 2 surveys (2% of the total observations), indicating the presence of a strong vertical gradient.

The mean integrated (0-60m) values of the PN were in the range 0.46-2.56 mmol m^{-3} and the average value (2008-2009) was 1.03 mmol m^{-3} .

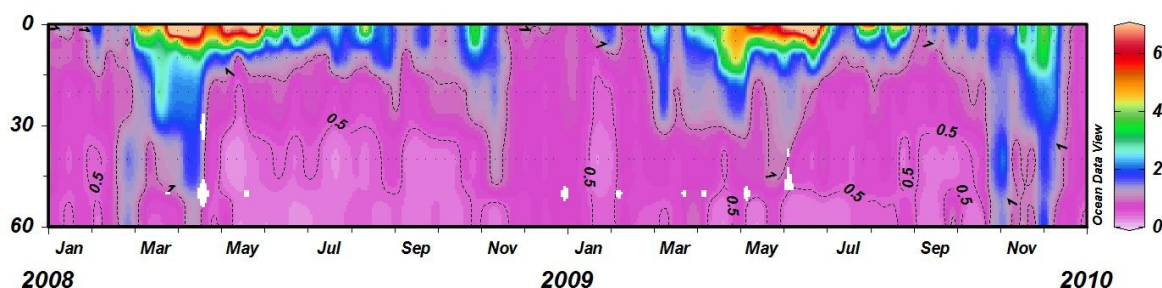


Fig. 5.5 – Temporal variability of the PN concentrations (mmol m^{-3}) at LTER-MC station (2008-2009).

During the two years, the average, minimum and maximum PN concentrations displayed similar values at all the investigated depths (Tab. 5.III).

Tab. 5.III – Yearly averaged values and standards deviations, minima, maxima of the PN concentrations at LTER-MC station (2008-2009).

Year	PN (mmol m^{-3})	Surface	-20m	-60m	Integrated mean value (0-60)
2008	AVG±SD	3.07±2.65	0.90±0.47	0.52±0.26	0.98±0.41
	MIN	0.63	0.35	0.24	0.49
	MAX	10.63	3.00	1.57	2.56
2009	AVG±SD	3.23±2.67	0.99±0.48	0.60±0.36	1.09±0.46
	MIN	0.54	0.42	0.24	0.46
	MAX	10.93	2.35	2.05	2.49

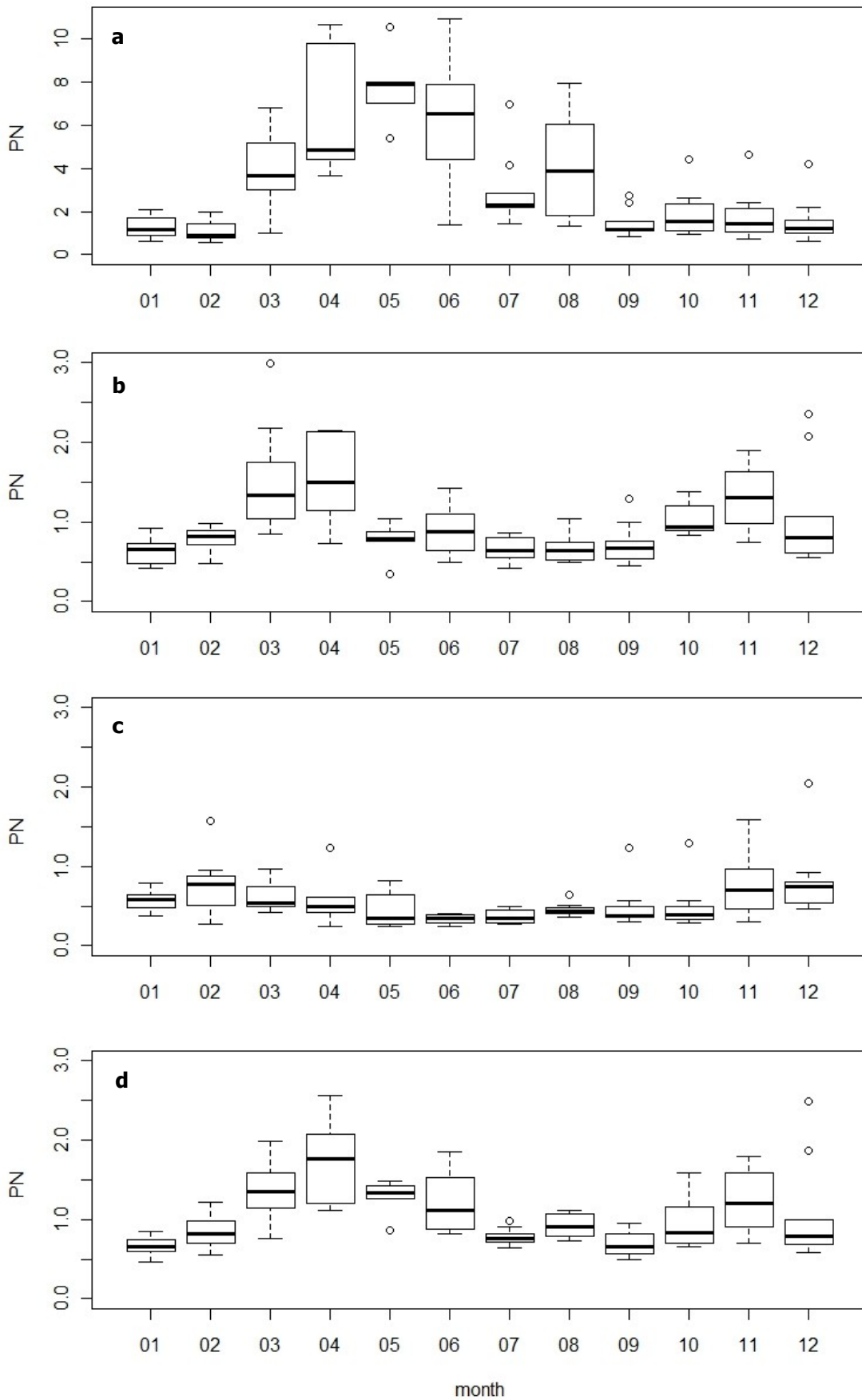


Fig. 5.6 –Seasonal cycle of PN (mmol m⁻³) at the surface **a**), 20m depth **b**), 60 m depth **c**) and as mean (0-60m) integrated value **d**), box-plot by month.

The seasonal patterns differ considerably, depending on the depth (Fig. 5.6). At the surface, the PN concentrations increase from January up to May and then decline up to September. In the period September-December the PN concentrations remain almost stable and show low values. The monthly average values range between 1.12 mmol m⁻³ (February) and 7.76 (May).

The PN concentrations at 20m, 60m and the mean integrated (0-60m) value show a similar seasonal pattern: two main period of higher values are recognizable in spring (March-June) and in autumn (October-November). However, at 60m, the PN shows a reduced variability compared to the other depths. The minima and maxima monthly averaged values at 20m are observed in January (0.62 mmol m⁻³) and March (1.54 mmol m⁻³), whereas at 60m they are recorded in June (0.33 mmol m⁻³) and December (0.82 mmol m⁻³). Finally, the mean integrated concentrations show the highest monthly averaged value in April (1.74 mmol m⁻³) and the lowest in January (0.67 mmol m⁻³).

5.3.2.2 Particulate Phosphorus

The particulate Phosphorus (PP) concentrations ranged from values <0.01 mmol m⁻³ (recorded at 60m, 40m and 20m) to 0.058 mmol m⁻³, observed at the surface (01/04/2008).

The contour plot of PP displays increased values in the upper layer of the water column, especially in spring. On the other hand, the PP concentrations below 20m are less variable and lower compared to the surface values (Fig. 5.7).

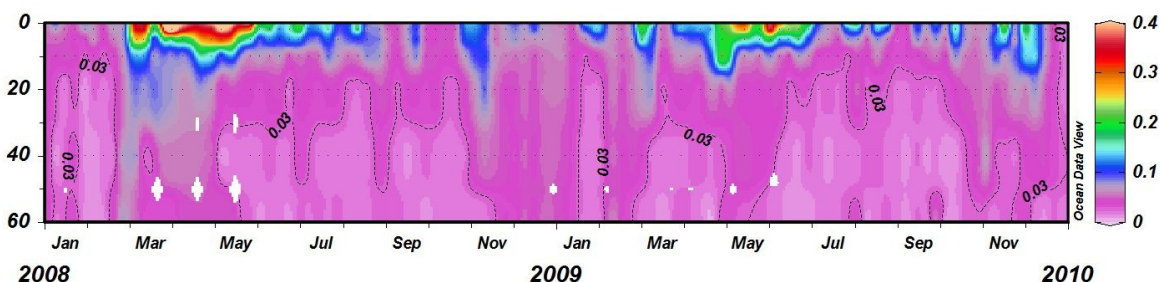


Fig. 5.7 – Temporal variability of the PP concentrations (mmol m⁻³) at LTER-MC station (2008-2009).

The mean integrated (0-60m) concentrations of the PP ranged from 0.02 mmol m⁻³ up to 0.12 mmol m⁻³, displaying an average value of 0.05 mmol m⁻³ and a CV of 43.

Tab. 5. IV – Yearly averaged values and standards deviations, minima, maxima of the PP concentrations at LTER-MC station (2008-2009).

Year	PP (mmol m ⁻³)	Surface	-20m	-60m	Integrated mean value (0-60)
2008	AVG±SD	0.15±0.12	0.04±0.02	0.03±0.02	0.05±0.02
	MIN	0.03	<0.01	<0.01	0.02
	MAX	0.58	0.10	0.08	0.12
2009	AVG±SD	0.14±0.10	0.04±0.02	0.02±0.01	0.04±0.02
	MIN	0.02	0.02	<0.01	0.02
	MAX	0.45	0.09	0.07	0.09

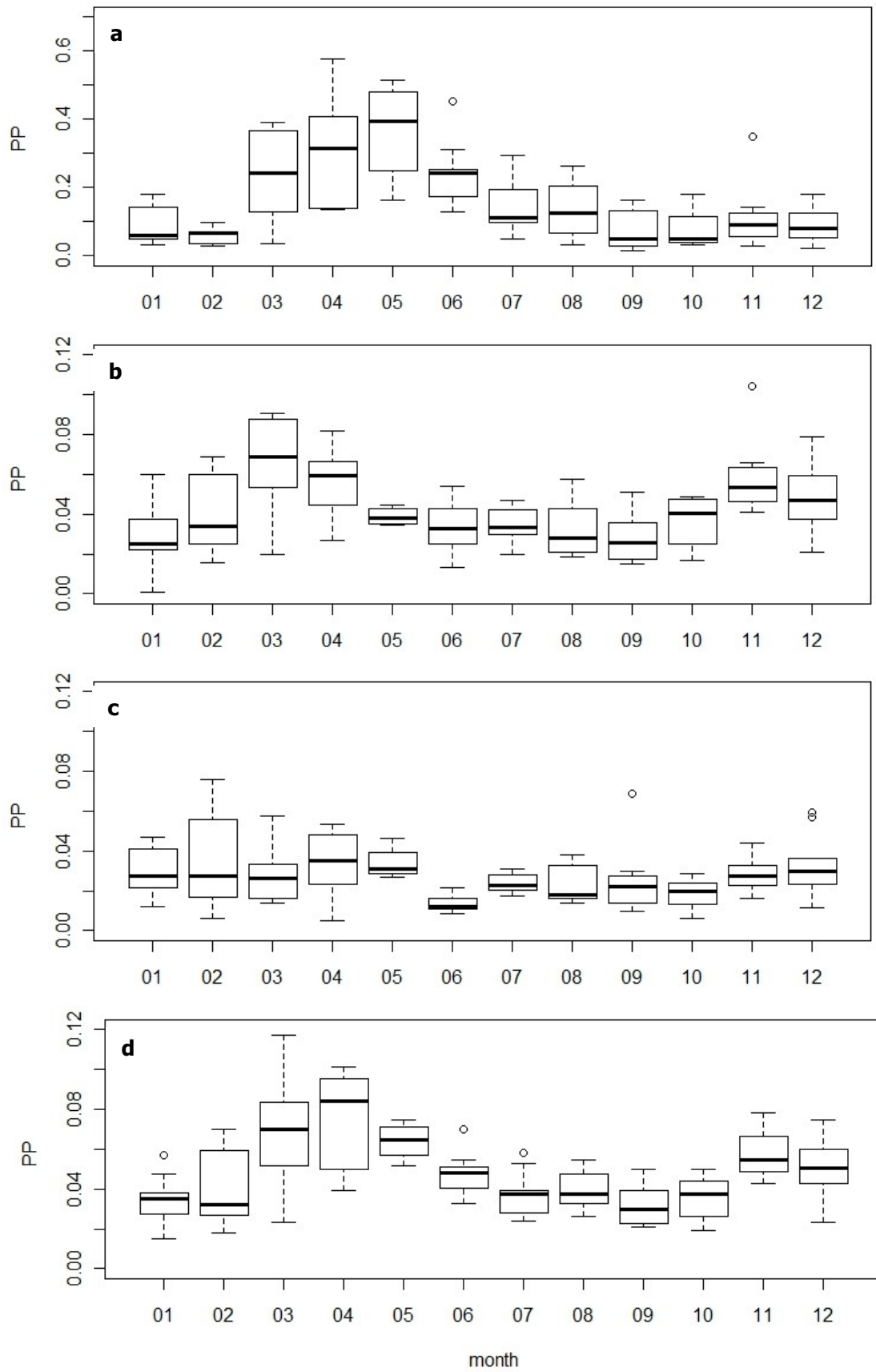


Fig. 5.8 –Seasonal cycle of PP (mmol m^{-3}) at the surface **a**), 20m depth **b**), 60 m depth **c**) and as mean (0-60m) integrated value **d**), box-plot by month.

The differences between the concentrations at 70m and at the surface were $>0.01 \text{ mmol m}^{-3}$ only in 1 sample (1% of the total observations).

In 2008 and 2009 the PP did not display significant differences in the yearly average, minimum and maximum values (Tab. 5.IV).

The seasonality (Fig 5.8) showed the same pattern observed in the previous paragraph for the PN: at the surface increasing PP concentrations are clearly observed in spring, whereas at 20m, 60m and in the mean integrated values, two main peaks of PP are recorded (spring and autumn).

The average monthly concentrations of the PP ranged from 0.06 mmol m^{-3} (February) up to 0.37 mmol m^{-3} (May) at the surface, from 0.03 mmol m^{-3} (December) up to 0.07 mmol m^{-3} (March) at 20m and from 0.01 mmol m^{-3} (June) up to 0.03 mmol m^{-3} (February) at 60m.

The mean integrated (0-60) concentrations displayed the maximum monthly value in March (0.12 mmol m^{-3}) and the lowest in September-October (0.05 mmol m^{-3}).

5.3.3 Dissolved Organic N and P

5.3.3.1 Dissolved Organic Nitrogen

The DON at LTER-MC ranged from 1.35 mmol m^{-3} up to $22.62 \text{ mmol m}^{-3}$, recorded respectively at 60m (2/12/2009) and 5m depth (10/03/2009).

The contour plot of DON did not display a clear vertical distribution (Fig. 5.9): the highest concentrations are generally recorded in the upper layer (0-10m). However enhanced values are recognizable over the whole water column.

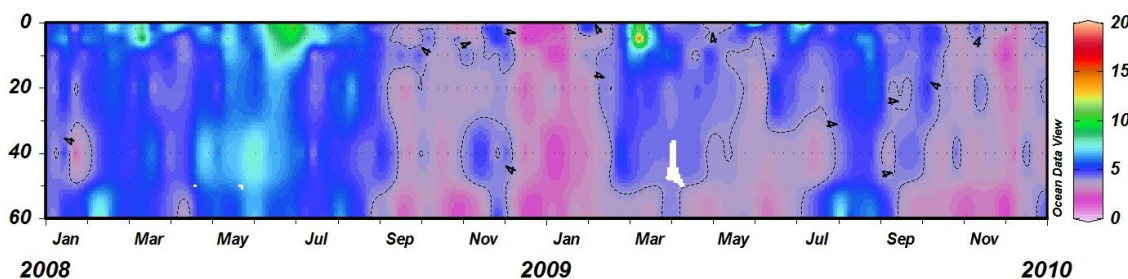


Fig. 5.9 – Temporal variability of the DON concentrations (mmol m^{-3}) at LTER-MC station (2008-2009).

The mean value at the surface, at 20m and 60m did not differ dramatically as found for PN (Tab 5.V). Moreover, the differences between the concentrations at 60m and at the surface were $>0.50 \text{ mmol m}^{-3}$ in 13 samples (16.25% of the total observations).

Tab 5.V – Yearly averaged values and standards deviations, minima, maxima of the PP concentrations at LTER-MC station (2008-2009).

Year	DON (mmol m^{-3})	Surface	-20m	-60m	Integrated mean value (0-60)
2008	AVG±SD	5.50±2.78	4.75±1.30	4.46±1.54	4.73±1.22
	MIN	1.92	2.15	1.81	2.11
	MAX	14.91	7.65	8.36	7.08
2009	AVG±SD	4.96±3.25	4.28±1.13	3.78±1.22	4.14±0.87
	MIN	1.85	2.32	1.35	2.28
	MAX	18.42	8.36	8.69	6.72

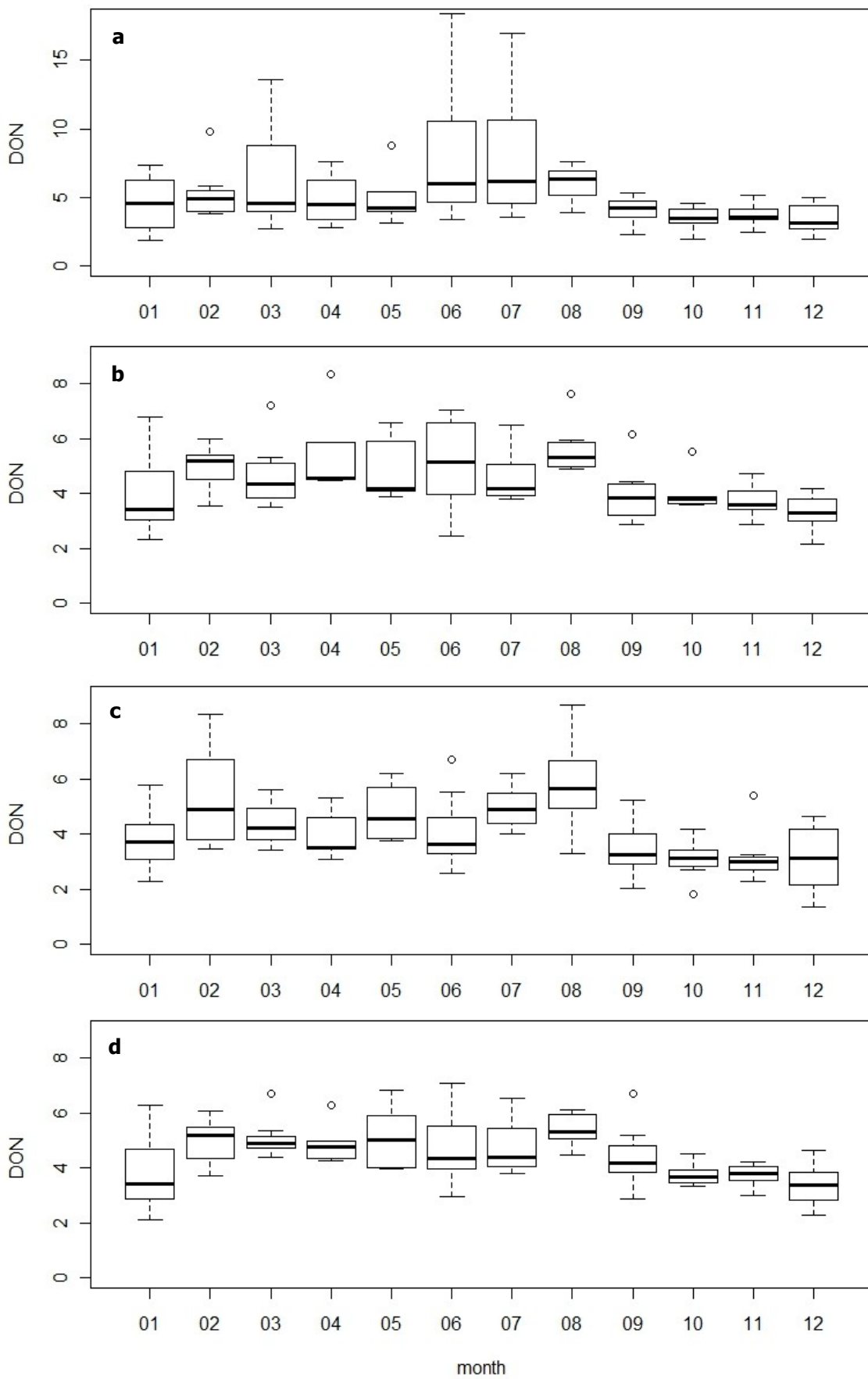


Fig. 5.10 –Seasonal cycle of DON (mmol m^{-3}) at the surface **a**), 20m depth **b**), 60 m depth **c**) and as mean (0-60m) integrated value **d**), box-plot by month.

The values in Tab 5.V do not change significantly during the two years of studies.

The DON shows higher concentrations in the period February-August, compared to the rest of the year, at all the selected depths (Fig. 5.10).

At the surface, the highest mean monthly value is observed in June (8.04 mmol m^{-3}), whereas at 20m and 60m it occurs in August (5.62 mmol m^{-3} and 5.81 mmol m^{-3} , respectively). On the other hand, the minimum monthly value are always observed in December (3.41 mmol m^{-3} at the surface, 3.32 mmol m^{-3} at 20m and 3.12 mmol m^{-3} at 60m).

The mean integrated concentrations display the maximum monthly mean in August (5.41 mmol m^{-3}), and the minimum in December (3.39 mmol m^{-3}).

5.3.3.2 Dissolved Organic Phosphorus

The Dissolved Organic Phosphorus (DOP) varied between 0.01 mmol m^{-3} (17/11/2009) and 1.06 mmol m^{-3} (03/06/2009), both recorded at the surface.

The data plotted in Fig 5.11 display an increase of concentration in summer over the whole water column, in both years.

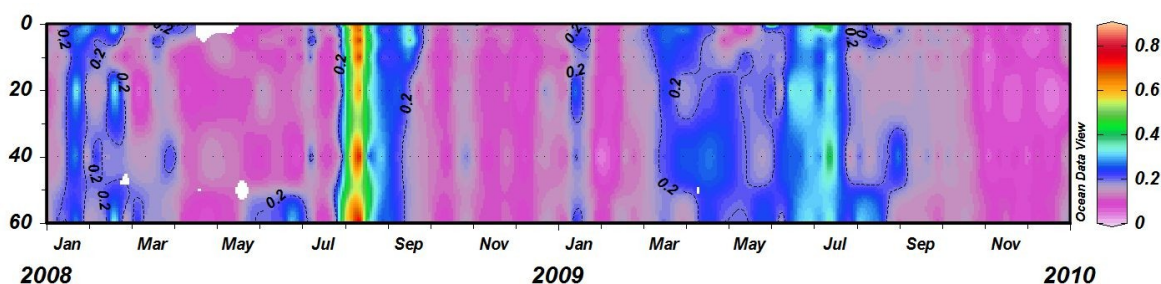


Fig. 5.11 – Temporal variability of the DOP concentrations (mmol m^{-3}) at LTER-MC station (2008-2009).

As observed also for the DON, the vertical distribution of DOP does not show a clear upward/downward vertical gradient but presents rather homogeneous vertical profiles. The differences between 60m depth and the surface were $>0.1 \text{ mmol m}^{-3}$ in 40 surveys (44% of the total observations), confirming the presence of downwards vertical gradients in DOP distributions. However, the highest concentrations were generally detected at the surface.

Tab. 5.VI – Yearly averaged values and standards deviations, minima, maxima of DOP concentrations at LTER-MC station (2008-2009).

Year	DOP (mmol m^{-3})	Surface	-20m	-60m	Integrated mean value (0-60)
2008	AVG±SD	0.20 ± 0.18	0.17 ± 0.14	0.19 ± 0.15	0.18 ± 0.15
	MIN	0.01	0.03	0.05	0.03
	MAX	0.94	0.78	0.92	0.89
2009	AVG±SD	0.18 ± 0.19	0.16 ± 0.10	0.18 ± 0.8	0.17 ± 0.08
	MIN	0.01	0.01	0.05	0.02
	MAX	1.06	0.43	0.39	0.44

The mean integrated DOP (0-60m) concentrations ranged between 0.02 mmol m⁻³ and 0.89 mmol m⁻³, the average value was 0.17 mmol m⁻³.

Tab 5.VI emphasizes the presence of marked differences in the maximum concentration at 20m, 60m and in the integrated value. As for the TP, these values were sensibly higher in 2008, due to an exceptional increase of DOP over the entire water column on the 12th of August. On the contrary, the average and minimum values did not display significant differences (Tab 5.VI).

The seasonal cycle of DOP is characterized by increased concentrations in July and August at all depths(Fig 5.12). At the surface, the DOP rises from January up to March, then decreases up to June and increases again from June to July-August. Starting from August up to December, the DOP concentrations decline again. The highest monthly value is observed in July (0.36 mmol m⁻³) and the lowest in December (0.10 mmol m⁻³).

At 20m and 60m, the DOP is almost stable from January to May. In June-August, the concentrations increase, whereas starting from September up to December a clear reduction of DOP is recognizable.

The integrated values show the same seasonal pattern observed at 20m and 60m.

The monthly mean value is maximum in August at 20m (0.31 mmol m⁻³) at 60m (0.38 mmol m⁻³) and as integrated value (0.34 mmol m⁻³). The minimum monthly values are observed in November at 20m (0.08 mmol m⁻³) and 60m (0.10 mmol m⁻³), and as integrated mean concentrations (0.09 mmol m⁻³).

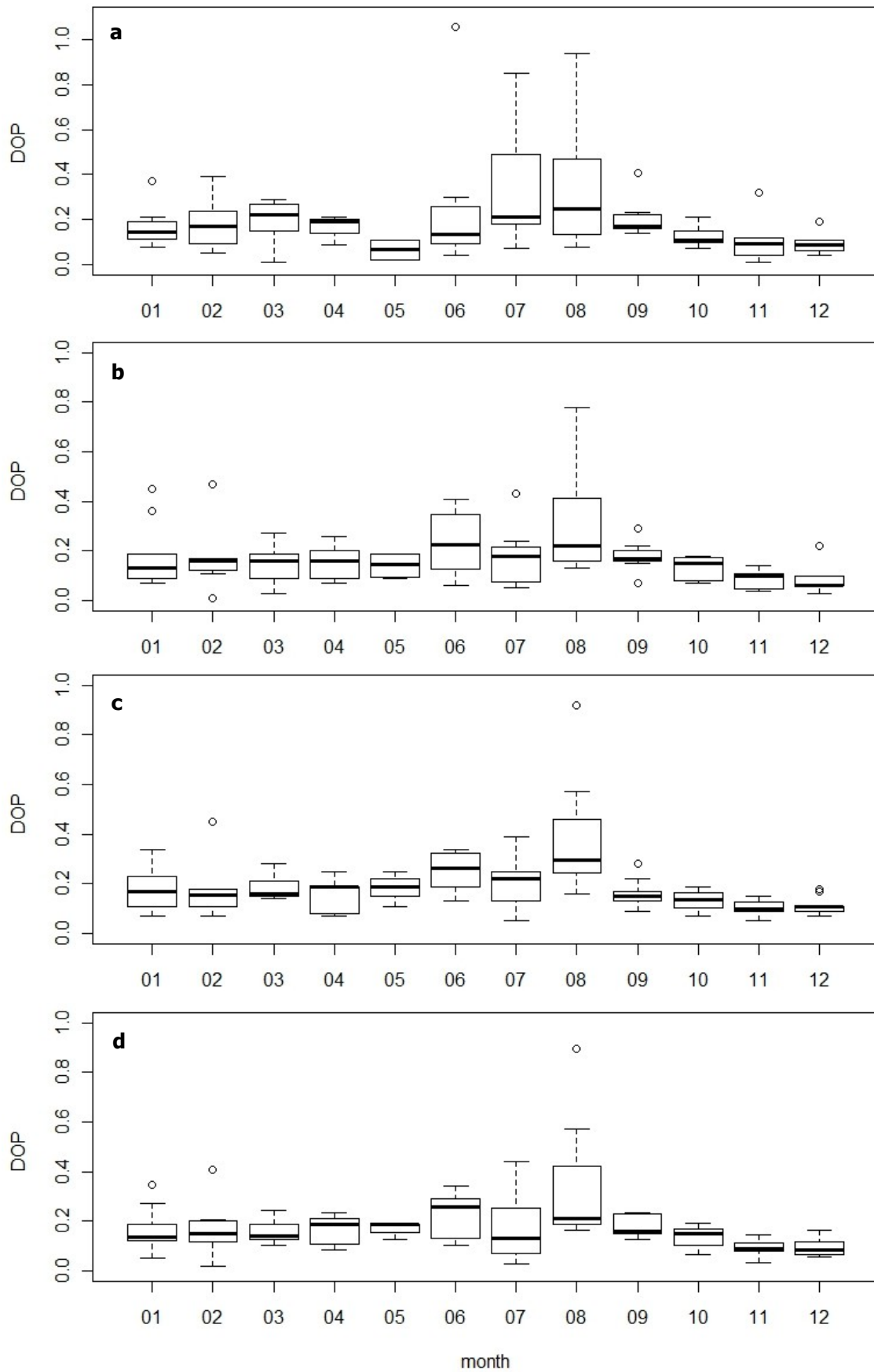


Fig. 5.12 –Seasonal cycle of DOP (mmol m^{-3}) at the surface **a**), 20m depth **b**), 60 m depth **c**) and as mean (0-60m) integrated value **d**), box-plot by month.

5.3.4 N and P compositions

In this section, the N and P percentage compositions at the surface, at 20m, at 60m and the 0-60m integrated mean have been investigated. More in details, the average percentage of the NO_3 , NH_4 , PN and DON has been analyzed in order to characterize the N pools, whereas PO_4 , PP and DOP have been taken into account to study the P composition.

The average composition has been reported at each selected depth, in order to characterize the vertical distribution of N and P compounds, and as integrated mean value to give an idea of the bulk properties of the whole water column.

Finally, the percentage composition of the N and P pools has been studied on monthly time-scale in order to investigate their seasonality.

5.3.4.1 N inventory

The N averaged compositions, as shown in Tab.V.II, indicate that the main N pool is the dissolved organic (DON) over the whole water column. However, significant differences can be identified among the different depths.

At the surface, the N composition shows the highest diversity: the DON accounts for half of TN, while the PN and DIN show similar percentages (~25%).

In the subsurface layers (20m and 60m), the DON accounts for more than 70% of the TN. However, at 20m the second N pool is the particulate, while at 60m it is the dissolved inorganic (mainly NO_3).

Tab. 5.VII – Averaged (2008-2009) percentage contribution of the main N pools to the TN at the surface, at 20m, at-60m and as mean integrated (0-60m) values at LTER-MC station.

N pool	Surface	-20m	-60m	Integrated mean value (0-60)
NO_3 (%)	7.42	4.00	9.05	5.22
NH_4 (%)	8.56	5.93	3.94	5.78
DON (%)	53.98	72.45	71.51	69.21
PN (%)	27.63	15.74	10.53	16.22

The seasonality of N compounds shows the highest variability at the surface and the lowest at 60m (Fig. 5.13).

At the surface the most important N pool is the DON all year long, except for April and May, when the PN is the most abundant N form. NO_3 and NH_4 account for around 30% of the TN from November to January and in March, while from May to August it attains below less than 5%.

At 20m the DON represents more than 60% of the TN all year long. In March and April, a slight increase of PN can be observed, while in October, November and December the cumulative NO_3 and NH_4 percentages are higher than 10%.

At 60m, the seasonal pattern of the N resembles that observed at 20m. However, the sum NO_3+NH_4 is always >10% of the TN and the PN fluctuations are less pronounced compared to 20m.

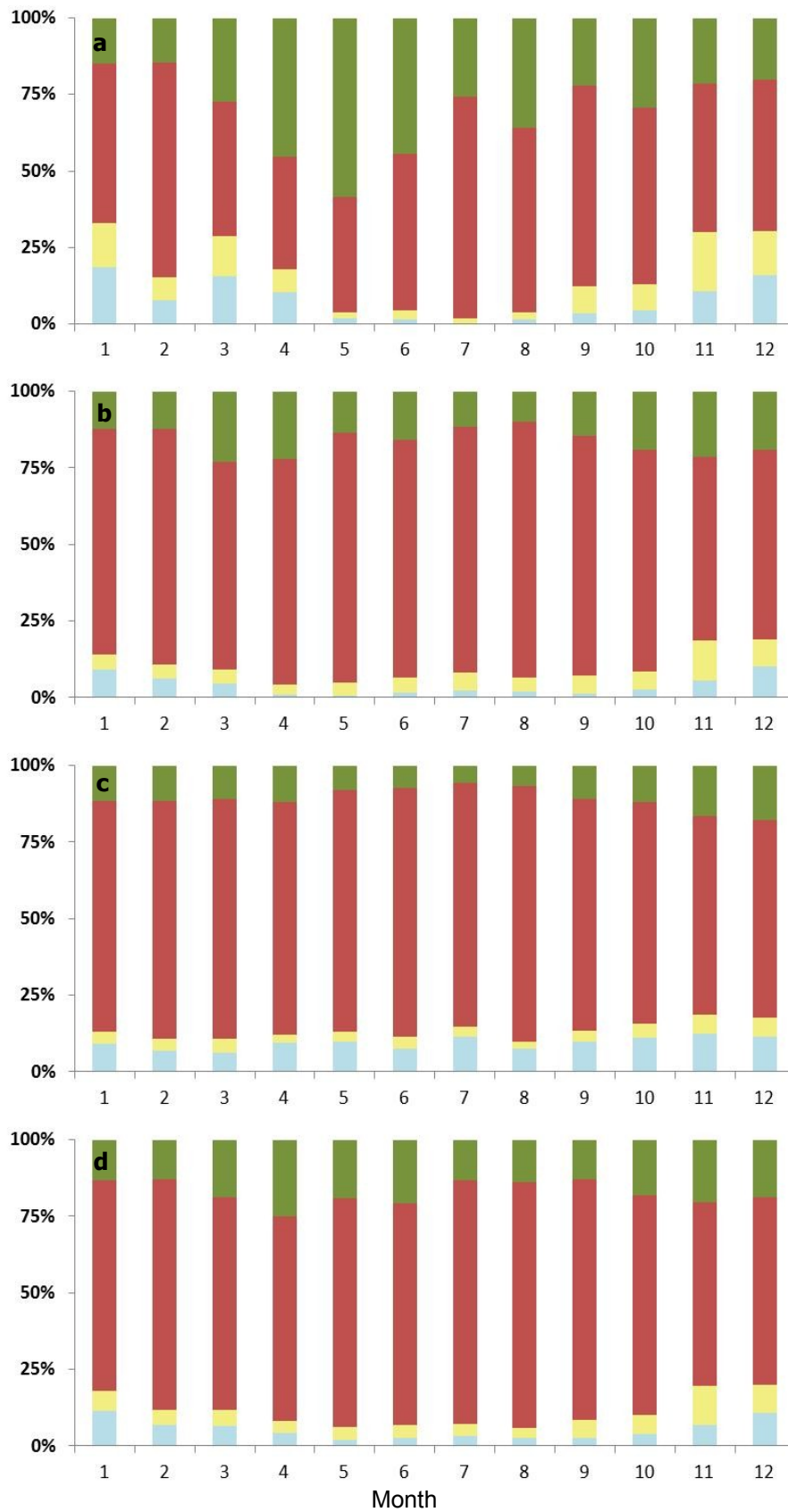


Fig. 5.13— Monthly percentage composition of TN (NH_4 , NO_3 , DON and PN) at the **a**) surface, **b**) 20m, **c**) 60m and **d**) as integrated mean (0-60m) values at LTER-MC (2008-2009).

As integrated values, the DON represents always more than 60% of the TN. The PN percentages increase in spring (March-June) and autumn (October-December) and the sum of NH₄ and NO₃ displays the highest contribution from November till to January.

5.3.4.2 P inventory

The percentage distribution of the P among the different pools is similar to that observed for N in the previous section. The main component of P is the DOP at all depths. However, the percentage of DOP is slight lower than DON.

At the surface, the P composition is more heterogeneous compared to the other depths. The DOP accounts for half of the TP, followed by the PP accounting for about one third.

At 20m and 60m, the DOP represents more than 60% of the TP, and its relative contributions increase with depth. On the contrary, the PP displays a negative vertical gradient (Tab. 5.VIII).

Tab. 5.VIII – Averaged (2008-2009) percentage contribution of the main P pools to the TN at the surface, at 20m, at 60m and as mean integrated (0-60m) values at LTER-MC station.

P pool	Surface	-20m	-60m	Integrated mean value (0-60)
PO ₄ (%)	19.49	12.72	18.11	14.45
DOP (%)	48.99	66.25	69.90	63.99
PP (%)	31.51	21.03	11.99	21.44

The seasonal pattern of P is somehow similar to that of N (Fig. 5.14). At the surface, it is possible to observe the highest variability among the different P pools. The highest percentage of PP are observed from March up to August, reaching more than 50% in April and May. On the contrary, the DOP displays the lowest percentage from May up to June and the highest relative values from July up to September. The phosphate contribution to the TP is higher from November up to January compared to the rest of the year.

At 20m and 60m, the variability in the composition of the P pool is drastically reduced compared to the surface. At 20m, the seasonal variability is largely due to the PP, that increases its percentage in spring (March and April) and autumn (November). At 60m the variability of the P composition is related mainly to the PO₄, whereas the PP accounts for less than 10% all year long.

As integrated mean value, the PP displays the highest percentages in spring and autumn, while the phosphates are highest from November till January.

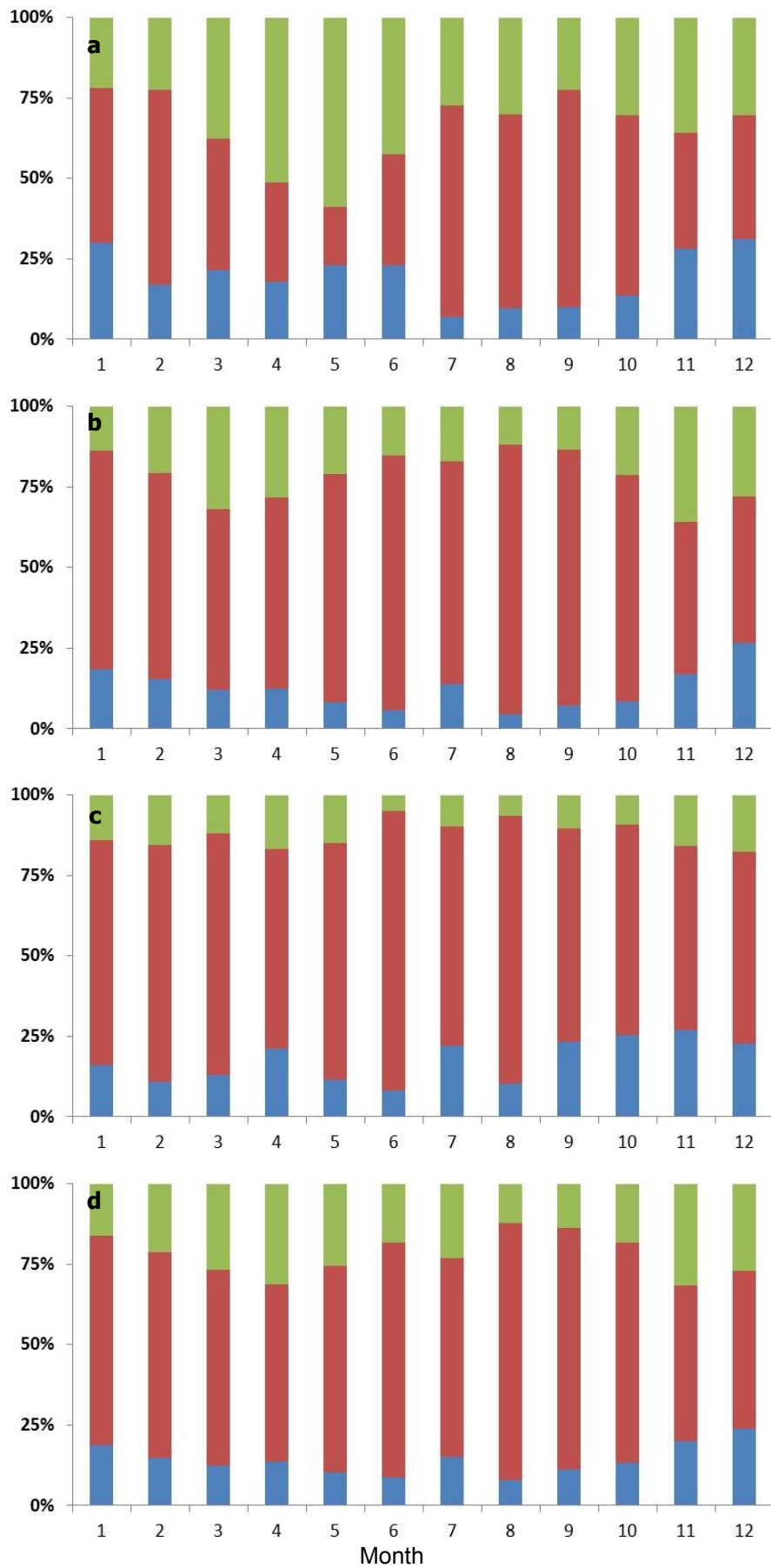


Fig. 5.14– Monthly percentage composition of TP (■ PO₄, ■ DOP and ■ PP) at the **a)** surface, **b)** 20m, **c)** 60m and **d)** as integrated mean (0-60m) values at LTER-MC (2008-2009).

5.3.5 N/P ratios

In this section, the N/P ratio has been investigated in the total, in the particulate and in the dissolved organic pools. For each pool the temporal variability of the N/P ratio over the whole water column and the seasonality at selected depths (0m, 20m, 60m and as integrated mean value in the layer 0-60m) have been analyzed.

5.3.5.1 N/P ratio in the Total Pool

The TN/TP ratio ranged between 4.72 and 132, both recorded at 30m (12/08/2008 and 29/07/2008, respectively).

The data plotted in Fig. 5.15 point out the ratio is higher than 20 most of the time. In fact, the (2008-2009) mean values were >25 at all depths (28.33, 30.73, 25.69 and 28.5 at the surface, 20m, 60m, and as integrated mean value, respectively).

Values less than 20 were mainly observed in the layer 20-60m in late spring-summer.

A clear vertical pattern was not detectable, the ratio seems enough uniform over the water column and sporadic and localized increases were observed mainly in the layer 20-60m.

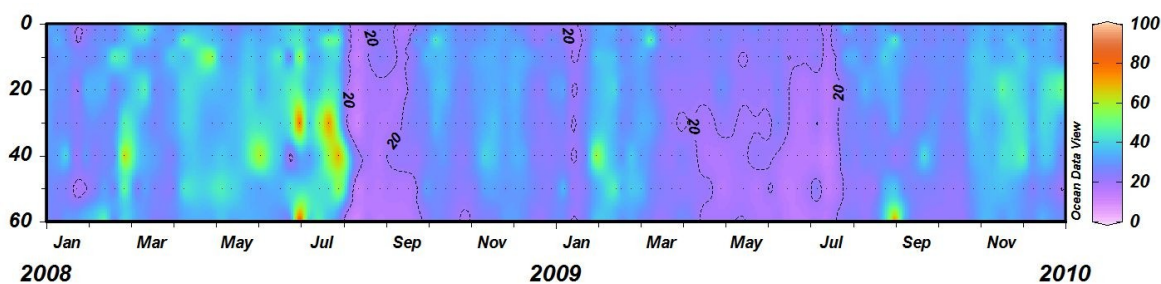


Fig. 5.15 – Temporal variability of the TP/TN ratio (mol/mol) at LTER-MC station (2008-2009).

The seasonality was analyzed by means of monthly box plots (Fig 5.16), looking at the surface, 20m, 60m and at the mean integrated value (0-60m).

At the surface, the TN/TP ratio does not display any seasonality. The median values are almost stable and attain around 27. In July, it is possible to observe the highest variability of the TN/TP ratio.

At 20m, a drop of the ratio occurs from July till September. In these months, the TN/TP shows a median value around 23-24. On the contrary, in November and December the highest values of this ratio are observed (median values ~ 37).

At 60m, the seasonal cycle is more pronounced compared to 0m and 20m. The ratio is maximum in February (median value 40) and shows high values from November till February. In contrast, in the period March-October, the N/P ratio displays a strong reduction reaching median values near 20.

The integrated mean value in the layer 0-60m did not display a clear seasonal signal. The highest median values are observed in February, May and November (>33) and the lowest (<24) in June and August.

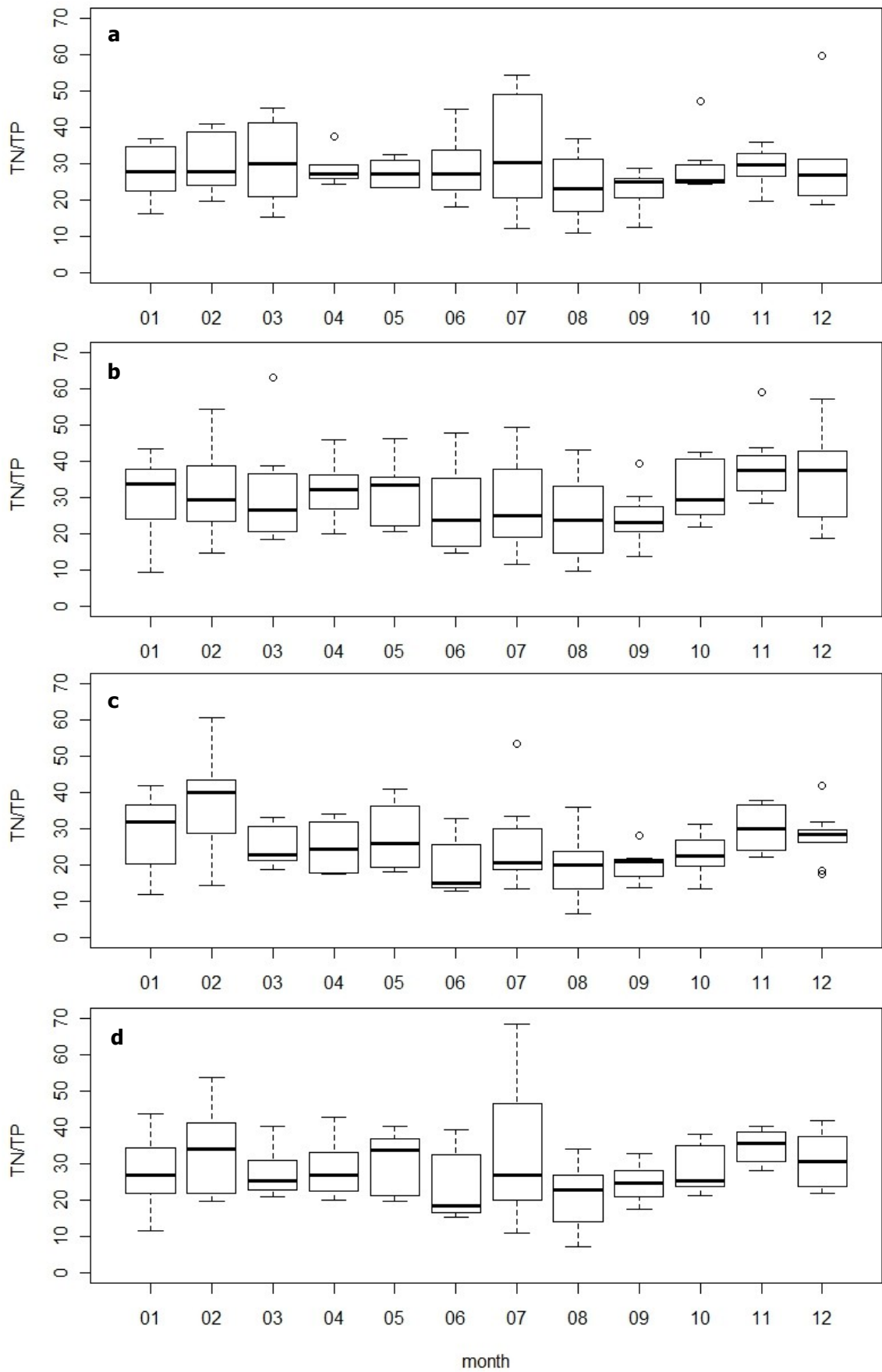


Fig. 5.16 –Seasonal cycle of TN/TP (mol mol⁻¹) at the surface **a**), 20m depth **b**), 60 m depth **c**) and as mean (0-60m) integrated value **d**), box-plot by month.

5.3.5.2 N/P ratio in the Particulate Pool

The N/P ratio in the Particulate pool displays lower variability compared to the Total.

Indeed, the PN/PP ratio was within the range 9.34 - 72.20, recorded at 60m (15/09/2009) and 40m (12/03/2008), respectively. This ratio is rather homogeneous with depth: the mean ratio is around 23-25 at each depth (23.33, 25.27, 23.38 and 25.13 at the surface, 20m, 40m and 60m and as integrated mean value, respectively). However, higher values are occasionally detected, mainly at 40m and 60m depth (Fig. 5.17).

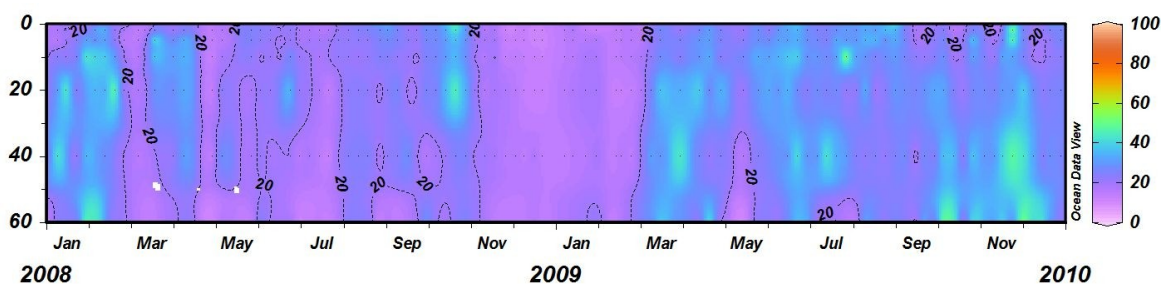


Fig. 5.17 – Temporal variability of the PN/PP ratio (mol/mol) at LTER-MC station (2008-2009).

The seasonal cycle of the PN/PP ratio at the surface shows a clear temporal pattern (Fig. 5.18, a). The ratio rises from January up to August and then decreases till December. Starting from March up to October, the median values of the ratio are >20 , whereas, in the rest of the year, they are <20 . The monthly median values ranged from 15 (January) up to 29 (August).

At 20m, the N/P particulate ratio depletes from October (median value ~ 31) till February (median value ~ 14). It sharply increases in March and April, then slightly decreases, oscillating around 20-26 from May up to August, and finally raise again in September-October (Fig. 5.18, b).

At 60m, a clear seasonality is not recognizable, but a stronger variability is found in autumn (Fig. 5.18, c). The lowest median values are detected in May (~ 14) and July (~ 15), and the highest in March (~ 26).

As integrated mean in the layer 0-60m, the PN/PP ratio displays low values in January and March. An abrupt increment is evident in March (median value ~ 34), and the ratio progressively decreases till August (median value ~ 15). It increases again in September and October, and finally declines in November and December (Fig. 5.18, d).

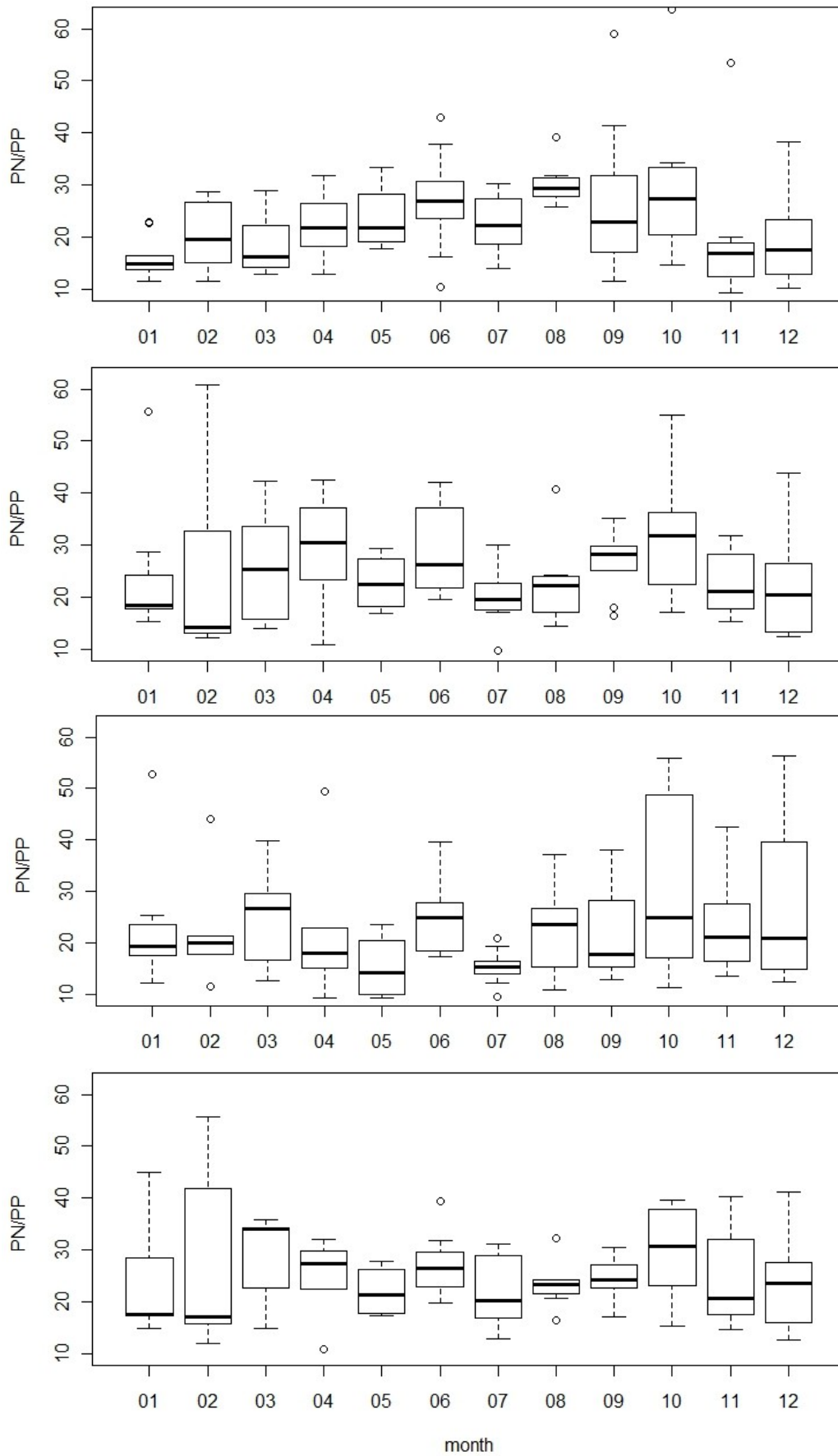


Fig. 5.18—Seasonal cycle of PN/PP (mol mol⁻¹) at the surface **a**), 20m depth **b**), 60 m depth **c**) and as mean (0-60m) integrated value **d**), box-plot by month.

5.3.5.3 N/P ratio in the Dissolved organic Pool

The N/P ratio in the dissolved organic pool displays an intense variability, higher than those observed in the other pools. The DON/DOP ratios were in the range 4.52-172.85, with both extreme values observed at 10m (12/08/2008 and 17/06/2008).

The DON/DOP ratio is higher in the layer 0-20m compared to the layer 40-60m. Indeed, the mean DON/DOP values are 37.7, 37.9 and 28.78 at 0m, 20m and 60m, respectively. The average ratio as (0-60m) integrated mean value is 35.40.

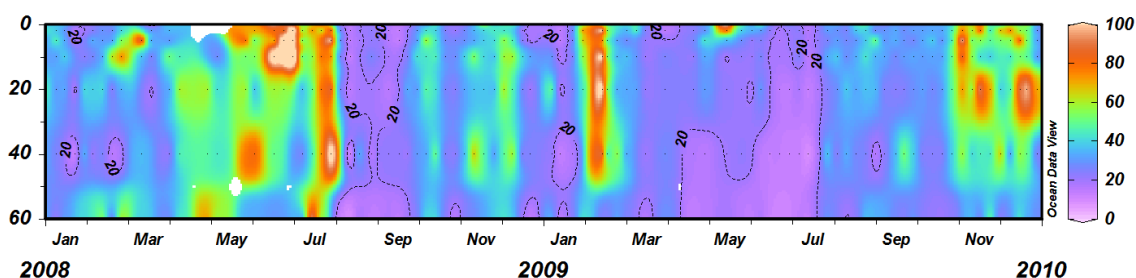


Fig. 5.19 – Temporal variability of the DON/DOP ratio (mol/mol) at LTER-MC station (2008-2009).

The lowest ratio are generally observed in July-August over the entire water column, whereas the highest values are mainly observed in spring (April-June) in the upper layer (0-10m), especially in 2008 (Fig. 5.19).

Looking at monthly distribution (Fig. 5.20), the DON/DOP at the surface is sensibly higher in May (median value 88) and June compared to the rest of the year. Enhanced values are observed also in November and December, whereas in the rest of the years the DON/DOP ratio are less variable, with median values in the range 16-30.

At 20m, the DON/DOP ratio is less variable compared to the surface: the median monthly values ranged from 47 (December) to 23 (September). The DON/DOP ratios slightly decrease starting from January up to September, even if a strong variability is observed in April and July. From September up to December, the ratio increases again.

At 60m, the seasonal pattern resembles that observed at the surface. However, the decreasing phase ends in June (median~16) and, successively, the DON/DOP ratio increases again up to February (median~39).

As integrated mean value (0-60m), the DON/DOP ratio displays high values from November up to February (in this period the median values are in the range 36-49), and sensibly lower ratios in March-September (median values 22-30).

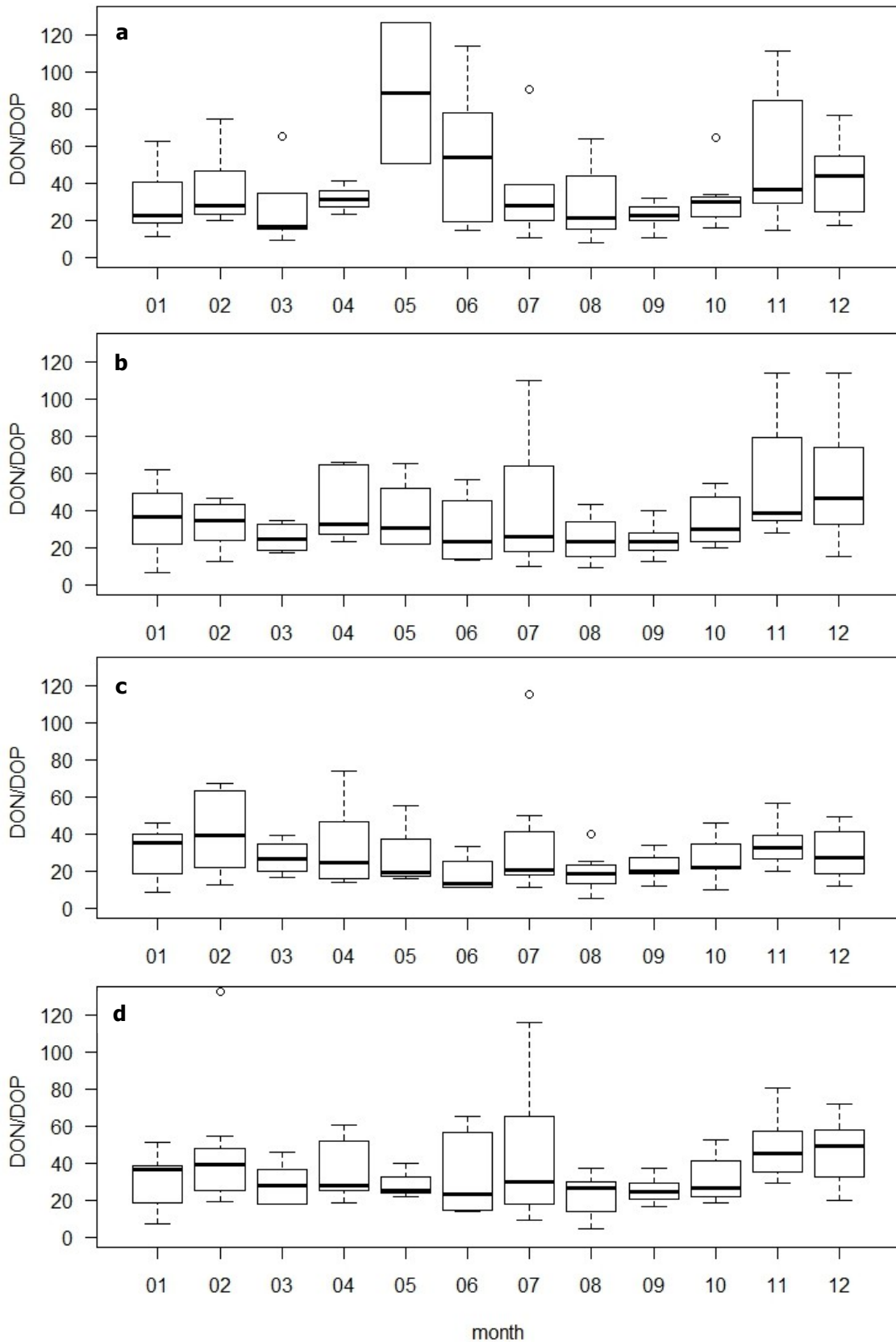


Fig. 5.20—Seasonal cycle of DON/DOP (mol mol⁻¹) at the surface **a**), 20m depth **b**), 60 m depth **c**) and as mean (0-60m) integrated value **d**), box-plot by month.

5.3.6 Heterotrophic bacteria

During 2008-2009, the heterotrophic bacteria (HB) abundances ranged between $2.3 \cdot 10^5$ cells ml⁻¹ (11/11/2008) and $4.4 \cdot 10^6$ cells ml⁻¹ (25/3/2009), recorded at 70m and 2m, respectively.

The highest abundances were always recorded in the upper part of the water column (0-10m) and the lowest in the 50-70m layer (Fig. 5.21). Indeed, the difference of HB abundance at 60m and at the surface was positive in 3 surveys (~3% of the total observations).

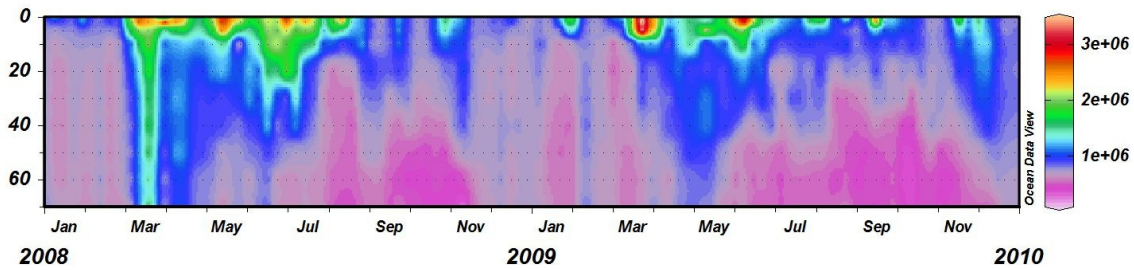


Fig. 5.21 – Time variability of the Heterotrophic bacteria abundances (cells ml⁻¹) at LTER-MC station (2008-2009).

The yearly mean abundances, as well as the yearly minimum values, were similar in the two years (Tab. V.IX). On the contrary, the maxima observed in 2008 at 20m and 60m were significantly higher than in 2009, mainly due to a winter event that affected the whole water column (observed on 19/3/2008).

Tab. 5.IX – Yearly averages, standard deviations, minima, maxima of HB abundances (cells ml⁻¹) at LTER-MC station (2008-2009).

Year	HB (cells ml ⁻¹)	Surface	-20m	-60m	Integrated mean value (0-60)
2008	AVG±SD	1.5E+06±8.0E+05	9.4E+05±3.7E+05	6.7E+05±2.0E+05	9.1E+05±2.8E+05
	MIN	6.9E+05	5.1E+05	4.0E+05	6.1E+05
	MAX	3.9E+06	2.2E+06	1.5E+06	1.9E+06
2009	AVG±SD	1.5E+06±8.2E+05	8.3E+05±1.8E+05	5.9E+05±1.3E+05	8.4E+05±2.1E+05
	MIN	6.3E+05	4.6E+05	3.2E+05	6.0E+05
	MAX	4.2E+06	1.2E+06	8.7E+05	1.7E+06

As integrated mean values (0-60m), the mean HB abundance was $8.7 \cdot 10^5$ cells ml⁻¹. Corresponding yearly mean, minimum and maximum values did not significantly changed in 2008 and 2009 (Tab.5.IX).

The seasonality of the HB is very pronounced at the surface. The HB abundances are sensibly higher in all the period March-August, while in the rest of the year they reduce to almost one half. At 20m, the HB abundance increases from March till June, when the maximum median value is reached. Starting from July up to February, the HB abundances remain stable, and the median fluctuates around $7 \cdot 10^5$ cells ml⁻¹.

At 60m, highest HB abundances are recorded from January till May, especially in April-May. Starting from June up to October, a clear decline of the HB concentrations is observed, followed by a new increase up to December.

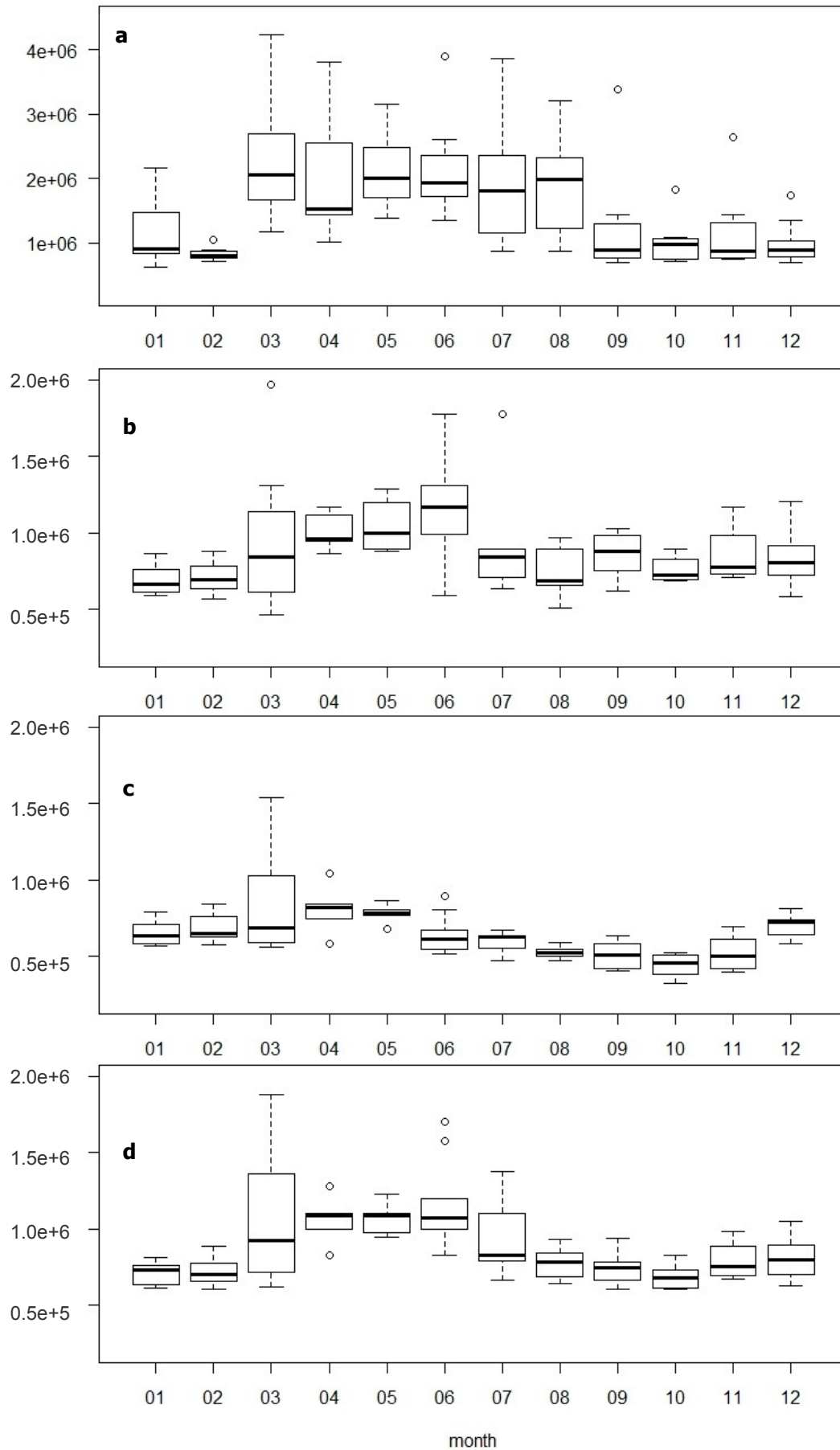


Fig. 5.22 –Seasonal cycle of HB abundances (cells ml⁻¹) at the surface **a**), 20m depth **b**), 60 m depth **c**) and as mean (0-60m) integrated value **d**), box-plot by month

As integrated mean values, the HB exhibit the highest abundances in the period April-June. March and June display a large variability and high median values. In the other months, the HB concentrations are low and more stable.

5.3.7 Carbon distribution and ratios in heterotrophic bacteria and phytoplankton

In this section, we investigated the relative contribution of heterotrophic bacteria and phytoplankton in terms of carbon, as described in the material and methods chapter. The results are reported as percentages of the HB carbon.

The minimum percentage of the HB (6%) was recorded at 5m depth, and the maximum (76%) at 60m, recorded in the surveys carried out on the 10/3/2009 and 19/3/2008, respectively. The relative proportion of HB increases with depth, varying from a mean value of 35% at the surface to 54% at 60m depth.

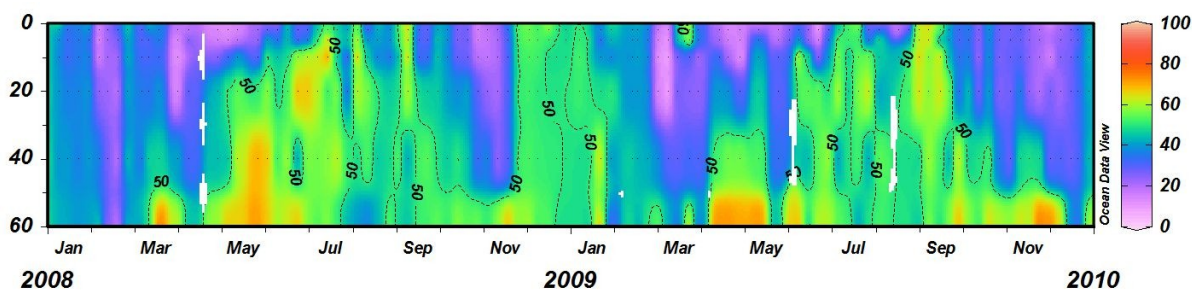


Fig. 5.25 – Percent contribution of heterotrophic bacterial carbon to total carbon (phytoplankton plus bacteria) at LTER-MC station (2008-2009).

The relative proportion of the HB displays an intense temporal variability. The HB biomass is higher than phytoplankton during oligotrophic conditions, while phytoplankton dominates during the main blooms (spring and autumn) over the whole water column (Fig. 5.25).

The seasonal cycle completely differed among the investigated depths (Fig. 5.26): at the surface, the highest relative proportion of HB was found in summer (mainly July and September) and the lowest in spring (from April up to June), indicating decoupling phase of development between bacteria and phytoplankton. However, the median values of HB are always <50, indicating a dominance of autotrophs at the surface.

At 20 m, the HB dominate the microbial assemblage throughout the late spring-summer, while the phytoplankton in the rest of the year (mainly in March and November).

At 60m the HB percentage is high (median values >60%) from March up to June and low in January-March (median values <40%). In the rest of the years the relative contribution of HB is less variable and the median values fluctuate around 50-60%.

As integrated mean value (0-60m), the HB show their highest relative proportion in late spring-summer (from May up to September), whereas phytoplankton dominate in the rest of the years.

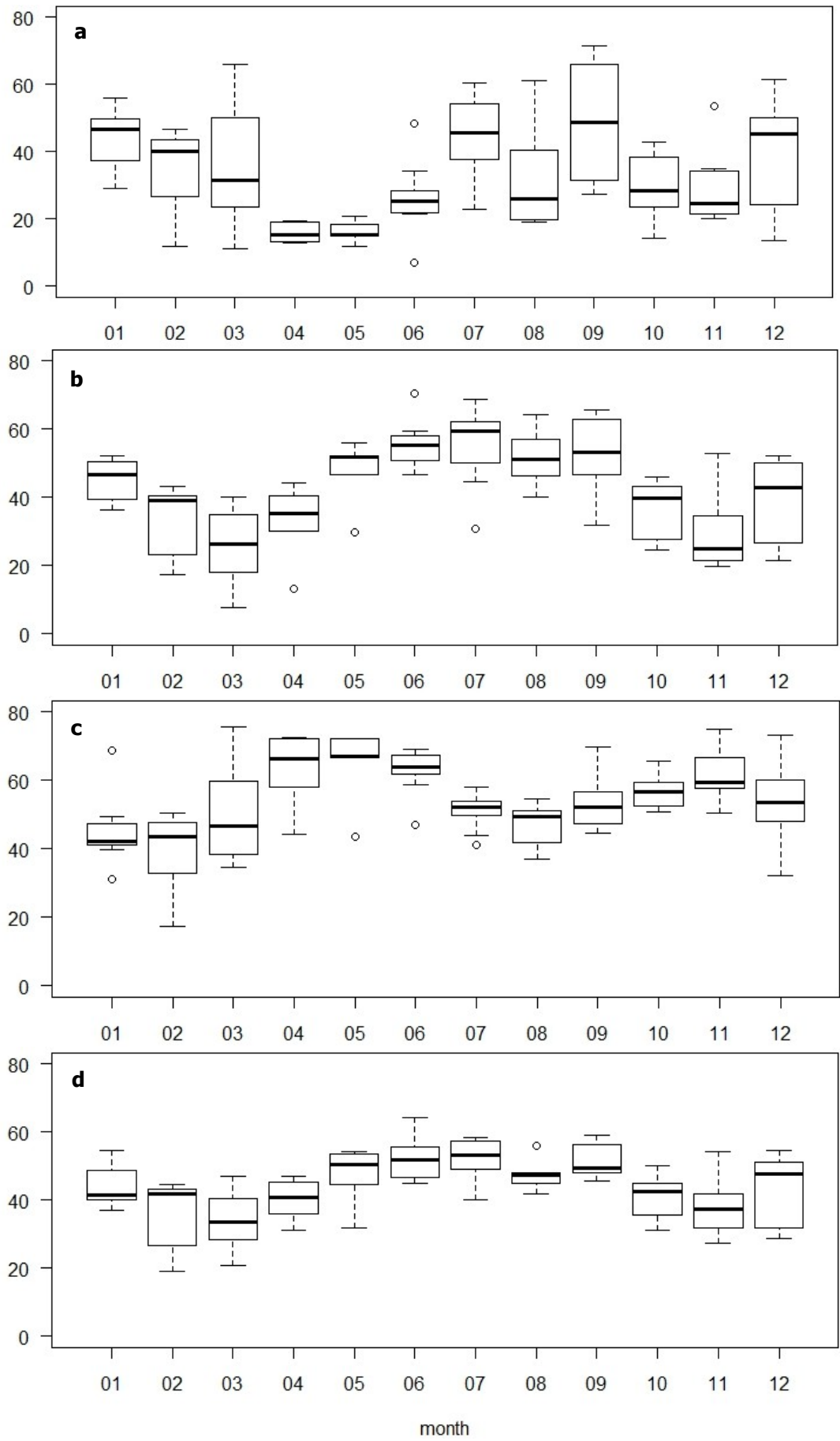


Fig. 5.26 –Seasonal cycle of the percentage ratio of heterotrophic bacteria carbon on the total carbon (phytoplankton plus heterotrophic bacteria) at the surface **a**), 20m depth **b**), 60 m depth **c**) and as mean (0-60m) integrated value **d**), box-plot by month.

5.3.8 Hydrolytic enzyme activities

The aminopeptidase (AMA) and the alkaline phosphatase (APA) activities showed similar ranges of variability. AMA hydrolysis rates ranged from 5.0 nM h⁻¹ up to 1125.85 nM h⁻¹, recorded at 60 m (23/06/2009) and at the surface (16/6/2009). The lowest value of APA activity was 0.18 nM h⁻¹ (22/01/2009 at 20 m) and the highest 1250.62 nM h⁻¹ (23/06/2009 at the surface).

The vertical distributions of the hydrolytic enzyme activities showed a clear vertical gradient for both AMA and APA. The highest hydrolysis rates were observed in the summer period, while they were low in winter over the whole water column.

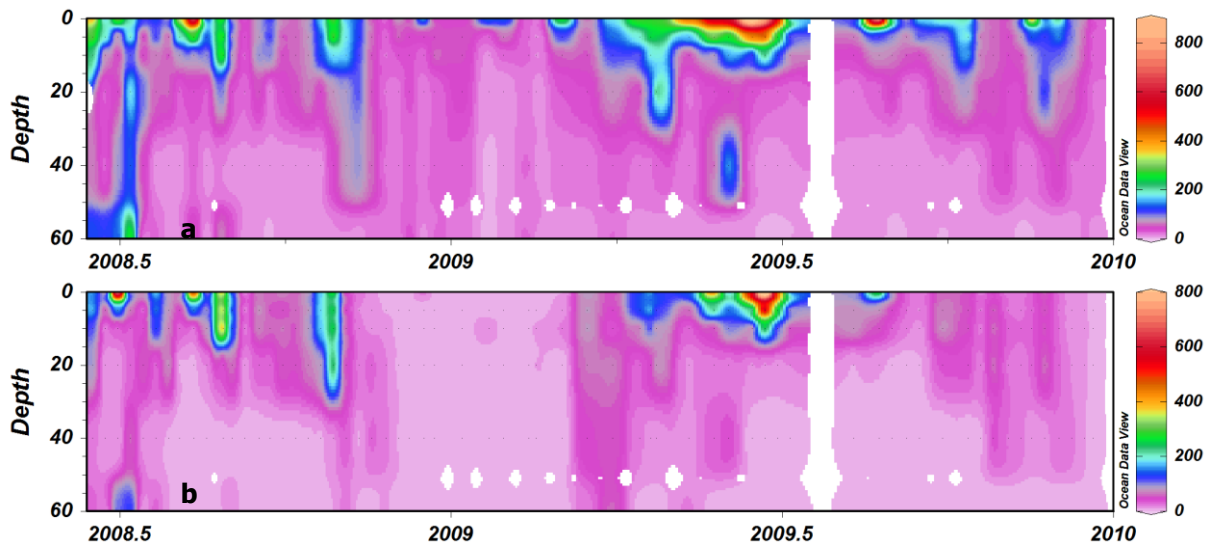


Fig. 5.27 – Time variability of the a) AMA and b) APA activities (nM h⁻¹) at LTER-MC station (2008-2009).

At the surface (Fig. 5.28) AMA e APA display a similar seasonal variability. High enzymes activities were observed in summer and, with the only exception of July, AMA overpasses APA all yearlong. The maximum and minimum monthly values are observed in June and in February for both enzymes.

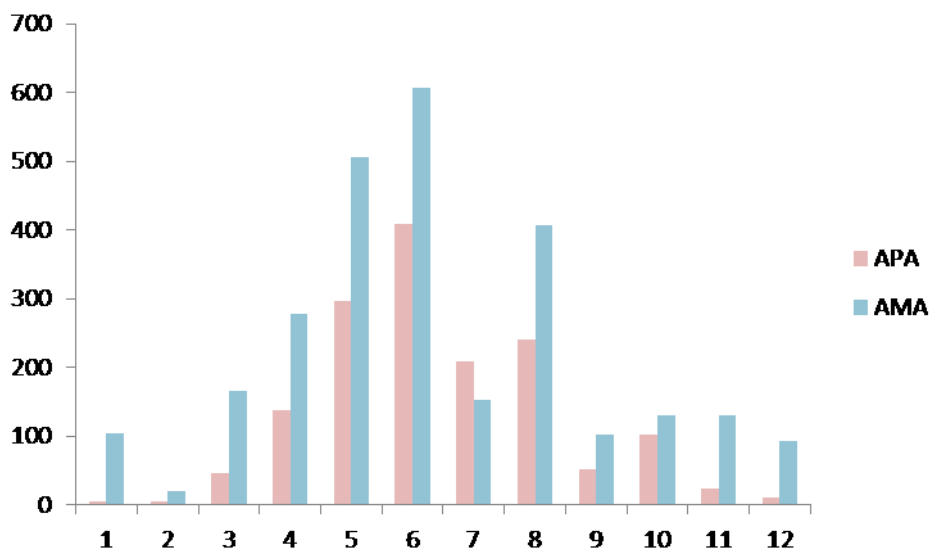


Fig. 5.28 – Monthly mean values of AMA and APA activities (nM h⁻¹) at the surface at LTER-MC station (2008-2009)

At 20 m, APA and AMA display different seasonal patterns (Fig.5.29). The highest mean monthly value of AMA has been observed in July, while the maxima hydrolytic rate of APA occurs in October. The differences between AMA and APA, in terms of mean monthly values, are less pronounced compared to the surface.

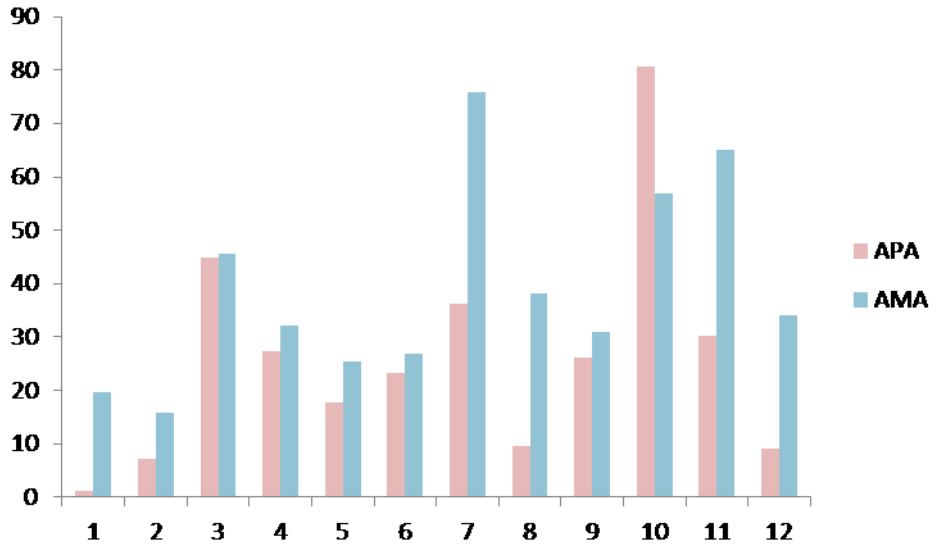


Fig. 5.28 – Monthly mean values of AMA and APA activities (nM h⁻¹) at 20m depth at LTER-MC station (2008-2009)

At 60 m, the enzymatic activities are low all yearlong (Fig.5.30). APA shows two relative maxima, in March and July, while AMA displays the highest values in June and July. As already observed the surface, the AMA activity rates are generally higher than APA.

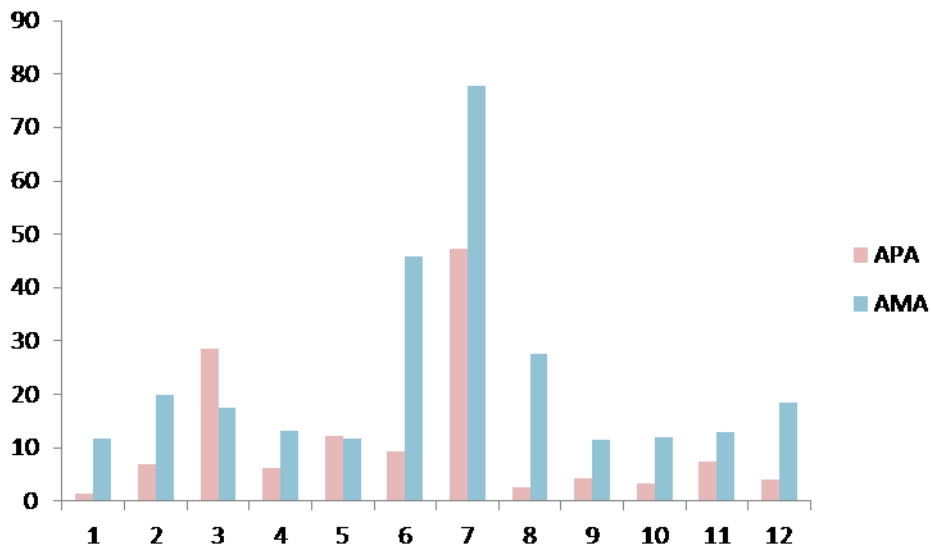


Fig. 5.28 – Monthly mean values of AMA and APA activities (nM h⁻¹) at 60m depth at LTER-MC station (2008-2009)

5.4 Discussion

N and P inventories

In this Chapter, the composition of the different N and P pools has been investigated in order to characterize their vertical and temporal distribution in terms of availability, partition, as well as stoichiometry. This is the first time a similar analysis is carried out at LTER-MC, even if the time-series has been sampled since 1984, because previous works were mainly focused on plankton (Ribera d'Alcalà et al., 2004, Modigh, 2001; Modigh and Castaldo, 2002; Zingone et al., 2010b; Mazzocchi et al., 2011), and no measures of organic (dissolved and particulate) N and P were collected until the beginning of study.

Moreover, also at different sites, studies centred on N and P dynamics within the different pools, inorganic and organic (dissolved and particulate), are mainly related to single surveys, and only during few multi-year researches the N and P compositions have been investigated in detail (English Channel (Butler et al., 1979), ALOHA station (Karl et al., 2001), (Bay of Blanes (Lucea et al., 2005), Gulf of Trieste (Lipizer et al., 2011)).

In all these studies, a high variability of the N and P dynamics has been found among the different pools and in their relative ratios, not only in coastal areas, but also in the open subtropical ocean (ALOHA station). Furthermore, the variations in the inventories and stoichiometries can have broad implications on the plankton, including population adaptation and community succession, and can ultimately influence the sequestration of atmospheric carbon dioxide (Karl et al., 2001), which makes this issue particularly important.

As a first step, we have compared the N and P data collected at LTER-MC in 2008-2009 with the other two multiyear studies carried out in the Mediterranean Sea. At LTER-MC, the N and P concentrations in all the pools are lower than those observed in the Gulf of Trieste (Lipizer et al., 2011), which is highly influenced by the Isonzo River, but are higher than the values in the Bay of Biscay (Lucea et al., 2005), that is located in an open oligotrophic coastal area. This finding supports the results of the previous chapter: at LTER-MC station, a strong impact of the terrestrial loads is well recognizable, which significantly affect also the organic pools of N and P.

As already found for the dissolved inorganic nutrient and for the phytoplankton biomass in the previous chapter, the upper part of the water column (0-10m) is the most dynamic layer. In fact, the highest variability in terms of concentrations, composition and relative ratios was recorded in this layer.

More in details, N and P in the total pools showed surface concentrations comparable to those recorded for the coastal stations affected by terrestrial loads (TN=19.85 mmol m⁻³, TP=0.69 mmol m⁻³), indicated as Group 3 in the Chapter 3, and are also quite similar to those observed in the outer station off Naples (NA6). On the other hand, surface TN and TP concentrations at MC are higher than the typical values of the stations located in the pristine area (TN=5.03 mmol m⁻³, TP=0.19 mmol m⁻³), indicated as Group 4 in Chapter 3. However, the observed differences are restricted to the first layer of the water column (0-10m), whereas the concentrations below 10 m depth do not differ dramatically neither the values characteristic of Group 4, nor from the

concentrations recorded in the open waters of the Western Mediterranean Sea (Moutin and Raimbault, 2002). This indicates that terrestrial inputs mainly affect the surface. The ratio between TN and TP at the surface is almost constant all yearlong (27), on the contrary at 20m and 60m the ratio displays lower values in the summer period compared to the rest of the year.

The surface PN and PP data recorded at LTER-MC are similar to those estimated for the coastal station off Naples (NA4) and sensibly higher than the coastal stations in the pristine area (PL and PT). Moreover, the surface particulate N and P values at LTER-MC are considerably higher than the typical values of the open Mediterranean Sea (Moutin and Raimbault, 2002; Puyo-Pay et al., 2011). This signal is still detectable at 20m, whereas at 60m the differences with the open waters are almost negligible.

Finally, the mean values of N and P in the dissolved organic matter were similar to those observed in the open Mediterranean Sea (Moutin and Raimbault, 2002, Puyo-Pay et al., 2011), indicating that the terrestrial loads influence more the dissolved inorganic and the particulate N and P pools. However, the maximum values observed both for DON and DOP are far from the range of variability of the open waters.

N and P dynamics

To test the relationships among the different N and P pools (inorganic, particulate and dissolved organic) and physical (temperature and salinity) and biological (phytoplankton biomass, heterotrophic bacteria biomass, aminopeptidase and alkaline phosphatase) properties, multivariate multiple regression analyses were performed at three different depths (0, 20, and 60 m).

At the surface, the variability in the composition of inorganic nutrient pools is best explained by a combination of physical (temperature and salinity) and biological (PON and POP) factors, whereas at 20m depth the role of physical processes is not significant. At the deepest depth salinity became again one of the most important factors explaining the composition of the inorganic nutrient pool (Fig.5.31).

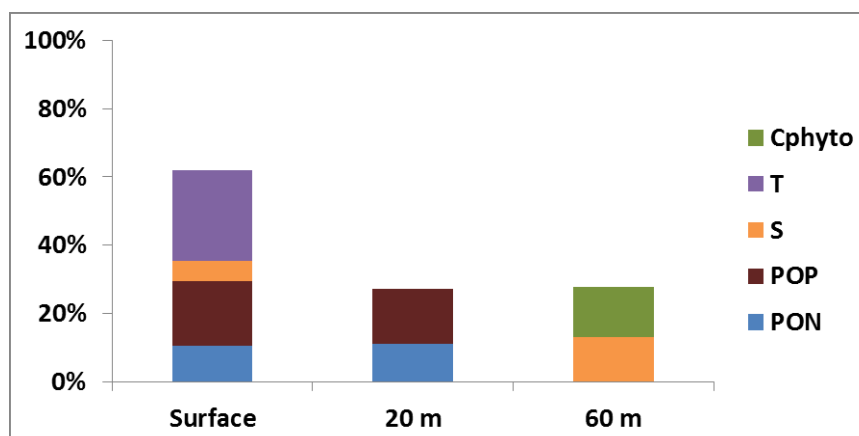


Fig. 5.31 - Percentages of explained variance in the composition of the inorganic nutrient pools.

These results indicate that changes in the overall physical conditions, including terrigenous transport, strongly modify waters. According to this, we indeed observed that values of the N/P ratio mostly increased concomitantly with the periods of maximum river discharge/precipitations,

whereas dropped to the lowest values in summer. This result allows us to depict the variations in the composition of the inorganic nutrients pool as an alternation of allochthonous 'supply' mechanisms and *in situ* consumption mechanisms. The allochthonous supply is clearly related to the physical and chemical properties of the terrigenous inputs, whereas *in situ* consumption appears to be tightly linked to the biological activity.

Moreover, this scenario confirms the prominent role of the terrestrial inputs in driving the variations observed at the surface at seasonal scale either in the DIN/PO₄ and NO₃/PO₄ ratios. As shown in the previous chapter, the increase of these ratios is typically associated with the presence of terrestrial inputs, but another possible mechanistic explanation of this pattern can be identified. In fact, as derived from the multiple regression tests, the PN and PP strongly influence the composition the inorganic nutrients pool. In this work, it was shown that the PN:PP ratio in the surface waters varies seasonally, with the highest values recorded from June to September, as a possible consequence of an accumulation of organic nitrogen in the particulate pool. It can be thus concluded that the observed seasonal variability in the N/P ratios at the surface is determined by the combination of both inorganic nutrient allochthonous supply mechanisms and *in situ* removal processes.

The multiple regression analysis applied to the organic pools reveals that, at all depths, a large part of the variations in the particulate organic N and P pools is related to the biological activity, either in terms of organic matter degradation activities or biomass stocks (Fig. 5.32).

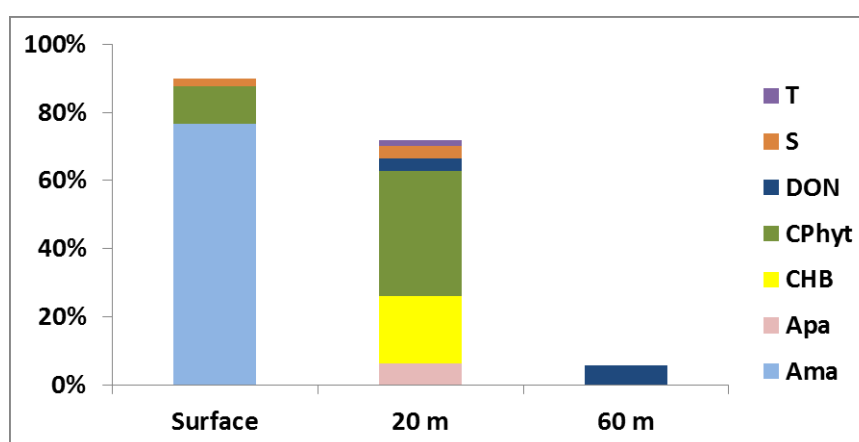


Fig. 5.32 - Percentages of explained variance in the composition of the particulate organic N and P pools.

However, this result is difficult to interpret under a simple mechanistic explanation, as the stoichiometry of the particulate organic pools can be highly affected by the algal physiology (Geider and La Roche, 2002; Arrigo, 2005), the taxonomic composition of the microbial assemblages (Quigg et al., 2003), and many different environmental constrains (Klausmaier et. al, 2004). For instance, Klausmaier and coauthors (2004) predict that the optimal composition of phytoplankton under exponential growth is associated with N/P ratios of about 8.2. Under nitrogen limitation this ratio approximates 37.4, whereas under phosphorus limitation it reaches values as high as 45.0. Recent studies (Sanudo-Wilhelmy et al. 2004; Fu et al., 2005) indicate that a large

fraction of particulate organic P is adsorbed at the cell surface (at rates even larger than the intracellular P). The fraction of scavenged P increases in senescent phytoplankton populations.

At LTER-MC, the low PN:PP ratio observed at the surface in winter-early spring, namely in conditions of replete nutrients (Chapter 4, Zingone et al., 2010), thus seems to be related to the physiology of the phytoplankton communities. In this season, the phytoplankton increase their allocation of resources toward the 'growth machinery', e.g. with the production of ribosomal RNA, which is high in both N and P, in agreement with the conceptual model proposed by Arrigo (2005). The high N/P ratio observed in summer, when the DIN concentrations are low, can then be explained by non-optimal growth conditions. Under these circumstances, the 'acquisition machinery' is favoured (Klausmaier et. al, 2004; Arrigo, 2005), and the phytoplankton synthesize additional resources (such as proteins, enzymes pigments) which are characterized by a high N/P ratio.

On the other hand, only a limited number of possible factors has been taken into account in the present study, so that the results of the multiple regression analyses should be considered with some caution. Nevertheless, at least at the surface, it was shown that aminopeptidase activities explain more than 75% of the total variance in the composition of the particulate organic pools. This result would support the hypothesis of a prominent role of degradation activities on the temporal variability of the particulate organic pools. However, it must be taken into account that under nutrient limitation, phytoplankton can produce large amounts of proteolytic enzymes to take advantage of the dissolved organic pools, so that the role of organic matter degradation hypothesised above should be investigated together with an analysis of the DOM uptake mechanisms by planktonic algae. Unfortunately, the lack of synoptic estimates of the heterotrophic production rates in our dataset does not allow a definitive confirmation of this hypothesis. As an additional remark, it should be kept in mind that non-optimal growth conditions for the phytoplankton can also determine the adsorption of P on cell surface, and, consequently, can alter the N/P ratio.

At all depths, only a small fraction of the variance in the dissolved organic pool is explained by the analysed variables. However, at each investigated layer, the role of the biological activity apparently overpasses that of the physical forcing (Fig. 5.33).

DON and DOP concentrations generally increase from June to August at all depths. A similar seasonal pattern has been observed by Butler et al (1979), who documented a steady increase in DON concentrations from January through August and then a steady decline from August to December.

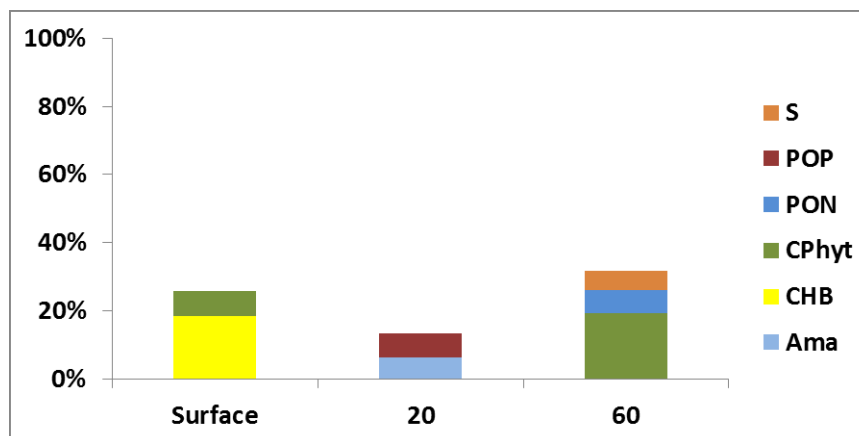


Fig. 5.33 - Percentages of explained variance in the composition of the dissolved organic N and P pools.

Net production of dissolved organic matter is due to the temporal and spatial uncoupling of *in situ* biological production and removal processes (Carlson, 2002). DON and DOP originate from a number of biotic and abiotic sources: the abiotic sources include DON and DOP transport via overland runoff, rivers, streams and groundwater (Tobias et al., 2001; Valiela et al., 1990; Tobias et al., 2001); the biotic sources include the phytoplankton, bacteria, microzooplankton and zooplankton releases (Carlson, 2002). The decline of phytoplankton blooms has been shown to be a period of significant DOM release due to such processes as physiological stress or high grazing pressure (Carlson et al., 1994, Jenkinson and Bidbanda, 1995). Due to the minimum of precipitations and river runoff recorded during these months at LTER-MC, the biotic source seems to be the more plausible source. Moreover, at LTER-MC, the highest values of mesozooplankton biomass are generally recorded in mid spring (April-May) and summer (July-September), and the annual maxima of microzooplankton are usually observed in late spring though peaks are observed whole the period of stratification (Ribera d'Alacalà et al., 2004). Thus, the increase of DON and DOP during the summer period seems to be related to the biological activity.

Regarding to the distribution of N and P among the different pools, the organic dissolved forms are the most abundant compounds over the whole water column. However, a strong seasonal variability has been observed at the surface. In May and June, when the autotrophic phytoplankton show their highest relative contribution, a strong increase in of PP and PN has been recorded. On the contrary, from July up to September, when the percentage of heterotrophic bacteria is maxima, particulate P and N decrease and DON and DOP increase.

Chapter 6: Conclusions

The research carried out during this Ph.D. thesis has been focused on the study of the Nitrogen and Phosphorous dynamics in the marine ecosystems along the coasts of Campania region (Southern Italy). More in details, the interactions between N and P space and time variability and selected physical parameters and forcings, as well as their relation to the microbial community, have been investigated in order to achieve a better understanding of ecosystem functioning in different coastal environments.

The research approach chosen involved increasing levels of complexity. In synthesis, in Chapter 3, the space-time variability has been described by analyzing the data collected over a wide area in the framework of a national monitoring program, but only on a limited number of parameters, with reduced vertical resolution. Chapter 4 was thus devoted to the analysis of the N and P dynamics along the water column and to its relation to local and large scale physical processes, concentrating on a station located inside the Gulf of Naples. Standard and advanced statistical techniques were applied to these historical data. As a final step, specific experimental activities have been carried out during the first two years of the Ph.D., setting up additional chemical and biological analyses at the MareChiara station. As described in Chapter 5, the analysis of the more complete dataset collected in 2008-2009 allowed to highlight the role of the biology in modulating the N and P dynamics inside the Gulf of Naples.

The analysis of the surface nutrient concentrations highlighted the presence of different trophic regimes along the Campania coasts (Chapter 3). The Gulf of Naples and the Gulf of Gaeta are in fact strongly impacted by terrigenous nutrient loads. In the first, the Sarno River DIN composition at its mouth clearly shows poor water quality reflecting the heavy industrial and sewage inputs along its path to the sea. Instead, the stations located in the southernmost part of the Gulf of Salerno display clear oligotrophic characteristics and their chemical properties do not significantly differ from the typical conditions of the open waters of the Tyrrhenian Sea.

An objective classification of the different coastal areas based upon their environmental conditions has been obtained, through a Principal Component Analysis of their chemical properties. The main mechanisms influencing the N and P dynamics in each class have then been identified. The inorganic fraction predominates in the stations close to river mouths, while the organic pools were mainly dominating the remaining sites. Among the rivers, the dissimilarity observed in the composition of the DIN reflects the differences in the contributing waters. Reasonably, the Volturno and Picentino watersheds are mainly impacted by agricultural activities, whereas industrial and domestic wastewaters strongly impact the Sarno basin. At the coastal station of the Gulf of Naples, the terrestrial inputs determine increasing concentrations of PO_4 , NH_4 , SiO_4 , TN and TP, probably originating from sewages and industrial wastewaters. Finally, despite the marked variability observed in terms of N and P inventories and dynamics, a strong seasonal signal in the

N/P ratios in the dissolved inorganic pool has been recorded at all the sampling sites, which appears to be mainly related to NO_3 seasonality.

As an additional remark, it was observed that the interannual variability of the physical parameters (salinity and temperature) was dominated by large-scale processes at all sampling sites. Therefore, monitoring programs and long time-series studies are to be considered powerful tools to identify basin scale variations, and to reveal larger spatial scale physical processes with sensibly reduced effort. This result is of particular relevance, if related to the long-term monitoring of climate variability and global change, and of their potential impact on the Mediterranean ecosystems.

In Chapter 4, the vertical distribution of P and N was more thoroughly analyzed. The study was performed on the 2002-2009 data collected at a station located in the Gulf of Naples (LTER-MareChiara). Within the DIN pool, ammonium predominates in the surface layer, and it is mainly related to terrigenous inputs. Conversely, the variations in nitrate distribution is associated with two different enrichment mechanisms. In the surface layer, terrigenous input prevails, whereas in the deeper part of the water column remineralization and sub-surface circulation (i.e. the advection/mixing of deep offshore waters) are the dominant processes. Indeed, the exchange between coastal and offshore waters after winter-mixing events plays a key role in fuelling nitrate at LTER-MC. Precipitations generally drive an increase in N and P, but induce an increase in the N/P ratio. It has been shown that the surface nutrient dynamics in the Gulf of Naples is highly dependent upon several factors (local and large scale circulations, meteorological forcing, river discharges etc.) and it cannot be explained by a simple correlation between nutrient and salinity and/or precipitations. In order to understand the processes that drive the nutrient dynamics in coastal waters, the long term-series of a single station can thus provide only limited information, because of the lacking knowledge of the dynamical conditions and associated advection regimes. As shown in section 4.4, new technologies, such satellite imagery or HF radars, in combination with in situ measurements, represent useful tools to fill this gap. However, the knowledge of the chemical features of the area can help in determining the source of nutrients. In fact, it has been shown that the relative contribution of the NH_4 and NO_3 to the DIN can be used as a marker of the origin of the water masses at least at surface.

Finally, the vertical distribution of N and P within the different pools (Chapter 5) reveals a stronger influence of the terrigenous loads on the dissolved inorganic and particulate pools, in terms of average composition, compared to the dissolved organic forms. However, the terrestrial inputs are generally confined to the upper part of the water column. By looking at the distribution of N and P among the different pools, the organic dissolved forms are the most abundant over the whole water column. However, at surface a strong seasonal variability has been observed. In May and June, when the autotrophic phytoplankton show their highest relative contribution, a strong increase in PP and PN has been recorded. On the contrary, from July up to September, when the percentage of heterotrophic bacteria is highest, particulate P and N decrease and DON and DOP increase.

At surface, the N/P stoichiometry displays an opposite temporal pattern between the dissolved inorganic and the particulate pools. The seasonal variability in the NO_3/PO_4 ratios at the surface thus appears to be determined by the combination of inorganic nutrient allochthonous supply and *in situ* removal processes.

References

Allen, J. R., D. J. Slinn, T. M. Shammon, R. G. Hartnoll, and S. J. Hawkins (1998), Evidence for eutrophication of the Irish Sea over four decades., *Limnology and Oceanography*, 43, 1970-1974.

Alongi, D. M. (2004), Ecosystem types and processes, in *Global coastal ocean: interdisciplinary regional studies and synthesis, Part A - Ecosystem dynamics and interactions The Sea*, edited by A. R. a. B. Robinson, K., pp. 317-352, Harvard University Press.

Andersen, J. H., L. Schluter, and G. Ærtebjerg (2006), Coastal eutrophication: recent developments in definitions and implications for monitoring strategies, *Journal of Plankton Research* 28(7), 621–628.

Anderson, L. A. (1995), On the hydrogen and oxygen content of marine phytoplankton, *Deep Sea Research I*, 42(9), 1675-1680.

Arrigo, K. R. (2005), Marine microorganisms and global nutrient cycles, *Nature*, 437, 349-355.

Azam, F., T. Fenchel, J. G. Field, J. S. Gray, L. A. Meyer-Reil, and F. Thingstad (1983), The ecological role of water-column microbes in the sea, *Marine Ecology Progress Series*, 10, 257-263.

Benitez-Nelson, C. R. (2000), The biogeochemical cycling of phosphorus in marine systems., *Earth-Science Reviews* 51, 109-135.

Benner, R. H. (2002), Chemical Composition and Reactivity, in *Biogeochemistry of Marine Dissolved Organic Matter*, edited by D. A. Hansell and C. A. Carlson, pp. 59-90, Accademic Press, San Diego.

Bizsel, N., and O. Uslu (2000), Phosphate, nitrogen and iron enrichment in the polluted Izmir Bay, Aegean Sea, *Marine Environmental Research*, 49(2), 101-122.

Bodeanu, N. (1993), Microalgal blooms in the Romanian area of the Black Sea and contemporary eutrophication conditions, 203-209 pp., Amsterdam.

Bonsdorff, E., E. M. Blomqvist, J. Mattila, and A. Norkko (1997), Coastal eutrophication: causes, consequences and perspectives in the Archipelago areas of the northern Baltic Sea., *Estuar Coast Shelf Sci*, 44(Suppl A), 63-72.

Borkman, D., H. Baretta-Bekker, and P. Henriksen (2009), Special Issue Long-term Phytoplankton Time Series Workshop: Time Series Data Relevant to Eutrophication and Ecological Quality Indicators WKEUT 11-14 September 2006, Tisvildeleje, Denmark Introduction, *Journal of Sea Research*, 61(1-2), 1-2.

Boukthir, M., and B. Barnier (2000), Seasonal and inter-annual variations in the surface freshwater flux in the Mediterranean Sea from the ECMWF re-analysis project, *Journal of Marine Systems*, 24(3-4), 343-354.

Bronk, D. A. (2002), Dynamics of DON, in *Biogeochemistry of Marine Dissolved Organic Matter*, edited by D. A. a. C. Hansell, C.A., pp. 153-247, Academic Press, San Diego.

Buonocore, B., D. Cianelli, P. Falco, R. Guida, M. Uttieri, G. Zambardino, and E. Zambianchi (2010), Hydrocarbon dispersal in the Gulf of Naples: a parametric study. , *Rapp Comm int Mer Médit* 39, 725

Butler, E. I., S. Knox, and M. I. Liddicoat (1979), The relationship between inorganic and organic nutrients in sea water., *Journal of the Marine Biological Association of the United Kingdom*, 59, 239-250.

Cadée, G. C. (1992), Phytoplankton variability in the Marsdiep, the Netherlands, *ICES Mar Sci Symp*, 195, 213-222.

Cadée, G. C., and J. Hegeman (2002), Phytoplankton in the Marsdiep at the end of the 20th century; 30 years monitoring biomass, primary production, and Phaeocystis blooms *Journal of Sea Research*, 48(2), 97-110.

Campbell, L., H. A. Nolla, and a. D. Vulot (1994), The importance of *Prochlorococcus* to community structure in the central North Pacific Ocean, *Limnology and Oceanography*, 39(4), 954-961.

Canals, M., P. Puig, X. D. de Madron, S. Heussner, A. Palanques, and J. Fabres (2006), Flushing submarine canyons, *Nature*, 444(7117), 354-357.

Carlson, C. A. (2002), Production and Removal Processes, in *Biogeochemistry of Marine Dissolved Organic Matter*, edited by D. A. Hansell and C. A. Carlson, pp. 91-152, Accademic Press, San Diego.

Carlson, C. A., H. W. Ducklow, and A. F. Michaels (1994), Annual flux of dissolved organic carbon from the eutrophic zone in the northwestern Sargasso Sea, *Nature*, 371, 405-408.

Carpenter, E. J., J. P. Montoya, J. Burns, M. R. Mulholland, A. Subramaniam, and D. G. Capone (1999), Extensive bloom of a N₂-fixing diatom/cyanobacterial association in the tropical Atlantic Ocean, *Marine Ecology Progress Series*, 185, 273-283.

Carrada, G. C., E. Fresi, D. Marino, M. Modigh, and M. Ribera d'Alcalà (1981), Structural analysis of winter phytoplankton in the gulf of Naples. , *Journal of Plankton Research*, 3(2), 291-313.

Carrada, G. C., T. S. Hopkins, G. Bonaduce, A. Ianora, D. Marino, M. Modigh, M. Ribera d'Alcalà, and B. Scotto di Carlo (1980), Variability in the hydrographic and biological features of the gulf of Naples, *Marine Ecology*, 1, 105-120.

Casotti, R., C. Brunet, B. Aronne, and M. R. d'Alcala (2000), Mesoscale features of phytoplankton and planktonic bacteria in a coastal area as induced by external water masses, *Marine Ecology-Progress Series*, 195, 15-27.

Celico, P., A. Malafrente , and V. Piscopo (1991), Bilancio idrologico e idrodinamica della Piana del Sarno (SA), in *Convegno Nazionale Giovani Ricercatori in Geologia Applicata* edited, pp. 297-306, Gargnano (BS).

Cianelli, D., M. Uttieri, B. Buonocore, P. Falco, G. Zambardino, and E. Zambianchi (2011), Dynamics of a very special Mediterranean coastal area: the Gulf of Naples., in *Mediterranean Ecosystems: Dynamics, Management and Conservation.*, edited by F. Columbus, Nova Science Publishers, New York.

Cloern, J. E. (2001), Our evolving conceptual model of the coastal eutrophication problem, *Marine Ecology Progress Series*, 210, 223–253.

Cloern, J. E., and A. D. Jassby (2010), Patterns and Scales of Phytoplankton Variability in Estuarine-Coastal Ecosystems, *Estuaries and Coasts*, 33(2), 230-241.

Cociasu, A., L. Dorogan, C. Humborg, and L. Popa (1996), Long-term ecological changes in Romanian coastal waters of the Black Sea., *Marine Pollution Bulletin*, 32, 32-38.

Comín, F. A., M. Menéndez, and J. A. Herrera (2004), Spatial and temporal scales for monitoring coastal aquatic ecosystems, *Aquatic Conservation: Marine and Freshwater Ecosystems*, 14(1), S5–S17.

Cooper, S. R. (1995), Chesapeake Bay watershed historical land use: impact on water quality and diatom communities., *Ecol Appl*, 5, 703-723.

De Blasio, A. (1993), *Annali Idrologici*, edited by U. I. e. M. d. Napoli, Istituto Poligrafico dello Stato, Roma.

De Maio, A., M. Moretti, E. Sansone, G. Spezie, and M. Vultaggio (1983), Dinamica delle acque del Golfo di Napoli e adiacenze. Risultati ottenuti dal 1977 al 1981, *Annali Istituto ersitario Navale*, 1-58.

Di Capua, I., and M. G. Mazzocchi (2005), Lo studio dello zooplancton nel monitoraggio delle acque marino-costiere della Campania, in *Gestione e tutela dell'ambiente marino-costiere in Campania* edited by L. Capobianco, S. Del Gaizo, V. Saggiomo and E. Zucaro, pp. 53-64, Napoli.

Duarte, C. M., J. Cebrian, and N. Marbà (1992), Uncertainty of detecting sea change, *Nature*, 356, 190.

Duarte, C. M., S. Agusti, H. Kennedy, and D. Vaque (1999), The Mediterranean climate as a template for Mediterranean marine ecosystems: the example of the northeast Spanish littoral, *Progress in Oceanography*, 44(1-3), 245-270.

Fleming, L. E., K. Broadb, A. Clement, E. Dewaillyd, S. Elmira, A. Knape, S. A. Pomponig, S. S. G. Smitha, H., and P. Walsh (2006), Oceans and human health: Emerging public health risks in the marine environment, *Marine Pollution Bulletin*, 53(10-12), 545-560.

Flo, E., E. Garces, M. Manzanera, and J. Camp (2011), Coastal inshore waters in the NW Mediterranean: Physicochemical and biological characterization and management implications, *Estuarine Coastal and Shelf Science*, 93(4), 279-289.

Fu, F. X., Y. Zhang, K. Leblanc, S. A. Sanudo-Wilhelmy, and D. A. Hutchins (2005), The biological and biogeochemical consequences of phosphate scavenging onto phytoplankton cell surface., *Limnology and Oceanography*, 50, 1459-1472.

Fuhrman, J. A., T. D. Sleeter, C. A. Carlson, and L. M. Proctor (1989), Dominance of bacterial biomass in the Sargasso Sea and its ecological implications, *Marine Ecology-Progress Series* 57(3), 200-217.

Gambi, M. C., F. Barbieri, S. Signorelli, and V. Sagggiomo (2010), MORTALITY EVENTS ALONG THE CAMPANIA COAST (TYRRHENIAN SEA) IN SUMMERS 2008 AND 2009 AND RELATION TO THERMAL CONDITIONS, *Biol. Mar. Mediterr.*, 17(1), 126-127.

Garrabou, J., et al. (*Glob. Change Biol.*, 15: 1090-1103.), A new large scale mass mortality event in the NW Mediterranean rocky benthic communities: effects of the 2003 heat wave., 2009, 15(1090-1103).

Geider, R. J., and J. LaRoche (2002), Redfield revisited: variability of C:N:P in marine microalgae and its biochemical basis, *European Journal of Phycology*, 37, 1-17.

Gravili, D., E. Napolitano, and S. Pierini (2001), Barotropic aspects of the dynamics of the Gulf of Naples (Tyrrhenian Sea). *Continental Shelf Research*(21), 455-471.

Grieco, L., L. B. Tremblay, and E. Zambianchi (2005), A hybrid approach to transport processes in the Gulf of Naples: an application to phytoplankton and zooplankton population dynamics, *Continental Shelf Research*, 25(5-6), 711-728.

Grignon, L., D. A. Smeed, H. L. Bryden, and K. Schroeder Importance of the variability of hydrographic preconditioning for deep convection in the Gulf of Lion, NW Mediterranean, *Ocean Science*, 6(2), 573-586.

Gruber, N. (2008), The Marine Nitrogen Cycle: Overview and Challenges, in *Nitrogen In The Marine Environment*, edited by D. G. Capone, D. A. Bronk, M. R. Mulholland and E. J. Carpenter, pp. 469-509, Elsevier, Burlington.

Hansen, H. P., and K. Grasshoff (1983), Automated chemical analysis, in *Methods of seawater analysis*

edited by K. Grasshoff, M. Ehrhardt and K. Kremling, Verlag Chemie, Weinheim.

Harding, L. W. J., and E. S. Perry (1997), Long-term increase of phytoplankton biomass in Chesapeake Bay, 1950-94., *Mar Ecol Prog Ser*, 157, 39-52.

Hays, G. C., A. J. Richardson, and C. Robinson (2005), Climate change and marine plankton, *TRENDS in Ecology and Evolution*, 20(6), 337-344.

Holm-Hansen, O., C. J. Lorenzen, R. W. Holmes, and J. D. H. Strickland (1965), Fluorimetric determination of chlorophyll., *J. du Conseil perm. internat. Expl. de la Mer*, 30, 3-15.

Hoppe, H. G. (1993), Use of fluorogenic model substrates for extracellular enzyme activity (EEA) measurement of bacteria., in *Handbook of Methods in Aquatic Microbial Ecology*, edited by P. F. Kemp, B. F. Sherr, E. B. Sherr and J. J. Cole, pp. 423-431, CRC Press, Boca Raton.

Hutchins, D. A., and F.-X. Fu (2008), Linking the Ocean biogeochemistry of iron and phosphorus with the marine nitrogen cycle, in *Nitrogen in the marine environment*, edited by D. G. Capone, D. A. Bronk, M. R. Mulholland and E. J. Carpenter, pp. 1627-1666, Elsevier, Burlington.

Ianora, A., M. G. Mazzocchi, and B. Scotto di Carlo (1985), Zooplankton community structure for coastal waters of the gulf of Naples. Summer of 1983. , *Rapp. Comm. Int. Mer. Medit.*, 29, 299-300.

Jackson, J. B. C., et al. (2001), Historical Overfishing and the Recent Collapse of Coastal Ecosystems, *Science*, 293, 629-638.

Jenkinson, I. R., and B. A. Bidbanda (1995), Bulk-phase viscoelastic properties of seawater: Relationship with plankton components. , *Journal Plankton Reserch*, 17, 2251-2274.

Jickells, T. D. (1998), Nutrient Biogeochemistry of the Coastal Zone, *Science*, 281, 217-222.

Jordan, M. B., and I. Joint (1998), Seasonal variation in nitrate : phosphate ratios in the English Channel 1923-1987, *Estuarine Coastal and Shelf Science*, 46(1), 157-164.

Karl, D. M., and K. M. Bjorkman (2002), Dynamics of DOP, in *Biogeochemistry of Marine Dissolved Organic Matter*, edited by D. A. a. C. Hansell, C.A., pp. 249-366, Academic Press, San Diego.

Karl, D. M., K. M. Bjorkman, J. E. Dore, L. Fujieki, D. V. Hebel, T. Houlihan, R. M. Letelier, and L. M. Tupas (2001), Ecological nitrogen-to-phosphorus stoichiometry at station ALOHA, *Deep-Sea Research Part II-Topical Studies in Oceanography*, 48(8-9), 1529-1566.

Kester, D. R., and R. M. Pytkowicz (1967), Determination of the apparent dissociation constants of phosphoric acid in seawater., *Limnology and Oceanography*, 12, 243-252.

Kirchman, D. L., and P. A. Wheeler (1998), Uptake of ammonium and nitrate by heterotrophic bacteria and phytoplankton in the sub-Arctic Pacific, *Deep-Sea Res. I*, 45, 347-365.

Kirchman, D. L., H. W. Ducklow, J. J. McCarthy, and C. Garside (1994), Biomass and nitrogen uptake by heterotrophic bacteria during the spring phytoplankton bloom in the North Atlantic Ocean., *Deep-Sea Res. I*, 41, 879-895.

Klausmeier, C. A., E. Litchman, and S. A. Levin (2004), Phytoplankton growth and stoichiometry under multiple nutrient limitation., *Limnology and Oceanography*, 49, 1463-1470

Kocak, M., N. Kubilay, S. Tugrul, and N. Mihalopoulos (2010), Atmospheric nutrient inputs to the northern levantine basin from a long-term observation: sources and comparison with riverine inputs, *Biogeosciences*, 7(12), 4037-4050.

Lehninger, A. L. (1975), *Biochemistry: The Molecular Basis of Cell Structure and Function*, New York,.

Lejeusne, C., P. Chevaldonné, C. Pergent-Martini, C. F. Boudouresque, and T. Pérez (2009), Climate change effects on a miniature ocean: the highly diverse, highly impacted Mediterranean Sea, *Trends in Ecology and Evolution*, 25(4).

Lipizer, M., G. Cossarini, C. Falconi, C. Solidoro, and S. F. Umani (2011), Impact of different forcing factors on N:P balance in a semi-enclosed bay: The Gulf of Trieste (North Adriatic Sea), *Continental Shelf Research*, 31(16), 1651-1662.

Liu , K. K., L. Atkinson, R. A. Quinones, and L. Talaue-McManus (2010), Biogeochemistry of Continental Margins in a Global Context in *Carbon and Nutrient Fluxes in Continental Margins*, edited by L. K. K., L. Atkinson, R. A. Quinones and L. Talaue-McManus, Springer-Verlag, Berlin-Heidelberg.

Lopez-Jurado, J.-L., C. Gonzalez-Pola, and P. Vélez-Belchi (2005), Observation of an abrupt disruption of the long-term warming trend at the Balearic Sea, Western Mediterranean Sea, in summer 2005, *Geophysical Research Letters*, 32, L24606.

Lucea, A., Duarte C. M., Agusti S., and Sondergaard M. (2003), Nutrient (N, P and Si) and carbon partitioning in the stratified NW Mediterranean, *Journal of Sea Research*, 49, 157-170.

Lucea, A., C. M. Duarte, S. Agusti, and H. Kennedy (2005), Nutrient dynamics and ecosystem metabolism in the Bay of Blanes (NW Mediterranean), *Biogeochemistry*, 73(2), 303-323.

Ludwig, W., E. Dumont, M. Meybeck, and S. Heussner (2009), River discharges of water and nutrients to the Mediterranean and Black Sea: Major drivers for ecosystem changes during past and future decades?, *Progress in Oceanography*, 80(3-4), 199-217.

Luterbacher, J., M. A. Liniger, A. Menzel, N. Estrella, P. M. Della-Marta, C. Pfister, T. Rutishauser, and E. Xoplaki (2007), Exceptional European warmth of autumn 2006 and winter 2007: Historical

context, the underlying dynamics, and its phenological impacts, *Geophysical Research Letters*, 34(12).

Marasovic, V., Z. Nincevic, G. Kuspilic, S. Marinovic, and S. Marinov (2005), Long-term changes of basic biological and chemical parameters at two stations in the middle Adriatic, *Journal of Sea Research*, 54(1), 3-14.

Margalef, R. (1969), Composicion especifica del fitoplancton de la costa catalano-levantina (Mediterraneo occidental) en 1962-1967, *Invest. Pesq.*, 33, 345-380.

Marie, D., F. Partensky, S. Jacquet, and D. Vaulot (1997), Enumeration and cell cycle analysis of natural populations of marine picoplankton by flow cytometry using the nucleic acid stain SYBR Green I, *Applied and Environmental Microbiology*, 63, 186-193.

Marino, M., M. Modigh, and A. Zingone (1984), General features of phytoplankton communities and primary production in the Gulf of Naples and adjacent waters, in *Marine Phytoplankton and Productivity*, edited by O. Holm-Hansen, L. Bolis and R. Gilles, pp. 89-100, Springer-Verlag, Berlin.

Mariotti, A., M. V. Struglia, N. Zeng, and K. M. Lau (2002), The hydrological cycle in the Mediterranean region and implications for the water budget of the Mediterranean Sea, *Journal of Climate*, 15(13), 1674-1690.

Marty, J. C., and J. Chiaverini (2010), Hydrological changes in the Ligurian Sea (NW Mediterranean, DYFAMED site) during 1995-2007 and biogeochemical consequences, *Biogeosciences*, 7(7), 2117-2128.

Marty, J. C., J. Chiaverini, M. D. Pizay, and B. Avril (2002), Seasonal and interannual dynamics of nutrients and phytoplankton pigments in the western Mediterranean Sea at the DYFAMED time-series station (1991-1999), *Deep-Sea Research Part II-Topical Studies in Oceanography*, 49(11), 1965-1985.

Maso, M., and E. Garces (2006), Harmful microalgae blooms (HAB); problematic and conditions that induce them., *Mar. Pollut. Bull.*, 53, 620-630.

Mazzocchi, M. G., P. Licandro, L. Dubroca, I. Di Capua, and V. Saggiomo (2011), Zooplankton associations in a Mediterranean long-term time-series, *Journal of Plankton Research*, 33(8), 1163-1181.

- Menna, M., A. Mercatini, M. Uttieri, B. Buonocore, and E. Zambianchi (2007), Wintertime transport processes in the Gulf of Naples investigated by HF radar measurements of surface currents., *Nuovo Cimento* (30(C)), 605-622.
- Modigh, M. (2001), Seasonal variations of photosynthetic ciliates at a Mediterranean coastal site, *Aquatic Microbial Ecology*, 23, 163–175.
- Modigh, M., and S. Castaldo (2002), Variability and persistence in tintinnid assemblages at a Mediterranean coastal site, *Aquatic Microbial Ecology*, 28, 299–311.
- Modigh, M., V. Saggiomo, and M. R. d'Alcalà (1996), Conservative features of picoplankton in a Mediterranean eutrophic area, the Bay of Naples, *Journal of Plankton Research*, 18(1), 87-95.
- Moore, L. R., A. F. Post, G. Rocap, and S. W. Chisholm (2002), Utilization of different nitrogen source by the marine cyanobacteria *Prochlorococcus* and *Synechococcus*, *Limnology and Oceanography*, 47(4), 989-996.
- Moutin, T., and P. Raimbault (2002), Primary production, carbon export and nutrients availability in western and eastern Mediterranean Sea in early summer 1996 (MINOS cruise), *Journal of Marine Systems*, 33, 273-288.
- Mozetic, P., V. Malacic, and V. Turk (2008), A case study of sewage discharge in the shallow coastal area of the Northern Adriatic Sea (Gulf of Trieste), *Marine Ecology-an Evolutionary Perspective*, 29(4), 483-494.
- Nehring, D. (1992), Eutrophication of the Baltic Sea., *Sci Total Environ (Suppl)*, 673-682.
- Paerl, H. W., L. M. Valdes, B. L. Peierls, J. E. Adolf, and L. W. J. Harding (2006), Anthropogenic and climatic influences on the eutrophication of large estuarine ecosystems., *Limnol. Oceanogr.*, 51, 448-462.
- Paytan, A., and K. McLaughlin (2007), The Oceanic Phosphorus Cycle, *Chemical Reviews*, 107, 563-576.
- Picot, B., G. Pena, C. Casellas, D. Bondon, and J. Bontoux (1990), INTERPRETATION OF THE SEASONAL-VARIATIONS OF NUTRIENTS IN A MEDITERRANEAN LAGOON - ETANG-DE-THAU, *Hydrobiologia*, 207, 105-114.

Povero, P., T. S. Hopkins, and M. Fabiano (1990), Oxygen and nutrient observations in the Southern Tyrrhenian Sea, *Oceanologica Acta*, 13(3), 299-305.

Pujo-Pay, M., and P. Raimbault (1994), Improvement of the wet-oxidation procedure for simultaneous determination of particulate organic nitrogen and phosphorus collected on filters, *Marine Ecology Progress Series*, 105, 203-207.

Pujo-Pay, M., P. Conan, L. Oriol, V. Cornet-Barthaux, C. Falco, J. F. Ghiglione, C. Goyet, T. Moutin, and L. Prieur (2011), Integrated survey of elemental stoichiometry (C, N, P) from the western to eastern Mediterranean Sea, *Biogeosciences*, 8(4), 883-899.

Quigg, A., Z. V. Finkel, A. J. Irwin, Y. Rosenthal, T. Y. Ho, J. R. Reinfelder, O. Schofield, F. M. M. Morel, and P. G. Falkowski (2003), The evolutionary inheritance of elemental stoichiometry in marine phytoplankton, *Nature*, 425.

Rabouille, C., F. T. Mackenzie, and L. M. Ver (2001), Influence of the human perturbation on carbon, nitrogen, and oxygen biogeochemical cycles in the global coastal ocean, *Geochimica et Cosmochimica Acta*, 65(21), 3615-3641.

Ribera d'Alcalà, M., M. Modigh, M. Moretti, V. Saggiomo, S. M., S. G., and Z. A. (1989), Una storia infinita. Eutrofizzazione nella baia di Napoli. , *Oebalia*, 15, 491-501.

Ribera d'Alcalà, M., et al. (2004), Seasonal patterns in plankton communities in a pluriannual time series at a coastal Mediterranean site (Gulf of Naples): an attempt to discern recurrences and trends, *Scientia Marina*, 68, 65-83.

Rinaldi, E., B. B. Nardelli, E. Zambianchi, R. Santoleri, and P. M. Poulain (2010), Lagrangian and Eulerian observations of the surface circulation in the Tyrrhenian Sea, *Journal of Geophysical Research-Oceans*, 115.

Rio, M. H., P. M. Poulain, A. Pascual, E. Mauri, G. Larnicol, and R. Santoleri (2007), A Mean Dynamic Topography of the Mediterranean Sea computed from altimetric data, in-situ measurements and a general circulation model, *Journal of Marine Systems*, 65(1-4), 484-508.

Sanudo-Wilhelmy, S. A., A. Tovar-Sanchez, F.-X. Fu, D. G. Capone, E. J. Carpenter, and D. A. Hutchins (2004), The impact of surface-absorbed phosphorus on phytoplankton Redfield stoichiometry, *Nature*, 432, 897-901.

Schär, C., P. L. Vidale, D. Lüthi, C. Frei, C. Häberli, M. A. Liniger, and C. Appenzeller (2004), The role of increasing temperature variability in European summer heatwaves, *Nature*, *427*, 332-336.

Schiaparelli, S., M. Castellano, P. Povero, G. Sartoni, and R. Cattaneo-Vietti (2007), A benthic mucilage event in North-Western Mediterranean Sea and its possible relationships with the summer 2003 European heatwave: short term effects on littoral rocky assemblages, *Marine Ecology*, *28*, 341-353.

Schroder, K., G. P. Gasparini, M. Tangherlini, and M. Astraldi (2006), Deep and intermediate Water in the western Mediterranean under the influence of the Eastern Mediterranean Transient, *Geophysical Research Letters*, *33*, L21607.

Schroeder, K., S. A. Josey, M. Herrmann, L. Grignon, G. P. Gasparini, and H. L. Bryden (2010), Abrupt warming and salting of the Western Mediterranean Deep Water after 2005: Atmospheric forcings and lateral advection, *Geophysical Research* *115*, 1-18.

Scotto di Carlo, B., et al. (1985), Uno studio integrato dell'ecosistema pelagico costiero del Golfo di Napoli. , *Nova Thalassia*, *7*, 98-128.

Seitzinger, S. P., and J. A. Harrison (2008), Land-based nitrogen sources and their delivery to coastal systems, in *Nitrogen in the marine environment*, edited by D. G. Capone, D. A. Bronk, M. R. Mulholland and E. J. Carpenter, pp. 469-510, Elsevier, Burlington.

Sfriso, A., B. Pavoni, A. Marcomini, and A. A. Orio (1988), ANNUAL VARIATIONS OF NUTRIENTS IN THE LAGOON OF VENICE, *Marine Pollution Bulletin*, *19*(2), 54-60.

Siano, R. (2007), The phytoplankton of Campania coasts: an ecological and taxonomic study, PhD thesis, 1-242 pp, Università di Messina.

Smith, V. H. (2006), Responses of estuarine and coastal marine phytoplankton to nitrogen and phosphorus enrichment., *Limnology and Oceanography*, *51*, 377-384.

Souchu, P., A. Gasc, Y. Collos, A. Vaquer, H. Tournier, B. Bibent, and J. M. Deslous-Paoli (1998), Biogeochemical aspects of bottom anoxia in a Mediterranean lagoon (Thau, France), *Marine Ecology-Progress Series*, *164*, 135-146.

Suttle, C. A., J. A. Fuhrman, and D. G. Capone (1990), Rapid ammonium cycling and concentration-dependent partitioning of ammonium and phosphate: Implications for carbon transfer in planktonic communities, *Limnology and Oceanography*, *35*, 424-433.

Sverdrup, H. U., M. W. Johnson, and R. H. Fleming (1942), *The oceans*, Prentice-Hall, Englewood Cliffs.

Tobias, C. R., J. W. Harvey, and I. C. Anderson (2001), Quantifying groundwater discharge through fringing wetlands to estuaries: Seasonal variability, methods comparison, and implications for wetland-estuary exchange., *Limnology and Oceanography*, *46*, 604-615.

Ulses, C., C. Estournel, P. Puig, X. Durrieu de Madron, and P. Marsaleix (2008), Dense shelf Water cascading in the northwestern Mediterranean during the cold winter 2005: Quantification of the export through the Gulf of Lion and the Catalan margin, *Geophysical Research Letters*, *35*, L07610.

Uttieri, M., D. Cianelli, B. B. Nardelli, B. Buonocore, P. Falco, S. Colella, and E. Zambianchi (2011), Multiplatform observation of the surface circulation in the Gulf of Naples (Southern Tyrrhenian Sea), *Ocean Dynamics*, *61*(6), 779-796.

Valderrama, J. C. (1981), THE SIMULTANEOUS ANALYSIS OF TOTAL NITROGEN AND TOTAL PHOSPHORUS IN NATURAL-WATERS, *Marine Chemistry*, *10*(2), 109-122.

Valiela, I., J. Costa, K. Foreman, J. M. Teal, B. Howes, and D. Aubrey (1990), Trasport of groundwater-borne nutrients from watersheds and their effects on coastal water., *Biogeochemistry*, *10*, 177-197.

Vitousek, P. M., H. A. Mooney, J. Lubchenco, and J. M. Melillo (1997), Human domination of Earth's ecosystems, *Science*, *277*, 494-499.

Winder, M., and J. E. Cloern (2010), The annual cycles of phytoplankton biomass, *Philosophical Transactions of the Royal Society B-Biological Sciences*, *365*(1555), 3215-3226.

Worm, B., H. K. Lotze, H. Hillebrand, and U. Sommer (2002), Consumer versus resource control of species diversity and ecosystem functioning, *Nature*, *417*, 848-851.

Zehr, J. P., and B. B. Ward (2002), Nitrogen cycling in the ocean: New perspectives on processes and paradigms, *Appl. Environ. Microbiol.*, *68*(3), 1015-1024.

Zingone, A., M. Montresor, and D. Marino (1990), Summer phytoplankton physiognomy in coastal waters of the gulf of Naples., *Marine Ecology*, *11*(2), 157-172.

Zingone, A., R. Casotti, M. R. d'Alcalà, M. Scardi, and D. Marino (1995), ST-MARTINS SUMMER - THE CASE OF AN AUTUMN PHYTOPLANKTON BLOOM IN THE GULF OF NAPLES (MEDITERRANEAN-SEA), *Journal of Plankton Research*, 17(3), 575-593.

Zingone, A., E. J. Philips, and P. J. Harrison (2010a), Multiscale Variability of Twenty-Two Coastal Phytoplankton Time Series: a Global Scale Comparison, *Estuaries and Coasts*, 33(2), 224-229.

Zingone, A., L. Dubroca, D. Iudicone, F. Margiotta, F. Corato, M. Ribera d'Alcalà, V. Saggiomo, and D. Sarno (2010b), Coastal Phytoplankton Do Not Rest in Winter, *Estuaries and Coasts*, 33(2), 342-361.